

Early stage drug discovery screening for novel
compounds active against the persister phenotype in
Burkholderia thailandensis

Submitted by Samuel Peter Barker to the University of Exeter
as a thesis for the degree of Doctor of Philosophy in Biological
Science

April 2016

This thesis is available for Library use on the understanding
that it is copyright material and that no quotation from the thesis
may be published without proper acknowledgement.

I certify that all material in this thesis which is not my own work
has been identified and that no material has previously been
submitted and approved for the award of a degree by this or
any other University.

Signature

.....

Acknowledgements

I would like to thank my supervisor Dr Nic Harmer for his significant intellectual contributions and support throughout my PhD. I would also like to thank Dr David Gray of the DDU for his expert advice and tuition in drug discovery.

I would also like to thank Dr Sarah Harding, Dr Helen Atkins and all involved in the project at DSTL who funded the project. Also thank you to Dr Claudia Hemsley and Professor Rick Titball at the University of Exeter.

My thanks go to Dr Karen Moore, Dr Audrey Farbos and Dr Konrad Paszkiewicz of the Exeter Sequencing Service for their assistance in library preparation and interpretation of sequencing results.

On a personal note, I would also like to thank my friends and family.

Abstract

Many pathogenic microorganisms are believed to stochastically switch into low metabolic states that display resistance to supra-lethal levels of antibiotics. These so-called “persister” cells have been associated with recurrent infections and the development of antibiotic resistance. Whilst a compound that eliminates *Staphylococcus aureus* persister cells has been described, it is not active against Gram-negative bacteria. The aim of my PhD project was to develop a high-throughput assay for compounds that eradicate persister cells in the β -proteobacterium *Burkholderia thailandensis*. Further to this, I aimed to develop “hit” compounds from screening into lead series through investigation of structure activity relationships and, use a chemical genetics approach to elucidate potential mechanisms of action.

I developed a phenotypic assay to identify compounds that eradicate persister cells. The assay was based on the reduction of the resazurin based dye PrestoBlue. Optimization of the assay gave a Z' prime of 0.41 when screened in high throughput at the DDU.

Screening of the library of 61,250 compounds identified 2,127 compounds that gave a statistically significant reduction in persister cell numbers. Follow-up assays highlighted 29 compounds with a pIC_{50} greater than five. Detailed investigation allowed me to down select to six “best in class” compounds, which included the licensed drug chloroxine. A time dependent killing assay showed that chloroxine reduced levels of persister cells by three orders of magnitude over 72 hours ($P = 0.01$). Hit expansion around chloroxine using commercially available compounds did not identify any more potent compounds, but did highlight key features of the molecule for activity. Assay protocols were provided to collaborators at DSTL who were able to

show that chloroxine is also active against persister cells formed by the tropical pathogen and Tier 1 biological agent *Burkholderia pseudomallei*. Investigations into the mechanism of action of chloroxine used Next Generation Sequencing of an over expression library, identifying two putative genes involved in inhibition of persister cells by chloroxine.

My findings demonstrate a phenotypic assay against persister cells in Gram-negative bacteria, which has the power to identify potent anti-persister agents to assist in chemotherapy. Structural activity relationship and mechanism of action investigations have indicated lead series and genetic starting points for future development of this research. My PhD project has concluded with sufficient data for continuation of research following a number of leads and is at an ideal stage for instigation of a medicinal chemistry program for development of chloroxine as a clinical option for treatment of persistent melioidosis.

Table of Contents

Early stage drug discovery screening for novel compounds active against the persister phenotype in <i>Burkholderia thailandensis</i>	i
Acknowledgements.....	ii
Abstract	iii
Table of Contents	v
List of Abbreviations	viii
Organism Abbreviations	xi
Table of Figures.....	xii
Table of Tables.....	i
1. Introduction	1
1.1. Melioidosis	1
1.2. Persister Cells	15
1.3. Project Brief.....	29
2. Assay Development	33
2.1. Overview	33
2.2. Assay Specifications	35
2.3. Assay controls.....	36
2.4. Preliminary Assays.....	38
3. High-Throughput Compound Screening.....	71
3.1. Overview	71
3.2. Assay optimization	78

3.3.	Experimental Procedures for Screening.....	79
3.4.	Results	83
3.5.	Discussion.....	97
4.	Activity Confirmation	99
4.1.	Overview	99
4.2.	Activity confirmation	99
4.3.	Experimental Procedure.....	102
4.4.	Results	105
4.5.	Discussion.....	154
5.	Series Expansion	158
5.1.	Overview	158
5.2.	Experimental Procedure.....	158
5.3.	Results	159
5.4.	Discussion.....	205
6.	Mechanism of action studies.....	210
6.1.	Overview	210
6.2.	Chemical genetics approach.....	211
6.3.	Resistance generation	212
6.4.	Experimental procedures	212
6.5.	Results	215
6.6.	Discussion.....	226

7. Conclusions and Outlook	231
References	237

List of Abbreviations

Standard abbreviations are used without definition in accordance to the instruction for authors for submission to the Journal of Antimicrobial Chemotherapy. The following abbreviations are also provided for the reader.

ADMET	absorption, distribution, metabolism and toxicity
BLAST	basic local alignment search tool
BSL3	biological safety laboratory class III
CDC	Center for Disease Control
CFU	colony forming units
ChIP-Seq	chromatin immunoprecipitation sequencing
CI	confidence interval
cLogP	A measure of lipophilicity in drug discovery.
CPS	capsular polysaccharide
CNS	central nervous system
CT	computed tomographic (scan)
DDU	Drug Discovery Unit, University of Dundee
DMSO	Dimethyl Sulfoxide
FDA	Food and Drug Administration – federal agency of the United States

gDNA	genomic DNA
GI	gastrointestinal
HTS	high throughput screening
IC ₅₀	half maximal inhibitory concentration
LB	Luria Bertani
MACS	model based analysis for ChIP-Seq
MDT	multi drug tolerance
MIC	minimum inhibitory concentration
MIQE	minimum information for publication of quantitative real-time PCR experiments
MLST	multi-locus sequence typing
MOA	mechanism of action
MW	molecular weight
NADH	nicotinamide adenine dinucleotide
NGS	next generation sequencing
NME	new molecular entity
PBP	penicillin binding protein
PCR	polymerase chain reaction
R&D	research and development

SD	standard deviation
TA	toxin – antitoxin
UV	ultraviolet
v/v	volume by volume
WT	wild-type
w/v	weight by volume

Organism Abbreviations

<i>B. burgdorferi</i> (Borrelia)	<i>Borrelia burgdorferi</i>
<i>B. melitensis</i> (Brucella)	<i>Brucella melitensis</i>
<i>B. mallei</i>	<i>Burkholderia mallei</i>
<i>B. pseudomallei</i>	<i>Burkholderia pseudomallei</i>
<i>B. thailandensis</i>	<i>Burkholderia thailandensis</i>
<i>C. trachomatis</i> (Chlamydia)	<i>Chlamydia trachomatis</i>
<i>E. coli</i>	<i>Escherichia coli</i>
<i>K. pneumoniae</i>	<i>Klebsiella pneumoniae</i>
<i>M tuberculosis</i> (Tuberculosis)	<i>Mycobacterium tuberculosis</i>
<i>P. aeruginosa</i>	<i>Pseudomonas aeruginosa</i>
<i>S. enterica</i>	<i>Salmonella enterica</i>
<i>S. aureus</i>	<i>Staphylococcus aureus</i>
<i>S. pyogenes</i>	<i>Streptococcus pyogenes</i>

Table of Figures

Figure 1.1: Predicted Global Distribution of Melioidosis and locations of occurrence.	4
Figure 1.2: Clinical events after infection with <i>B. pseudomallei</i> .	7
Figure 1.3: The structure of ceftazidime, a third generation cephalosporin used in frontline treatment for melioidosis.	11
Figure 1.4: The cycle of persister cells.	18
Figure 1.5: Survival frequency of <i>Burkholderia thailandensis</i> treated with ceftazidime and ciprofloxacin.	20
Figure 1.6: Structure of HicA protein, shown in the cartoon format, coloured blue to red from the N-terminus to the C-terminus. Reproduced with permission from N. Harmer (Butt et al., 2014a).	25
Figure 2.1: Investigated options for a full kill, negative control using PrestoBlue.	37
Figure 2.2: Persister frequency in response to treatment with ceftazidime. Persister frequency for: 1 = 0.59 +/- 0.8; 2 = 0.028 +/- 0.03; 3 = 0.033 +/- 0.033.	42
Figure 2.3: The luciferase reaction from BactTiter-Glo Microbial Viability Assay (Promega)	43
Figure 2.4: Assay development using Bactiter Glo.	45
Figure 2.5: Assay development for qPCR.	48
Figure 2.6: Plasmid map of pBHR4-groS-RFP, conjugated into <i>B. thailandensis</i> to express red fluorescent protein.	51
Figure 2.7: Assay development using recombinantly expressed Red Fluorescent Protein.	52
Figure 2.8: Residual fluorescence of Red Fluorescent Protein	53
Figure 2.9: Assay development using LIVE / DEAD cell viability reagent.	56
Figure 2.10: Reduction of resazurin to Resorufin.	57

Figure 2.11: A PrestoBlue cell viability reagent based persister cell assay.	60
Figure 2.12: DMSO tolerance of persister cells.	65
Figure 2.13: Edge effect for a 384 well plate.	66
Figure 2.14: Ceftazidime MIC determination	67
Figure 2.15: Screening of a fragment library with the PrestoBlue persister cell assay.	70
Figure 3.1: A checkboard of persister cell culture to show positional plate effects...	85
Figure 3.2: Distributional effects of persister cells in 384 well assay plate.	86
Figure 3.3: Determining the optimum incubation time for a robust Z' value.....	87
Figure 3.4: Comparison of heat killed cells to minimal media for use as a positive control.	88
Figure 3.5: Distribution of percentage inhibition for screening batches.	90
Figure 3.6: Distribution of percentage inhibition for high throughput screening.....	91
Figure 3.7: Primary dose response assays for “Hit compounds”.....	96
Figure 4.1: Structure of 3.....	108
Figure 4.2: Concentration dependent killing from 3.....	109
Figure 4.3: Structure of 5.....	110
Figure 4.4: Concentration dependent killing from 5.....	111
Figure 4.5: Structure of 7.....	112
Figure 4.6: Concentration dependent killing from 7.....	113
Figure 4.7: Structure of 8.....	115
Figure 4.8: Concentration dependent killing from 8.....	116
Figure 4.9: Structure of chloroxine	117
Figure 4.10: Concentration dependent killing from chloroxine.....	118
Figure 4.11: Structure of 11.....	119

Figure 4.12: Concentration dependent killing from 11.....	120
Figure 4.13: Structure of 13.....	121
Figure 4.14 Concentration dependent killing from 13.....	122
Figure 4.15: Structure of 15.....	123
Figure 4.16: Concentration dependent killing from 15.....	124
Figure 4.17: Structure of 16.....	125
Figure 4.18: Concentration dependent killing from 16.....	126
Figure 4.19: Structure of 17.....	127
Figure 4.20: Concentration dependent killing from 17.....	128
Figure 4.21: Structure of 18.....	129
Figure 4.22: Concentration dependent killing from 18.....	130
Figure 4.23: Structure of 19.....	131
Figure 4.24: Concentration dependent killing from 19.....	132
Figure 4.25: Structure of 20.....	133
Figure 4.26: Concentration dependent killing from 20.....	134
Figure 4.27: Structure of 21.....	135
Figure 4.28: Concentration dependent killing from 21.....	136
Figure 4.29: Structure of 22.....	137
Figure 4.30: Concentration dependent killing from 22.....	138
Figure 4.31: Structure of 23.....	139
Figure 4.32: Concentration dependent killing from 23.....	140
Figure 4.33: Structure of 24.....	141
Figure 4.34: Concentration dependent killing from 24.....	142
Figure 4.35: A broth microdilution determination of minimum inhibitory concentration (MIC) determination for chloroxine.....	149

Figure 4.36: Confirmation of chloroxine activity in <i>B. pseudomallei</i> . Data provided by DSTL.....	151
Figure 4.37: Time dependent killing for 6 compounds with promising activity indicated from dose response assays.	153
Figure 5.1: Dose response assay for a fresh stock of hit compound 7. $pIC_{50} = 6.3$ (95% CI: 6.9 to 5.8)	164
Figure 5.2: Structure of 7.....	164
Figure 5.3: 27 from series expansion of 7.	165
Figure 5.4: Structure of 27.....	165
Figure 5.5: 28 from series expansion of 7.	166
Figure 5.6: Structure of 28.....	166
Figure 5.7: 29 from series expansion of 7.	167
Figure 5.8: Structure of 29.....	167
Figure 5.9: 30 from series expansion of 7.	168
Figure 5.10: Structure of 30.....	168
Figure 5.11: 31 from series expansion of 7.	169
Figure 5.12: Structure of 31.....	169
Figure 5.13: 32 from series expansion of 7.	170
Figure 5.14: Structure of 32.....	170
Figure 5.15: 33 from series expansion of 7.	171
Figure 5.16: Structure of 33.....	171
Figure 5.17: Dose response assay for original hit compound 23.....	177
Figure 5.18: Structure of 23.....	177
Figure 5.19: 39 from series expansion of 23.	178
Figure 5.20: Structure of 39.....	178

Figure 5.21: Dose response assay for 40 from series expansion of 23.....	179
Figure 5.22: Structure of 40.....	179
Figure 5.23: 41 from series expansion around the structure of compound 23.....	180
Figure 5.24: Structure of 41.....	180
Figure 5.25: Series expansion around hit compound 16	184
Figure 5.26: Dose response assay for a fresh stock of hit compound 16.....	185
Figure 5.27: Structure of 16.....	185
Figure 5.28: Dose response assay for 44 from series expansion of 16.....	186
Figure 5.29: Structure of 44.....	186
Figure 5.30: Dose response assay for 45 from series expansion of 16.....	187
Figure 5.31: Structure of 45.....	187
Figure 5.32: Dose response assay for 48 from series expansion of 16.....	188
Figure 5.33: Structure of 48.....	188
Figure 5.34: Dose response assay for 52 from series expansion of 16.....	189
Figure 5.35: Structure of 52.....	189
Figure 5.36: Structure of Chloroxine.....	191
Figure 5.37: Dose response assay for 55 from series expansion of chloroxine.	195
Figure 5.38: Structure of 55, also known as broxyquinoline.....	195
Figure 5.39: Dose response assay for 65 from series expansion of chloroxine	196
Figure 5.40: Structure of 65.....	196
Figure 5.41: Dose response assay for 54 from series expansion of chloroxine.	197
Figure 5.42: Structure of 54.....	197
Figure 5.43: Dose response assay for 57 from series expansion of chloroxine.	198
Figure 5.44: Structure of 57.....	198
Figure 5.45: Dose response assay for 61 from series expansion for chloroxine. ...	199

Figure 5.46: Structure of 61.....	199
Figure 5.47: Dose response assay for compound 62 from series expansion of chloroxine.....	200
Figure 5.48: Structure of 62.....	200
Figure 5.49: Dose response assay for 63 from series expansion of chloroxine.	201
Figure 5.50: Structure of 63.....	201
Figure 5.51: Dose response assay for 64 from series expansion of chloroxine.	202
Figure 5.52: Structure of 64.....	202
Figure 5.53: Compounds tiliquinol (left) and tilbroquinol (right).	207
Figure 6.1: Agarose gel of products of miniprep for Next Generation Sequencing.	217
Figure 6.2: Kegg pathway for BTH_I0185, a gene involved in ascorbate and aldarate metabolism.....	222
Figure 6.3: Kegg pathway for gene BTH_I0313 a gene included in a pathway for degradation of ketone bodies.	224

Table of Tables

Table 1.1: Target Product Profile for a drug to recurrent infection through persister cell survival in melioidosis.....	32
Table 3.1: Summary of screen outcome for diversity library.....	92
Table 4.1: Compounds identified as exhibition dose dependent inhibition of persister cells.....	107
Table 4.2: Results from activity confirmation.....	148
Table 5.1: Series expansion around hit compound 7	163
Table 5.2: Series expansion around parent 23	176
Table 6.1: Sample conditions for round one of Next Generation Sequencing	216
Table 6.2: Pathways in <i>B. thailandensis</i> identified through two rounds of next generation sequencing of persister cells from an over expression library treated with chloroxine.....	218

1. Introduction

1.1. Melioidosis

Burkholderia pseudomallei is the causative agent of melioidosis, a disease highly endemic to Southeast Asia and Northern Australia with an increasing global presence (Figure 1.1) (Wiersinga et al., 2012). Commonly characterised by pneumonia and abscesses, melioidosis is a significant cause of community acquired sepsis in endemic regions such as northeast Thailand, where it is the third most common cause of death from infectious disease after HIV/AIDS and tuberculosis (Limmathurotsakul et al., 2010a).

Melioidosis was first characterised in 1912 by the pathologist Alfred Whitmore who during a post-mortem in Rangoon identified a glanders-like disease. However, upon culturing the bacteria and studying the disease in guinea-pig model it became apparent that the bacteria was not *Burkholderia mallei* (formerly *Bacillus mallei*) but a new bacteria he named as *B. pseudomallei* (Whitmore, 1913).

Melioidosis is a serious public health concern in Southeast Asia and Australia. In Thailand, 2000 culture-confirmed cases of melioidosis are reported each year, with a fatality rate of up to 40% (Limmathurotsakul et al., 2010b). It is also prevalent in an increasing number of tropical developing countries as an emerging infectious disease. It is recognised as a serious public health concern in Malaysia, Singapore, Vietnam, Cambodia and Laos with recent reports that the endemic zone has expanded to include the Indian subcontinent, southern China, Hong Kong, Taiwan, various Pacific and Indian Ocean islands (Figure 1.1) (Wiersinga et al., 2012).

A further concern is that due to limitations in diagnosis of melioidosis (Hoffmaster et al., 2015) the global distribution of *B. pseudomallei* is still unknown. Furthermore, a recent study into the ability of *B. pseudomallei* to become established in soils through importation by infected human and animals, has predicted that the bacteria is likely to be ubiquitous throughout many tropical regions (Limmathurotsakul et al., 2016). This study has been seen as a turning point in recognition of melioidosis as a disease of global concern estimating that 89,000 people will die globally in 2015 with > 99 % of all deaths occurring in low and middle income countries. The study also identified geographical environments in Japan and southern parts of Louisiana and Texas in the US, where *B. pseudomallei* may establish if introduced. Given a recent, unintentional release at the Tulane National Primate Research Centre, this is not as unlikely as one may predict (Prevention, 2015).

Melioidosis exhibits a wide range of clinical presentations and pathogenesis varying from rapidly fatal septicaemia to the formation of abscesses and chronic infection (Wiersinga et al., 2012). Asymptomatic exposure can also occur resulting in seroconversion (Inglis et al., 2006) and the disease can lie dormant for years before symptoms manifest (Currie et al., 2000b, White, 2003).

B. pseudomallei also has a unique potential to be used as a bioterrorism agent (Gilad et al., 2007). Features that contribute to the potential of *B. pseudomallei* to be used as a bioterrorism agent include its ability to infect through inhalation, ingestion and percutaneous inoculation at low infective doses. The bacteria is also incredibly easy to selectively culture from soil samples using Ashdown's media. Additionally, there is no available vaccine, diagnosis is difficult unless melioidosis is suspected, it is difficult to stockpile appropriate antibiotics, and large scale treatment would overwhelm medical facilities.

One redeeming feature of *B. pseudomallei*'s categorisation as a Tier one select agent by the CDC (Butler, 2012), is that new streams of funding for research into the disease, treatments and vaccines have opened up than would usually be available to a neglected tropical disease.

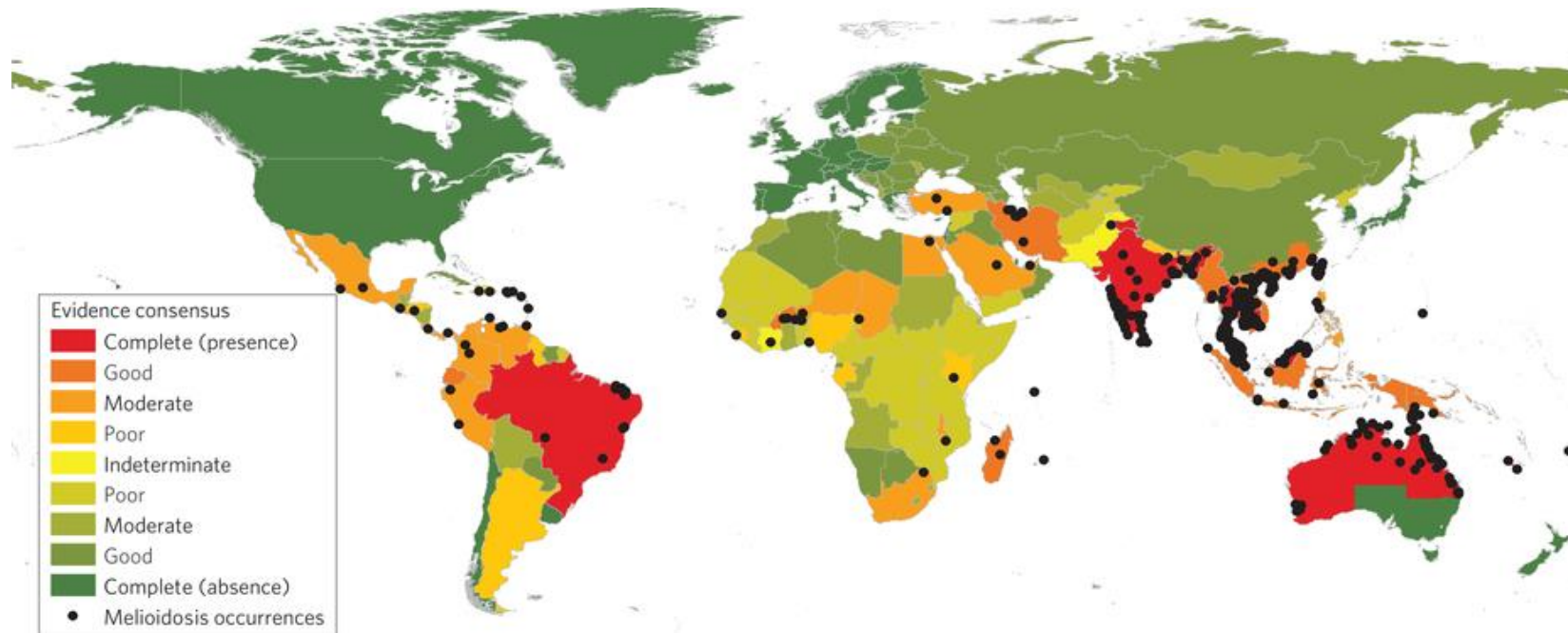


Figure 1.1: Predicted Global Distribution of Melioidosis and locations of occurrence.

Country colouring is based on evidence-based consensus, with green representing a complete consensus on absence of *B. pseudomallei* and red a complete consensus on presence of *B. pseudomallei*. Black dots represent geo-located records of melioidosis cases or presence of *B. pseudomallei*. Reproduced with permission from Limmathurotsakul D et al. *NMicrobiol* 2016;15008.

Transmission and routes of infection

Infection with melioidosis primarily occurs by subcutaneous inoculation, often through exposure of an open wound to soil or water (White, 2003). A demographic of people at greater risk of infection includes farmers who work in rice paddy fields in endemic areas where the saprophyte resides in soil and water. The disease can also be contracted through ingestion of contaminated food or water. Inoculation through inhalation is also a significant concern. This is most common during rainy season, severe weather events or through deliberate release.

Clinical manifestations of melioidosis can vary enormously making early diagnosis a challenge. Once referred to as the “mimicker of maladies”, melioidosis can be mistaken for a number of other diseases such as cancer, *Pseudomonas* infection or tuberculosis without appropriate diagnosis (John, 2004). Figure 1.2 shows clinical events after infection with *B. pseudomallei* leading to the most common clinical manifestations. The primary presentation in over half of patients is pneumonia with other presentations include genitourinary infection, skin infections, bacteraemia, arthritis and osteomyelitis (Currie et al., 2010). It is also common for abscesses to form in internal organs and for presentations to differ based on the geographical location of the patient.

Risk Factors

Fatal outcomes of melioidosis in healthy persons are very rare so long as the infection is diagnosed early and appropriate treatment is administered. Risk factors can significantly increase mortality rates in patients with acute melioidosis (Cheng et al., 2004, Limmathurotsakul et al., 2010a). This includes diabetes mellitus, excess alcohol consumption (Rode and Webling, 1981), chronic renal failure, and chronic lung

disease (Peacock et al., 2008, Currie et al., 2004). Up to 80% of affected adults have underlying diseases which predispose them to melioidosis (Currie et al., 2000b, Currie et al., 2004, Suputtamongkol et al., 1999). Diabetes is a predominant risk factor in melioidosis with 37% of mortalities recorded in a prospective study of melioidosis in northern Australia having the condition (Currie et al., 2000b). This risk factor is of increasing concern in the treatment of melioidosis as diabetes is a growing global health problem. The greatest increase is seen in economically developing countries such as Thailand, with a projected 300 million sufferers worldwide by 2020 (Aekplakorn et al., 2011, King et al., 1998). Additionally, there is a growing public health concern that the rise in alcohol abuse may be a compounding factor in the severity of melioidosis incidences (Ogeil et al., 2015).

Environmental risk factors which have been shown to increase rates of melioidosis have been described. These include heavy rainfall, intensive agricultural work and also inhalation of airborne dust (Currie et al., 2004). Weather events such as are a significant contribution factor to cases of melioidosis with the 20 year Darwin study reporting 81 % of incidents occurring during monsoon season (Currie et al., 2010).

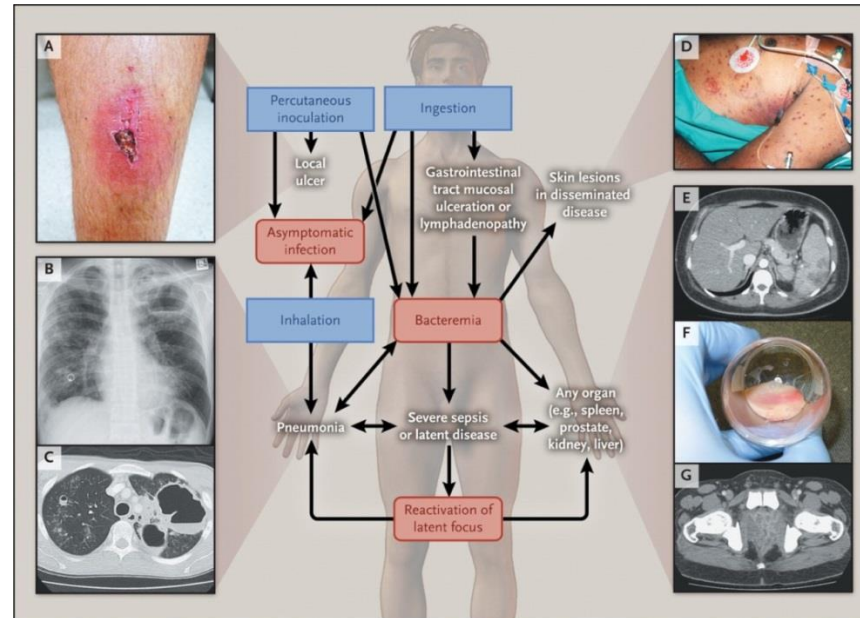


Figure 1.2: Clinical events after infection with *B. pseudomallei*.

Shown are the routes of infection, the natural history of infection, and the diverse disease manifestations (white text). Panel A: cutaneous melioidosis in a healthy host. B: lung abscesses on the chest radiograph of a patient with acute melioidosis pneumonia, and C: the corresponding CT scan. D: the skin manifestations in a fatal case of disseminated melioidosis. E: splenic abscesses on an abdominal CT scan. F: aspirated pus in a patient abscesses, and G: the abscesses on a CT scan from the patient. Reproduced with permission from Wiersinga WJ et al. N Engl J Med 2012;367:1035-1044, Copyright Massachusetts Medical Society.

Diagnosis and under-reporting

Early diagnosis of melioidosis is proven to be critical in attaining a non-fatal outcome. This is because the frontline antibiotic for melioidosis (ceftazidime) is not an agent of choice for empirical antibiotic regimes for suspected bacterial sepsis. In contrast, in endemic areas, agents with activity against *B. pseudomallei* are recommended for patients with community acquired pneumonia and melioidosis risk factors.

Clinical diagnosis is difficult as melioidosis has no pathognomonic clinical manifestations. The gold standard diagnosis method is through culture. However, despite being easy to grow on agar and having characteristic universal resistance to gentamicin and colistin, it is difficult to make a positive identification of *B. pseudomallei* if the laboratory does not suspect melioidosis (Hoffmaster et al., 2015). This is because Ashdown's medium is required to isolate the bacteria from non-sterile samples. False diagnoses are a particular problem when the patient's symptoms or history do not imply melioidosis.

The "gold standard" test for diagnosis of melioidosis is isolation through culture from samples of blood, urine, pus or sputum. This method takes from three to seven days and incidences of misidentification can occur. *B. pseudomallei* can be identified by DNA amplification with PCR. However, this assay can be less sensitive, especially in blood samples (Merritt et al., 2006). Recent attempts to introduce simple and rapid diagnostic tests have led to the development of lateral flow antigen detection assays which are promising alternatives, especially in laboratories with less frequent exposure to melioidosis (Houghton et al., 2014). This is particularly vital as early diagnosis and treatment with appropriate antibiotics has been attributed to significant improvements in falling mortality rates (Currie et al., 2010).

Treatment and antibiotic resistance

Treatment of melioidosis is drawn out and requires extensive periods of hospital admission. International guidelines recommend initial treatment consisting of 10 to 14 day intravenous administration of ceftazidime or meropenam (Dance, 2014b). However, a recent study has found that increased duration of intensive phase treatment to 26 days leads to an almost total reduction in cases of relapse (one patient in a study of 215 relapsed) (Pitman et al., 2015). Intensive phase treatment is followed by oral eradication therapy with co-amoxiclav or a combination of chloramphenicol, doxycycline and co-trimoxazole lasting between 3 and 6 months (Wiersinga et al., 2012). Patients with access to adequate diagnosis and treatment facilities have seen reduced mortality rates due to developments in treatment with a 50 % reduction in mortality following the introduction of ceftazidime in 1986 (Dance, 2014a, Pitman et al., 2015). The cost of this treatment regime is high and the burden of disease in developing countries such as Cambodia prevents those in need from being treated (Rammaert et al., 2011, Vlieghe et al., 2011).

B. pseudomallei is inherently resistant to many frontline antibiotics including; penicillin, ampicillin, first-generation and second-generation cephalosporins, gentamicin, tobramycin, streptomycin and polymyxin (Wiersinga et al., 2012). Recently, a mutation in *penA* has resulted in resistance development to ceftazidime through modifications to a β -lactamase enzyme which is a concern for the treatment of acute melioidosis should a patient become infected with a resistant strain (Chantratita et al., 2011, Sarovich et al., 2012). However, there is no evidence for human to human transmission of melioidosis which means that ceftazidime resistance is, for now, less of a priority.

Ceftazidime

Ceftazidime is a semisynthetic injectable third-generation cephalosporin active against Gram-negative bacilli including *B. pseudomallei* and *B. thailandensis* (Figure 1.3).

Ceftazidime is a β -lactam agent with bactericidal effects on growing cultures of Gram-positive and Gram-negative bacteria. Synthesis of bacterial cell walls is inhibited through high-affinity binding of ceftazidime to penicillin-binding protein (PBP), an essential protein to cell division, and subsequent inhibition of peptidoglycan cross-linking (Hayes and Orr, 1983, Choi and Koh, 2012, Rains et al., 1995, Richards and Brogden, 1985). This lethal disruption to cell division leads to formation of spheroplasts and ultimately cell lysis.

The β -lactam class of antibiotics are 'time-dependent' antimicrobial agents; as such the bacterial killing observed is proportional to the duration of time that the concentration of the drug is above the MIC in serum and tissue. (Hyatt et al., 1995) The pharmacokinetic / pharmacodynamics profile of ceftazidime could explain improved treatment outcomes with increased duration of intravenous phase treatment (Pitman et al., 2015).

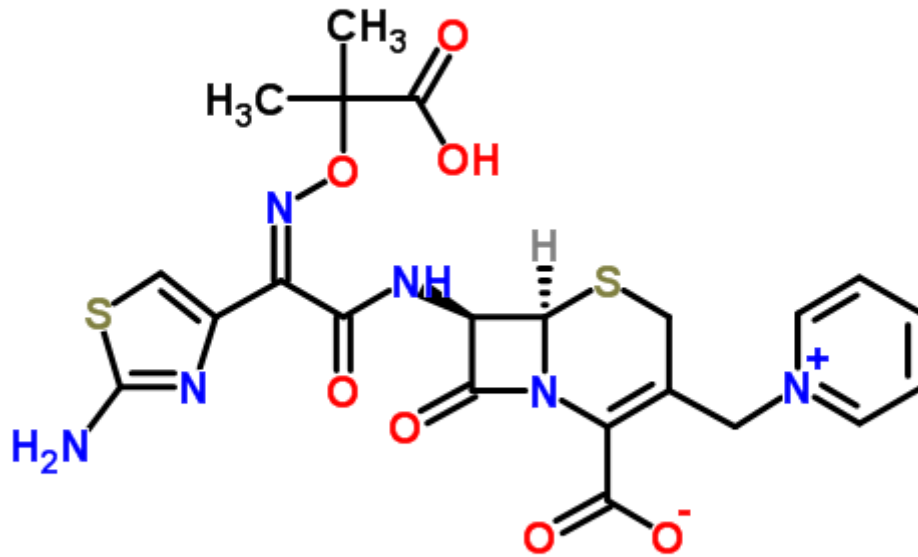


Figure 1.3: The structure of ceftazidime, a third generation cephalosporin used in frontline treatment for melioidosis.

Treatment shortcomings and vaccine development

The cost of prolonged intravenous antibiotic treatment is high (Dance, 2014b) and the burden of disease in developing countries can prevent those in need from being treated adequately (Nhem et al., 2014). As an example, in Cambodia where incidents of melioidosis are becoming increasingly prevalent (Rammaert et al., 2011, Pagnarith et al., 2010), one study experienced a 52% fatality rate due to inappropriate antibiotic treatment (Vlieghe et al., 2011). These pressures present an urgent unmet need for improved diagnostic technologies and affordable drugs to reduce the cost and duration of treatment and to prevent relapse of infection (Lipsitz et al., 2012, Sarovich et al., 2014).

There is currently no vaccination able to give sterilising immunity to melioidosis. Whilst research into vaccine development around capsular polysaccharide (CPS), lipopolysaccharide (LPS) and outer membrane vesicle has been shown to confer some protection in murine models, there is no clinically available option (Ngugi et al., 2010, Sarkar-Tyson et al., 2007, Sarkar-Tyson et al., 2009, Nieves et al., 2014).

Recurrent melioidosis

A significant problem in treating melioidosis is the propensity for relapse of disease which can occur months or years after treatment of the initial infection. Whilst the top priority in treating acute melioidosis is to prevent a fatal outcome, a subsequent task is to address recurrent infection in patients following successful antibiotic treatment.

Relapse is defined as a new presentation of acute culture confirmed melioidosis, with a repeat infection occurring after resolution of an initial infection of over two weeks treatment with intravenous antibiotics (Currie et al., 2000a). The majority of relapse

infections have been shown to have been caused by an identical strain to the initial infection indicating that *B. pseudomallei* is able to persist in the body in a non-disease causing state for long periods of time (Currie et al., 2000a, Maharjan et al., 2005, Vadivelu et al., 1998). This was described by use of multi-locus sequence typing (MLST) to determine whether re-presentation of infection was relapse or a reinfection. MLST is a technique, which uses sequencing of seven housekeeping gene fragments to unambiguously characterise isolates of bacterial species. Point mutations within the housekeeping genes are used to differentiate allelic profiles. Studies showed that of the total cases of melioidosis between 3 and 9.7% presented with relapse of infection (Chaowagul et al., 1993, Haraga et al., 2008a, Currie et al., 2000a). Incidences of recurrence are reducing. Prior to September 2003, the Darwin Prospective Melioidosis Study in Northern Australia recorded a reduction from 6.4% to only 1.2% (Sarovich et al., 2014). This reduction was attributed to the introduction of extended periods of intravenous therapy with ceftazidime (Sarovich et al., 2014). Direct causes of relapse are unproven. However, patients who have not completed their antibiotic regime and individuals who are immunocompromised are at greater risk of relapse (Chaowagul et al., 1993, Limmathurotsakul et al., 2006). Relapse cases are also far more likely in patients with systemic melioidosis infections than in cases of localised disease. A likely cause of this is that symptoms of infection may be treated without entirely eradicating reservoirs of infection (Chaowagul et al., 1993).

Burkholderia pseudomallei* and *Burkholderia thailandensis

B. pseudomallei is a Gram-negative, oxidase positive, β -proteobacterium. Its 7.2 Mb genome consists of two chromosomes of 4.1 Mb and 3.2 Mb (Holden et al., 2004) which encode different genes for core functions, cellular processes and for host pathogenicity and virulence (Holden et al., 2004). There is evolutionary evidence for

acquired antibiotic resistance which includes efflux pumps, enzymatic inactivation, bacterial-cell-membrane impermeability, alterations to antibiotic target site, and amino acid changes in *penA*, a gene which encodes for a highly conserved class A β -lactamase (Cheng et al., 2008, Wuthiekanun et al., 2011). *B. pseudomallei* is an intracellular pathogen able to survive phagocytosis and dwell within macrophages, epithelial cells, polymorphonuclear and mononuclear leukocytes and alveolar macrophages (Pruksachartvuthi et al., 1990, Jones et al., 1996, Ahmed et al., 1999). *B. pseudomallei*'s ability to persist in macrophages is hypothesised to cause late onset septicemic infections after long disease free periods of up to 62 years post exposure (Jones et al., 1996, Sanford and Moore, 1971, Inglis et al., 2001, Ngauy et al., 2005). It is known that bacterial persisters also colonise the gastric tract (Huddleston, 2014). As the gastric environment is devoid of immune factors this is a further way in which reservoirs of infection are able to persist and evade immune clearance (Lewis, 2001). Further hypotheses are that the bacteria are able to evade clearance by the host immune system by formation of biofilms and the presence of glycocalyx structures which form enclosed microcolonies with large amounts of fibrous material inhibiting effective phagocytosis and contributing to the chronic persistent infections observed in melioidosis (Vorachit et al., 1995).

B. pseudomallei is a close evolutionary relative of *B. mallei*, the causative agent of glanders disease, and *B. thailandensis*, which is mostly avirulent in immunocompetent humans (Haraga et al., 2008b, Brett et al., 1998, Brett et al., 1997). MLST analysis of the three species genomes shows a high degree of genetic similarity and evolutionary lineage (Godoy et al., 2003).

First phylogenetically distinguished from *B. pseudomallei* in 1998, (Brett et al., 1998) *B. thailandensis* shows over 85% gene conservation with *B. pseudomallei* and exhibits

similar biochemical and genetic properties (Yu et al., 2006). However, *B. thailandensis* differs from the virulent *B. pseudomallei* in colony morphology, the ability to assimilate arabinose and the absence of capsular polysaccharide. *B. thailandensis* is nevertheless a useful surrogate (Reckseidler et al., 2001, Smith et al., 1996, Majerczyk et al., 2014). This is particularly so as work with *B. thailandensis* does not require containment level III laboratory conditions, enabling a wider range and greater expedience of experiments. *B. pseudomallei* is currently classed by the US Centers for Disease Control (CDC) as a Tier 1 select agent which adds additional difficulties to working with the bacterium (Centers for Disease et al., 2012).

B. thailandensis is generally avirulent in humans with two exceptional cases of infection in the USA where acquisition of a CPS virulence cluster is predicted to have enabled infection of humans (Glass et al., 2006, Sim et al., 2010). The CPS virulence cluster encodes an extracellular polysaccharide capsule, which contributes to protection from the host immune system through resistance to phagocytosis via reducing Complement Factor C3b deposition on the bacteria surface (Reckseidler-Zenteno et al., 2005). There is also evidence to show that carbohydrates such as the CPS, which are T cell-independent type 2 antigens, induce a poor immunological memory and do not provoke a strong isotype-switching response, which gives additional protection to the bacteria from host immune responses (Weintraub, 2003).

1.2. Persister Cells

Persister cells were first identified in 1944 by Joseph Bigger. An army physician, Bigger observed that the newly available antibiotic penicillin (Fleming, 1946) failed to completely sterilise staphylococcal infections in wounds resulting in recurrent infections. This led Bigger to postulate the presence of insusceptible “persisters”

(Bigger, 1944). Persister cells are tolerant to supralethal concentrations of antibiotics and in chronic infections can protect bacterial populations from clearance by the host's immune system (Keren et al., 2004a). Transient inhibition of antimicrobial targets, minimal metabolic activity and slow or non-existent growth (Balaban et al., 2004) have been postulated as causes of the observed tolerance to super lethal concentrations of multiple antibiotics (Wood et al., 2013).

Persister cells are phenotypic variants recognisably different to resistant mutants as persister populations do not multiply in the presence of the antibiotic. Once treatment is withdrawn growth resumes and, unlike resistant mutants, the recrudescence organism is equally as sensitive to the drug as the naïve population (Figure 1.4) (Lewis, 2007).

Persister cells have been identified in numerous bacterial species, including the prominent pathogens *Mycobacterium tuberculosis*, *Salmonella enterica*, *Chlamydia trachomatis*, *Brucella melitensis*, *Borrelia burgdorferi*, *Pseudomonas aeruginosa*, pathogenic *Escherichia coli*, *Staphylococcus aureus* and *Streptococcus pyogenes* (Monack et al., 2004, Palmer et al., 2009). It is recognised that the clinical burden of microbial persistence is increasing (Cohen et al., 2013) with persister cells shown to play an integral role in chronic infections (Fauvart et al., 2011) especially in tuberculosis (McCune and Tompsett, 1956) and cystic fibrosis patients (McCune and Tompsett, 1956, Mulcahy et al., 2010a).

Once antibiotic treatment is ceased, persister cell resuscitation can lead to repopulation of the infection, often through the presence of biofilms. These are bacterial communities that settle and establish on surfaces covered by an exopolymer matrix (Lewis, 2010, Conlon et al., 2015, Lewis, 2008b, Dorr et al., 2009). The CDC

calculate that 65% of all infections in developed countries are caused by biofilms (Hall-Stoodley et al., 2004).

Persister cells in biofilms

The discovery of persister cells in biofilms (Brooun et al., 2000, Spoering and Lewis, 2001) has marked this phenomenon as a potential target for new treatments of recalcitrant infections. It has also been suggested that persister cells could enhance the development of inherited genetic resistance (Cohen et al., 2013) by acting as a reservoir of actively and adaptively evolving organisms that when treated with antibiotics induce a selective preference for mutants that produce increased persister numbers in chronic diseases (Mulcahy et al., 2010a, Cohen et al., 2013).

Persister cell numbers are highly enriched in biofilms which are complex, surface associated communities of microbes protected by a polymeric matrix (Roberts and Stewart, 2005) (Lewis, 2001). Biofilms can provide protection to cells from clearance by host immune mechanisms and antibiotics. They can also lead to limited nutrient availability. Under these conditions entering a metabolically dormant state is advantageous to microbes. Multi drug tolerant (MDT) persister cells can confer benefits to the whole cell population through their ability to survive (Lewis, 2008a, Lewis, 2010).

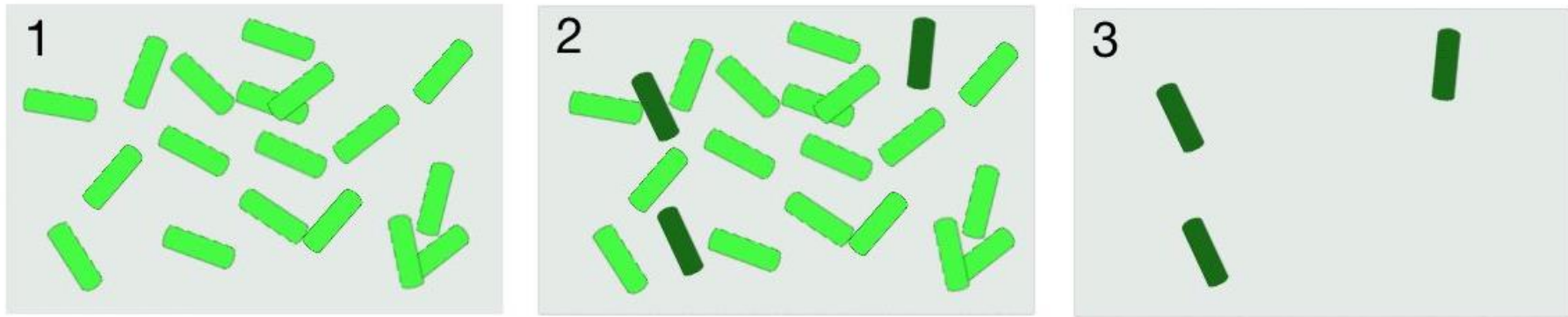


Figure 1.4: The cycle of persister cells.

Panel 1 (left) shows an antibiotic sensitive population of bacterial cells. Phenotypic variants form at low frequency reaching a maximum number at stationary growth phase in panel 2 (centre). After antibiotic treatment with ceftazidime 99% of cells are killed leaving only the persistent fraction as shown in panel 3 (right). These cells are tolerant to the antibiotic and, upon removal of ceftazidime and resuspension in fresh media will resume growth and return to the original state in panel 1.

Persister cells in melioidosis.

The role that persister cells play in *B. pseudomallei* infections is not fully understood. However, persister cells account for approximately 0.1 % of cells in *B. pseudomallei* cultures in vitro, which is significantly higher than observed for other species (Hemsley et al., 2014, Lewis, 2007). It is hypothesised that this reservoir of infection is responsible for the recurrent infections observed and need for such a protracted duration of therapy as previously described (Fauvart et al., 2011). Although not clinically proven, initial in vitro studies into persister cells in *B. thailandensis* are concurrent with other persister producing species. A time dependent killing assay treatment with 100 X MIC of the antibiotics ceftazidime and ciprofloxacin results in a biphasic killing pattern (Figure 1.5) (Hemsley et al., 2014). During the initial phase of antibiotic exposure susceptible cells are killed rapidly. This is followed by a secondary phase where the rate of cell death is significantly reduced. After 48 hours treatment a surviving fraction of approximately 0.1 % viable cells remains.

It has been shown that persister cells form stochastically in populations prior to antibiotic treatment (Balaban et al., 2004). This would imply that persister formation provides a level of evolutionary or survival benefit to the bacteria. Bacterial populations are at their most susceptible during growth and so entering a persistent state can provide an advantage in evading host recognition. However, as *B. pseudomallei* is a non-obligate pathogen, evolution has occurred in the environment rather than within a host. As *Burkholderia sp.* produce high levels of persister cells, this suggests that this transient state provides a survival advantage to environmental stresses such as nutrient deficiency, desiccation and attack from other microorganisms (Balaban et al., 2004, Dhar and McKinney, 2007).

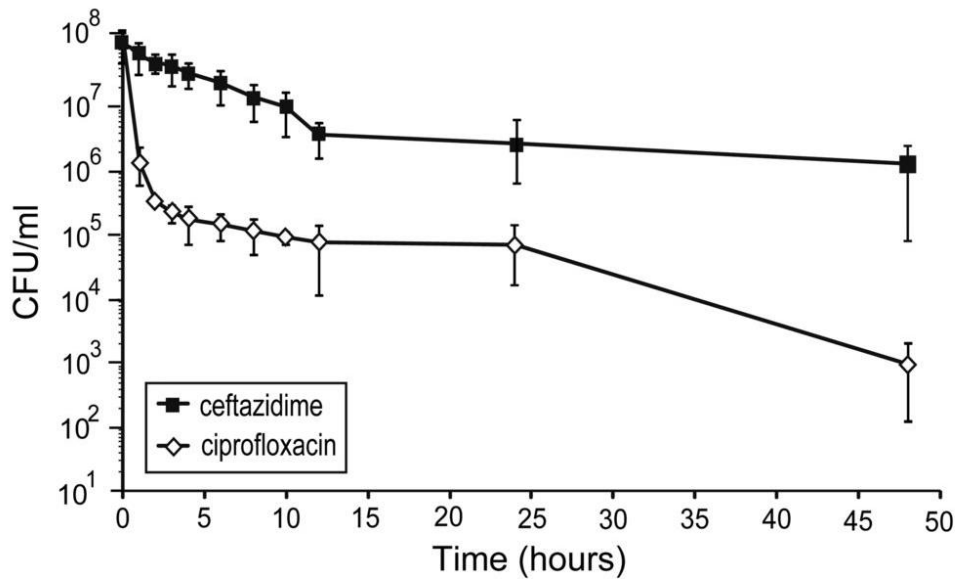


Figure 1.5: Survival frequency of *Burkholderia thailandensis* treated with ceftazidime and ciprofloxacin.

Aliquots of bacteria were incubated in the presence of 100× the MIC of ceftazidime hydrate or ciprofloxacin. The surviving proportion was enumerated at the indicated time points and is plotted on a logarithmic scale over time. Survival frequency was assessed following 48 h incubation of serial dilutions on non-selective media and is defined as the number of cells that survived the antibiotic treatment. The error bars represent the standard deviation (Crocker et al.) over the mean from three independent experiments. Reproduced with permission from Hemsley et al. (2014).

Dormancy

Persister cells are often termed “transiently dormant” due to their non-growing state. Time-lapse fluorescence microscopy has been used to visualise growth inhibited cells from high persister mutants which are able to survive prolonged antibiotic treatment and resume growth on cessation of treatment. This demonstrates that persister cells can originate from non-growing cells (Balaban et al., 2004). However, it has not been definitively proven that that growth inhibition and metabolic dormancy are required for persister cell formation or antibiotic tolerance (Orman and Brynildsen, 2013). Further to this, it is more probable, as suggested by recent studies, that bacterial populations may harbour a diverse collection of heterogeneous persisters with multiple pathways inducing the persistent state (Allison et al., 2011a). Further weight is added to this argument by transcriptomic profiling of persister cells in *Burkholderia* which suggests that multi drug tolerance (MDT) can be attributed to up regulation of anaerobic nitrate respiration, efflux pumps, β -lactamases, and stress response proteins (Hemsley et al., 2014). Anaerobic nitrate respiration is of importance in species of bacteria, such as *B. pseudomallei*, which form anoxic granulomas. In these circumstances nitrate acts as a terminal electron acceptor in the absence of oxygen (Cole, 1996).

Initiation of persistence

Persister cell formation is thought to be a stochastic process within an isogenic population with the persistent fraction in bacterial populations increasing rapidly during mid-exponential phase in most species (Lewis, 2007).

Triggers of the persistent state have not been fully characterised. However, initiation of persistence by environmental conditions has been shown, such as is seen under active starvation (Nguyen et al., 2011). Nguyen et. al showed that whilst a common

hypothesis of persistence attributes growth arrest as a central pathway to multidrug tolerance through inactivity of key antimicrobial targets, this is not sufficient as a sole mechanism. Using *Pseudomonas aeruginosa*, a bacteria which causes acute and chronic infections, as a model organism Nguyen et al. investigated active starvation responses with a particular focus on the stringent response. The stringent response is a stress response in bacterial to amino acid starvation. The response is initiated through accumulation of the effector nucleotides ppGpp and pppGpp, levels of which are controlled by the enzymes RelA and SpoT (Figure 1.6). RelA synthesises ppGpp in response to uncharged tRNA which stalls the active site in the ribosome as a consequence of amino acid starvation. SpoT is a hydrolyse enzyme which catalyses the degradation of ppGpp but also has weak synthase activities. Nguyen et al. inactivated *relA* and *spoT* through mutation, eliminating signal transduction through production of the 'alarmone' (Caglic et al.)ppGpp. Using this model it was shown that whilst serine-starvation in wild-type bacteria supported tolerance to antimicrobial killing, the *relA spoT* mutant showed significantly less killing despite both strains showing arrested cell growth.

The role of the alarmone ppGpp in persistence has been further described in (Caglic et al.) (Maisonneuve et al., 2013). This study further investigated the signal cascade that causes stochastic switching of subpopulations into slow growth and persistence in response to environmental factors. Maisonneuve and Gerdes build upon previous literature on molecular regulation of persistence showing that overproduction of PolyP or (p)ppGpp leads to dramatic overproduction of persister cells. Furthermore a hierarchically structured pathway has been established for the regulation of persistence by (p)ppGpp. As in Figure 1.6, (p)ppGpp produced by RelA inhibits exopolyphosphate (PPX), which is a cellular enzyme that degrades PolyP. Shyp et al.,

have already established that (p)ppGpp forms a positive feedback loop with RelA instigating a fast amplification of small signals (Shyp et al., 2012). This contributes to Maisoneuve and Gerdes hypothesis that (p)ppGpp controls stochastic induction of persistence as small fluctuation in the cell may have significantly amplified effects of transcription. Further down the pathway from (p)ppGpp, transcription of TA operons is regulated by conditional cooperativity (Afif et al., 2001). This is so named as the toxin may act as a corepressor and depressor of the cognate TA operon depending on relative concentration of antitoxin. During persister cell formation there is a high level of (p)ppGpp. This creates free toxin as antitoxin present is rapidly degraded by the Lon / PolyP complex present as a consequence of (p)ppGpp. This results in toxin binding to the TA promoter and transcription of the operon causing slow cell growth and multidrug tolerance.

Specific genes that may contribute towards the persistent state have also been identified whereby persistent cells display increased expression of toxin – antitoxin (TA) modules (Keren et al., 2004c, Shah et al., 2006). For example, the *hipAB* TA module (Yamaguchi and Inouye, 2011a, Moyed and Bertrand, 1983, Rotem et al., 2010, Germain et al., 2013a, Kaspy et al., 2013a) encodes HipA, a serine-protein kinase (Schumacher et al., 2009, Schumacher et al., 2012, Correia et al., 2006). This induces dormancy through phosphorylation of glutamyl-transfer RNA synthase (Germain et al., 2013b, Kaspy et al., 2013b). HipB, a DNA-binding protein, forms a complex with HipA and promoter DNA in non-persistent states, thus inactivating HipA. An example of TA regulated persistence is explained in Figure 1.6. This example of a toxin-antitoxin module is the most deeply studied persister inducing mechanism and has very recently been identified as a basis of heritability in multi drug tolerance (MDT) (Yamaguchi and Inouye, 2011b, Balaban, 2011, Schumacher et al., 2015).

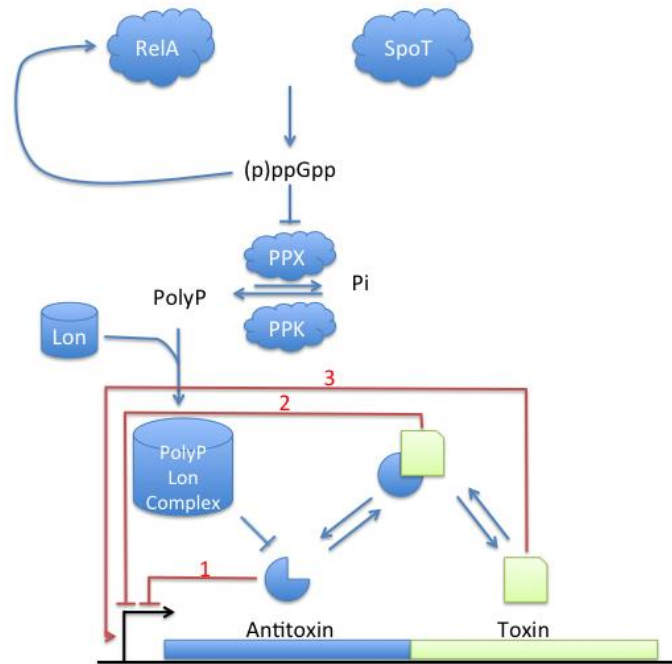


Figure 1.6: A regulatory mechanism of persistence through (p)ppGpp mediated toxin antitoxin transcriptional regulation. RelA and SpoT are enzymes which synthesis (p)ppGpp. (p)ppGpp inhibits PPX, which is a cellular enzyme that degrades PolyP. PolyP forms a complex with Lon in *E. coli* to degrade antitoxin thus allowing inhibition of translation and cell growth via the toxin. Red arrows 1 and 2 show that when $[antitoxin] > [toxin]$ the TA complex binds tightly to the TA promoter and strongly represses the operon. In contrast, red arrow 3 shows that when $[antitoxin] < [toxin]$ the toxin destabilises the TA bound promoter and induces transcription of the operon. In the case of persister cells and high (p)ppGpp levels the antitoxin is rapidly degraded by Lon and PolyP resulting in high levels of unbound toxin and transcription of persister genes and cell growth arrest (Cataudella et. Al., 2012).

A number of other persister related genes have also been identified such as *rmf*, a stationary state inhibitor of translation (Yoshida et al., 2002) and the septation inhibitor *sulA* (Walker and Levine, 1996). In *B. pseudomallei*, a very closely related organism

to *B. thailandensis*, overexpression of the toxin HicA (Figure 1.7) causes growth arrest and an increased persister fraction within the population with a differential response to different classes of antibiotic with modulation of HicA expression. It has been shown that HicA toxin induces cleavage of mRNA and tmRNA preventing translation in persister cells (Butt et al., 2014b, Jorgensen et al., 2009).

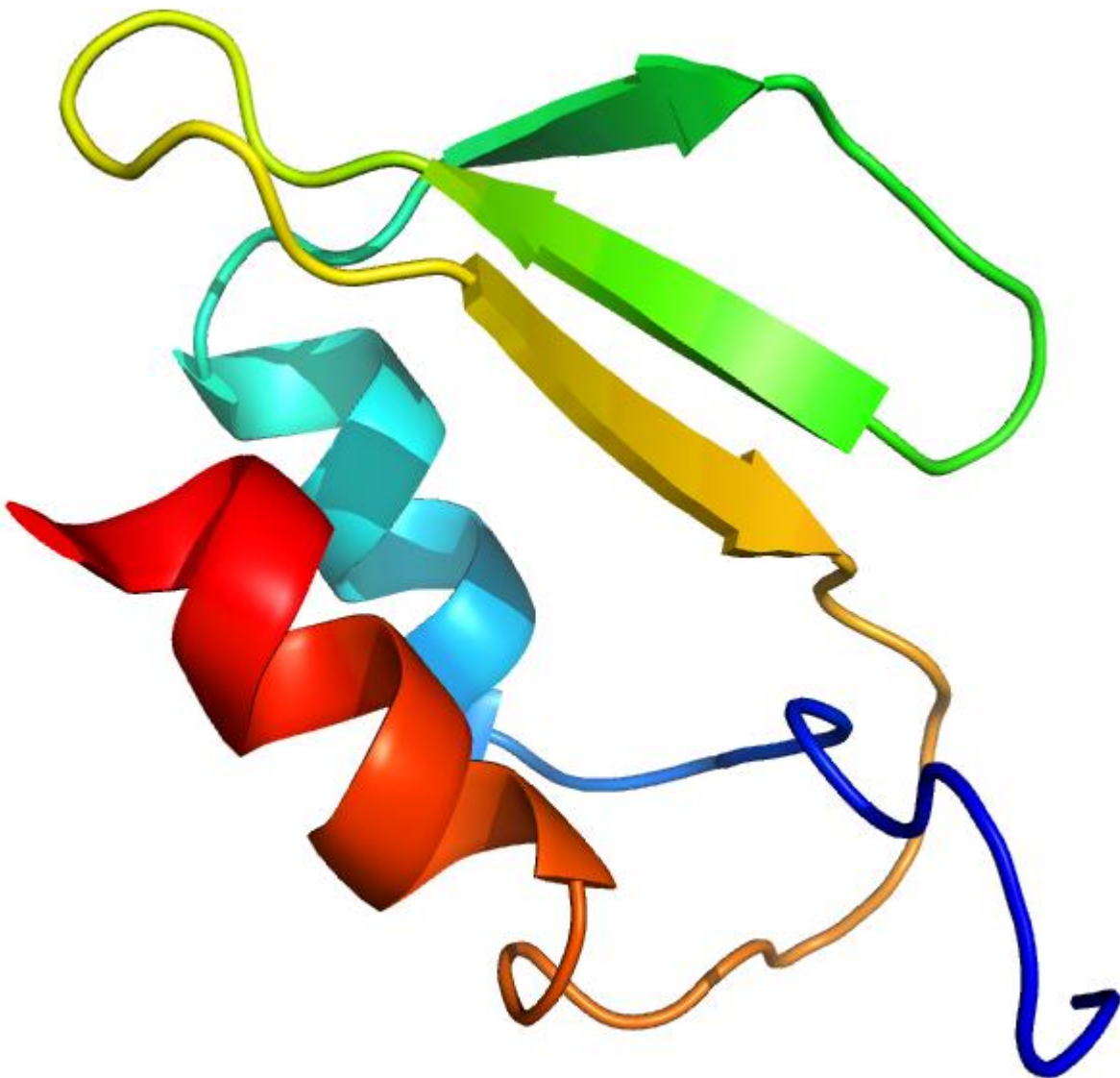


Figure 1.7: Structure of HicA protein, shown in the cartoon format, coloured blue to red from the N-terminus to the C-terminus. Reproduced with permission from N. Harmer (Butt et al., 2014a).

Study of persister cells

Persister cells have, up to recently, been overlooked as targets for antimicrobial drug therapy. This may have been due to an inherent experimental difficulty in working with persister cells. In addition, medical science has benefited from an era of effective antibiotic treatment. However, as antibiotic resistance continues to develop against even the last line of antibiotic defence (Bathorn et al., 2016) there is an urgent need to diversify away from traditional, “silver bullet” approaches and searching for broad spectrum antibiotics. A proposed strategy is to look to persister cells as potential targets of new therapies (Helaine and Kugelberg, 2014, Allison et al., 2011b, Balaban et al., 2013, Conlon et al., 2013, Maisonneuve et al., 2013, Nguyen et al., 2011).

The majority of microbiological studies focus on culturable bacteria. The persistent fraction in most bacteria is less than 0.01% which presents difficulties in developing methods to reliably screen for new targets for drug discovery. To this point *Burkholderia* is an especially suitable species for studying persister cells due to the exceptionally high surviving fraction observed.

It is becoming clear that use of ceftazidime against persister cells may not be an appropriate use. An observation that there is an inverse relationship between ceftazidime killing and atmospheric oxygen levels leads to that conclusion that under anaerobic conditions, ceftazidime’s activity is severely reduced. This may be explained by transcriptome analysis of persister cells which showed a reduced level of expression for cell division and replication genes which in turn reduces the available target of ceftazidime activity (Hemsley et al., 2014). It is known that ceftazidime is rarely active against anaerobic microbes, in which case if persister cells are formed or

survive in oxygen limited environments, ceftazidime will not be successful in resolving these reservoirs of infection (Richards and Brogden, 1985).

As persisters form such a small proportion of a population, methods to isolate persister cells have been developed. One approach is by antibiotic sedimentation of susceptible cells (Keren et al., 2004b). This allows population level studies of persister cells. However, this may miss single cell events and does not allow for the study of heterogeneity in persister populations. It is also possible to use high persistence (Okiror et al.) mutants with an increased proportion of persister cells (Moyed and Bertrand, 1983, Wolfson et al., 1990) or fluorescently marked cells. This latter approach has been made possible through the use of microfluidics (Unger et al., 2000, McDonald et al., 2000, Balaban et al., 2004), microscopy, and flow cytometry (Helaine and Holden, 2013).

Current thoughts in eradication of Persister cells

Mathematical models for existing antibiotic treatments have been used to design periodic dosing regimens or “pulse dosing” whereby persisters are allowed to resuscitate after antibiotic treatment before being treated again with antibiotic whilst in a susceptible state (De Leenheer and Cogan, 2009, Cogan et al., 2013, Sharma et al., 2015). Increased duration of antibiotic treatment has also been considered in cases of *M. tuberculosis* and *P. aeruginosa*. However, this is a contentious point as prolonged exposure could select for *hip* mutants which produced more persister cells (Keren et al., 2012).

Several strategies have been proposed for clearance of the antibiotic tolerant fraction. These include targeting TA modules to initiate exit of persistent state (enabling the antibiotic to be fully effective) or alternatively inhibiting an essential persister protein

(Lewis, 2007). An example of this includes the mutation in the essential *Escherichia coli* gene encoding PlsB. PlsB was identified through antibiotic tolerance selection for a genomic over-expression library (Rottig A et al., 2015). PlsB is a sn-glycerol-3-phosphate acyltransferase shown to be essential and conserved in persister cells (Spoering et al., 2006) although the exact mechanism in persistence is still to be determined. What is known is that PlsB plays a key role in coordinating fatty acid and phospholipid synthesis (Parsons et al., 2013) and that by inactivating PlsB through mutation a 2–3 log drop in the frequency of persister formation is observed (Nystrom, 2003).

A further application of activation and corruption of a target came from the Kim Lewis's lab at Northeastern University in 2013 which identified ADEP4, an acyldepsipeptide antibiotic which activates ClpP to become a non-specific protease, degrading over 400 proteins and resulting in cell death. A combination of ADEP4 with rifampicin showed complete clearance of a *Staphylococcus* biofilm (Conlon et al., 2013). The role of ClpP in a normal cell environment is to recognise and proteolyse misfolded proteins in a complex with ATP-dependent ClpX, C or A subunits. Upon ADEP4 binding, the ClpP catalytic chamber is maintained in its "open" state allowing entry of proteins and peptides and ATP independent cleavage (Conlon et al., 2013). Rifampicin functions as an antibiotic by inhibiting bacterial DNA dependent RNA synthesis through inhibition of DNA dependent RNA polymerase (Calvori et al., 1965). This is the most compelling anti-persister treatment published to date.

1.3. Project Brief

Antibiotics were once hailed as a revolutionary end to infectious diseases. It has now been recognised that this “golden age” is over and antibiotic efficacy can no longer be relied on to give rapid and complete clearance of infection (Conlon et al., 2013).

It is evident that there is an acute need for novel therapeutics to improve treatment outcomes in melioidosis. I propose that persister cells represent a previously unexploited target for new therapies for melioidosis. Furthermore, by gaining a greater understanding of proteins complicit in the generation and maintenance of persistence, it may be possible to identify future targets to be used in drug discovery not only in *B. pseudomallei*, but also other Gram-negative pathogens for which MDT is a public health concern (Pendleton et al., 2013).

A proposed approach to producing an “anti-persister” drug to improve upon current treatment of *B. pseudomallei* would be to combine the current frontline antibiotic, ceftazidime, with an inhibitor of an essential persister protein. The desired therapeutic may either inhibit persistence or force cells to leave their persistent state and become susceptible to antibiotic killing.

Project Objectives

- Design a bioassay capable of detecting compounds which reduce persister cell survival
- Use this assay to screen a compound library to identify hit compounds with drug like physiochemical properties and suitable activity
- Confirm hits and look to improve activity through series expansion
- Identify the genetic mechanism of action

Target Product Profile

In many countries where melioidosis is endemic, cost of medications and hospital care are significant barriers to effective treatment. As well as improving upon current treatments in terms of efficacy in clearing the disease, a previously unmet need in treating melioidosis is to make available therapies cheaper and more easily accessible. To achieve this, throughout this project I have been working toward goals described in the Target Product Profile (TPP) as laid out in Table 1.1.

A TPP is a planning tool for therapeutic candidates based upon FDA guidance to provide a structure for development of a new drug allowing all parties involved in the project to work concertedly. The TPP for this project describes an orally administered drug with minimal side effects that will reduce the burden of persister cells when administered alongside ceftazidime to give improved successful treatment outcomes and reduce the incidents of relapse.

Product Properties	Minimum acceptable result	Ideal Result
Primary indication	Reduction of persister cell number in melioidosis preventing relapse of infection. To be administered alongside parenteral treatment and into the oral eradication phase	Eradication of all reservoirs of infection resulting in relapse of melioidosis. To be administered alongside parenteral treatment.
Patient population	Patients with chronic or acute melioidosis	Patients with acute melioidosis
Treatment duration	Less than 6 months	In line with a typical course of oral antibiotic treatment
Delivery mode	Oral	Oral
Dosage form	Tablet or capsule	Tablet or capsule
Regimen	1-2 x / day	1 x / day
Efficacy	Decrease from 3 % relapse in cases of melioidosis	Eradication of relapse of disease
Side effects	Minor or moderate CNS side effects Minor or moderate GI side effects	No CNS side effects No GI side effects

Table 1.1: Target Product Profile for a drug to recurrent infection through persister cell survival in melioidosis.

2. Assay Development

2.1. Overview

The starting point for this drug discovery program to identify compounds with anti-persister activity in *Burkholderia pseudomallei* was development of a robust and reliable assay for use with high throughput screening (HTS) of a compound library.

In this section of work, carried out at the University of Exeter between May 2012 and October 2013, a number of approaches to developing a suitable assay were explored. By developing an assay capable of quantifying persister cell numbers the focus of assay development was to enable accurate and reliable detection of a four-fold difference in persister numbers allowing identification of compounds which inhibit their formation and survival.

As described in chapter 1, *Burkholderia thailandensis* shares over 85% of its genes with *B. pseudomallei* but is avirulent in immunocompetent humans (Majerczyk et al., 2014). For this reason, and to facilitate HTS without requiring biological safety laboratory class III (BSL3) facilities, *B. thailandensis* was chosen for screening with hit compounds. The intention was to confirm activity in *B. pseudomallei* at a later stage.

From conception of the project I decided to use a phenotypic, whole cell assay. Phenotypic screening has multiple advantages over the alternative target-based screens. Whilst a number of potential pathways involved in the induction and maintenance of persister cells have been identified as discussed in chapter 1, target based screening could limit the scope of this drug discovery program. Additionally, compounds identified through target-based screening can often interact with, on average, six other targets. These off-target effects can have serious down-stream

implications (Mestres et al., 2009). Using phenotypic screening of a whole cell assay opens up possibilities of discovering novel targets in the treatment of persister cells. In the past decade phenotypic screening has produced significantly more first-in-class small-molecule drugs than target-based approaches. One study investigating new medicines approved by the FDA between 1999 and 2008 finding 60% of new biologics and small molecules were discovered through phenotypic screening (Swinney and Anthony, 2011).

In addition to this, it is hypothesised that persistence is multigenic with significant redundancy of genetic pathways leading to the persistent phenotype (Helaine and Kugelberg, 2014). By using a phenotypic assay, only compounds which elicit an effect are detected reducing the effect of redundancy. This also ensures that all hits are able to permeate cells and have activity under the severely retarded cellular metabolism observed in persister cells. Whilst phenotypic assays have many benefits, they do also have shortcomings when compared to target based assays. Phenotypes observed may occur through modulation of a number of different pathways and so target identification can be significant task downstream of high throughput screening. Because of this, although hit rates for phenotypic screening may be higher than other methods, hits compounds are more likely to attrite later in the drug discovery pipeline, particularly with viability readouts which have many potential non target mechanisms of action.

This chapter documents the design and evaluation of seven potential assays covering a number of orthogonal mechanisms of action. It was important to cover a breadth of designs to ensure that the selected assay was biologically relevant in quantifying persister cells and that it met specifications for sensitivity and reliability criteria of a suitable HTS bioassay.

2.2. Assay Specifications

Developing a bioassay with adequate sensitivity, reliability and robustness was pivotal to this project. Given the substantial investment involved in screening at the DDU and downstream processes it was essential that the screening assay worked reliably and would be transferrable to the DDU facilities. Most critically the focus on assay design was to ensure the data collected would identify changes in persister cell numbers when incubated with molecules active against persister cells.

Stipulations for a suitable assay included the ability to detect a four-fold change in cell numbers with 99% confidence and a Z' prime > 0.5 .

Assay Robustness

Assay robustness in drug discovery is quantified by the industry standard Z' statistic defined in Equation 2.1 (Zhang et al., 1999). To meet requirements set by collaborators at the DDU, the assay was developed and optimized to provide a Z' greater than 0.5 for a four-fold difference in cell numbers. Z' is more widely used in drug discovery than a t–statistic p-value as this can be highly influenced by the sample size of the controls and has been largely discredited (Halsey et al., 2015).

$$Z' \text{ factor} = 1 - \frac{3(\sigma_p + \sigma_n)}{|\mu_p - \mu_n|}$$

Equation 2.1: An equation for calculating Z' prime

Z' prime is a measure of statistical effect size used in HTS to evaluate assay reliability and robustness. Z' prime is defined in terms of four parameters: the mean (μ) and standard deviation (σ) of positive (Caglic et al.) and negative (n) controls.

Initial tests for assays were performed by seeding with two-fold increases of cell concentrations to test the assay's ability to differentiate. Whilst assay development took place using 96 well microtiter plates, screening at the DDU would take place using 384 well plates. An important consideration in assay development was to ensure that methods would be able to translate to using smaller volumes without losing assay robustness to changes such as those caused by edge effects (Maddox et al., 2008).

2.3 Assay controls

A full kill negative control was developed in order to provide a means to detect a decrease in viable cell numbers, to be implemented as a positive control for active compounds in screening. Options tested included treatment with 1 M hydrochloric acid; 10 % (v/v) ethanol; exposure to UV light and heating samples at 90 °C prior to incubation (Figure 2.1). Upon further consideration of these methods it was decided that addition of ethanol or hydrochloric acid should be avoided due to their likely effects on the cell viability reagents used in the assay. Instead, further investigation was carried out into heat treatment and exposure to UV radiation. Heat treatment of cells at 90 °C for 5 minutes prior to incubation led to a reduction in PrestoBlue fluorescence (2.4.8) comparable with background fluorescence, with the 'full kill' being confirmed by absence of growth when grown on LB agar.

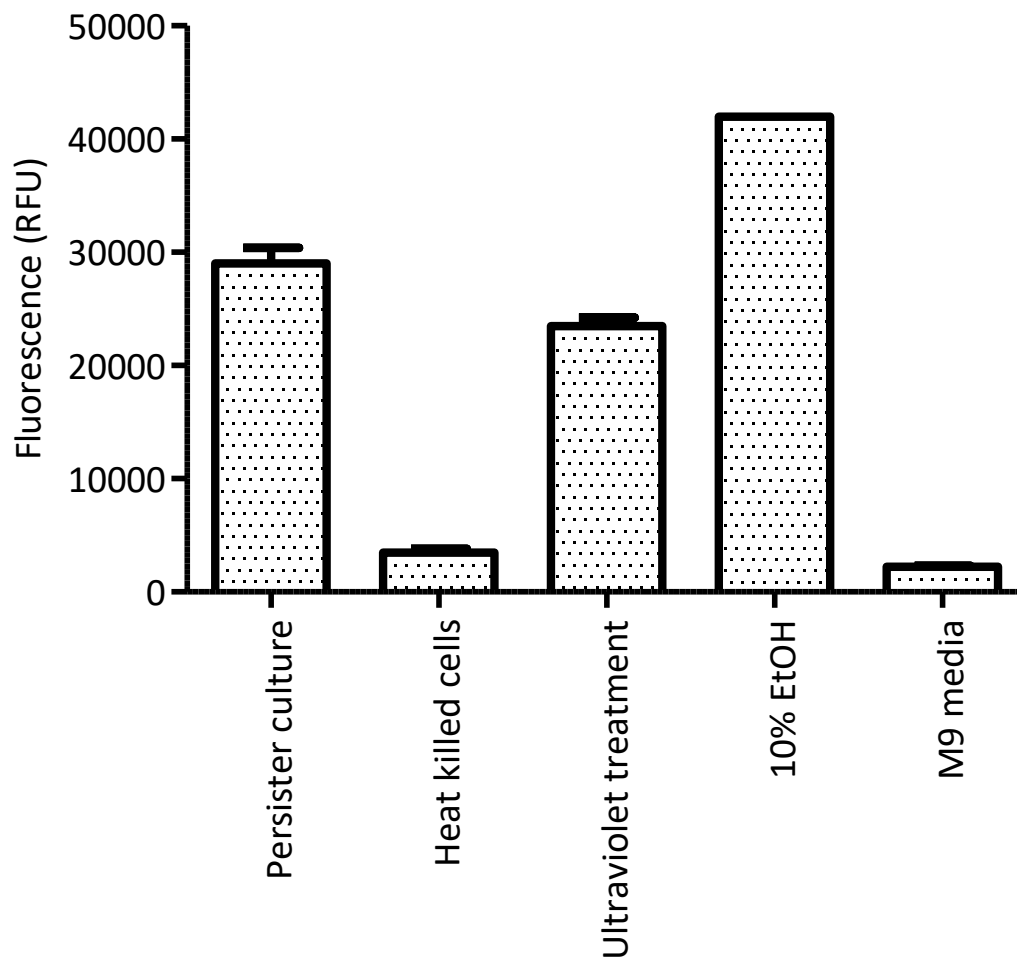


Figure 2.1: Investigated options for a full kill, negative control using PrestoBlue.

Persister cells were treated and incubated for 24 hours in the presence of 100X MIC ceftazidime. Of the potential negative controls tested, heat treatment of cells gave a 'full kill' reading comparable to the M9 media blank. No growth when incubated on agar confirmed this result.

2.4. Preliminary Assays

2.4.1. Generation of persister cell culture by treatment with ceftazidime.

As previously described, frontline treatment of melioidosis is parenteral administration of the third-generation cephalosporin antibiotic ceftazidime.

Initial tests in persister cell generation through treatment with antibiotics showed that both persister frequency and reversion periods to normal phenotype are dependent on the class of antibiotic used (Hemsley et al., 2014). This may indicate that persistence is not a single phenotype but likely to be dependent on the cause of formation. As ceftazidime is currently chosen as the first line treatment and any 'anti-persister' compounds discovered are intended to be used in conjunction with treatment, it was chosen for assay development (Pitman et al., 2015).

Previous studies into persister cells have generated and isolated persisters through antibiotic sedimentation of susceptible cells (Keren et al., 2004b). A surviving fraction of bacteria, hypothesised to be persister cells, was produced upon treatment of *B. thailandensis* with ceftazidime (Figure 1.5). Upon this evidence it was decided to use antibiotic treatment with ceftazidime to generate persister cells for screening of compounds.

Experimental procedure

All experiments carried out in assay development used *B. thailandensis* strain E264. Bacteria were grown in high salt LB broth at 37 °C with aeration at 200 rpm.

A persister cell culture was produced for a culture of *B. thailandensis* grown overnight to stationary phase in LB broth from which cells were harvested by centrifugation at

10,000 x g. Cell pellets were resuspended in M9 minimal media (Harwood C. R., 1990) and persister cells generated by treatment with 400 µg/ml ceftazidime (Melford Laboratories Ltd.). Antibiotic stock was produced by preparing dilutions from a freshly prepared stock at 10 mg/ml active component in 0.1 M NaOH. This method of generating persister cells was kept consistent throughout assay development to allow accurate comparison between methods.

2.4.2. Colony culturing and counting

A visible colony count style experiment was carried out using serial dilutions of cultures before and 24 hours after treatment with 100 X MIC ceftazidime to calculate the persister subpopulation (Figure 2.2).

Experimental procedure

A culture of *B. thailandensis* was grown to stationary phase in LB broth. Cell density was measured by absorbance at 600 nm and cultures were diluted with fresh broth to OD 0.2, approximately equal to 2×10^8 CFU/ml. The colony forming units (CFU) will be determined before (t_0) and after the treatment (t_{24}) where the former represents the input number of bacteria and the latter the surviving fraction, persister cells.

For t_{24} samples a solution of 800 µg/ml ceftazidime hydrate (200 X MIC) in LB was produced using antibiotic from a stock solution. In three wells of a 24 well plate, 500 µl of prepared bacterial culture was mixed with 500 µl ceftazidime hydrate solution. To one well 1 ml LB was added as a control and plates were incubated statically at 37 °C for 24 hours. Following incubation the assay mixture was transferred to a 1.5 ml reaction tube and centrifuged at 14,000 rpm using a desktop microcentrifuge for four minutes to pellets cells. The supernatant was discarded and a wash step using 1 ml fresh LB was performed before resuspension in 1 ml fresh LB.

To perform CFU counts a dilution series of the bacterial suspension was prepared using nine x 10-fold dilution steps. This was performed by addition of 10 µl bacterial suspension to 90 µl LB in wells of a 96 well plate. 10 µl of each dilution was dropped on the surface of a dry LB agar plate, allowed to dry and plates incubated overnight at 37 °C. Cells were enumerated for an appropriate dilution at which 10 to 50 colonies were visible; averages from triplicates were then adjusted for the dilution factor to give results in CFU/ml. Persister frequency = CFU at t_{24} / CFU at t_0 . This experiment was repeated over 3 consecutive days to give independent biological replicates.

Results and Evaluation

Colony counting has previously been considered the gold-standard method for quantifying persisters (Feng et al., 2015); however for this application it was not deemed suitable as a primary assay due to difficulties in scaling up for HTS and variance between biological repeats (Figure 2.2). In addition, colony counting would only quantify persister cells that have survived antibiotic treatment and are able to revert to the normal phenotype and reproduce to form colonies on agar within a 24 hour period. This may limit the assay's ability to detect possible phenotypic differences in persister cells.

The experiment was repeated on three separate occasions to precisely determine persister frequency of *B. thailandensis* at stationary phase and to indicate the reproducibility of this assay. Whilst the standard deviation observed between technical repeats (Figure 2.2) was low, the difference seen between biological repeats of the experiment indicate the assay is not suitably reliable. In addition, whilst the assay is able to detect differences in cell numbers on the log scale shown, it is not sensitive enough to detect a four-fold change as desired.

2.4.3. Measuring cell density by absorbance

Absorbance at 600 nm was considered as a method to calculate cell density. However, as the persister fraction is estimated to comprise just 0.1% of cell numbers at stationary phase in *Burkholderia* species, this would be below the detection limit and significantly outside experimental ability to resolve a four-fold difference in cell numbers. In addition, this method was deemed unsuitable as it gives no indication of cell viability or evidence of metabolism. No data is shown for this method as it was clear from the outset that the method would not have the sensitivity required for a persister detecting assay.

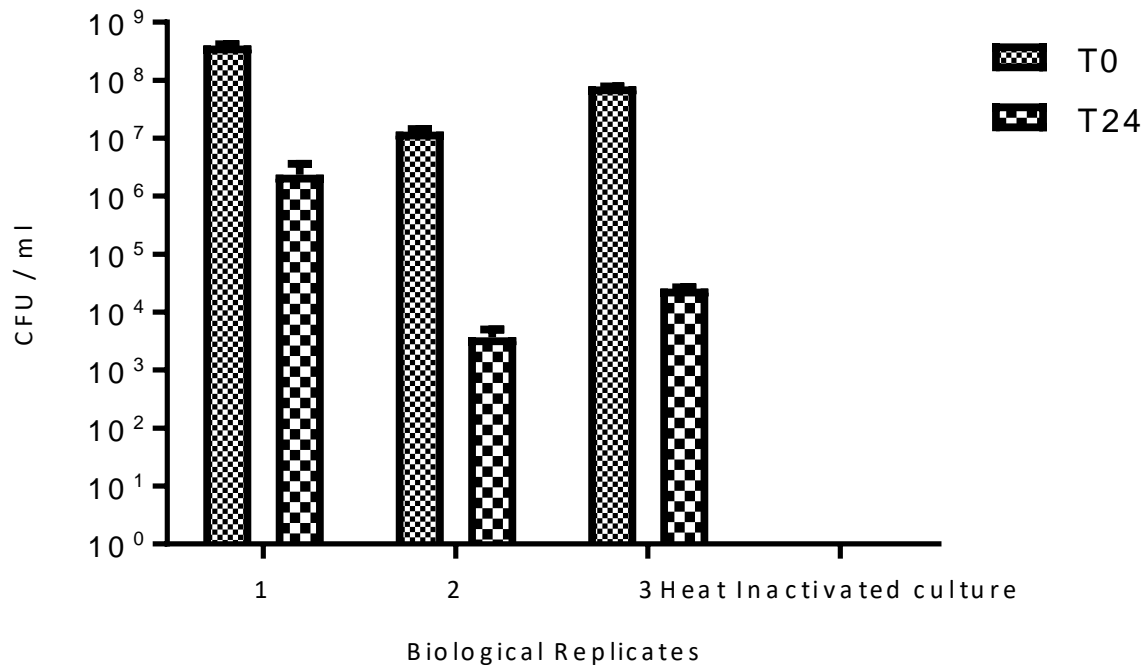


Figure 2.2: Persister frequency in response to treatment with ceftazidime. Persister frequency for: 1 = 0.59 +/- 0.8; 2 = 0.028 +/- 0.03; 3 = 0.033 +/- 0.033

A culture of *B. thailandensis* was treated with 400 µg/ml ceftazidime hydrate and incubated in a 24 well plate. Samples were taken after 24 hours, cells harvested and resuspended in fresh LB media before serial dilution and enumerating on agar. Results show technical repeats for three biological replicates. Error bars indicate standard deviation. This method shows large standard deviation and variance between biological repeats over consecutive experiments.

2.4.4. Quantification of persister cells by BacTiter-Glo Microbial Cell Viability Assay

Preliminary investigations were carried out to quantify persister cell generation using the BacTiter-Glo™ Microbial Cell Viability assay (Promega). This homogeneous cell viability reagent can be added directly to culture where viable cells are quantified through the reagent's reaction with intracellular ATP. This is linearly related to luminescent signal intensity the reaction (Figure 2.3).

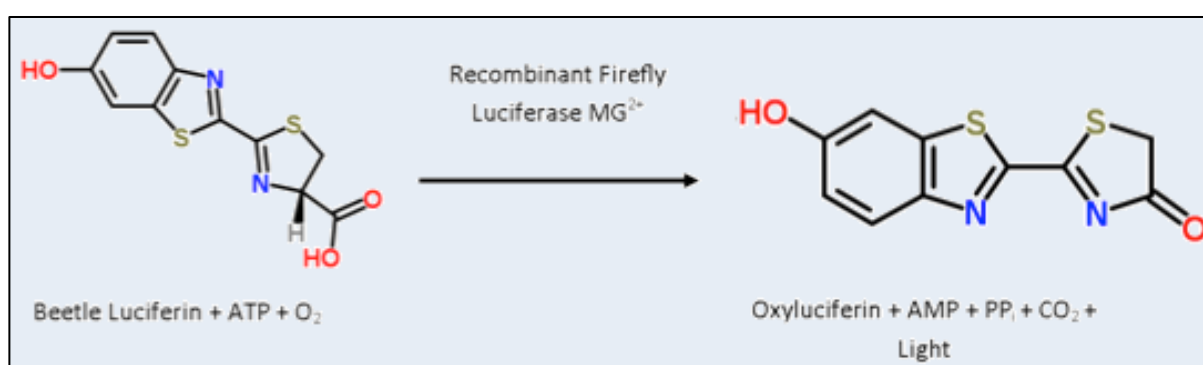


Figure 2.3: The luciferase reaction from BacTiter-Glo Microbial Viability Assay (Promega)

Experimental Procedure

A culture of *B. thailandensis* was grown to a cell density of OD₆₀₀ 1.6, equivalent to 1.6 x10⁹ CFU/ml. As per the colony counting method described above, samples of t₀ and t₂₄ were produced with the t₂₄ persister culture incubated statically for 24 hours at 37 °C. Dilution series of t₀ and t₂₄ were prepared for visible colony count quantification using 10-fold dilution steps of 90 µl LB to 10 µl bacterial suspension in a 96 well plate.

ATP concentration was determined against an ATP ladder produced from a 10 µM stock solution of ATP in LB which was serially diluted using seven, 10-fold dilution steps of 90 µl LB to 10 µl ATP solution in a 96 well plate.

Aliquots of 100 µl for all samples; t_0 , t_{24} and ATP standards were added to wells of an opaque, white walled 96 well plate (Corning: Catalogue no. #3917) and 100 µl BacTiter-Glo reagent added. Plates were mixed using an orbital shaker and incubated at room temperature for 5 minutes before luminescence was read using an Infinite M200 Pro (Tecan) plate reader.

Results and Evaluation

Dilutions of an overnight culture of *B. thailandensis* were tested with BacTiter-Glo Microbial Cell Viability Assay (Figure 2.4). From a starting cell density of OD₆₀₀ 1.6, equivalent to approximately 1.6×10^9 CFU/ml the figure shows detection of two-fold dilutions in untreated cultures. Results are shown for *B. thailandensis* culture in a 96 well format.

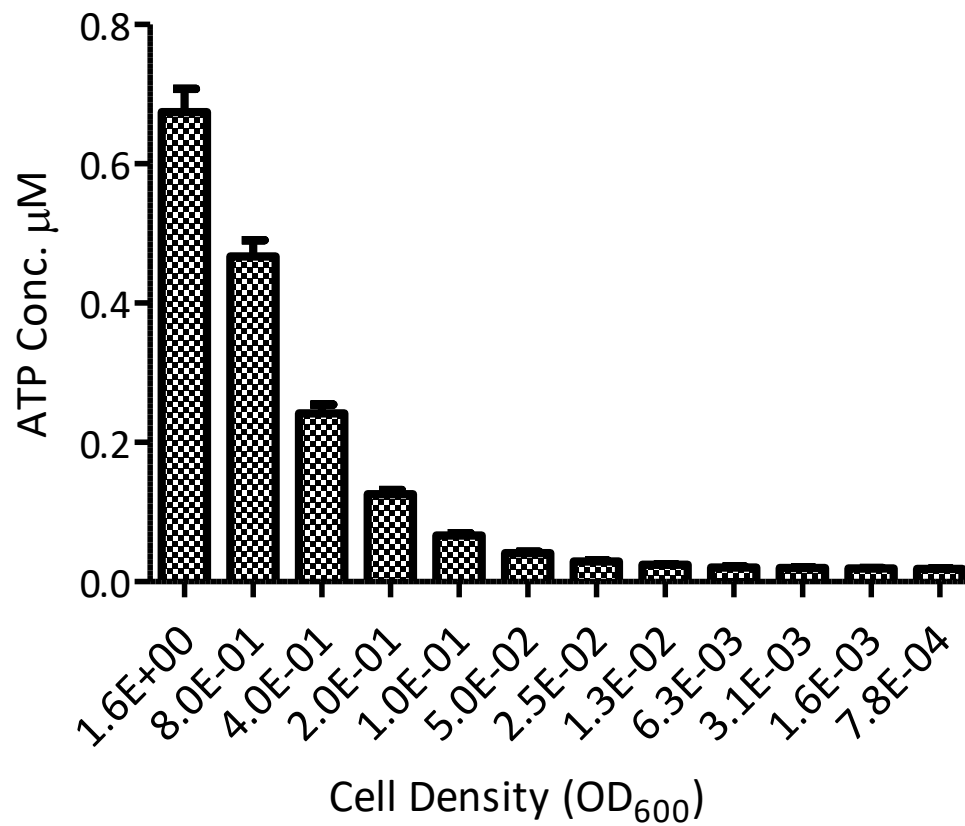


Figure 2.4: Assay development using Bactiter Glo.

An untreated culture of *B. thailandensis* quantified with Bactiter Glo reagent. Signal is representative of average bacterial ATP concentrations from three replicates. Error indicates 95% confidence intervals. Z' for 0.8 to 0.4 = 0.61

2.4.5. QPCR

It is possible to absolutely and relatively quantify cell numbers through real-time PCR. It was hypothesized that changes in persister cell numbers could be accurately determined by comparing persister culture gDNA to a known standard curve.

Gene BTH_II0730, a putative sugar binding protein previously validated for identification of *Burkholderia* species was chosen (Koh et al., 2012). This gene is known to be highly conserved in *Burkholderia* sp. Initial studies were carried out using SYBR Green Real-Time PCR reagent, a nucleic acid stain which binds dsDNA and is suitable for DNA quantification.

Experimental Procedure

An experiment was designed according to the minimum information for publication of quantitative real-time PCR experiments (MIQE) guidelines (Bustin et al., 2009). Primers were designed for gene BTH_II0730 using Applied Biosystems Primer Express 3.0 software for a 709 bp amplicon.

Genomic DNA (gDNA) was extracted from a stationary culture of *B. thailandensis* using a GeneJET Genomic DNA Purification Kit (ThermoFisher) and the concentration was determined to be 19.4 ng/μl using a NanoDrop 2000c spectrophotometer. gDNA was then diluted to 2 ng/μl and seven 10-fold dilutions were made with ddH₂O for a standard curve.

Two-fold dilutions of *B. thailandensis* from a stationary culture in LB were produced from OD₆₀₀ 1.6 to 0.2.

qPCR was carried out using SYBR Green Real-Time PCR Master Mix (ThermoFisher) on an Applied Biosystems StepOne Real-Time PCR System. PCR was performed in

a total volume of 15 μ l containing 5 μ l of purified genomic DNA or cell culture, 0.2 mM of each dNTP, 2 mM MgCl₂, 0.2 μ M primers BTH_II0730 forward (AGCTCGCAGATGAACTGGAT) and reverse (GCTGATCGTTGTTTCGTCGTA). The amplification condition was initiated with denaturation at 95 °C for 3 min, followed by 30 cycles at 95 °C for 20 s, 59 °C for 35 s, and 72 °C for 30 s. The amplification took approximately 1 hour and 20 minutes.

Results and Evaluation

This method has potential to detect and quantify exceedingly small quantities of bacterial DNA. Real-time PCR is capable of giving both relative and absolute quantification of total bacteria through use of the universal probe, SYBR Green, and conserved primers. SYBR green intercalates double stranded DNA binding to the minor groove (Zipper et al., 2004).

The standard curve gives a good dynamic range (Figure 2.5: upper). However, upon testing the assay with serial dilutions of a culture of *B. thailandensis*, no discrimination was observed for reduction in cells numbers (Figure 2.5: below). I hypothesize that this is due to DNA from dead or dying cells remaining in culture and contributing to the total DNA present.

It became evident that the cost and complexity of this method would be prohibitive for use in high-throughput screening. The rate of DNA degradation in dead cells was also a concern as DNA from non-viable cells may still be amplified. A wash step would reduce this risk but also add a further step increasing cost, difficulty and error.

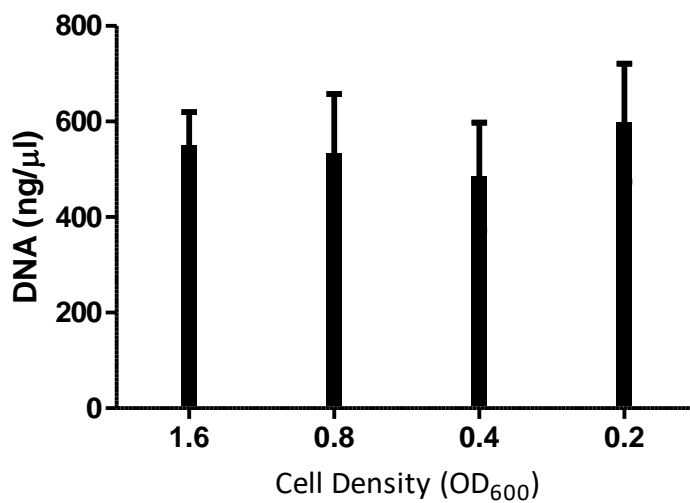
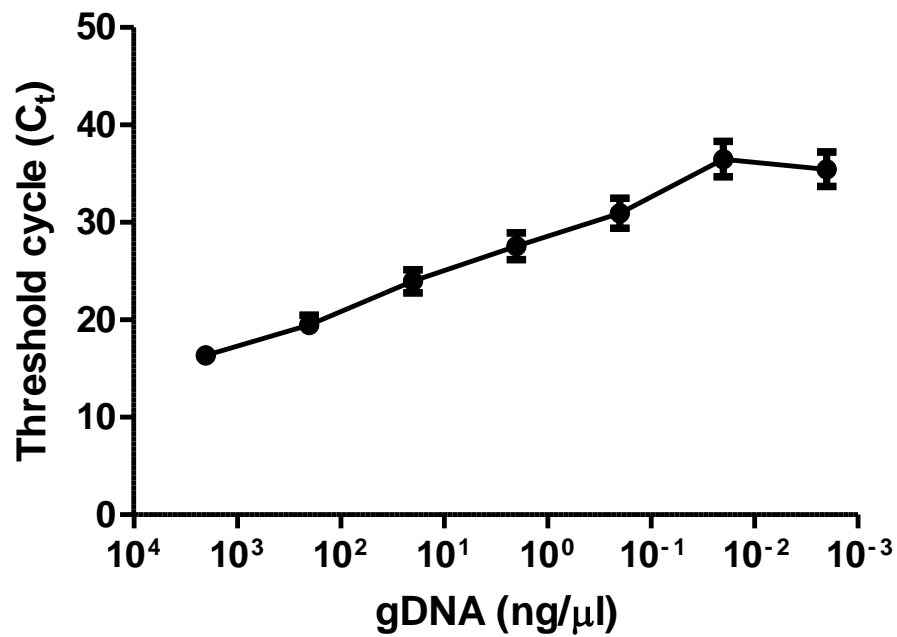


Figure 2.5: Assay development for qPCR.

Above: Standard curve created from gDNA dilutions. Below: Calculated DNA quantities from a culture of *B. thailandensis*. QPCR of *B. thailandensis* cells with SYBR green probe showed a detectable difference in 10 fold dilutions of cell culture against a 1:10 genomic DNA standard. $y = -1.5\ln(x) + 26$; $R^2 = 0.99$.

2.4.6. Plasmid encoded fluorescent protein

A further candidate for assay development used detection of a constitutively expressed red fluorescent protein to quantify cell numbers.

Experimental Procedure

The plasmid pBHR4-groS-RFP (Figure 2.6) was conjugated into *B. thailandensis* E264 from the carrier *Escherichia coli* S17 containing a chloramphenicol resistance gene (Appendix iv). A culture was grown to OD₆₀₀ 1.6 before being centrifuged to pellet cells and resuspended in fresh LB containing 750 µg/ml chloramphenicol. The culture was optically adjusted to OD₆₀₀ 0.8 and two-fold dilutions made in a black-walled 96 well assay plate (Corning, 07-200-567) in LB media.

To test with persister cells, a persister culture was produced as in 2.4.1 by centrifuging the sample at 10000 x g for 10 minutes before resuspending the cell pellet in LB media with 400 µg/ml ceftazidime and incubated for 24 hours.

Fluorescence was read at ex 588 nm and em 635 nm using an Infinite M200 Pro (Tecan) plate reader.

Results and Evaluation

Despite having a significantly slowed metabolism persister cells are still able to produce proteins (Rotem et al., 2010). Whilst this option gave excellent resolution in detecting a two-fold difference in seeded cell numbers and displaying a suitable dynamic range as shown in Figure 2.7, this option could not be selected for HTS. This was due to the expressed fluorophore accumulating in solution and inhibiting the detection of reductions of cell numbers (Figure 2.8). Effectively, the fluorescent protein accumulated in dead cells. This resulted in an overall increase in fluorophore over time

and reduced the signal to noise ratio of live cells to background fluorescence. Figure 2.8 shows measured fluorescence for a culture of cells prior to antibiotic treatment compared to a culture treated with ceftazidime, which has previously been shown to be lethal to cells. A reduction in fluorescence under treatment with antibiotic was not observed. A treated cell culture was centrifuged to pellet cells and the supernatant read: this gave a very low signal indicating that fluorophore is contained within cell bodies or cell debris. Antibiotic treated media only control showed very little fluorescence confirming that this did not significantly contribute to background fluorescence.

Initial investigations into RFP quantification used pBHR4-groS-RFP, a constitutively expressed plasmid. However due to issues arising from fluorophore persisting in solution, an approach to control fluorophore expression by including a rhamnose inducible promoter to the plasmid was considered. The intention was to perform the screen and subsequently induce expression of RFP in surviving cells. This was expected to be representative of the quantity of cells present. The attempt used Gibson cloning of a RhaB2 promoter into the pBBR-RFP plasmid. However, due to concerns of selective pressure introducing bias and difficulties in cloning; this could not be achieved within the time constraints imposed by the need to provide the Drug Discovery Unit with a validated assay.

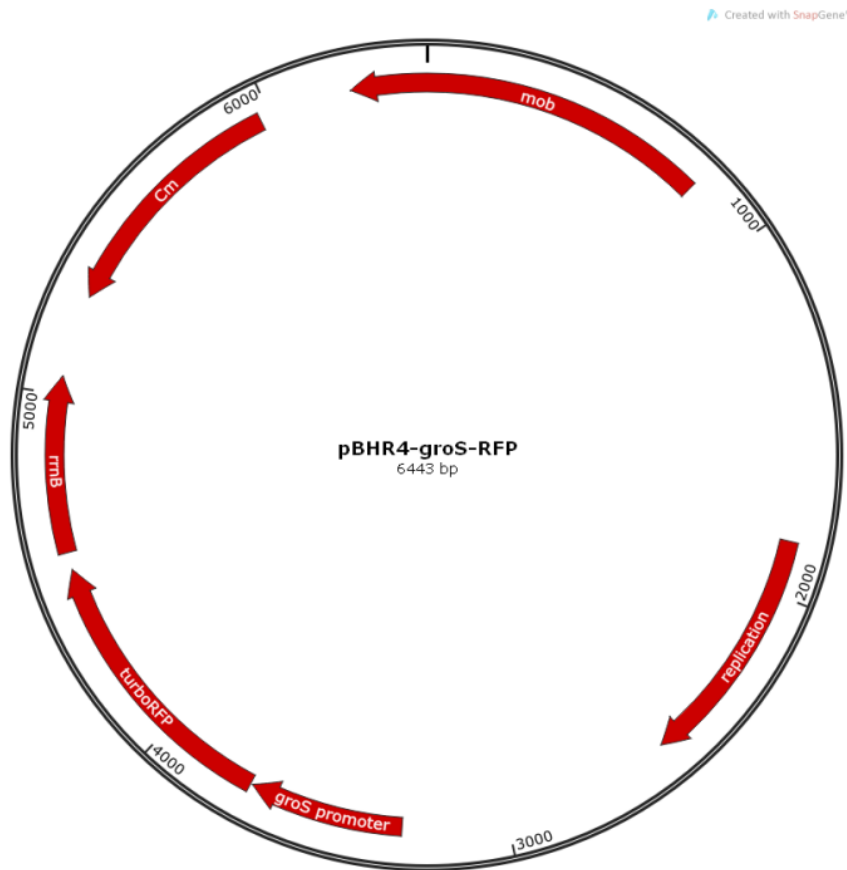


Figure 2.6: Plasmid map of pBHR4-groS-RFP, conjugated into *B. thailandensis* to express red fluorescent protein.

TurboRFP is a red fluorescent protein (Maximum excitation/emission wavelengths are 588 and 635 nm respectively). The plasmid contains a chloramphenicol resistance cassette (CM) and a constitutive promoter (groS). Figure created using Snapgene v.

2.

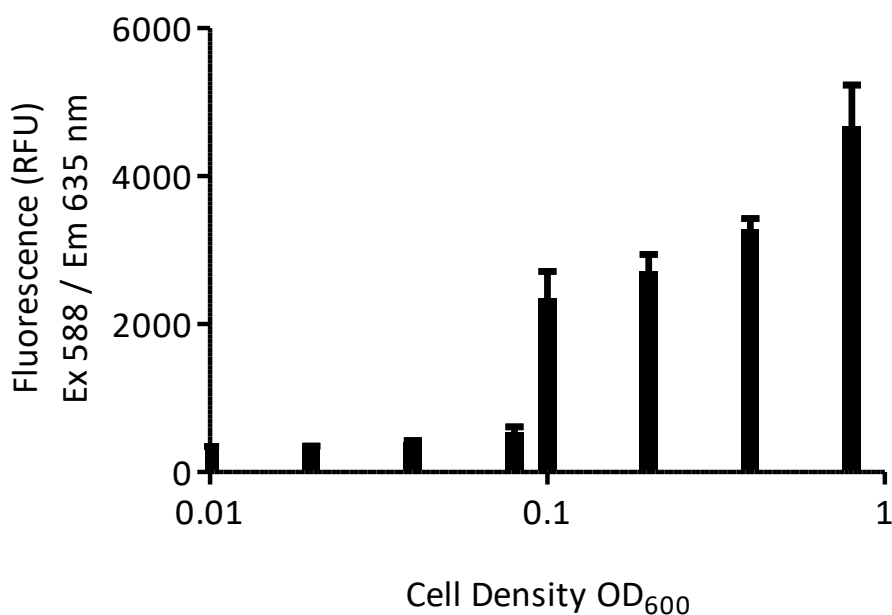


Figure 2.7: Assay development using recombinantly expressed Red Fluorescent Protein.

Fluorescence of a *B. thailandensis* persister culture expressing a plasmid encoded Red Fluorescent Protein (RFP) shows clear resolution of two-fold differences in cell numbers. Z' prime for a two – fold difference from 0.8 to 0.4 = 0.5. Persister culture is generated by treatment with 400 µg/ml ceftazidime. Results shown are in triplicate, error indicates standard deviation.

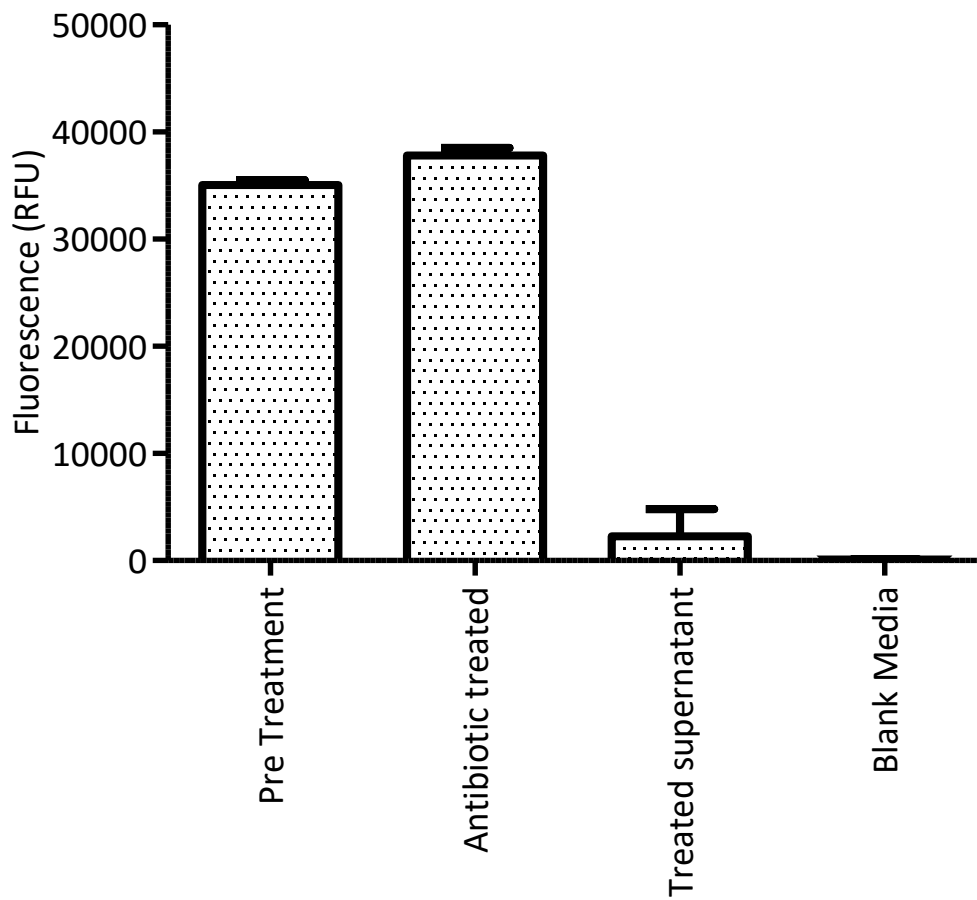


Figure 2.8: Residual fluorescence of Red Fluorescent Protein

Residual fluorescence of constitutively expressed red fluorescent protein inhibited assay's ability to detect decreases in cell numbers despite giving excellent results for different seeding of cells.

2.4.7. LIVE/DEAD cell viability staining

LIVE/DEAD® BacLight™ Cell viability staining is a two-colour fluorescence assay. As methods relying on metabolism of bacteria don't work for all bacterial groups, this method was also considered. In addition, there is a possibility that screening compounds may react with other fluorophores. This assay uses SYTO9, a green fluorescent nucleic acid stain and the red fluorescent nucleic acid stain propidium iodide to assess membrane integrity. When used as a sole reagent, SYTO9 will penetrate and label all bacteria in a population. However, propidium iodide is only able to penetrate bacteria with damaged cell membranes. When both dyes are present in a cell, the propidium iodide will cause a reduction in the fluorescence of SYTO9. This cell viability staining kit has potential for the persister assay as the ratios of dyes can be optimised for *B. thailandensis* and fluorescence can be read rapidly in a microplate reader to give quantitative data.

Experimental Procedure

A mastermix of equal volume SYTO9 to propidium iodide was prepared and 3 µl added to wells containing an overnight persister culture generated as in section 2.4.1 and mixed thoroughly. Initially the experiment was carried out in LB media. The method was then developed to include a centrifugation step of 5 minutes at 8000 x g after which cell pellets were resuspended in M9 media with 400 X MIC ceftazidime.

Plates were incubated at room temperature in the dark for 15 minutes and fluorescence was read at ex 480 / em 500 nm for SYTO9 stain and ex 490 / em 635 nm for propidium iodide.

Results and Evaluation

Initially this method did not give an acceptable signal to noise ratio (data not shown). However, the assay was optimised to use M9 minimal media which reduced background fluorescence. Further optimisation included incubation with a breathable membrane. This reduced signal variability between wells by equalizing gaseous exchange and reducing evaporation from wells around the edge of plates.

These steps improved the assay to give LIVE / DEAD staining a suitable dynamic range (Figure 2.9) and differentiating ability (Stiefel et al., 2015). Following assay optimisation to use M9 minimal media, which reduces background noise in fluorescence, LIVE / DEAD staining met the criteria of a suitable assay.

Considerations for use of LIVE/DEAD staining are that it would be more expensive than some alternatives in high throughput. Also, methods that assess membrane integrity often suffer from high background fluorescence and results aren't necessarily representational of viable cells. This is a significant concern in studying persister cells. An additional concern with the LIVE/DEAD reagent is that the wavelengths used are known to be troublesome for compound effects. For use with the DDU library red wavelengths are preferred.

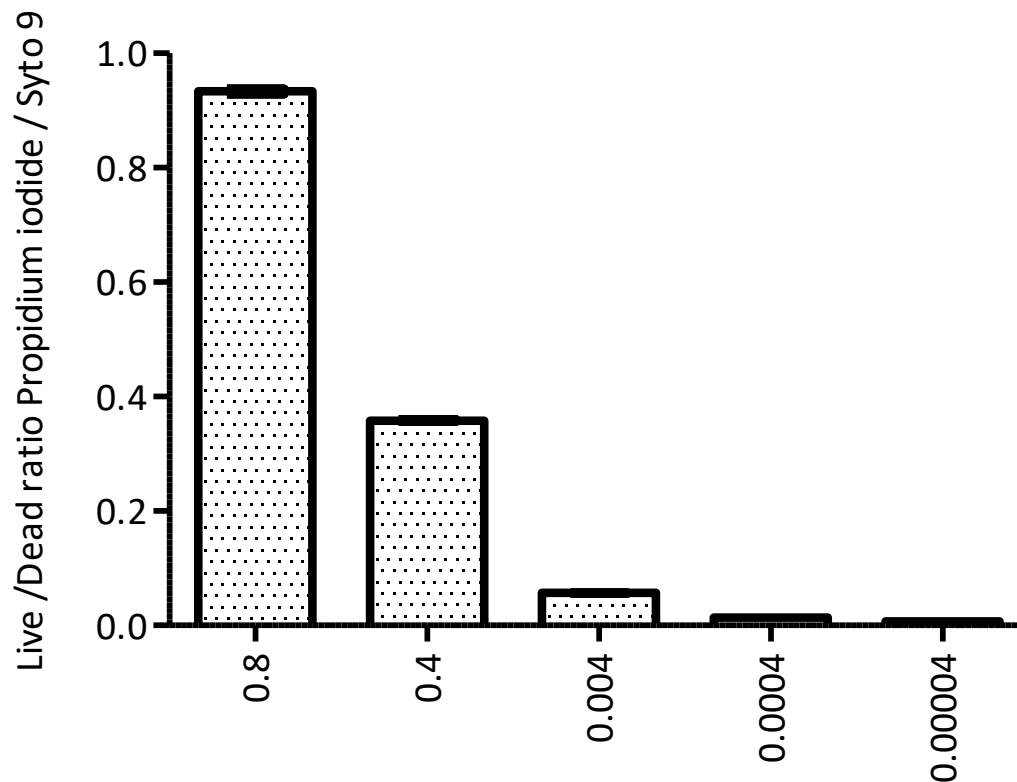


Figure 2.9: Assay development using LIVE / DEAD cell viability reagent

The LIVE/DEAD reagents SYTO9 and Propidium Iodide were used to quantify viability as a function of the membrane integrity of the cell. Dilutions of *B. thailandensis* culture were added to a 96 well plate and a persister culture generated by treatment with 100X MIC ceftazidime hydrate. Plates were incubated for 24 hours at 37 °C before addition of LIVE/DEAD cell viability reagents and reading fluorescence. Results show four biological replicates with error bars indicating standard deviation.

2.4.8. PrestoBlue Cell viability assay

PrestoBlue (ThermoFisher) is a cell viability assay that allows cell quantification by the irreversible intracellular reduction of resazurin to the fluorescent resorufin (Figure 2.10) (Lall et al., 2013). This method is particularly well suited to this application as PrestoBlue fluorescence is dependent only on the reducing environment of viable cells independent of the state of the cell membrane, ability to divide or protein expression.

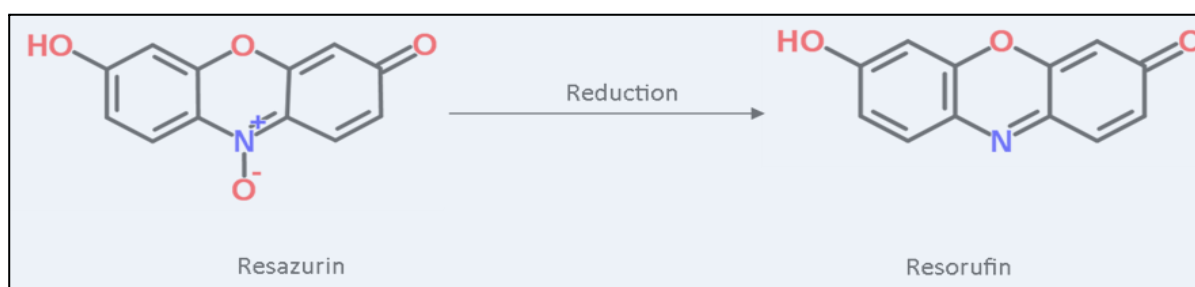


Figure 2.10: Reduction of resazurin to Resorufin.

PrestoBlue contains the agent resazurin which is reduced intracellularly in viable cells to produce the highly fluorescent dye resorufin. The fluorescence intensity is proportional to the number of viable cells present (Leveau et al., 2001).

Experimental Procedure

A persister cell culture was generated as previously described (as in 2.4.1). The culture was centrifuged and resuspended in M9 with 400 µg/ml ceftazidime before being serially diluted in an equal volume of M9 media to produce 11 x two-fold dilutions. The positive control contained cells untreated with ceftazidime and for the negative control, cells were heat killed at 90 °C for 2 minutes. Plates were incubated at 37 °C overnight before addition of PrestoBlue reagent and reading of fluorescence as described previously.

Detection of cell viability with PrestoBlue (Life Technologies) was performed in 96 and 384 well, black walled assay plates with reagent added 10% (v/v) to the persister culture (10 μ l PrestoBlue to 90 μ l persister culture). After addition of reagent, plates were incubated at room temperature for one hour and fluorescence was read at ex 540 / em 590 nm at Dundee by an Envision plate reader (PerkinElmer) and at Exeter by an Infinite M200 Pro (Tecan). All liquid handling in primary screening and series expansion was automated.

Results and Evaluation

PrestoBlue was able to discriminate a four-fold change in persister cell numbers (Figure 2.11). A four-fold change in persister cell numbers from OD₆₀₀ 0.078 to 0.019 gave $Z' = 0.41$ as indicated by *.

PrestoBlue is more amenable to HTS than LIVE/DEAD as only a single fluorescence reading is taken per well. From my personal experience in this project this keeps experimental time to a minimum and enables larger batches to be tested, reducing inter-batch error.

Results indicate that fluorescence intensity is representative of cell number (Figure 2.11). Whilst not empirically determined in this project it was hypothesised in assay development the fluorescence intensity would not be directly proportional to CFU counts. It is postulated that this could be as a result of persister cells being unable to revive and produce colonies on agar under the defined experimental parameters. This further favours the use of PrestoBlue for detection of compounds which inhibit the persister phenotype. Resazurin-based assays have been used previously in high-throughput screening for infectious diseases (Bowling et al., 2012).

Due to this method's ease of operation, range of detection and sensitivity to two-fold changes in cell numbers it was chosen for use with screening.

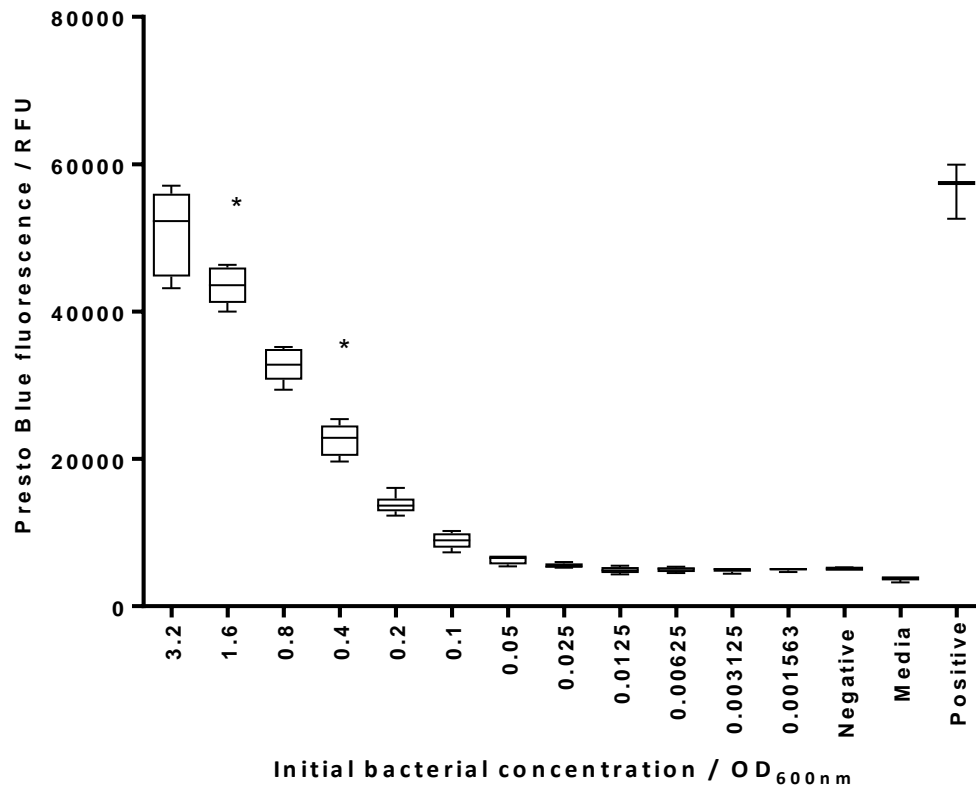


Figure 2.11: A PrestoBlue cell viability reagent based persister cell assay.

The PrestoBlue assay shows good discrimination of persister numbers. *B. thailandensis* persister culture was diluted to a range of optical densities at two-fold intervals. Samples were incubated statically at 28°C in 96 well plates. After 20 hours, PrestoBlue reagent was added and the fluorescence read with gain optimised for the highest bacterial concentration. The results show reliable distinction of two-fold differences in cell numbers as compared to a boiled cell negative control in M9 minimal media. * Indicates Z' for four-fold difference between OD_{600 nm} 1.6 and 0.4 = 0.41. $Z' < 0.5$ indicates a marginal effect size for screening however Z' is a tool measure statistical effect size and cell viability assays are unlikely to yield Z' scores as high as

biochemical assays due to the polyphenotypic nature of a cell culture. Data shows biological triplicates, whiskers indicate min and max results, box 25th to 75th percentile, central line indicates median.

2.4.9. Assay considerations and Optimisation for HTS

All compounds screened at the DDU are stored as a DMSO solution. As a precautionary measure to ensure that the results of screening the assay would not be masked by cytotoxicity of DMSO a minimum inhibitory concentration (MIC) experiment was run to determine survival of *B. thailandensis* under incubation with different concentrations of DMSO and to also ensure that the PrestoBlue reagent was also unaffected.

The effect of evaporation is increased when working in volumes of 50 µl. To maintain reliable results in transitioning from 96 to 384 well format, conditions such as temperature and humidity were considered. It was also hypothesized that by incubating assay plates with a breathable membrane (Sigma-Aldrich, Z380059) gaseous exchange would be more even across all well locations and evaporation reduced.

To optimize the PrestoBlue assay for HTS an experiment was carried out to evaluate the effect of incubating assay plates at a lower temperature of 28 °C to reduce evaporation and edge effect.

To ensure the efficacy of ceftazidime at the lower temperature, two broth microdilution MIC determinations were run at 37 and 28 °C.

Experimental procedure

DMSO tolerance was determined using a persister culture (as described in section 2.4.1) optically adjusted to OD₆₀₀ 0.4. 90 µl of culture were added to a 96 well plate and DMSO added over five concentrations from a maximum concentration of 10 % v/v. The plate was incubated at 28 °C for 24 hours before addition of 10 µl PrestoBlue.

The plate was centrifuged at 58 x g and left at room temperature for 30 minutes before fluorescence was read (as in 2.4.8).

To test reduction of edge effect and improvement of the assay through incubation at 28 °C, 90 µl persister culture was added to every well of two 96 well plates. A breathable membrane was applied and plates incubated at 28 and 37 °C for 18 hours before addition of 10 µl PrestoBlue reagent. Plates were centrifuged at 58 x g and left at room temperature for 30 minutes before fluorescence was read (as in 2.4.8).

To determine the effect of lower temperature on MIC of ceftazidime a 400 µg/ml solution of ceftazidime in M9 minimal media was produced. A 96 well assay plate was labelled to include samples in triplicate. 100 µL of M9 media was added to each well and a positive control of inoculated compound free broth and a negative control of uninoculated broth only were included. To the first well in the microdilution series 100 µL of the 128 µg/mL compound stock solution was added such that concentration = 128 µg/mL. From this well serial dilutions of 100 µl were performed to a final concentration of 0.03 µg/mL. The last aliquot was discarded (Ambaye et al., 1997).

B. thailandensis E264 was grown overnight in 10 mL of LB media and OD measured at 590 nm. The bacterial suspension was adjusted to the density of 0.01 and incubated for 1-2 hours at 37 °C. A viable count of the inoculum was performed to confirm concentration. 100 µL of the inoculum was then added to each well on the already prepared 96 well plate resulting in a maximum concentration of 64 µg/mL. Plates were incubated at 37 °C for 18 – 20 hours and adsorption at 590 nm read. MIC was determined as the lowest concentration of antibiotic in the original culture that inhibited bacterial growth over a four hour period.

Results and evaluation

For overnight incubation with two-fold increases of DMSO up to 10 % v/v, the maximum concentration of DMSO tolerated by *B. thailandensis* persister culture was 1.0 %. Approximately 50 % of cells were killed at 5.0 % DMSO (Figure 2.12). The maximum concentration of DMSO in any experiment in this project is 3.2 %. Therefore no action needed to be taken with regards to the use of DMSO in the PrestoBlue assay, particularly in HTS where the DMSO concentration does not exceed 0.05 %.

Incubation at the lower temperature of 28 °C displayed no difference to 37 °C for a standard MIC by microdilution experiment to determine the inhibitory concentration of ceftazidime. MIC for both temperatures was determined as 0.6 µg/ml (Figure 2.14).

The optimizations made and incubation at 28 °C gave rise to more consistent assay results and reduced plate effect however it was noted that corner wells still read anonymously low, a phenomenon that would be corrected by the DDU data handling software (Figure 2.13).

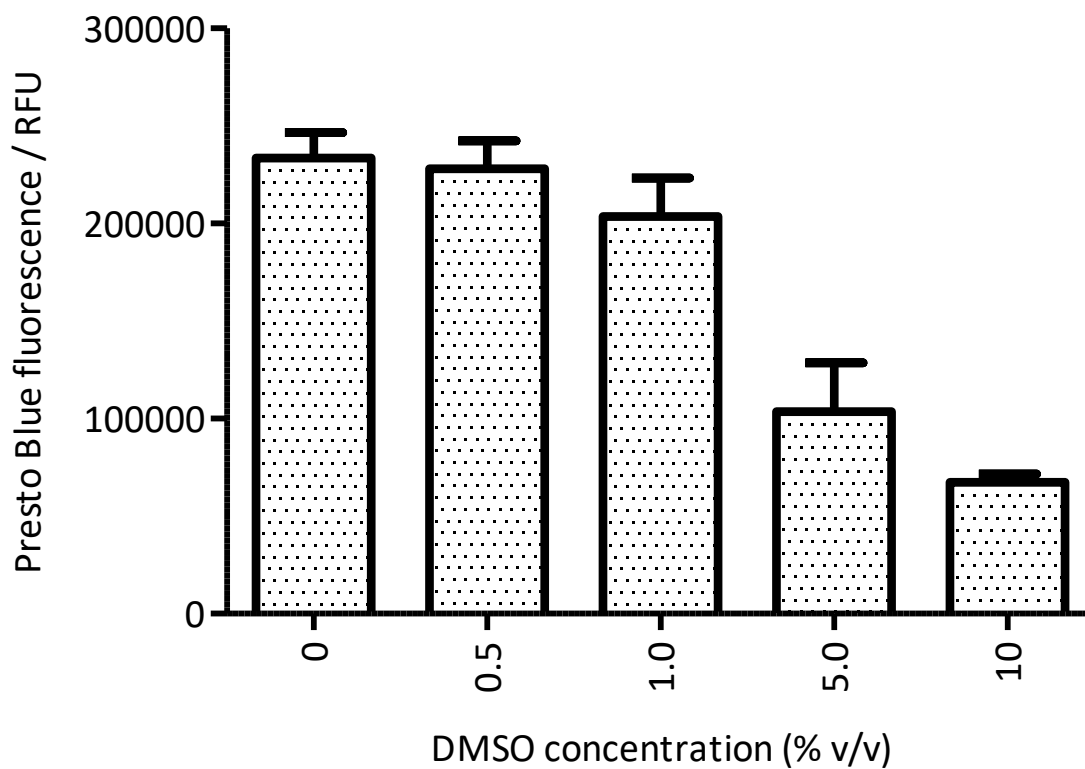


Figure 2.12: DMSO tolerance of persister cells.

Persister culture in a 384 well microplate was treated with increasing concentrations of DMSO and incubated at 28 °C for 24 hours. After incubation PrestoBlue reagent was added, plates incubated at room temperature for 30 minutes and fluorescence read. Results show average of 32 wells, error indicates standard deviation.

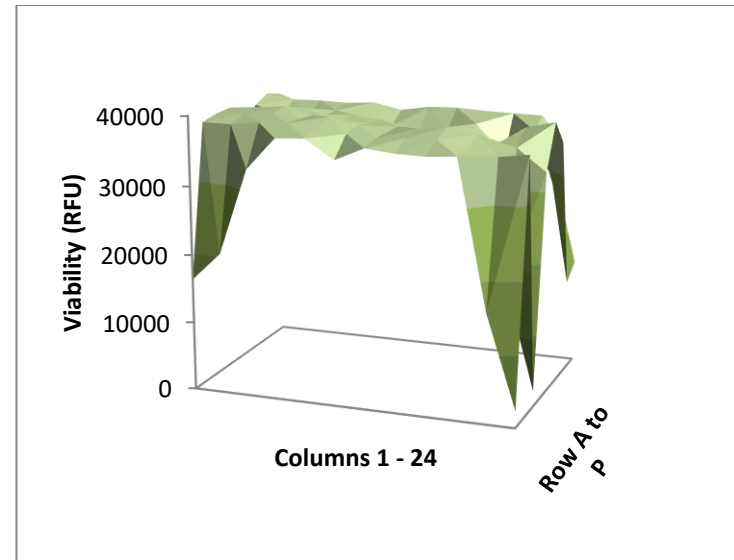
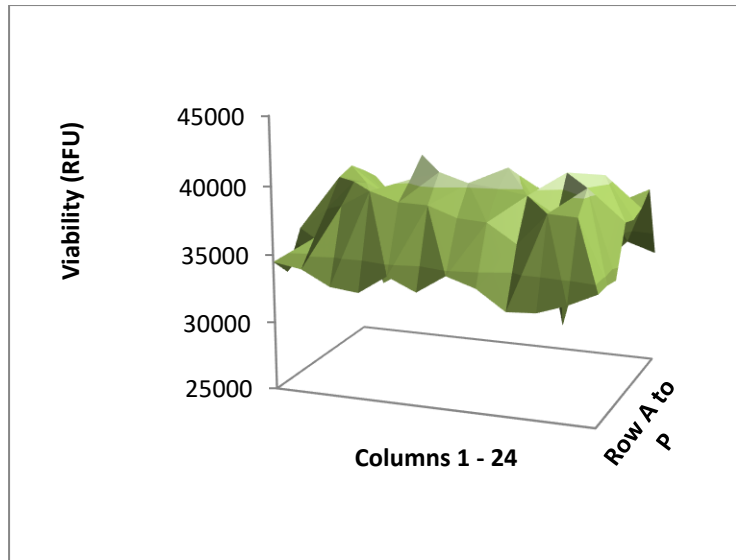


Figure 2.13: Edge effect for a 384 well plate.

Left: 100 μ l persister culture incubated at 37 $^{\circ}$ C with open wells shows large signal variance across x and y axis of the plate. Right: 100 μ l persister culture was added to all wells and incubated overnight at 28 $^{\circ}$ C with a breathable membrane, this reduced the coefficient of variation from 14 % to 8%. PrestoBlue was added to both plates following 18 hours static incubation and fluorescence read. A 3D map of fluorescent signal shows a significant improvement for addition of membrane and incubation at lower temperatures but corner wells still read low.

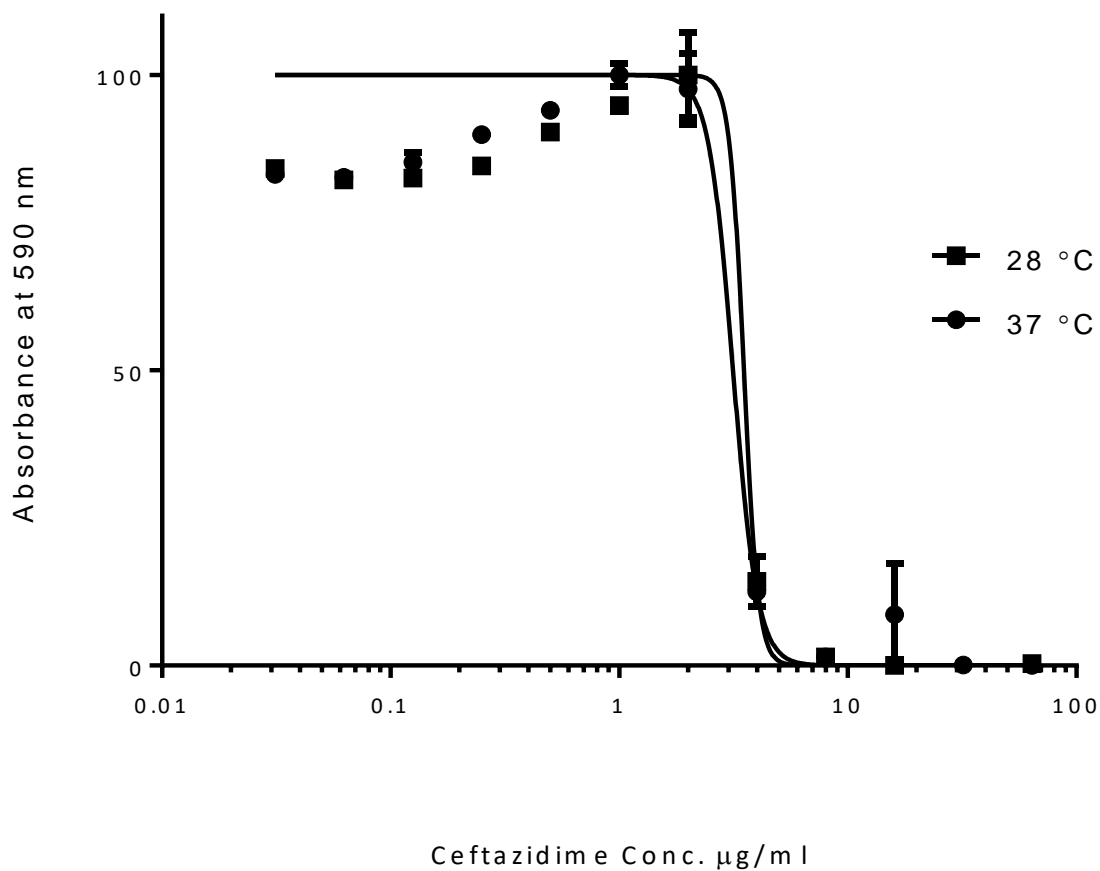


Figure 2.14: Ceftazidime MIC determination

Treatment of *B. thailandensis* culture with increasing concentrations of ceftazidime and overnight incubation determined that the MIC for ceftazidime not affected by incubation at the lower temperature of 28 °C. MIC for both temperatures was determined as 3.5 µg.ml⁻¹ +/- 0.4. There is a slight discernible upslope for concentrations up to 2 µg.ml⁻¹ which is caused by increasing concentration of compound in solution.

2.4.10. Maybridge screens

It was essential to carry out a proof of principle to make sure that PrestoBlue was not prone to providing false positive results. To do this, the assay was tested with a collection of fragment compounds from the Maybridge fragment compound library. This comprises of approximately 1000 small molecules which were tested at 1 mM. Initial screening provided operational optimisation of the assay and confidence in the assay's suitability.

Experimental Procedure

Burkholderia thailandensis E264 was cultured overnight in 100 ml LB media to OD₆₀₀ 1.6. 250 µl of culture was added to 10 X reaction tubes and centrifuged at 6000 x g for 5 minutes to pellet cells. Pellets were then resuspended to an optical density of OD₆₀₀ 0.4.

A persister solution for screening was created by resuspension in 1 ml M9 media with 400 µg/ml ceftazidime. Four fold upper and lower concentrations; 1.6 and 0.1 OD₆₀₀ were also produced. A negative, untreated control was created by resuspension in 1 ml M9 media and a positive control was made by heating in a block at 95 °C for 5 minutes allowing to cool and 500 µl M9 with 800 µg/ml ceftazidime added (M9ceft800).

43.6 µl of control solutions were added in triplicate to wells of a 384 well plate containing 1.6 µl DMSO.

Compounds in the Maybridge library are rule of three compliant and are provided in 96 well masterplates at 32 mM in DMSO solution. 1.6 µl of compounds from the Maybridge screens were aliquoted to the 384 well plate using a multichannel pipette before addition of 43.6 µl of *B. thailandensis* OD₆₀₀ 0.4. The maximum

DMSO concentration was 3.2%, and compounds were screened at 1 mM. The plate was centrifuged at 200 x *g* for 2 minutes before covering with a breathable membrane and incubating for 18 hours at 28 °C.

After incubation the membrane was removed and 5 µl PrestoBlue solution was added to each well of the assay plate then centrifuged at 200 x *g* for 2 minutes. The plate was left at room temperature for 30 minutes before reading fluorescence at ex 560 / em 590.

Results and Evaluation

Inhibiting activity of small molecules from 169 fragment compounds screened with the PrestoBlue persister assay is shown (Figure 2.15). Of 6 plates run; 2 gave Z' prime values greater than 0.5, which covered a total of 169 compounds. The distribution shows percentage inhibition for screening of 169 compounds at 1 mM in comparison to an untreated persister culture control. An untreated negative control and heat killed cell positive control were used to calculate Z' prime = 0.66 indicating a robust assay. There was a strong skew toward increased fluorescence with a median inhibition of -124.6, and standard deviation of 63.2. This high signal variability made it intractable to apply a statistical cut-off so, whilst two compounds appear to inhibit PrestoBlue fluorescence they cannot be deemed statistically significant.

For this experiment compounds were screened at 1 mM. This is significantly higher than is proposed for screening at the DDU, yet necessary when screening with fragment compounds due to their relatively low affinity binding to targets (Erlanson et al., 2004).

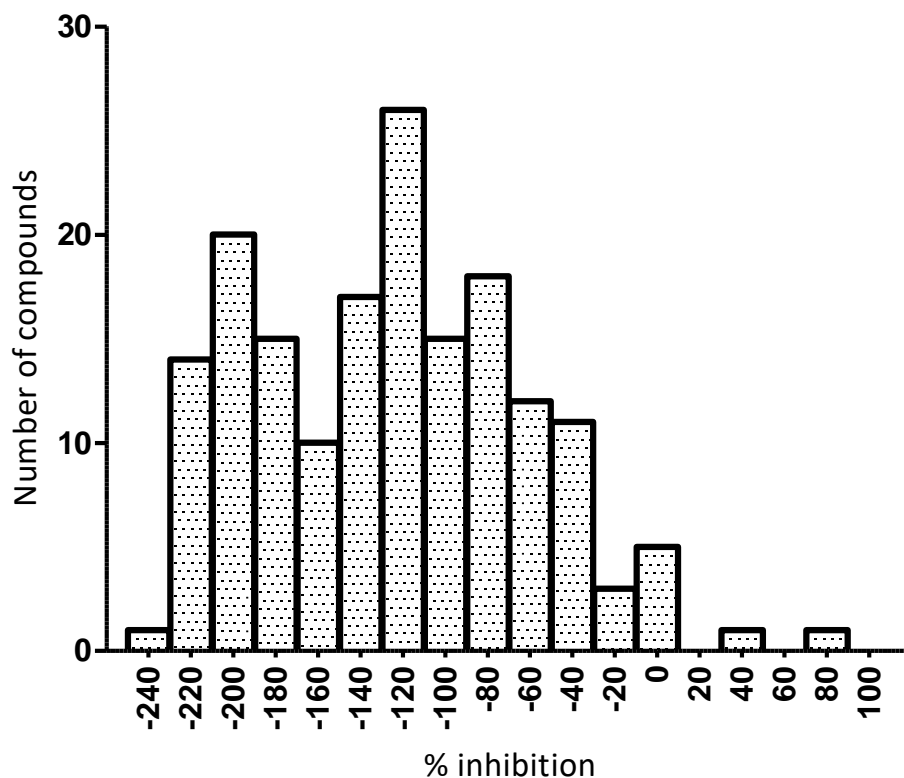


Figure 2.15: Screening of a fragment library with the PrestoBlue persister cell assay.

Distribution of a single point screen grouped in 10 % windows using the PrestoBlue cell viability assay against 169 compounds from plates 5 and 6 of the Maybridge fragment library. Positive and negative controls were embedded over several locations of a 24 well plate resulting in a Z' of 0.66 when comparing untreated persister culture to a killed cell control. Median activity was 124 % indicating that the majority of compounds tested resulted in an increase in fluorescence when compared to the persister culture control. Two compounds appear to reduced cell viability however due to the distribution and high standard deviation a statistical cut off could be applied.

3. High-Throughput Compound Screening

3.1. Overview

Work undertaken in chapter 3 was carried out at the Drug Discovery Unit (DDU), University of Dundee from October 2013 to March 2014. This chapter documents the optimisation and implementation of the PrestoBlue persistor cell assay developed and selected in chapter 2. In this section of work I carried out HTS of 61,250 compounds from the DDU's diversity library and the analysis and hit identification from the data collected.

The DDU collaborate with both academic research groups and the pharmaceutical industry to provide expertise and infrastructure for early-stage drug discovery. The DDU have a flexible business model collaborating with partners to translate academic led biological research into novel drug targets and candidate drugs. Typical projects for the DDU target diseases of the developing world and areas that are considered unprofitable for large pharmaceutical investment. From this point of view melioidosis fits clearly into their remit and this project benefited from their extensive portfolio and experience in screening biological assays.

Drug Discovery

This project was undertaken because, as outlined previously, there is an unmet clinical need for treatments to the disease melioidosis. My aim in this body of work was to identify active molecules and generate data to identify a target, to which activation or inhibition will result in a therapeutic effect.

Small molecule drugs make up the majority of conventional therapeutics. This is due to their low molecular weight, which allows them to diffuse across cell membranes, and the ability to bind to biopolymers such as proteins or nucleic acids to elicit an effect (Veber et al., 2002). More on small molecule pharmacology and drug suitability of small molecule compounds is covered later in this chapter.

The cost of drug discovery projects is continually increasing and the development pathway from discovering a hit compound to introduction of an approved clinical treatment is long and expensive (Duffy et al., 2012). A recent Deloitte analysis showed that the cost of developing a single asset increased from \$1.2 billion to \$1.6 billion between 2010 and 2015. Furthermore, the return on this research and development investment has approximately halved (Mullard, 2015). This can be attributed to market pressures and smaller patient volumes with drugs developing to become more targeted and specific. These figures are representative of the pharmaceutical industry as a whole. However, in recent years drug discovery investment into anti-infectives has seen significant cuts. This has been recognised by the industry, with particular focus on the development of new treatments to combat antibiotic resistance. At the 2016 World Economic Forum in Davos, Switzerland, a declaration was made by the Pharmaceutical, Biotechnology and Diagnostics Industries for alternative market structures to be implemented in combating antimicrobial resistance (Resistance, 2016). The declaration, signed by 85 companies, calls for governments to work with the industry to develop alternative market structures to provide a more stable model for research and development of new drugs and also to dissociate profitability of antibiotic drugs from the volume sold.

There are a number of approaches to drug discovery. Strategies for identifying hit compounds vary and the screening method employed must be suitable to the project requirements. One option is to use focussed screening where, if a potential target is known, computational modelling can be used to construct a 3D pharmacophore around known ligands. However, as mentioned previously, this method needs to start with a tractable target as a starting point (Valler and Green, 2000).

A hit compound can be defined as a molecule, which shows a robust dose-response activity in a primary screen. It is considered the output of screening (Valler and Green, 2000). Hit compounds provide a tangible starting point from which structural modifications can be made to improve potency and drug properties such as ADMET can be assessed for hit series (Duffy et al., 2012). Identified compound skeletons can then be manipulated to improve drug suitability and potency.

Label extension of existing drugs

One approach to addressing the urgent requirement for new treatments for neglected diseases has been to extend indications of current treatments (Rosenthal, 2003). This has the advantage of reducing the cost and time associated with drug discovery in an area which is unattractive to pharmaceutical investment. Successes in this approach include ivermectin. Initially indicated for use as a veterinary antiparasitic drug, ivermectin was shown to be effective in treating onchocerciasis, otherwise known as river blindness, a neglected tropical disease (Omura and Crump, 2004). A disadvantage of this approach is a risk of over reliance on label-extension and reluctance from the pharmaceutical industry

to allow their products to be extended to use in other patient classes for fear of unexpected toxicities (Pink et al., 2005).

Natural Products

Historically, the most successful drug leads have come from natural sources. Marine and terrestrial products have been administered through diet and natural remedies for millennia. Chemical purification and enhancement in the past centuries has improved the potency and scalability of these therapies (Dias et al., 2012) In addition to this, as that less than 10% of the world's biodiversity has been evaluated for drug activity, it is likely that there are many more natural product leads to discover (Cragg and Newman, 2013). Natural products are still a major source of new drug leads with over 100 new products in clinical development. The ease with which compounds can be produced using yeast and bacteria systems, and drug-like properties can be achieved through combinatorial chemistry, have modernised the use of natural products in drug discovery (Harvey, 2008).

The pharmaceutical industry has moved away from screening natural products in drug discovery over the past two decades (Lam, 2007). The rationale for this shift towards small molecule screening was the incompatibility of natural products with developing HTS technologies. Other difficulties included sourcing natural products and their isolation and structural characterisation. In addition, a lack of new discoveries led to the thinking that the "low-hanging fruit" had been exhausted as antibiotic resistance became ubiquitous (Singh and Barrett, 2006).

More recently, the value of natural antibiotics has been recognised once again and new methods of target identification such as the mining of biosynthetic

scaffolds have led rise to a fresh optimism (Johnston et al., 2016). This has also extended to the discovery of a new antibiotic termed teixobactin, which was discovered through screening of uncultivable bacteria in the soil environment (Ling et al., 2015).

High-Throughput Screening and Automated Liquid Handling

HTS allows testing of a large number of diverse chemical structures against targets or whole cells assays to identify hits. Although HTS incurs a greater input cost in assay development and significant investment in screening equipment, this is outweighed by many advantages. Significant improvements on traditional methods of drug discovery include greater reliability, high efficiency and a much greater scope for covering chemical space. The data harvest is also greatly increased (Liu et al., 2004). HTS is characterised by automated liquid handling, a specific and optimised bioassay, an extensive library of compounds and most crucially the information technology to acquire and analyse data. Detection by fluorescence is a favoured method as these methods are simple, fast and can be scaled down in volume. The ability to work in volumes in the microliter and nanoliter range also reduces reagent costs and enables more data to be acquired from precious resources (LaVan et al., 2002). Equipment such as the Echo 555 liquid handler (Labcyte) allows fast, accurate and precise transfers of nanoliter volumes without waste and minimal risk of contamination.

The DDU Diversity Compound Library

Screening took place with the DDU's 'diversity' set of compounds. This library differs in design from "Lipinski's rule of 5" for drug compounds being focused

towards 'lead compounds'. Compounds compliant with the "rule of five" have no more than 5 hydrogen bond donors; no more than 10 hydrogen bond acceptors; a molecular mass less than 500 daltons and an octanol-water partition coefficient ($\text{Log } P$) less than 5 (Lipinski et al., 2001). Intelligent sample synthesis and acquisition has created a library of molecules that improve coverage of chemical space using fewer compounds than traditionally used by the pharmaceutical industry. This has the advantage of reducing the operational requirements for screening and in making small molecule drug discovery accessible to a greater number of projects with less investment needed. The library is also strategically designed for antimicrobial discovery. This differs from most screening libraries which are based heavily on past discovery campaigns. These are heavily biased towards kinases, G protein coupled receptors and mammalian ion channels.

Molecules included in the DDU's diversity screen are typically around 200 to 300 daltons which is smaller than the 500 daltons stated by Lipinski's "rule of 5" (Lipinski et al., 2001). Smaller compounds are usually preferred in screening libraries due to strict limits of druggability in which properties such as low molecular weight, lipophilicity and the number hydrogen bond donors and acceptors can have a large effect on the suitability of a potential orally administered drug (Wenlock et al., 2003). Compound selection and pharmacology is discussed further in chapter 4.5.

Chemical space is the ensemble of all possible molecules in an energetically stable state (Reymond et al., 2010). Mathematically it is impossible to cover all possible drug molecules which have been estimated to exceed 10^{40} possible

molecules (Valler and Green, 2000). Whilst it is impossible to cover all of the space, the DDU diversity library aims to cover as large an area as is possible with 200-300 Da molecules. The aim in developing this library and a target for the whole drug discovery field is to increase the chances of identifying “winners” for target molecules.

Data acquisition and processing is the crucial step in transferring extensive screening data into meaningful results. The DDU use ActivityBase software (IBDS) screening data management software which collates every raw data file obtained in the facility automatically. Screening data can then be matched with chemical structure information using Vortex software (Dotmatics) and reports created using vast arrays of screening data. This enables staff at the DDU to cross reference screens and build up multiple assay data for each compound in the library.

Drug discovery in melioidosis

Drug discovery for neglected infectious diseases such as melioidosis is not economically attractive to the pharmaceutical industry. However, it is vital that new treatments for these diseases are developed to alleviate the burden of infectious disease. Neglected infectious diseases suppress economies of developing countries and more importantly prevent people living in these countries from having the prosperity and longevity we enjoy in developed nations (Katsuno et al., 2015).

In order to develop new treatments for melioidosis alternative streams of funding have to be sources. These are most likely to be government and academic based

drug discovery programs. As such new thinking and creativity is needed to discover high quality target leads with the restricted availability of resources.

One drug discovery program for melioidosis reports to have developed a whole animal HTS platform capable of screening 300, 000 compounds (Lakshmanan et al., 2014). However, it is worth noting that this study was published in an journal with impact factor = 1.2; which is not open access and has only been cited once, so I cannot comment on the legitimacy of this statement.

Other investigations include a structural biology approach targeting macrophage infectivity potentiators (Mips) (Begley et al., 2014). Furthermore, an early stage study has looked at novel targets for drug discovery in *B. pseudomallei* targeting CPS synthesis and the heptokinase WcbL (Vivoli et al., 2015).

3.2. Assay optimization

In order to be confident in using the PrestoBlue persistor assay for HTS, it was necessary to validate all aspects of the assay. From the work carried out in the assay development stage I had confidence that the assay was biologically and pharmacologically relevant. In the stages before HTS was carried out, it was necessary to confirm that the assay performance was robust and translated to the DDU facilities effectively.

Assays robustness is established through use of the Z' prime as previously covered (Equation 2.1). Assay performance tests also looked at signal variation using the coefficient of variation (% CV) to confirm that all wells of assay plates gave consistent results. The coefficient of variation is calculated as the ratio of standard deviation to the mean.

Controls

During assay development it was shown that a suitable positive control to show a “full kill” of all cells could be obtained by heating cells to 90 °C for 5 minutes. During preliminary screening at the Drug Discovery Unit this was repeated to determine that minimal difference in values and signal variation between heat treated cells and M9 minimal media were seen. Therefore it would be operationally beneficial to use media only as a lower fluorescence boundary for ‘hit’ selection as it is difficult to reliably heat kill large volumes of cells.

Screening with a Bioactive Set

A library consisting of 1,000 compounds from the DDU Diversity library was used as a preliminary screen for assay optimisation. The library was screened at 10 µM and 50 µM to determine an optimum concentration for the assay. The bioactive set contains a large diversity of compounds to cover the largest possible area of chemical space; this can be used in further analysis to identify trends in hit compounds.

3.3. Experimental Procedures for Screening

Large volume production of persister culture

As in section 2.3.1, a culture of *B. thailandensis* E264 was produced from a frozen glycerol stock streaked on LB agar and incubated for 20 hours at 37 °C. A single colony was picked to inoculate 1 L LB broth and incubated for 18 hours at 37 °C with aeration at 200 rpm. Cell density at OD₆₀₀ was measured and the volume of overnight culture required to make 1.5 L persister culture at OD₆₀₀ 0.4 was calculated. This volume was centrifuged at 600 x g for 10 minutes, the

supernatant discarded and cells resuspended in 1.5 L M9 minimal media (Harwood C. R., 1990). Ceftazidime hydrate dissolved in M9 was added to make total concentration 0.4 g/L.

Z' prime and signal variance determination:

To carry out a chequerboard experiment, 45 µl of persister culture was added to wells A1 – H12 and I13 – P24 of a black walled, clear bottom 384 well assay plate (Greiner: SKU – CLS3766) using a Matrix Wellmate microplate filler. 45 µl heat killed cell culture was added to all wells of the opposite well quadrants: I1 to P12 and A13 to H24. The plate was centrifuged for 2 minutes at 58 x g and incubated for 18 hours at 28 °C. After incubation 5 µl of PrestoBlue reagent was added to all wells. The plates were centrifuged at 58 x g for 2 minutes and left at room temperature for 1 hour. A PHERAstar microplate reader was used to measure fluorescence at ex 540 nm / em 590 nm with data directly uploaded to ActivityBase (IDBS). Repeated readings taken at 5 minute intervals from 15 minutes to 45 minutes.

A further experiment with persister culture in all wells was carried out by addition of 45 µl of persister culture was added to each well of a 384 well assay plate. A breathable membrane (Sigma-Aldrich: SKU Z380059) was added and the plate was centrifuged at 58 x g for 2 minutes before being incubated statically for 18 hours at 28 °C. Following incubation the membrane was removed and 5 µl PrestoBlue reagent added. The plate was centrifuged at 58 x g for 2 minutes and incubated at room temperature for 1 hour before fluorescence was read.

Assay plate preparation for screening

The DDU library contains 62,250 compounds prepared as 10 mM stock solutions in DMSO. Stocks are stored in 384-well echo plates under inert gas conditions. Assay plates were prepared from stock solutions using an Echo 550 liquid handling robot (Labcyte).

For the bioactive set, 45 nl of compound stock solution was acoustically dispensed from a DDU masterplate to a 384 well assay plate to screen at 10 μ M; for screening at 50 μ M, 225 nl was dispensed. Columns 23 and 24 of assay plates contained DMSO only.

For the diversity set, 135 nl of compound stock solution was added to each well resulting in a screening concentration of 30 μ M. Again columns 23 and 24 contained only DMSO as a control.

A Wellmate microplate filler (Matrix) was used to dispense 45 μ l of persistor culture to columns 1-23 of assay plates and 45 μ l M9 minimal media to column 24 to provide negative control.

A breathable membrane (Sigma – Z763624) was applied to assay plates which were then centrifuged at 58 x *g* for 5 minutes and incubated statically for 18 hours at 28 °C and 5% CO₂. After removal of the membrane, 5 μ l PrestoBlue reagent was dispensed to all wells. Plates were centrifuged at 58 x *g* for 5 minutes and incubated at room temperature for 1 hour before fluorescence was read at ex 540 nm, em 590 nm with a gain of 300 using a Pherastar plate reader writing directly to Activity Base (IDBS) data management platform.

Hit confirmation and Potency Determination

Hit compounds identified through single point screening were cherry-picked into 384 well Echo plates using the Biomek FX automated handling workstation (Beckman Coulter). Ten, two-fold serial dilutions of each compound with a maximum concentration of 100 μ M were performed using an Echo550. Plates were then treated as above and results analysed to determine potency through IC_{50} calculation.

Data Analysis

Data processing and analysis was conducted within Activity Base (IDBS) with report creation undertaken using Vortex. All IC_{50} curve fitting was undertaken within Activity Base XE utilising the underlying 'MATH IQ' engine of XLfit version 5.1.0.0 from IDBS. This is a functional add on to Microsoft Excel and fits dose-response curves using the same fitting formula as previous described in Prism Graphpad. A 4-parameter logistic dose-response curve was used for compound potency determination, which has been defined by reference to the negative log molar value at the point of inflection of any sigmoidal concentration-response curve generated (pIC_{50}). Equation: $y = A + (B - A) / (1 + ((10C) / x)^D)$, where A = % inhibition at bottom, B = % inhibition at top, C = 50 % effect concentration (IC_{50}), D = slope, x = inhibitor concentration and y = % inhibition. As IC_{50} values are Log normally distributed, data is presented as the pIC_{50} ($-\log_{10}[IC_{50}]$).

3.4. Results

Z' prime and Coefficient of variance

The coefficient of variation shows the extent of variability in relation to the mean. It is used in assay development alongside the Z' prime as a quality control where plate effect may occur and is useful for comparison between data sets.

To identify positional effects and calculate signal variance a chequerboard 384 well assay plate was incubated with two quadrants containing a persister cell culture and opposing quadrants containing a heat killed cell negative. For this experiment maximum signal variance was 11.2 %CV and the Z' prime was equal to 0.68 (Figure 3.1). The high signal variance identified an edge effect with wells on the edge of the plate displaying lower than average fluorescence.

In response to the high %CV observed in the chequerboard, the assay was modified to include the addition of a breathable membrane during the incubation step. In an experiment where all wells contained persister culture the %CV was reduced to a maximum of 8.7 % and edge effect was improved (Figure 3.2).

The chequerboard experiment was repeated and fluorescence read over a range of times for incubation with the PrestoBlue to determine the optimum time interval for incubation with the fluorescent reagent. It was important to determine an appropriate time window that gives acceptable Z' primes as this would impact on the batch size that can be run per day. Figure 3.3 shows that the robustness of the assay increases over incubation time with PrestoBlue. It took between 40 and 45 minutes of incubation at room temperature to achieve $Z' \geq 0.5$. Figure 3.3 shows readings between 15 and 45 minutes incubation time. The Z' prime may

have improved, as could be extrapolated from the graph, by incubating for longer. However, after 45 minutes the experiment met the threshold of $Z' > 0.5$ and the operational requirements of the DDU laboratory required the use of the plate reader leading to the experiment being stopped. I concluded that 40 minutes of incubation would be suitable and that whilst the assay may have been further improved given more time, HTS requires compromises to be made providing results meet the stipulated quality threshold.

Use of M9 media as a control for 100% inhibition was confirmed to be an acceptable alternative to heat killed cells with no significant difference between the two treatments (Figure 3.4). This was more convenient for running HTS and also removed the difficulty of completely sterilising large volumes of culture. A Z' of 0.25 was obtained for the difference between persister cell culture and M9 media; however this relatively low Z' value was mostly likely due to the large signal variance of 18.9 %CV observed in this experiment.

Preliminary experiments in preparing for HTS included comparing assay plates from five different manufacturers using Z' prime and signal variance as means of selection (Greiner 384 well, black walled, clear bottom, SKU – CLS3766). In addition, a chequerboard experiment was run to identify any plate effect or a systematic inconsistency between well locations (data not shown).

34541	32775	35775	33004	36496	32964	36523	32126	35959	32260	35325	31841	210004	225253	205696	226069	200933	211218	205364	214573	212510	187836	203116	184889
31582	36080	33931	37650	34433	37594	34104	37418	34369	36523	34015	37112	235332	227906	221007	209760	218491	215625	199173	198023	212103	197264	202371	223241
34943	32761	36844	34335	37885	34429	37561	34427	37648	34391	37441	34540	213365	228417	204055	212151	202811	204720	213632	204727	201299	196606	209503	197754
31726	36921	34372	38636	35476	39667	36043	38790	35669	38743	35357	39427	220863	215778	212778	215698	210209	217223	224542	213954	211402	205593	217257	230927
35709	33694	38365	36426	39970	36534	39737	35894	38975	36185	39666	36632	189598	204139	192276	196022	198076	205488	201450	211409	198597	212443	214718	215512
33377	38382	36669	41262	36784	40303	36165	40171	36288	40195	36998	42306	214520	214014	230949	221480	234197	218226	223538	220001	223456	211989	212381	241433
35181	35155	38535	36688	39396	36092	39295	36376	39834	36796	40419	38578	183646	188102	186348	187093	183376	186605	189411	201394	196263	194331	206111	206402
32864	37970	35594	39168	36674	40240	37579	40753	37465	41206	39216	45568	206793	195579	187348	176857	183050	177114	177928	178152	190132	192161	205727	213254
225576	209867	192895	208231	205862	210565	199409	208051	186366	193860	177716	174402	41477	39692	42520	37895	40363	36800	40277	36772	40331	36468	38848	33255
236213	225801	211980	201456	208455	206166	207486	216251	211237	198755	182641	170830	39142	41701	37183	41409	37115	40392	36957	40551	36802	40065	36290	36765
219699	210901	191825	203950	196248	203261	201973	217319	203294	205595	182324	172640	41288	38018	40430	37431	40054	36917	40106	37541	39950	36004	39161	33403
243570	215452	208501	204663	203431	203891	206505	210246	218473	198139	180887	163825	38766	41622	37190	40471	37372	40763	37507	41377	37193	40146	36189	37380
246860	205721	188813	195881	187330	193523	187624	205807	191689	211789	184580	177871	39922	36325	39470	36180	39920	36038	40005	36587	39732	35768	38799	33493
242669	216494	201911	191339	199826	186774	193955	194001	211770	202862	189730	177213	36584	39874	36028	40448	36478	39889	36439	40345	36534	39776	35520	36442
233801	207250	194067	188942	183822	183230	188818	199631	200106	196906	200999	189691	39989	36360	39433	36844	39661	36220	39758	36309	40082	35739	39266	33449
219512	225801	225767	204205	203441	203217	195996	212378	196398	216863	207373	206174	34225	38364	33948	38166	34666	38421	34182	38257	34098	36562	33690	33418

Figure 3.1: A checkboard of persister cell culture to show positional plate effects.

Persister culture is shown in red and heat killed cells green, Intensity of colour indicates the signal strength. Maximum signal variance was 11.2 %CV, $Z' = 0.68$. Persister culture (45 μ l) was added to all wells of a 384 well plate with live cells in wells shaded red and heat inactivated cells in green. The plate was incubated statically overnight. This experiment identifies positional effects on readings covering all relative positions on the plate with both positive and negative control values. Relative fluorescence units (RFU) are given for all wells showing significantly decreased fluorescence in edge and corner wells compared to central wells ($P = 0.011$).

	1	2	3	4	5	6	7	8	9	10	11	12	13	14	15	16	17	18	19	20	21	22	23	24	%cv
A	179057	174439	175471	182618	182260	177696	182589	179501	197458	180502	192266	193762	188194	188776	181983	187953	183682	180139	185258	193286	192992	182969	184526	196362	3.2
B	168385	175270	177513	192978	178931	192534	183322	187045	177136	188383	176572	188329	185876	184304	177130	185705	181113	197500	187096	208079	200029	185715	169832	172063	5.5
C	164518	180820	187172	184120	196307	185656	212968	190690	200019	185698	197153	186368	198862	183950	197453	184611	202479	196682	213379	191565	210413	192788	189399	168158	6.6
D	175267	208431	187443	208416	193053	216922	193523	214666	182645	192230	183267	195926	178412	195709	183810	195371	180927	213340	209429	228981	201509	204535	178973	192110	7.5
E	191915	186839	211151	187928	209740	194922	207707	190276	200922	186195	204192	187210	200860	196232	191389	179323	196899	200535	224845	203750	207476	195985	195498	190990	5.4
F	168690	213035	199265	220074	199352	215745	188061	203377	194359	213089	193984	205427	199967	211041	191730	205309	187735	222332	218138	241587	204795	211111	195629	204980	7.2
G	178954	174030	214730	184691	208873	179760	207666	188346	209589	200981	202289	182045	203691	192420	216651	196883	199845	199876	243704	210609	221248	198218	209416	188446	8.4
H	181303	210750	192547	220074	191292	211139	193642	212577	190557	219271	202272	213502	200826	211257	201656	207166	199868	220376	217721	229989	212117	215163	191329	203339	6.0
I	179564	190659	203951	189039	205448	189260	209602	191447	209608	197260	207698	212893	219715	227371	220306	201545	203228	210118	218809	210205	202405	194559	197489	195789	6.0
J	176052	219645	196600	214716	199198	213414	196333	215961	200407	211638	198144	213184	208361	215871	205693	203849	201603	215162	208010	226245	208831	207287	195311	210096	5.0
K	177058	186283	207811	193171	208674	175650	214445	199005	202958	182373	204600	208377	225043	213730	213393	199525	198265	197565	217050	206334	216341	190132	199349	189937	6.9
L	176660	218595	200065	200842	202219	212511	199158	218051	203494	203797	199058	211524	203104	210857	200979	202620	202962	209925	201762	229604	201881	206920	194487	210526	4.8
M	188549	186405	207884	186192	193139	189986	210415	191198	201117	181659	193444	196105	211473	207978	202156	192299	203752	195083	207263	193146	196739	188532	202949	200359	4.3
N	193056	214677	202381	223124	199943	221032	198099	219715	197165	218269	195311	202997	196643	206456	193729	217943	194240	205466	191317	205218	190861	195872	187548	208555	5.2
O	186167	178625	211032	188519	200032	193684	203862	194986	216953	182350	190856	197169	213132	190457	204253	193330	198635	192847	200017	191918	200307	200837	218763	199494	5.2
P	171174	199886	187392	219980	192533	206613	179519	190851	179529	190498	179473	200266	186908	197868	198648	199958	179928	205707	179082	198942	189866	223655	206931	207995	6.4
%CV	4.6	8.7	6.1	7.6	4.5	7.7	5.7	6.5	5.5	7.0	4.6	5.3	6.3	6.3	6.1	5.0	4.6	5.4	8.0	7.6	4.4	5.6	6.1	6.4	

Figure 3.2: Distributional effects of persister cells in 384 well assay plate.

A schematic of a 384 well assay plate with persister culture in all wells. 45 µl persister cell culture was added to all wells. %CV is shown across rows and down columns. Green indicates > 200, 000 RFU; red indicates < 190, 000 RFU. Intensity of colour indicates the deviation from the mean. An edge effect is apparent primarily in rows A, B and P and columns 1, 2, 23 and 24. Edge effect is observed where readings on the outer wells of a plate give anomalous readings often due to a higher rate of evaporation during incubation. The maximum % CV observed = 8.7 for column 2. This reduction from 11.2 % in Figure 3.1 is attributed to the addition of a breathable membrane during incubation.

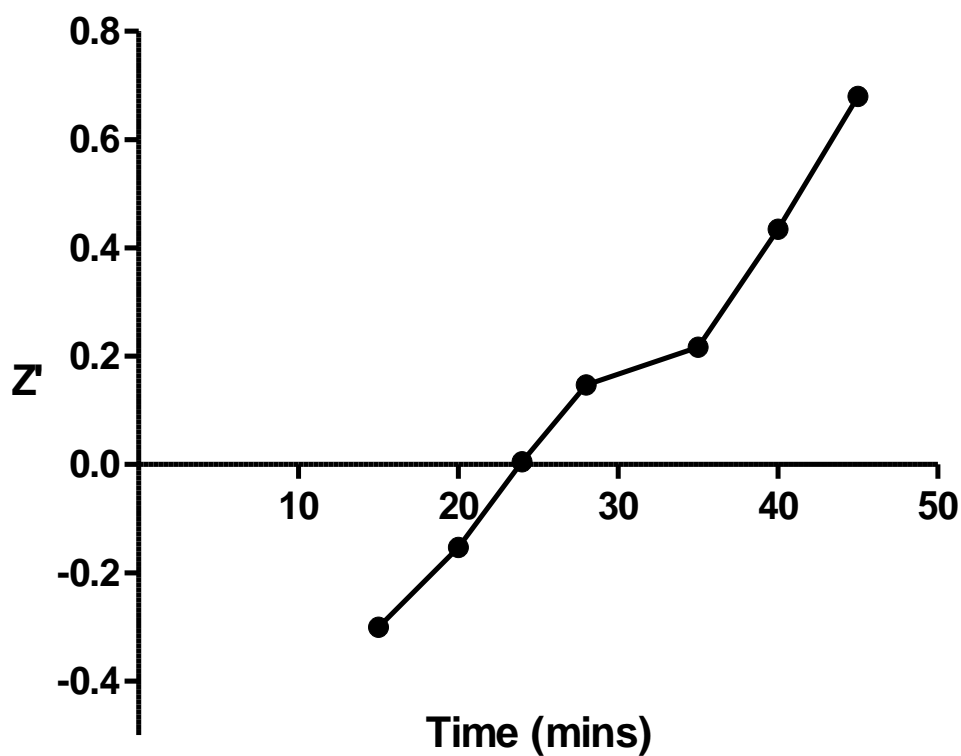


Figure 3.3: Determining the optimum incubation time for a robust Z' value.

5 μ l PrestoBlue was added to a chequer board of persister culture and heat killed cells and incubated at room temperature inside a plate reader with fluorescence read at 5 minute time intervals. It is hypothesised that the signal to noise ratio as interpreted through Z' improves due to the accumulation of the fluorophore rezorufin over time resulting in a higher relative fluorescence per viable cell. Z' prime was calculated to determine the optimum incubation time between addition of PrestoBlue and reading fluorescence.

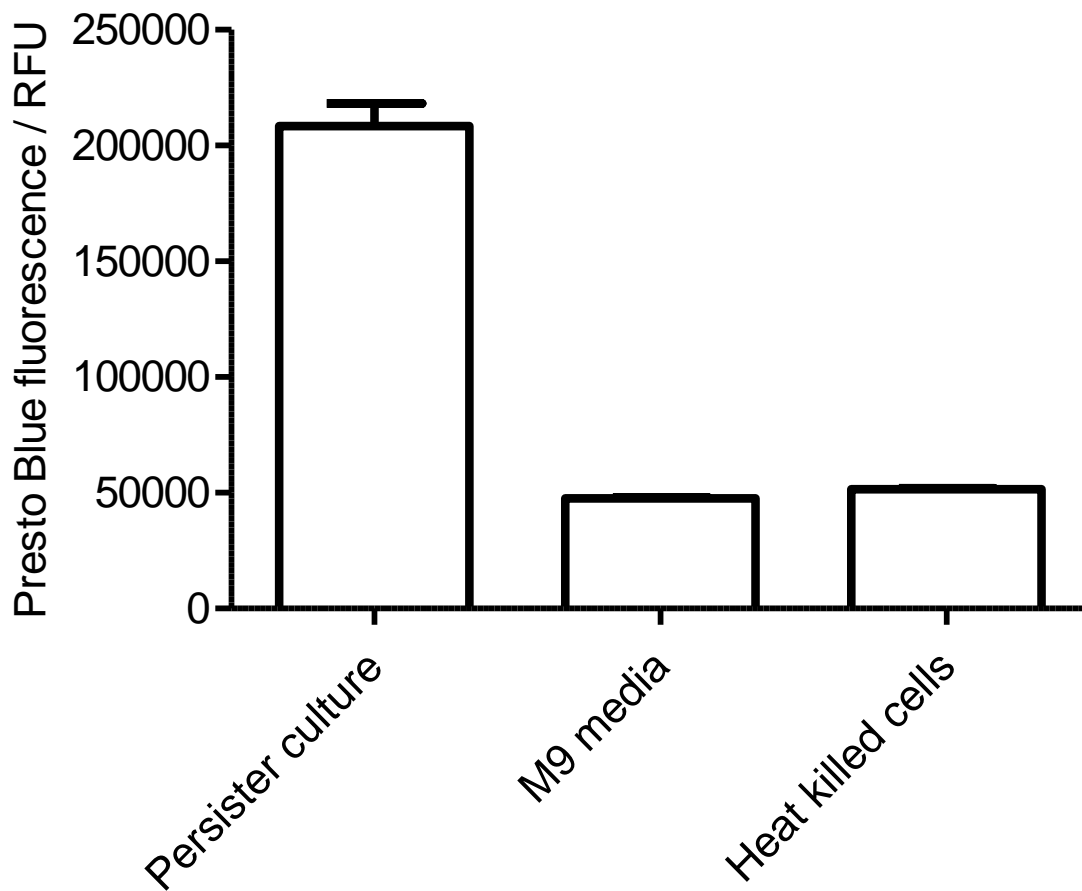


Figure 3.4: Comparison of heat killed cells to minimal media for use as a positive control.

A comparison of heat killed *B. thailandensis* cells to M9 media carried out at the DDU confirmed that M9 media could be used as an appropriate “100% inhibition” control. Results show mean for 16 replicates for each condition positioned down a column length of a 384 well assay plate. Error bars indicate standard error. Z' for persister culture to M9 media = 0.25; Z' for persister culture to heat killed cells = 0.22. The coefficient of variation (%CV) for persister culture = 18.9%; for M9 media = 2.1; for heat killed cells = 3.0.

Screening of BioActive Set (1,000 compounds)

Screening was carried out at 10 μM and 50 μM . 50 μM gave an optimum hit rate (i.e. greater than 0.5%) so would be a more suitable concentration to screen at. However, this uses a larger volume of compounds and takes significantly longer to create assay plates using the Echo liquid handler. Therefore, as a compromise it was decided to screen at 30 μM . This was also appropriate as any compounds active at 50 μM but not at 30 μM are unlikely to meet further criteria as a suitable drug compound.

Screening of Diversity Library

61,250 compounds tested were tested over a two week period. All plates passed quality control (robust Z' > 0.5) with the robust Z' prime for the overall screen of 177 assay plates being 0.71 +/- 0.12.

To define the criteria for selecting hits, the primary screen data was plotted as a frequency distribution graph (Figure 3.6). The data shows a relatively unusual distribution for a general screen. While the majority of compounds return a low percent effect value, there is an active negative tail where molecules look to have resulted in more growth, in some cases over the 100% control. This prevents the use of the distribution of the negative tail to calculate the statistical cut-off for identifying hits. In this case, the distribution of the positive tail was used to calculate the standard deviation, allowing for the small skew in the baseline. It should be noted that in four of the five single shot screening runs the positive skew was larger. In a single run, the skew was marginally negative. Because the skew was in the negative tail it is more likely that we encounter false negative hits than false positive.

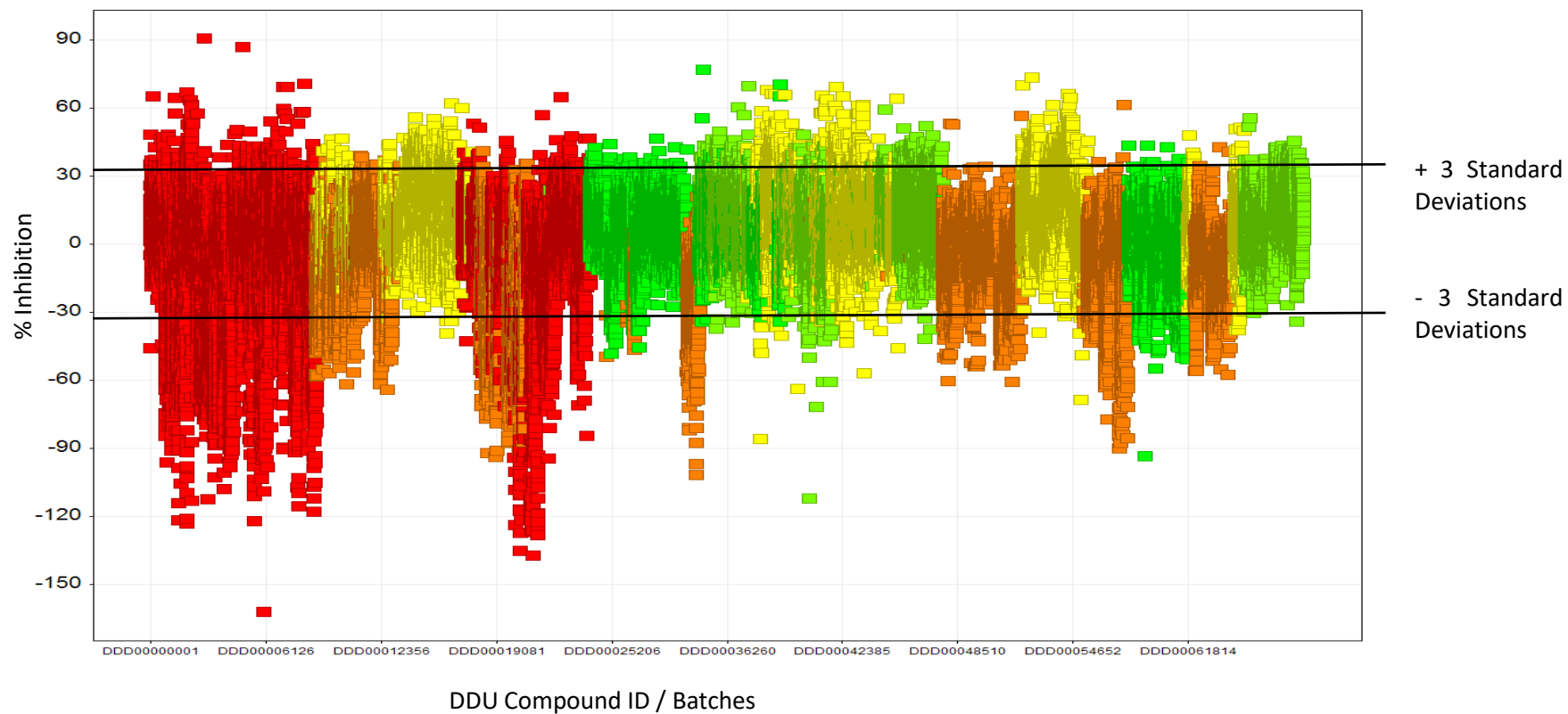


Figure 3.5: Distribution of percentage inhibition for screening batches.

Green results indicate first test sets through to yellow and red indicating latter test sets of screening. Results showing higher inhibition are more statistically robust than those showing reduced inhibition.

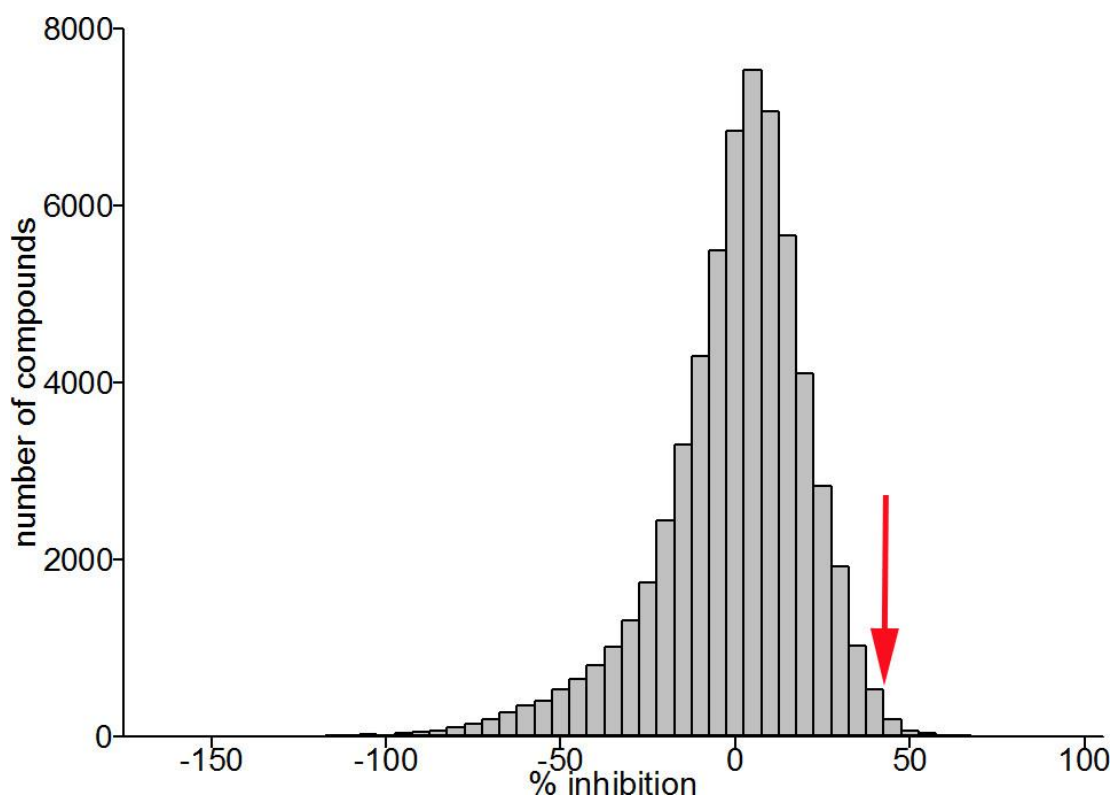


Figure 3.6: Distribution of percentage inhibition for high throughput screening.

Inhibiting activity of test compounds from 61,250 compounds screened with a phenotypic assay using a *B. thailandensis* persister culture as shown by PrestoBlue reduction. The distribution shows percentage inhibition grouped in 5% windows for high throughput screening of 61,250 compounds at 30 μ M, as compared to a heat killed cell control. The median activity is 5.3%. The standard deviation of the positive tail is 9.65%, giving a statistical cut-off for activity of 34.3% determined as the first bin at greater than three standard deviations from the mean. The arrow indicates the selected pragmatic threshold at 45%: 345 compounds were identified as 'hits' according to this criterion. 45% was chosen to reduce the number of hits to an amount considered amenable to downstream secondary assays. 309 compounds were selected based on high activity, or as analogues of compounds with high activity present in the collection, which have good physicochemical properties.

Output	Result	% of total
Number of compounds screened	61,250	
Hit Identification threshold	34.40%	
Putative hits > 33.8% inhibition	2,092	3.4
Compounds in full curve	309	0.5
Compounds with $pIC_{50} > 5$	29	0.05

Table 3.1: Summary of screen outcome for diversity library.

From initial screening 309 hits showing between 45.6 and 74.2 % inhibition were 'cherry picked' for further investigation, with the threshold for selection being determined from the distribution of compound inhibition (Figure 3.6) using three standard deviations from the mean as a guideline. "Cherry Picking is a term coined by Novartis to mean further testing of a smaller subset of compounds from a primary screen or statistical model.

Hit confirmation

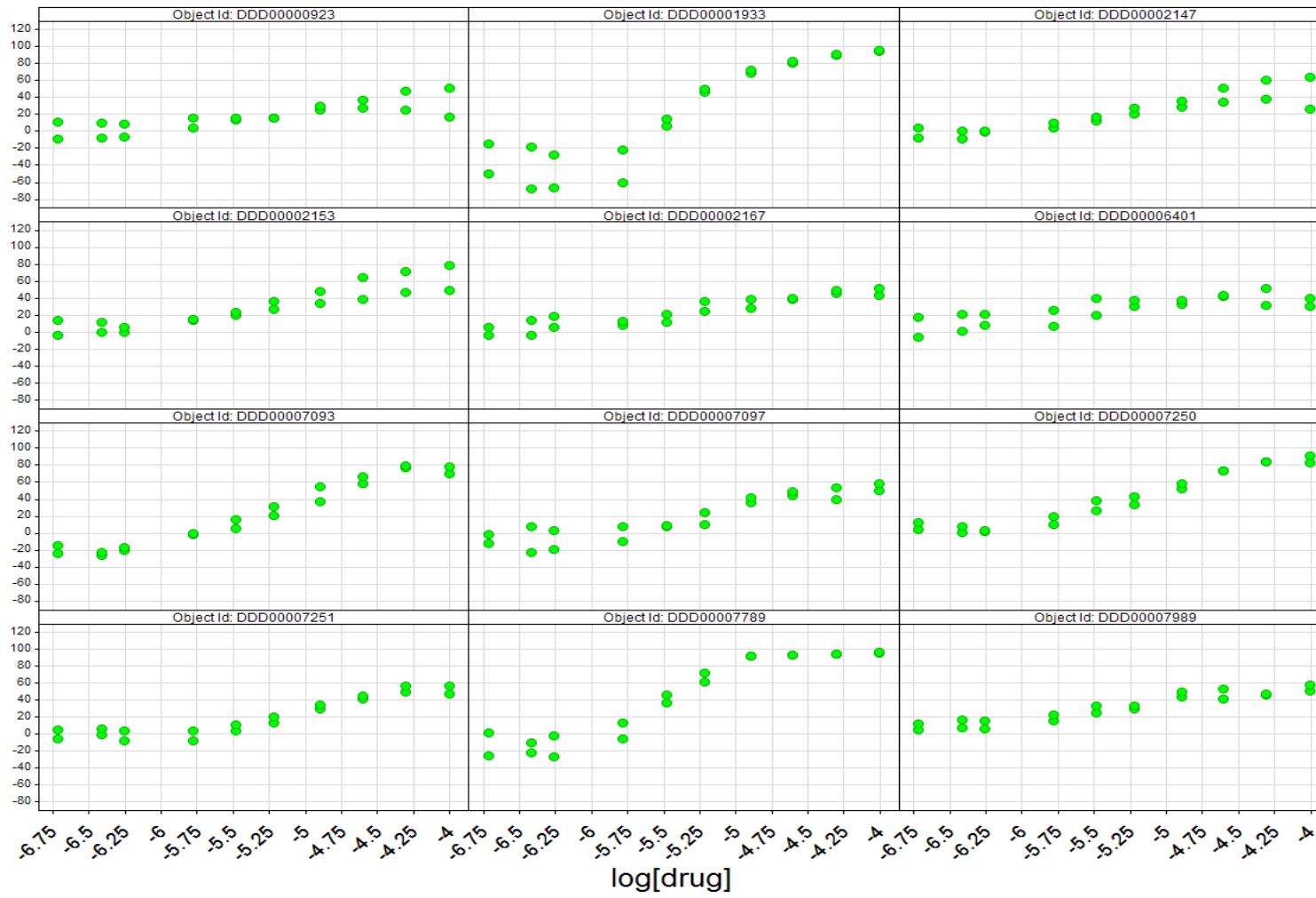
Primary single point screening took place for the 61,250 compounds. As expected, the majority of the compounds were inactive (Figure 3.6). Using the median percentage effect (5.3%) plus three standard deviations (9.7%), a statistically significant cut-off of 34.3% inhibition was determined. This identified 2,092 unique compounds as 'hits', exceeding the capability for downstream analysis. As a result, a pragmatic cut off of 45% inhibition was selected (Figure 3.6, red arrow), resulting in 345 unique compounds. Some of these were de-selected due to known promiscuity issues.

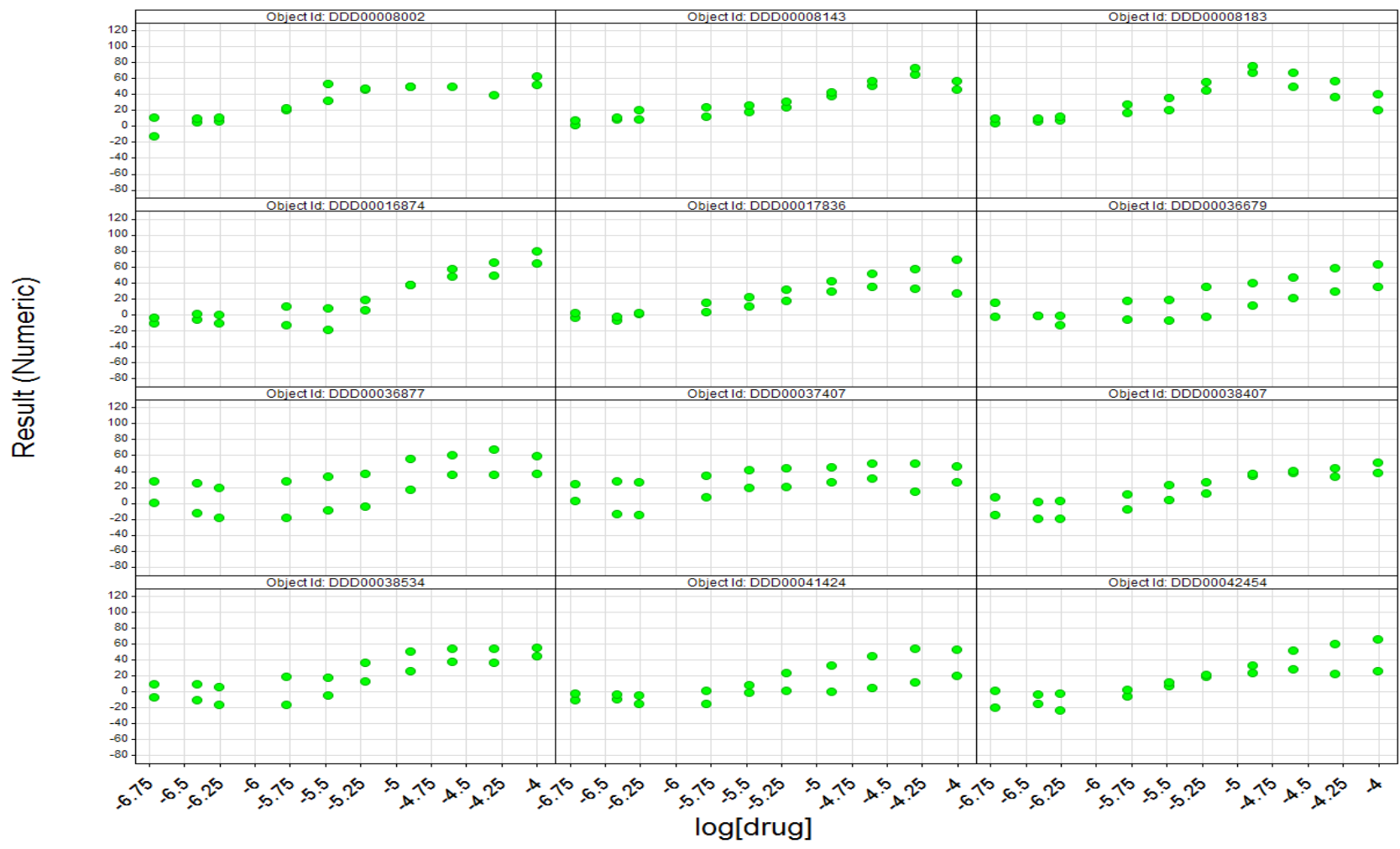
I selected 309 compounds for detailed screening: these included some near analogues to hits from within the DDU collection that show high activity and good physiochemical properties. For these 309 compounds, a ten point, 2-fold, concentration response assay was performed in duplicate (Figure 3.7) with criteria for a positive hit set as greater than 50% inhibition at the highest concentration tested (100 μ M). Acceptable concentration response relationships were returned for 58 compounds, of which 29 showed pIC_{50} values > 5 .

LC-MS confirmation of compound purity

Compound purity checked by liquid chromatography mass spectrometry (LCMS). This is an important consideration as impurities from the synthesis of compounds such as residual heavy metals can lead to false positives. The technique does have limitations for checking purity in that it is unlikely to resolve enantiomers. LCMS was carried out by DDU research staff. (Di and Kerns, 2006) (Table 5 in Appendix document DDU report)

Result (Numeric)





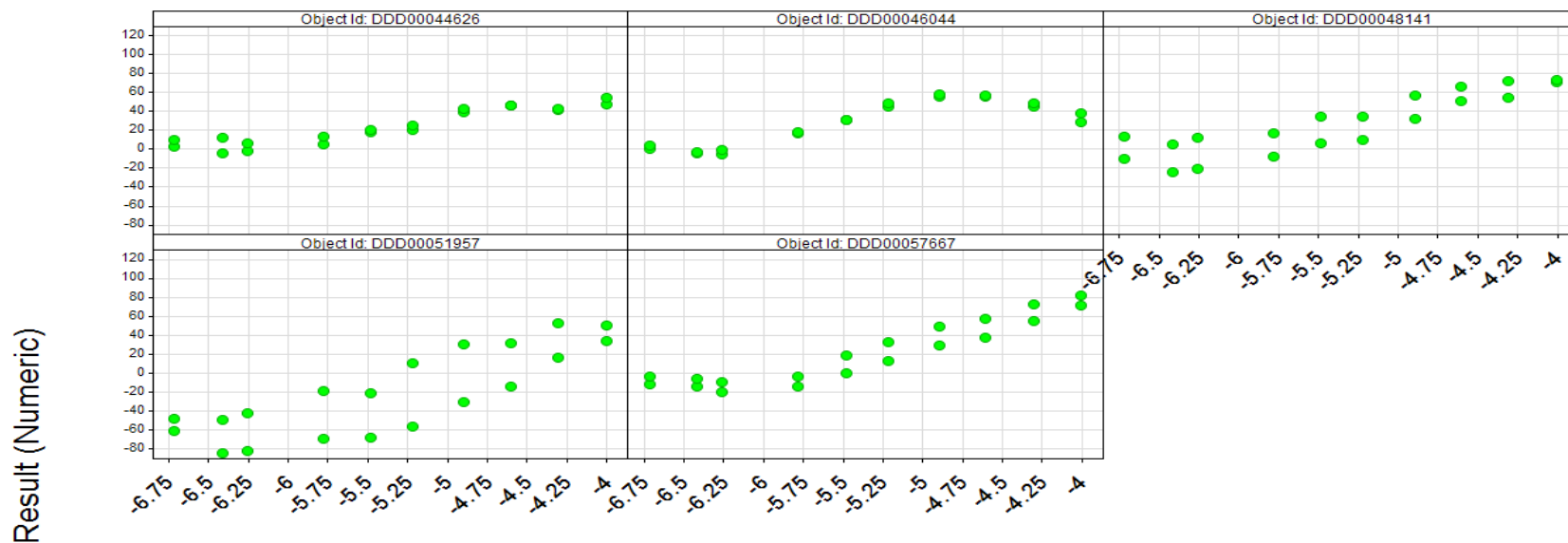


Figure 3.7: Primary dose response assays for “Hit compounds”.

Compounds cherry picked from an initial single point screen at 30 μM were selected for dose response investigation. Of 309 hit compounds 58 compounds exhibited concentration dependent killing of which the 29 compounds shown exhibited a $pIC_{50} > 5$. Results show % inhibition as measured by the PrestoBlue persister assay in comparison to a blank media control. Compounds were tested in duplicate using a standard ten point half logarithm concentration range from a top concentration of 100 μM .

3.5. Discussion

There are many different approaches to drug discovery and hit identification. This project benefited from the professional experience of scientists at the DDU. The assay used for HTS and methods employed were all approved by the DDU so, whilst some procedures may deviate from traditional means of screening, I am confident that my approach was appropriate and that the results of screening are legitimate.

One of the most frequent parameters used to assess screening results in drug discovery is the IC_{50} (Gubler et al., 2013). Where concentration effect relationships are evident, the IC_{50} denotes the concentration at which 50 % inhibition is attained, relative to the maximal and minimal effect observed. IC_{50} values can be used in drug discovery to prioritise compounds in order of potency (Sebaugh, 2011). In order to fit an IC_{50} curve, at least two points are required in the upper and lower plateaus of maximal and minimal effect in order to determine the relative IC_{50} accurately. In this study I have used pIC_{50} ($-\log_{10}[IC_{50}]$) where higher values indicate exponentially increasing potency (Selvaraj et al., 2011).

It was necessary to re-optimize the assay from its development at Exeter for use with the DDU facilities. Due to the differences in scale, significantly larger quantities of persister culture needed to be made with consistency. It was vital to the biology of the assay that the persister was prepared and treated identically to ensure the results were reliable. Another consideration was the importance of designing and working to a standard operating protocol (SOP). This ensured that although less time and attention were paid to individual batches, all plates in the screen would be consistent and meet quality control stipulations. Another cause for re-optimisation of the assay was to account for differences in the equipment used, such as the plate reader and automated

liquid handling. The SOP included an analysis template which stipulated control locations on the plate and barcoded details of assay plates and compound locations.

A possible source of error in this experiment is that for cost reasons the same Wellmate (Matrix) tubing was used to dispense persisters cells over the entire screening period of two weeks. The potential detriment to the experiment could involve biofilm formation on the interior surface of the tubes and subsequent shedding of cells into assay wells. To reduce this risk, tubes were flushed with 70% EtOH and dH₂O after each use. Results did not indicate any significant effect caused by this. However, Figure 3.5 does indicate that batches run later in screening had a broader distribution of inhibition indicating that error increased over subsequent batches of screening.

The primary screen gave a hit rate of 3.4%. Typically antagonist screening would see a hit rate of 2 – 3 % so this is marginally high. However, this is not unexpected as often inhibition assays detecting a decrease in signal will also detect compounds that interfere with signal generation (Hughes et al., 2011b).

It is possible that the number of compounds observed showing negative inhibition (i.e. growth) could have been caused by compounds reacting with the resazurin in PrestoBlue (Figure 3.6). Resazurin is highly sensitive to redox reactions; as such any compounds which are reducing agents could cause a false positive reading.

4. Activity Confirmation

4.1. Overview

Work undertaken in chapter 4 was carried out at the University of Exeter following compound screening at the DDU, which concluded in March 2014.

Following preliminary activity confirmation carried out at the DDU by means of a dose response assay in duplicate, I returned to the University of Exeter with 29 identified hit compounds (Table 3.1).

Hit to Lead: process and requirements.

Having identified hits in chapter 3 the first priority on return of work to Exeter was to triage these results and define which compounds had the most potential for further work. The hit to lead process aims to transform a series of hit compounds into a smaller number of druggable compounds with potential clinical use. This is a funnel-like process with down selection of compounds being made as more data is gained for the compounds (Duffy et al., 2012). Through activity confirmation I aimed to reduce the number of compounds to a more manageable quantity, re-confirm activity and cluster compounds into series. Through this, moderate quality hits could be developed for progression to leads.

In this section of work I was taking moderate quality hit and looking to narrow down to high quality hits which can progress to leads.

4.2. Activity confirmation

The first phase of activity confirmation was to generate dose response curves for compounds identified from the diversity compound library by the PrestoBlue persister

assay. Using newly sourced compounds, hit confirmation was carried out under more robust conditions, both performed in triplicate over a larger range of concentrations and alongside a secondary viability assay using the LIVE/DEAD cell viability reagent.

This refinement process seeks to show normal competitive behaviour in hits to indicate that the compound is inhibiting a target or non-target protein rather than interfering with another component of the assay at high concentrations.

Because HTS libraries, such as those at the DDU, are stored for long periods of time in DMSO solutions it was important to obtain fresh samples of hit compounds. This ensures that compounds have not been contaminated, modified, degraded or precipitated from solution.

Presto Blue Dose Response repeats

Preliminary dose response assays were carried out at the DDU in chapter 3. These were repeated at the University of Exeter using the freshly sourced compounds. The experiment was improved by increasing the range of concentrations to give 16 data points and running each concentration in triplicate.

Secondary LIVE/DEAD Assay

At this point a secondary assay using LIVE/Dead cell viability staining to quantify persister cells was used to confirm hits, particularly in a minority of compounds where signal interference was observed in the PrestoBlue assay. It is a standard procedure in drug discovery to employ a secondary, orthogonal assay to confirm activity (**Error! Hyperlink reference not valid.**). Whilst both PrestoBlue and LIVE/Dead are viability reagents the biochemical mechanism by which the fluorophore is produced differs.

Time Dependent Killing

The time kill curve is used to determine the bactericidal activity of compounds in combination with ceftazidime in contrast to ceftazidime alone. Previous studies in persister cells show a biphasic killing pattern upon treatment with super lethal concentrations on antibiotics as is shown for *B. thailandensis* previously (Figure 1.5). The biphasic pattern is attributed to initial, rapid killing of susceptible cells leaving antibiotic tolerant persister cells which are killed at a slower rate. To show if identified compounds were able to inhibit a persister culture through the “gold standard” colony counting method, an experiment was run to compare the survival of persister cells over time with addition of test compounds.

Minimum Inhibitory Concentration (MIC)

The previous results highlighted compounds with significant effects on persister numbers. A hypothesis was that these compounds either potentiated the effects of ceftazidime, or prevented the maintenance of the persistent state. However, I reasoned that they might be acting as antibiotics in their own right. I therefore performed a minimum inhibitory concentration (MIC) test for a select group of compounds (chapter 4.5). A MIC test determines the minimum concentration of compound required in a bacterial culture to inhibit growth. This is carried out through serial dilution of compound concentrations to determine the concentration at which the bacteria are able to grow and divide as measured by absorbance and an observed increase in turbidity. This was carried out according to the Clinical and Laboratory Standards Institute (CLSI) guidelines for antimicrobial susceptibility testing (Ambaye et al., 1997).

4.3. Experimental Procedure

Compounds were reconstituted in DMSO to a stock concentration of 36 mM and transferred to a 96 well, DMSO resistant microtiter plate referred to as a masterplate.

A persister culture was produced as described in chapter 3.3 through treatment of an overnight culture of *B. thailandensis* optically adjusted to OD₆₀₀ 0.4 with 400 µg/ml ceftazidime hydrate.

DMSO resistant assay plates were used to produce compound master plates. 40 µl of 36 mM compound in DMSO was added to wells of the masterplate and fifteen two-fold dilutions of 20 µl compound to 20 µl DMSO performed. This generated a set of solutions with the compound at concentrations from 36 mM to 1.1 µM.

To prepare assay plates, 2.4 µl of each dilution for compounds was transferred to wells of a black walled, clear bottomed, 96 well plate. To this, 37.6 µl of persister culture was added and mixed through pipetting. This provided a final concentration range of 1 mM to 61 nM. A breathable membrane was applied before plates were centrifuged at 58 x g for 2 minutes and incubated statically at 28 °C for 18 hours.

Presto Blue Assay

Following incubation, membranes were removed from assay plates and 5 µl of Presto Blue reagent was added to each well and mixed by pipetting. Plates were centrifuged at 58 x g for 2 minutes and incubated at room temperature for 40 minutes before fluorescence was read at ex 540 nm/ em 590 nm. This was carried out using a Tecan Pro 200 plate reader with settings: 20 µs integration time, 150 ms settle time. Z position and optimal gain were derived for individual plates. Fluorescence was read in triplicate for four loci on each well.

LIVE/DEAD Assay

The LIVE/DEAD assay is a viability assay that uses two fluorescent probes as indicators of cell viability. The assay consists of propidium iodide, which is a red fluorescent nucleic acid stain, and SYTO9, which is also a nucleic acid but fluoresces green. The two stains differ in ability to penetrate healthy cell membranes so whilst SYTO9 will label all cells in a population regardless of membrane integrity, propidium iodide can only penetrate cells with damaged membranes as such giving the proportion of the total cell population that is dead or dying. After incubation as above, 3 μ l of Live/Dead reagent (Life Technologies) was added to each well from an equal volume stock solution of SYTO9 and propidium iodide in DMSO and mixed thoroughly. Plates were incubated at room temperature in the dark for 15 minutes and fluorescence was read at ex 480 / em 500 nm for SYTO9 stain and ex 490 / em 635 nm for propidium iodide.

Data analysis of concentration dependent killing was carried out using GraphPad v5 (Prism) following a 4 parameter logistic equation: $y = A + (B - A) / (1 + ((10C) / x)^D)$, where A = % inhibition at bottom, B = % inhibition at top, C = 50 % effect concentration (IC_{50}), D = slope, x = inhibitor concentration and y = % inhibition. As IC_{50} values are Log normally distributed, data is presented as the pIC_{50} ($-\log_{10}[IC_{50}]$).

Error is presented as 95% confidence intervals (95% CI). As the IC_{50} is calculated as $\log_{10}[IC_{50}]$ it is not appropriate to use standard error (GraphPad Software, 2016). ~~56~~

Time Dependent Killing

A culture of initial bacterial optical density 0.4 at 600 nm was added in 1.5 ml aliquots to wells of a 24 well plate. A ceftazidime stock solution was produced to 24 mg/ml in 0.1 M NaOH. Wells were treated with 400 μ g/ml ceftazidime hydrate and 30 μ M of test

compound in triplicate and incubated statically. At specified time intervals samples of 1 ml were taken. These were centrifuged, washed and resuspended in 1 ml LB media. Cells were enumerated by serial dilution in LB media and incubation of 10 µl spots on LB agar for 24 hours at 37 °C before colonies were counted. The maximum DMSO concentration in any well was 0.1%.

MIC

A 10 mg/mL stock solution of compound in DMSO solution was produced from which 256 µL was taken and added to 9.744 mL of M9 minimal media (final concentration: 256 µg/mL). A 96 well assay plate was then labelled to include samples in triplicate. 100 µL of M9 media was added to each well and a positive control of inoculated compound free broth and a negative control of un-inoculated broth only were included. To the first well in the microdilution series 100 µL of the 256 µg/mL compound stock solution was added such that concentration = 128 µg/mL. From this well, serial dilutions of 100 µl were performed to a final concentration of 0.03 µg/mL. The last aliquot was discarded (Ambaye et al., 1997).

B. thailandensis E264 was grown overnight in 10 mL of LB media and OD measured at 590 nm. The bacterial suspension was adjusted to the density of 0.01 and incubated for 1-2 hours at 37 °C. A viable count of the inoculum was performed to confirm concentration. 100 µL of the inoculum was then added to each well on the already prepared 96 well plate resulting in a maximum concentration of 64 µg/mL. Plates were incubated at 37 °C for 18 – 20 hours and absorbance at 590 nm read. MIC was determined as the lowest concentration of antibiotic in the original culture that inhibited bacterial growth over a four hour period.

4.4. Results

Compounds identified from the DDU diversity screen were re-purchased from commercial suppliers and re-tested for inhibition against the phenotypic persister cell assay which was improved by the addition of triplicate testing and a greater range of compound concentrations

Dose Response Assays

Reference Table 4.1 shows compounds available to obtain from commercial suppliers through online catalogues based upon outcomes of preliminary dose response assays carried out at the DDU. In preliminary screening all compounds gave a $pIC_{50} > 5$.

As Table 4.1 shows, ten compounds which were originally thought to be commercially available were impossible to obtain at the time of testing. This was a frustration. However, it is worth noting that many compounds appeared to fall into a series of families based upon structural properties. The result of this was that the dropout rate for hits because of sourcing issues was not as significant as first thought as a similar compound would, hopefully, still identify potential lead series.

Compound Key and Reference Table

Key	Supplier reference	DDU reference	Figure
1	C218-0294	DDD00000923	Not available to buy
2	3731-0081	DDD00001933	Not available to buy
3	C206-0819	DDD00002132	Figure 4.2
4	C206-1078	DDD00002147	Not available to buy
5	C206-0883	DDD00002153	Figure 4.4
6	C206-0741	DDD00002167	Not available to buy
7	6049-2413	DDD00006401	Figure 4.6
8	4896-2436	DDD00007093	Figure 4.8
9	4896-0324	DDD00007097	Not available to buy
10	4896-5070	DDD00007250	Not available to buy
	3406-0528 (Chloroxine)	DDD00007789	Figure 4.10
11	5186-0396	DDD00007989	Figure 4.12
12	5186-0395	DDD00008002	Not available to buy
13	5408-0429	DDD00008143	Figure 4.14
14	5408-0603	DDD00008183	Not available to buy
15	C274-2532	DDD00017836	Figure 4.16
16	5916774	DDD00036679	Figure 4.17
17	5843290	DDD00036877	Figure 4.20
18	6073831	DDD00037407	Figure 4.21
19	7361758	DDD00038407	Figure 4.23

20	7353899	DDD00038534	Figure 4.26
21	7859704	DDD00041424	Figure 4.27
22	7852536	DDD00042454	Figure 4.29
23	7985493	DDD00044626	Figure 4.32
24	9000195	DDD00046044	Not available to buy
25	7706-0056	DDD00048141	Not available to buy

Table 4.1: Compounds identified as exhibition dose dependent inhibition of persister cells.

In total 28 hit compounds were identified from the DDU diversity library using the persister cell assay. Compound activity was confirmed in a standard ten point, two-fold, concentration response assay carried out in duplicate with all compounds giving p/C_{50} values > 5 (Figure 3.7). Compounds were supplied by ChemDiv and Chembridge.

3

pIC_{50} from dose response assay carried out at DDU was 5 with 77 % maximal inhibition and hill slope 0.8. The compound was obtained from ChemDiv and the name determined from the structure (Figure 4.1).

When repeated at Exeter the pIC_{50} for a dose response assay with PrestoBlue was 4.4. This was repeated with the LIVE/DEAD assay which gave a pIC_{50} of 4.5. For PrestoBlue the Hill slope was 1.7 and maximum inhibition = 39 % (Figure 4.2).

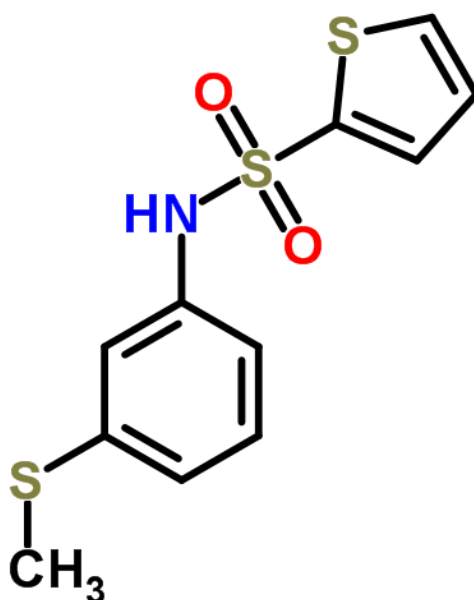


Figure 4.1: Structure of 3

Also known as N-[3-(Methylsulfanyl)phenyl]-2-thiophenesulfonamide

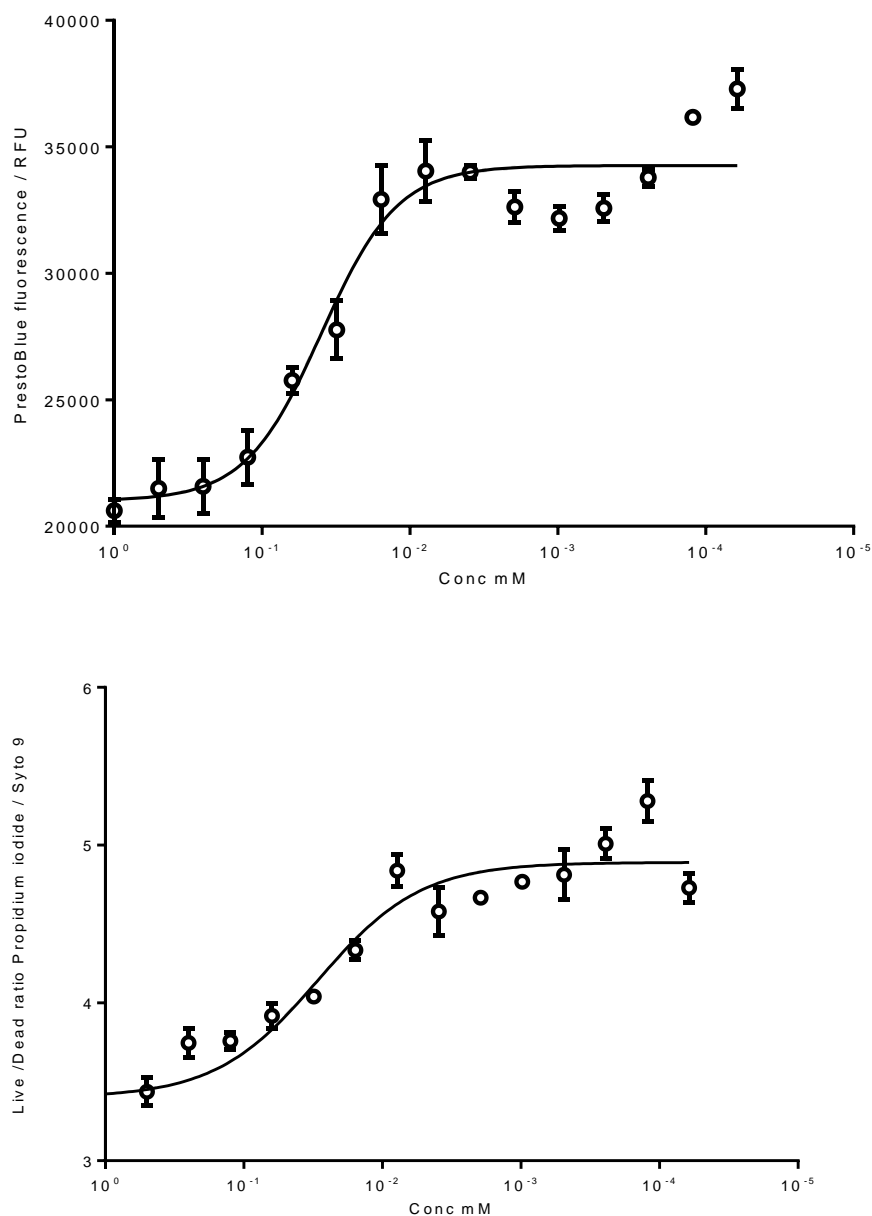


Figure 4.2: Concentration dependent killing from **3**.

Persister culture, generated by treatment with 100X MIC ceftazidime hydrate, was added to a 96 well plate containing two-fold dilutions of compounds in DMSO. Plates were incubated for 24 hours at 37 °C before addition of; Upper: PrestoBlue cell viability reagent; Lower: LIVE/DEAD and reading fluorescence. Results show three biological replicates with error bars indicating standard deviation. pIC_{50} for Upper = 4.4 (95% CI: 4.5 to 4.3); for Lower = 4.5 (95% CI: 4.9 to 4.2).

5

pIC_{50} from dose response assay carried out at DDU was 5.1 with 79 % maximal inhibition and hill slope 0.8. The compound was obtained from ChemDiv and the name determined from the structure (Figure 4.3).

When repeated at Exeter the pIC_{50} for a dose response assay with PrestoBlue was 4.4. This was repeated with the LIVE/DEAD assay which gave a pIC_{50} of 4.2. For PrestoBlue the Hill slope was 1.7 and maximum inhibition = 43 % (Figure 4.4).

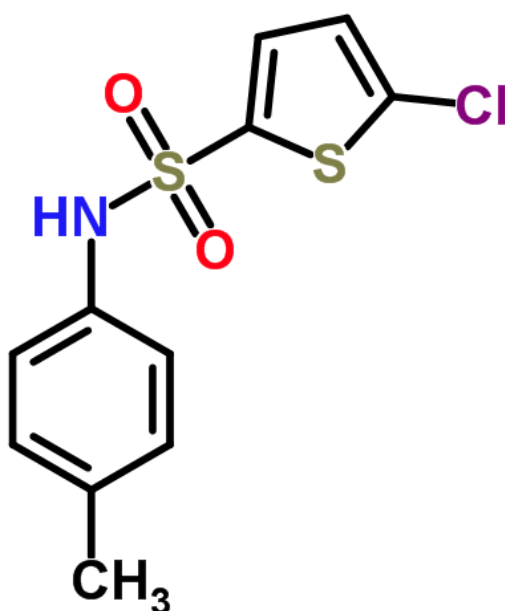


Figure 4.3: Structure of 5

Also known as 5-Chloro-N-(4-methylphenyl)-2-thiophenesulfonamide

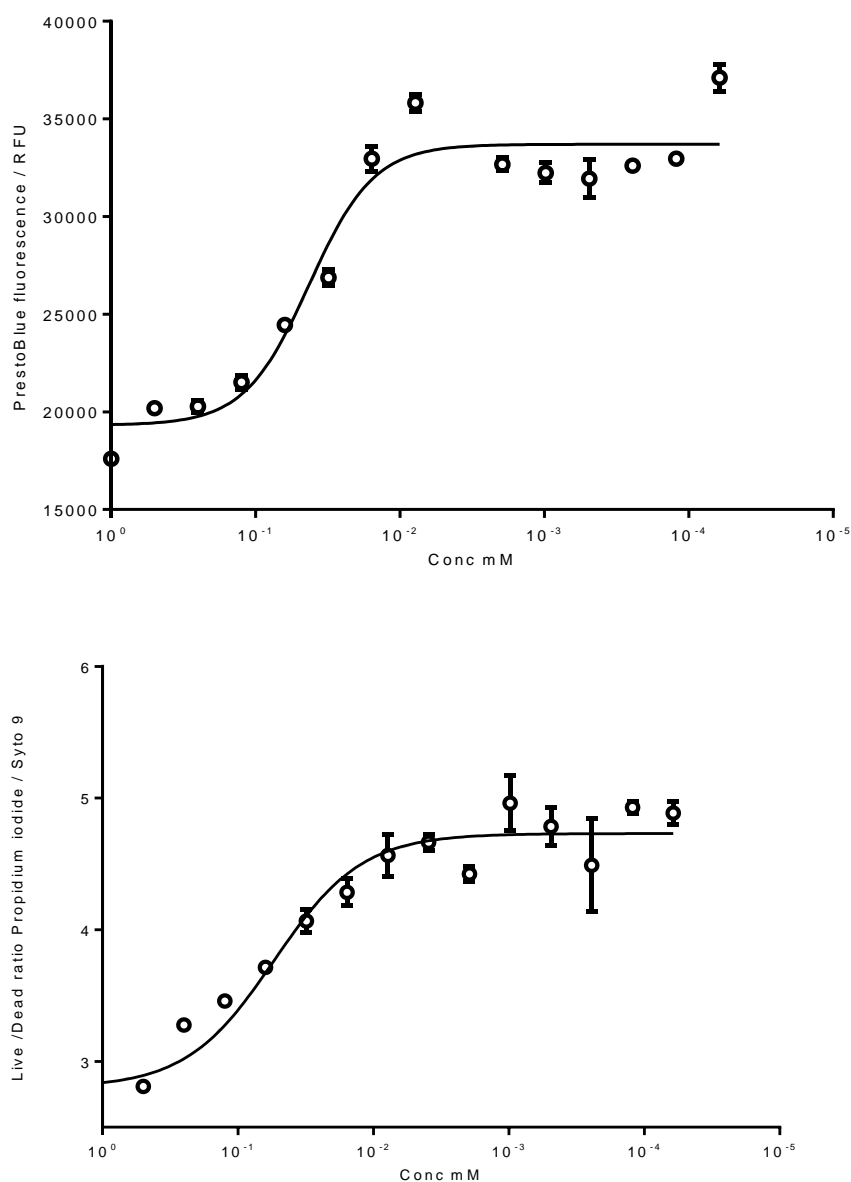


Figure 4.4: Concentration dependent killing from **5**.

Persister culture, generated by treatment with 100X MIC ceftazidime hydrate, was added to a 96 well plate containing two-fold dilutions of compounds in DMSO. Plates were incubated for 24 hours at 37 °C before addition of; Upper: PrestoBlue cell viability reagent; Lower: LIVE/DEAD and reading fluorescence. Results show three biological replicates with error bars indicating standard deviation. p/C_{50} for Upper = 4.4 (95% CI: 4.5 to 4.3); for Lower = 4.2 (95% CI: 4.5 to 4.0).

7

pIC_{50} from dose response assay carried out at DDU was 5.5 with 52% maximal inhibition and hill slope 1.4. The compound was obtained from ChemDiv and the name determined from the structure (Figure 4.5).

When repeated at Exeter the pIC_{50} for a dose response assay with PrestoBlue was 6.3, the Hill slope was 0.32 and maximum inhibition = 49 % (Figure 4.6). The assay was repeated with the LIVE/DEAD assay, which gave a pIC_{50} of 5.3 however, a large 95% confidence interval of 6.9 to 3.3 was observed.

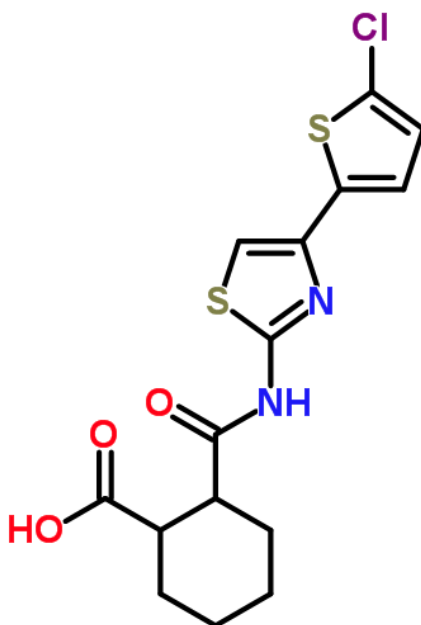


Figure 4.5: Structure of 7

Also known as 2-[[4-(5-Chloro-2-thienyl)-1,3-thiazol-2-yl] carbamoyl] cyclohexanecarboxylic acid.

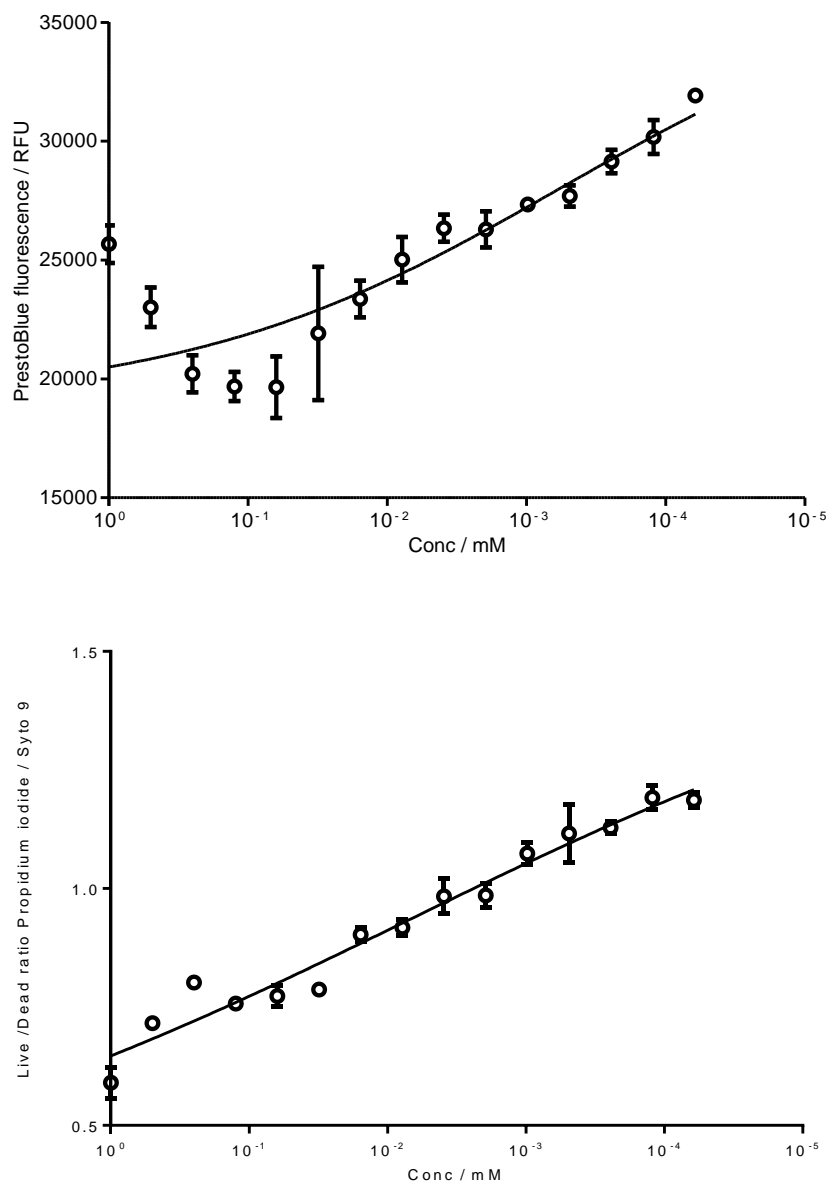


Figure 4.6: Concentration dependent killing from 7.

Persister culture, generated by treatment with 100X MIC ceftazidime hydrate, was added to a 96 well plate containing two-fold dilutions of compounds in DMSO. Plates were incubated for 24 hours at 37 °C before addition of; Upper: PrestoBlue cell viability reagent; Lower: LIVE/DEAD and reading fluorescence. Results show three biological replicates with error bars indicating standard deviation. p/C_{50} for Upper = 6.3 (95% CI: 6.5 to 6.0); for Lower = 5.3 (95% CI: 6.9 to 3.3). The shape of the dose response curve

is not indicative of an active compound, rather it shows a linear correlation between compound concentration and fluorescence. It is possible that this compound has an emission spectra that overlaps propidium iodide and rezazurin.

8

pIC_{50} from dose response assay carried out at DDU was 5.2 with 80 % maximal inhibition and hill slope 1.2. The compound was obtained from ChemDiv and the name determined from the structure (Figure 4.7).

When repeated at Exeter the pIC_{50} for a dose response assay with PrestoBlue was 4.3. Similar results were observed with the LIVE/DEAD assay which gave a pIC_{50} of 4.3. For PrestoBlue the Hill slope was 0.7 and maximum inhibition = 79 % (Figure 4.8).

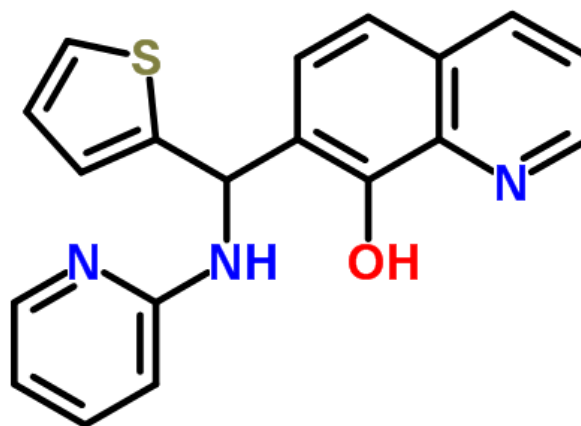


Figure 4.7: Structure of **8**

Also known as 7-[(Pyridin-2-ylamino)(2-thienyl)methyl]quinolin-8-ol.

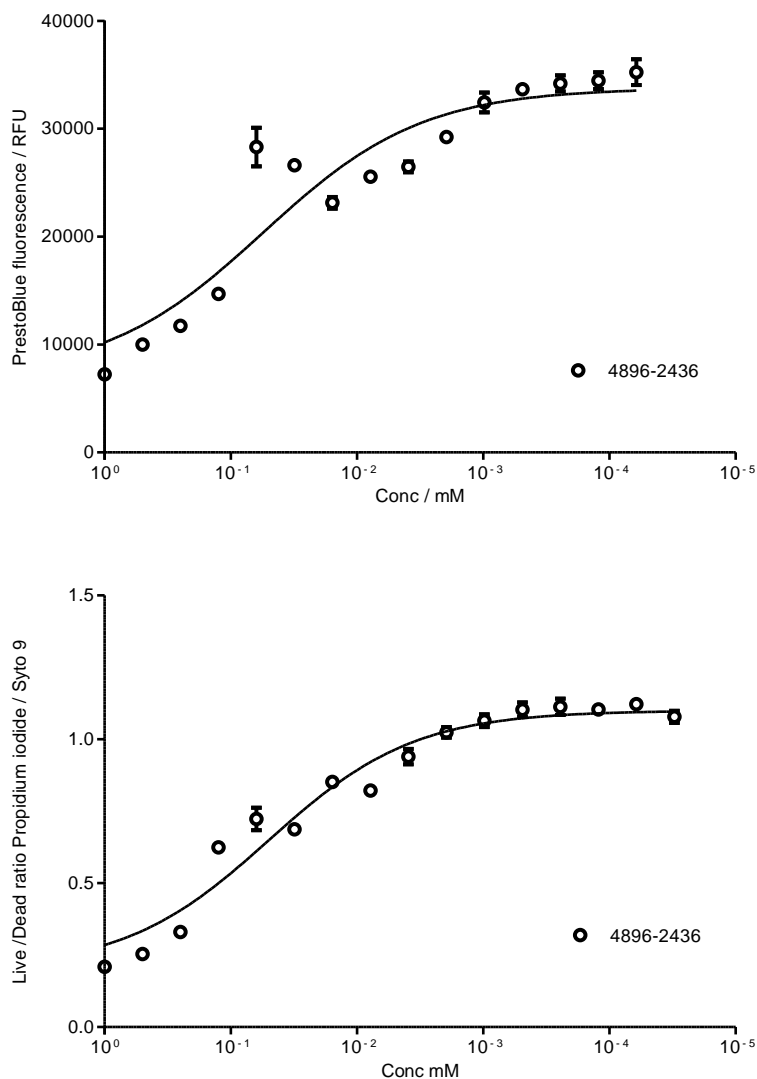


Figure 4.8: Concentration dependent killing from **8**.

Persister culture, generated by treatment with 100X MIC ceftazidime hydrate, was added to a 96 well plate containing two-fold dilutions of compounds in DMSO. Plates were incubated for 24 hours at 37 °C before addition of; Upper: PrestoBlue cell viability reagent; B – LIVE/DEAD and reading fluorescence. Results show three biological replicates with error bars indicating standard deviation. pIC_{50} for Upper = 4.3 (95% CI: 4.5 to 4.0); for Lower = 4.3 (95% CI: 4.4 to 4.2).

Chloroxine

pIC_{50} from dose response assay carried out at DDU was 5.47 with 96 % maximal inhibition and hill slope 2.2. The compound was obtained from Sigma-Aldrich (Reference number - D64600), and the compound structure is shown in Figure 4.9.

When repeated at Exeter the pIC_{50} for a dose response assay with PrestoBlue was 5.5, with a Hill slope of 1.7 and maximum inhibition = 72 % (Figure 4.10). Data obtained from the PrestoBlue assay were exceptionally good. However, chloroxine did not give a dose dependent result for the LIVE/DEAD assay. It was inferred that the compound interfered with the assay reagents although this should have been further investigated by assaying a titration of compound against the assay reagents alone to confirm this.

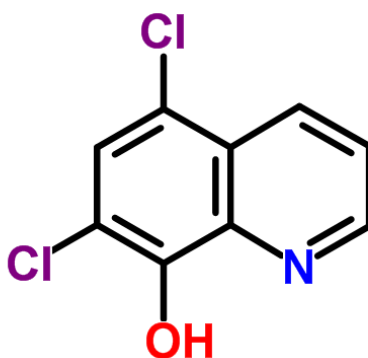


Figure 4.9: Structure of chloroxine

5,7-Dichloro-8-quinolinol is commercially known as chloroxine.

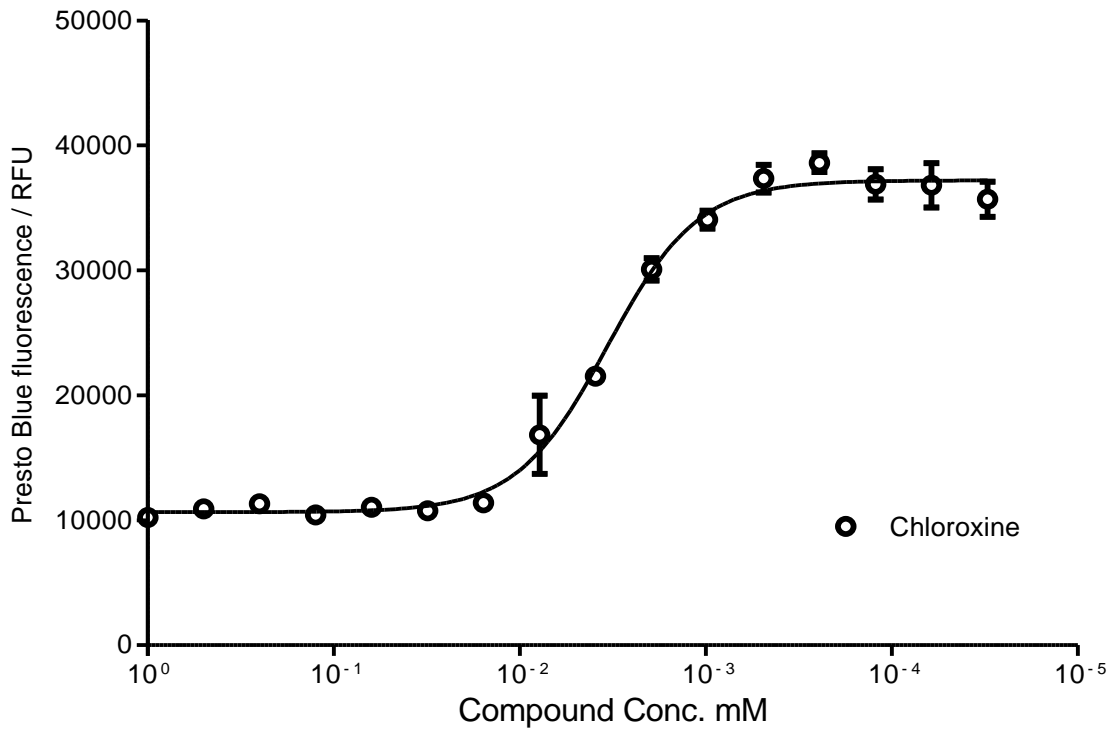


Figure 4.10: Concentration dependent killing from chloroxine.

Persister culture, generated by treatment with 100X MIC ceftazidime hydrate, was added to a 96 well plate containing two-fold dilutions of compounds in DMSO. Plates were incubated for 24 hours at 37 °C before addition of PrestoBlue cell viability reagent and reading fluorescence. Results show three biological replicates with error bars indicating standard deviation. $pIC_{50} = 5.5$ (95% CI: 5.5 to 5.4).

11

pIC_{50} from dose response assay carried out at DDU was 5.4 with 53 % maximal inhibition and hill slope 1.7. The compound was obtained from ChemDiv and the name determined from the structure (Figure 4.11).

When repeated at Exeter the pIC_{50} for a dose response assay with PrestoBlue was 3.9. The LIVE/DEAD assay gave a pIC_{50} of 4.4. For PrestoBlue the Hill slope was 0.9 and maximum inhibition = 67 % (Figure 4.12).

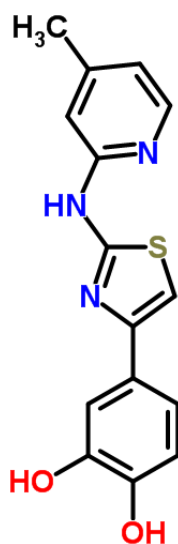


Figure 4.11: Structure of 11

Also known as 4-{2-[(4-Methyl-2-pyridinyl)amino]-1,3-thiazol-4-yl}-1,2-benzenediol.

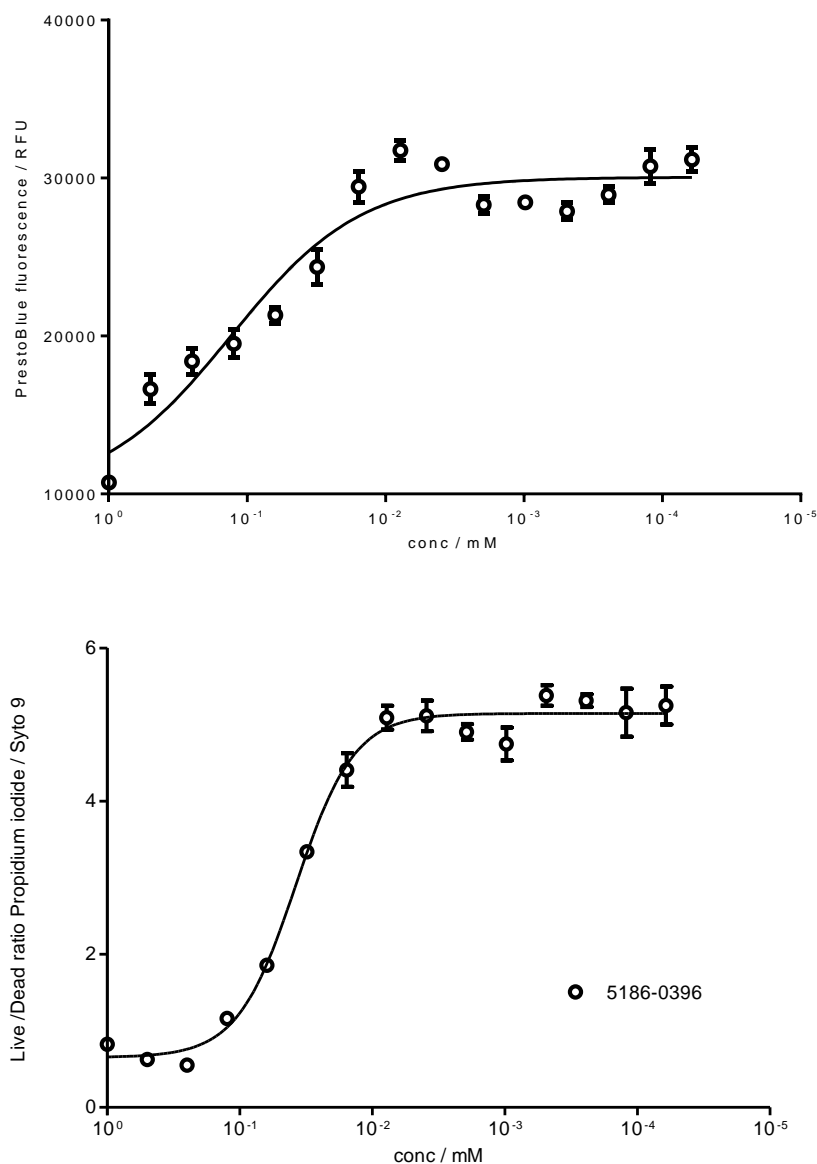


Figure 4.12: Concentration dependent killing from **11**.

Persister culture, generated by treatment with 100X MIC ceftazidime hydrate, was added to a 96 well plate containing two-fold dilutions of compounds in DMSO. Plates were incubated for 24 hours at 37 °C before addition of; Upper: PrestoBlue cell viability reagent; Lower: LIVE/DEAD and reading fluorescence. Results show three biological replicates with error bars indicating standard deviation. pIC_{50} for A = 3.9 (95% CI: 4.3 to 3.5); for B = 4.4 (95% CI: 4.5 to 4.4).

13

pIC_{50} from dose response assay carried out at DDU was 5.1 with 73% maximal inhibition and hill slope 0.9. The compound was obtained from ChemDiv and the name determined from the structure (Figure 4.13).

When repeated at Exeter the pIC_{50} for a dose response assay with PrestoBlue was 4.6. Similar results were obtained with the LIVE/DEAD assay which gave a pIC_{50} of 4.9. For PrestoBlue the Hill slope was 4.4 and maximum inhibition = 60 %. For the Live/Dead assay, 100 % inhibition was observed (Figure 4.14).

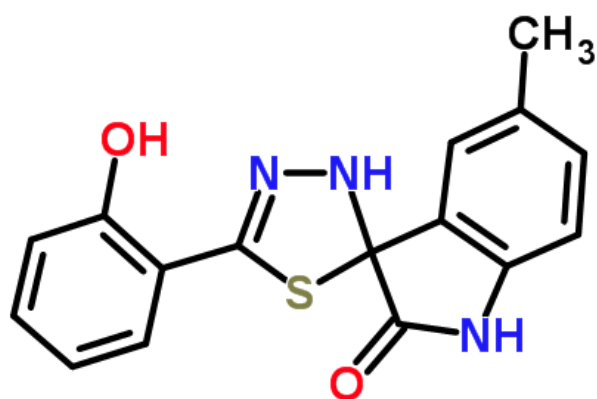


Figure 4.13: Structure of **13**

Also known as 5-Ethyl-5'-(2-hydroxyphenyl)-3'H-spiro[indole-3,2'-[1,3,4]thiadiazol]-2(1H)-one.

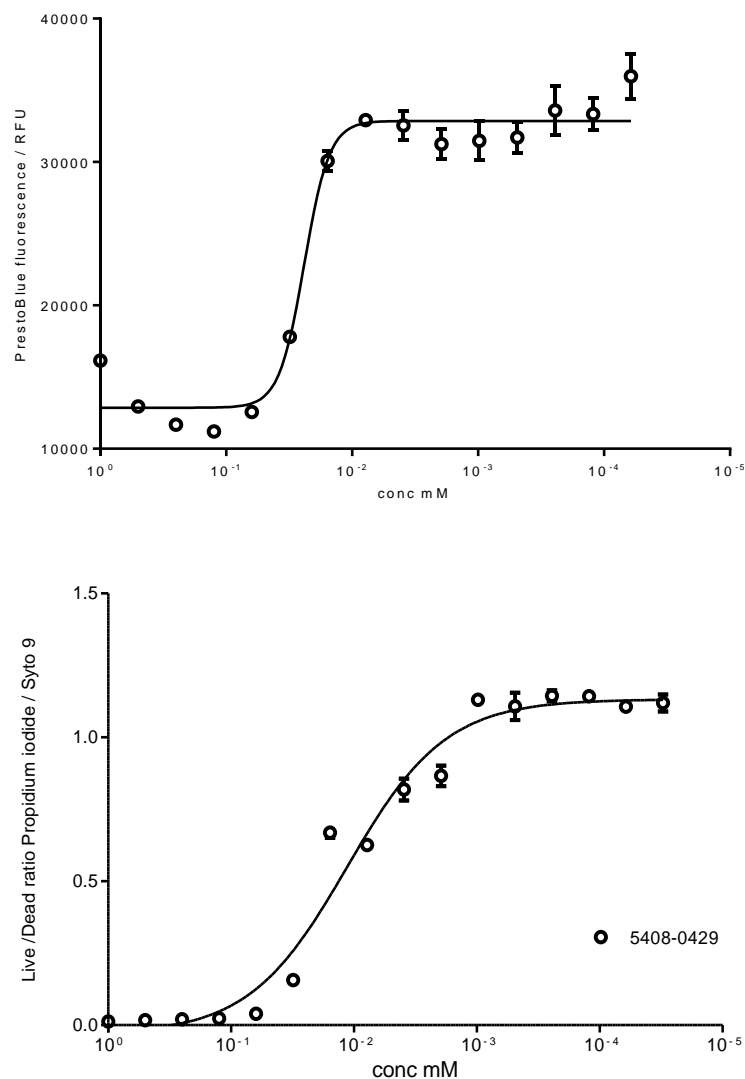


Figure 4.14 Concentration dependent killing from **13**.

Persister culture, generated by treatment with 100X MIC ceftazidime hydrate, was added to a 96 well plate containing two-fold dilutions of compounds in DMSO. Plates were incubated for 24 hours at 37 °C before addition of; Upper: PrestoBlue cell viability reagent; Lower: LIVE/DEAD and reading fluorescence. Results show three biological replicates with error bars indicating standard deviation. pIC_{50} for Upper = 4.6 (95% CI: 4.7 to 4.6); for Lower = 4.9 (95% CI: 5.0 to 4.8).

15

pIC_{50} from dose response assay carried out at DDU was 5.0 with 69 % maximal inhibition and hill slope 0.7. The compound was obtained from ChemDiv and the name determined from the structure (Figure 4.15).

When repeated at Exeter the pIC_{50} for a dose response assay with PrestoBlue was 4.3, PrestoBlue the Hill slope was 1.8 and maximum inhibition = 38 % (Figure 4.16). The assay repeated with the LIVE/DEAD assay. However, this gave inconclusive results. This was most likely due to a compound effect as fluorescence increased at higher concentrations of the compound.

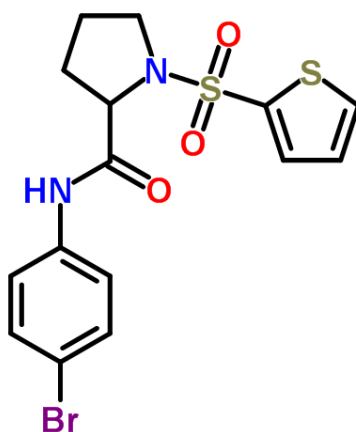


Figure 4.15: Structure of **15**

Also known as N-(4-Bromophenyl)-1-(2-thienylsulfonyl)prolinamide.

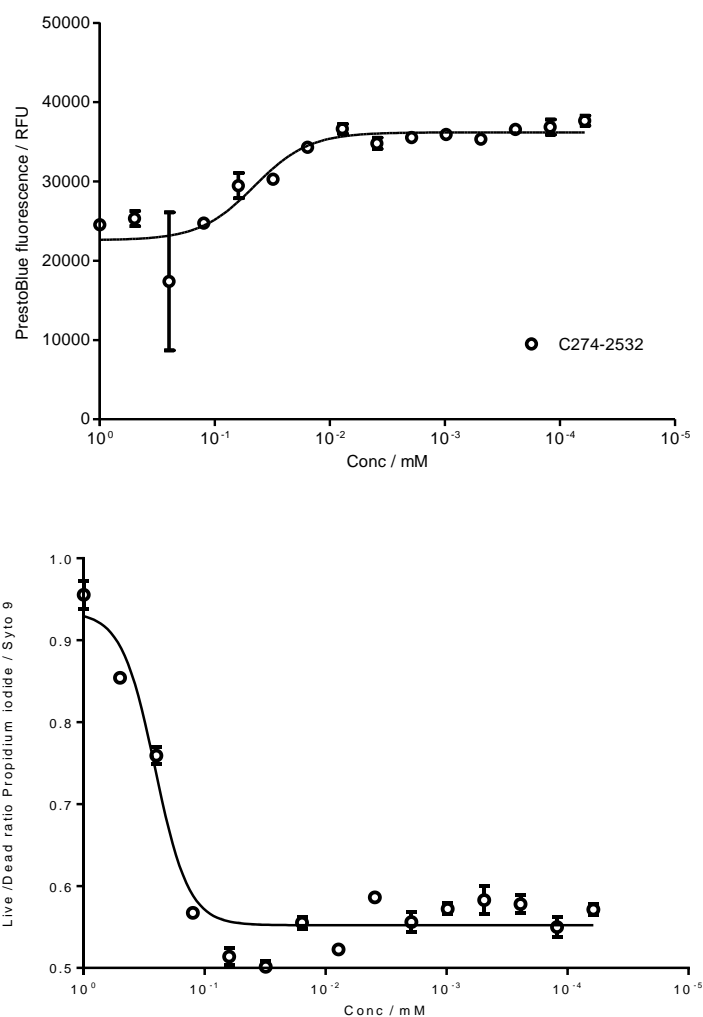


Figure 4.16: Concentration dependent killing from **15**.

Persister culture, generated by treatment with 100X MIC ceftazidime hydrate, was added to a 96 well plate containing two-fold dilutions of compounds in DMSO. Plates were incubated for 24 hours at 37 °C before addition of; Upper: PrestoBlue cell viability reagent; Lower: LIVE/DEAD and reading fluorescence. Results show three biological replicates with error bars indicating standard deviation. p/C_{50} for Upper = 4.3 (95% CI:4.6 to 4.1). An accurate dose response curve for LIVE/DEAD could not be fitted to obtain IC_{50} as limitations of solubility of the compound restricted use of test concentrations high enough to cause an upper plateau of data points.

16

pIC_{50} from dose response assay carried out at DDU was 5.1 with 63 % maximal inhibition and hill slope 1.0. The compound was obtained from ChemBridge (Hit2lead.com) and the name determined from the structure (Figure 4.17).

When repeated at Exeter the pIC_{50} for a dose response assay with PrestoBlue was 4.6 but showed a wide 95% confidence interval of 6.5 to 2.6 and only reached maximum inhibition of 12 % indicating the PrestoBlue assay did not work. The LIVE/DEAD assay gave a pIC_{50} of 3.9 with a Hill slope of 2.3, maximum 42 % inhibition and 95% confidence interval 2.73 to 2.68 (Figure 4.18). However, this activity is significantly lower than predicted by the DDU results.

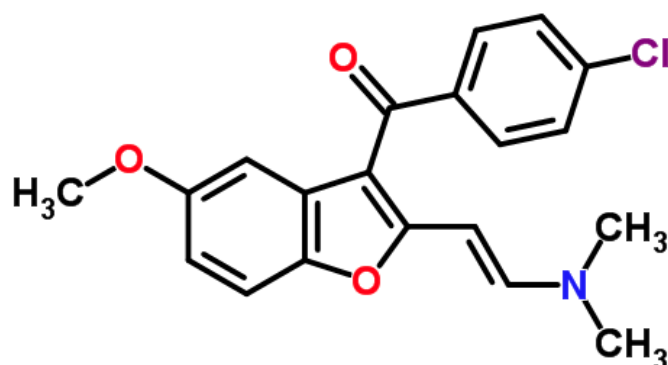


Figure 4.17: Structure of **16**

Also known as (4-chlorophenyl){2-[2-(dimethylamino)vinyl]-5-methoxy-1-benzofuran-3-yl}methanone.

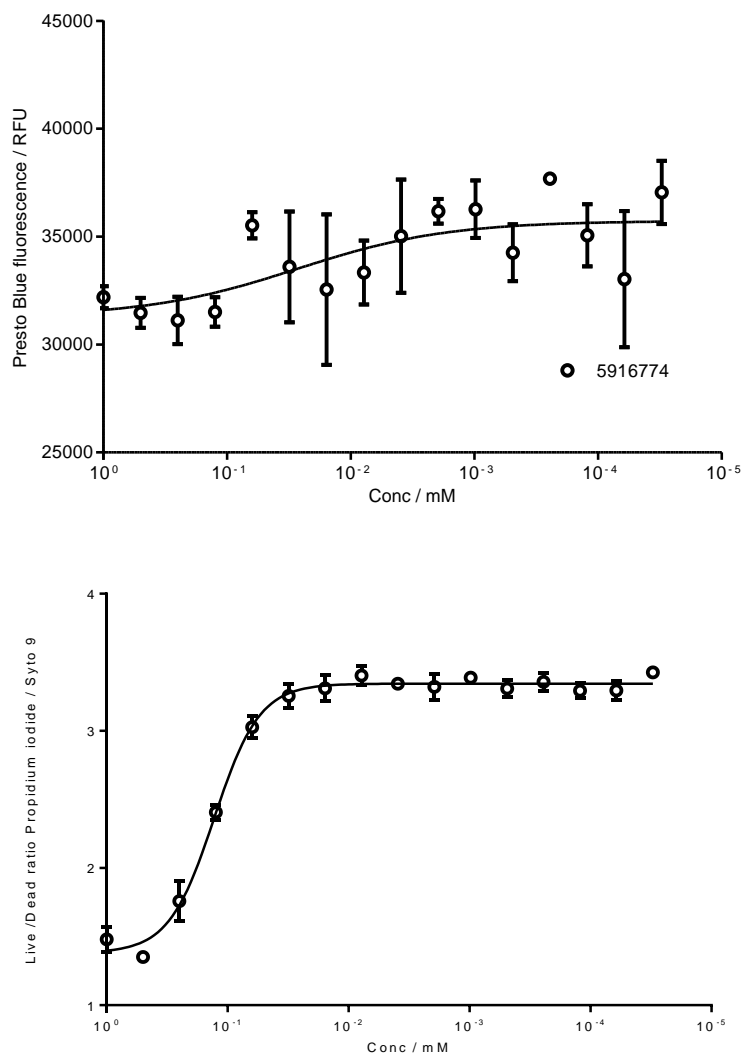


Figure 4.18: Concentration dependent killing from **16**

Persister culture, generated by treatment with 100X MIC ceftazidime hydrate, was added to a 96 well plate containing two-fold dilutions of compounds in DMSO. Plates were incubated for 24 hours at 37 °C before addition of; Upper: PrestoBlue cell viability reagent; Lower: LIVE/DEAD and reading fluorescence. Results show three biological replicates with error bars indicating standard deviation. pIC_{50} for Upper = 4.6 (95% CI: 6.5 to 2.6); for Lower = 3.9 (95% CI: 2.73 to 2.68).

17

pIC_{50} from dose response assay carried out at DDU was 5.1 with 67 % maximal inhibition and hill slope 2.1. The compound was obtained from ChemBridge (Hit2lead.com) and the name determined from the structure (Figure 4.19)

When repeated at Exeter the pIC_{50} for a dose response assay with PrestoBlue was 4.3, the Hill slope was 0.8 and maximum inhibition = 40 %. When repeated with the LIVE/DEAD assay, pIC_{50} was 4.0. The Live/Dead assay appeared to show a compound effect at higher concentrations of compound; as such the bottom value for calculation of \log/C_{50} was truncated to 3.1. However, a wide 95% CI indicated the fitted curve is not reliable (Figure 4.20).

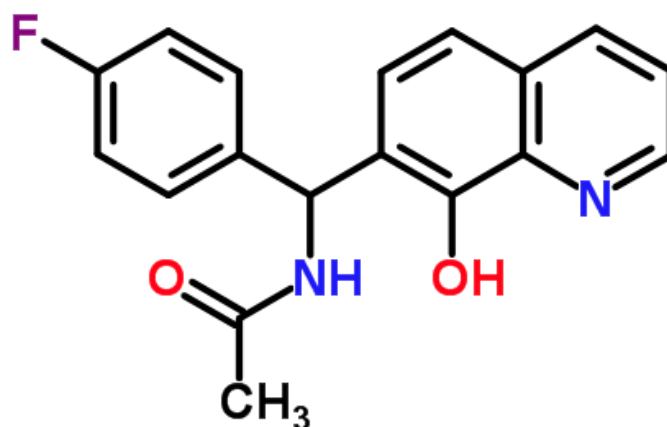


Figure 4.19: Structure of 17

Also known as N-[(4-fluorophenyl)(8-hydroxy-7-quinoliny)methyl]acetamide.

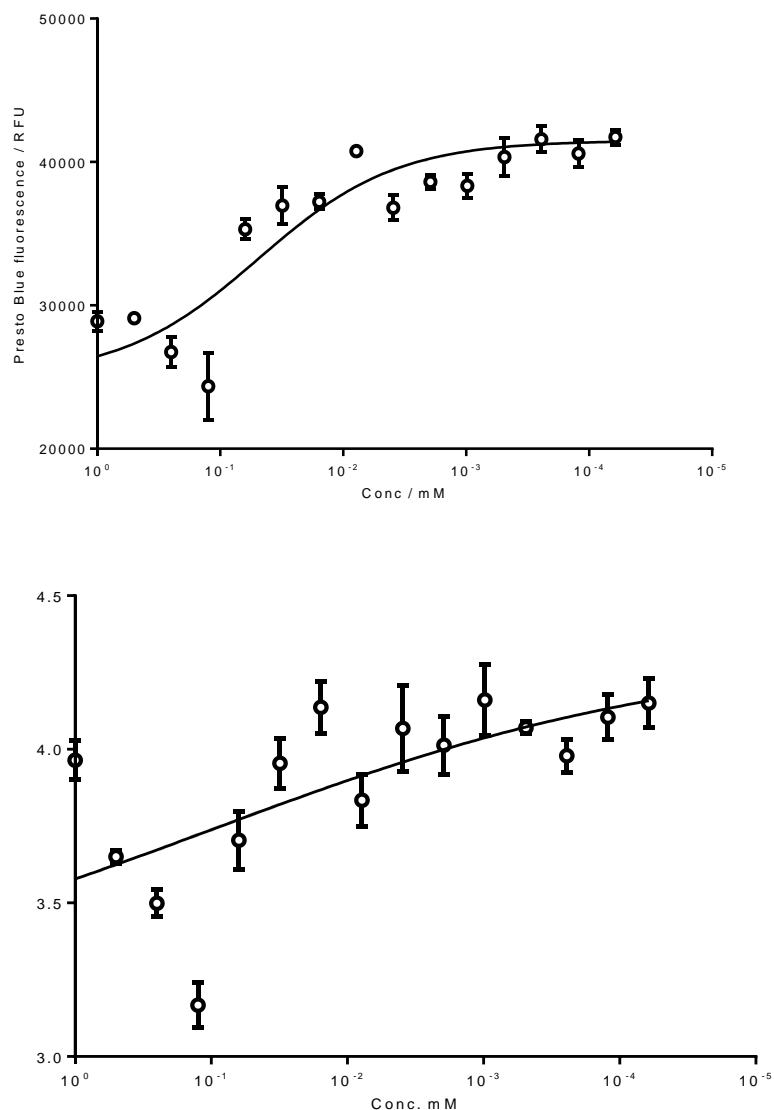


Figure 4.20: Concentration dependent killing from 17.

Persister culture, generated by treatment with 100X MIC ceftazidime hydrate, was added to a 96 well plate containing two-fold dilutions of compounds in DMSO. Plates were incubated for 24 hours at 37 °C before addition of; A - PrestoBlue cell viability reagent; B – LIVE/DEAD and reading fluorescence. Results show three biological replicates with error bars indicating standard deviation. pIC_{50} for Upper = 4.3 (95% CI: 4.5 to 4.1); for Lower = 4.0 (95% CI: 6.7 to 1.3).

18

$pI_{C_{50}}$ from dose response assay carried out at DDU was 5.7 with 67 % maximal inhibition and hill slope 1.4. The compound was obtained from ChemBridge (Hit2lead.com) and the name determined from the structure (Figure 4.21)

When repeated at Exeter the $pI_{C_{50}}$ for a dose response assay with PrestoBlue was 4.3. This was not repeatable with the LIVE/DEAD assay which gave inconclusive data. For PrestoBlue the Hill slope was 4.7 and maximum inhibition = 18 % (Figure 4.22).

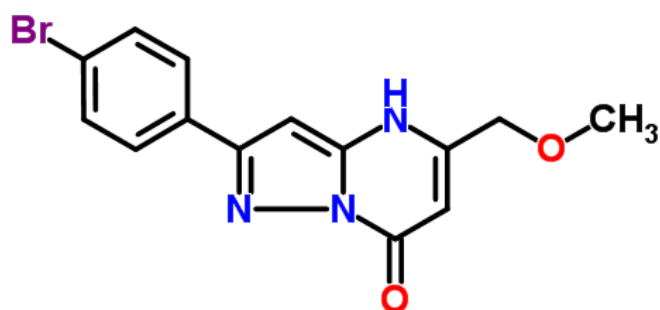


Figure 4.21: Structure of **18**

Also known as 2-(4-bromophenyl)-5-(methoxymethyl)pyrazolo[1,5-a]pyrimidin-7(4H)-one.

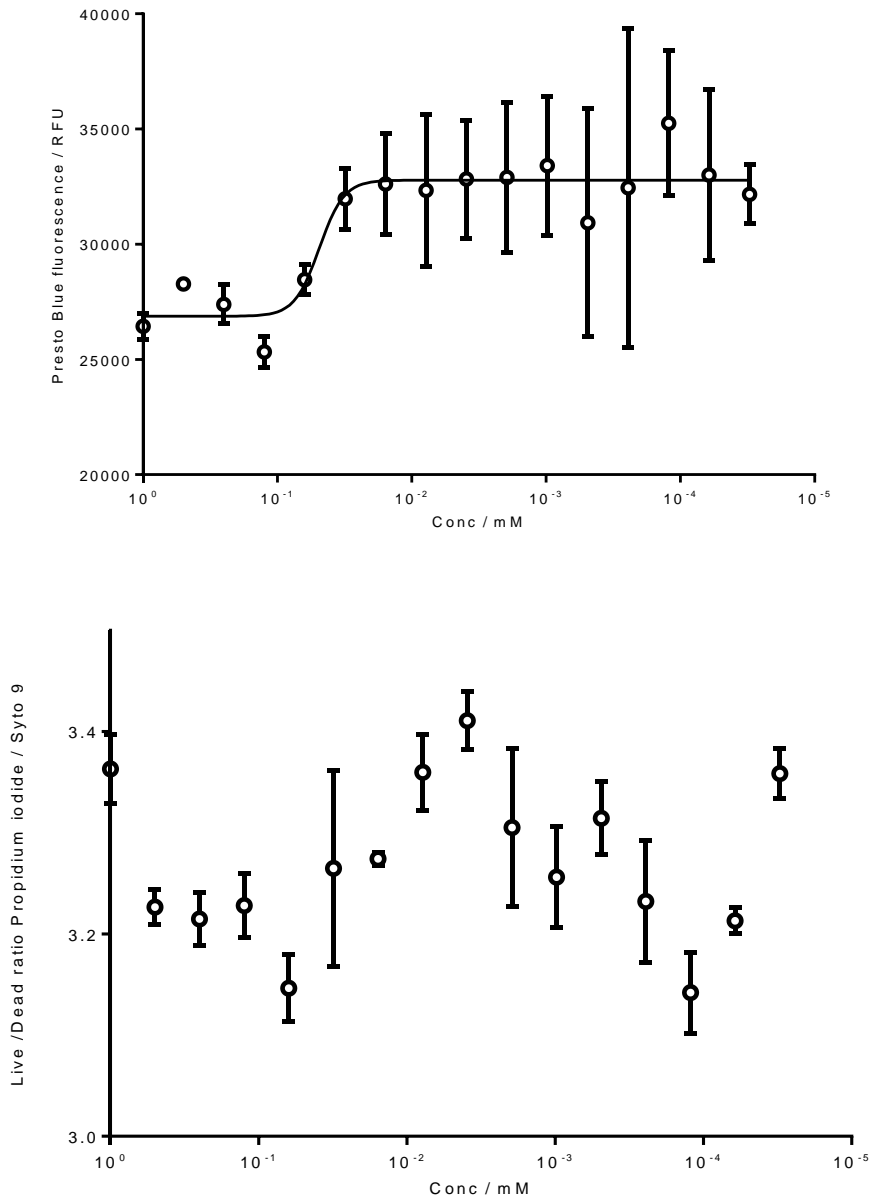


Figure 4.22: Concentration dependent killing from **18**.

Persister culture, generated by treatment with 100X MIC ceftazidime hydrate, was added to a 96 well plate containing two-fold dilutions of compounds in DMSO. Plates were incubated for 24 hours at 37 °C before addition of; Upper: PrestoBlue cell viability reagent; Lower: LIVE/DEAD and reading fluorescence. Results show three biological replicates with error bars indicating standard deviation. The large error observed is

likely a result of noise in the absence of a detectable treatment effect. pIC_{50} for A = 4.3 (95% CI: 4.6 to 4.0); B would not converge to provide a curve.

19

pIC_{50} from dose response assay carried out at DDU was 5.2 with 55 % maximal inhibition and hill slope 2.3. The compound was obtained from ChemBridge (Hit2lead.com) and the name determined from the structure (Figure 4.23)

When repeated at Exeter the pIC_{50} for a dose response assay with PrestoBlue was 4.8. This was also observed with the LIVE/DEAD assay which gave a pIC_{50} of 4.8. For PrestoBlue the Hill slope was 2.7 and maximum inhibition = 37 % (Figure 4.24).

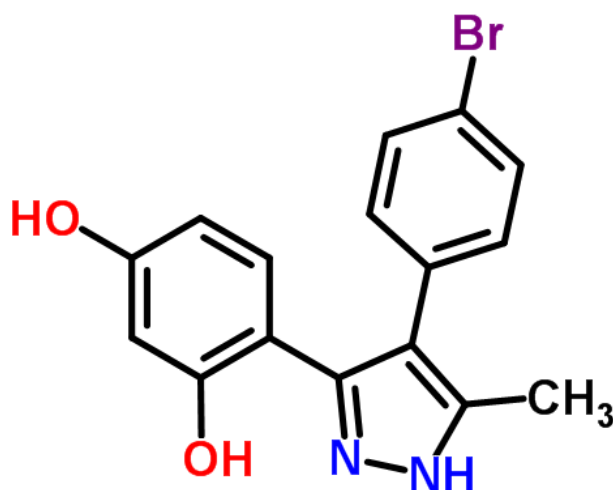


Figure 4.23: Structure of **19**

Also known as 4-[4-(4-bromophenyl)-5-methyl-1H-pyrazol-3-yl]-1,3-benzenediol.

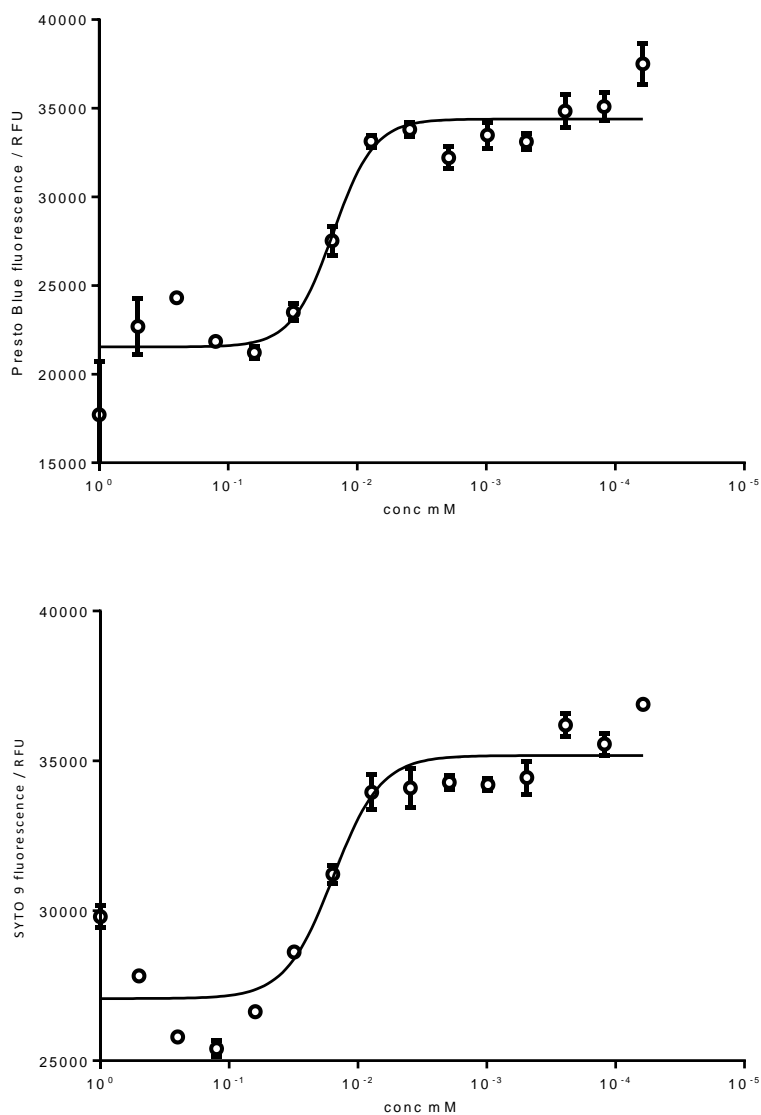


Figure 4.24: Concentration dependent killing from **19**.

Persistor culture, generated by treatment with 100X MIC ceftazidime hydrate, was added to a 96 well plate containing two-fold dilutions of compounds in DMSO. Plates were incubated for 24 hours at 37 °C before addition of; Upper: PrestoBlue cell viability reagent; Lower: SYTO9 nucleic acid stain and reading fluorescence. Results show three biological replicates with error bars indicating standard deviation. pIC_{50} for Upper = 4.8; for Lower = 4.8.

20

pIC_{50} from dose response assay carried out at DDU was 5.3 with 55 % maximal inhibition and hill slope 2.3. The compound was obtained from ChemBridge (Hit2lead.com) and the name determined from the structure (Figure 4.25)

When repeated at Exeter the pIC_{50} for a dose response assay with PrestoBlue was 4.7. An identical pIC_{50} was observed with the LIVE/DEAD assay. For PrestoBlue the Hill slope was 1.0 and maximum inhibition = 88 % (Figure 4.24).

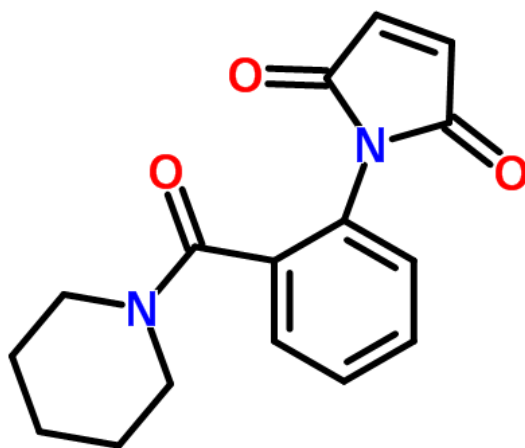


Figure 4.25: Structure of **20**

Also known as 1-[2-(1-piperidinylcarbonyl)phenyl]-1H-pyrrole-2,5-dione.

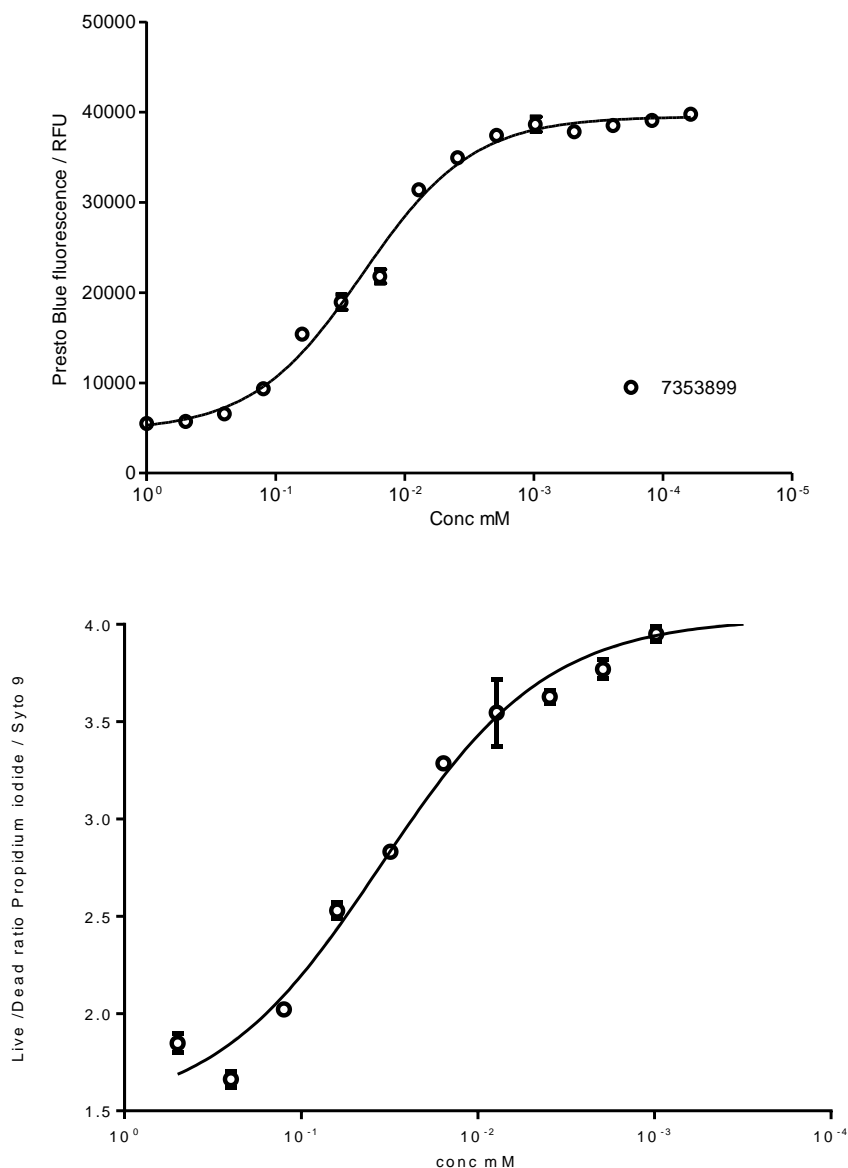


Figure 4.26: Concentration dependent killing from **20**.

Persister culture, generated by treatment with 100X MIC ceftazidime hydrate, was added to a 96 well plate containing two-fold dilutions of compounds in DMSO. Plates were incubated for 24 hours at 37 °C before addition of; A - PrestoBlue cell viability reagent; B – LIVE/DEAD and reading fluorescence. Results show three biological replicates with error bars indicating standard deviation. pIC_{50} for A = 4.7 (95% CI: 4.7 to 4.6); B = 4.7 (95% CI: 4.9 to 4.5).

21

pIC_{50} from dose response assay carried out at DDU was 5.1 with 54 % maximal inhibition and hill slope 1.3. The compound was obtained from ChemBridge (Hit2lead.com) and the name determined from the structure (Figure 4.27)

When repeated at Exeter the pIC_{50} for a dose response assay with PrestoBlue was 4.4. The LIVE/DEAD assay which gave inconclusive results. For PrestoBlue the Hill slope was 2.3 and maximum inhibition = 11 % (Figure 4.28).

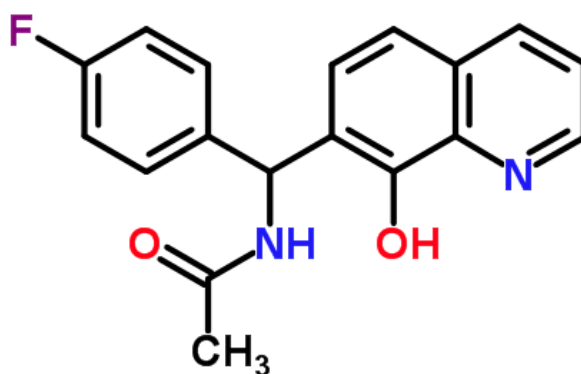


Figure 4.27: Structure of **21**

Also known as [1-(2-phenoxyethyl)-1H-benzimidazol-2-yl](phenyl)methanol.

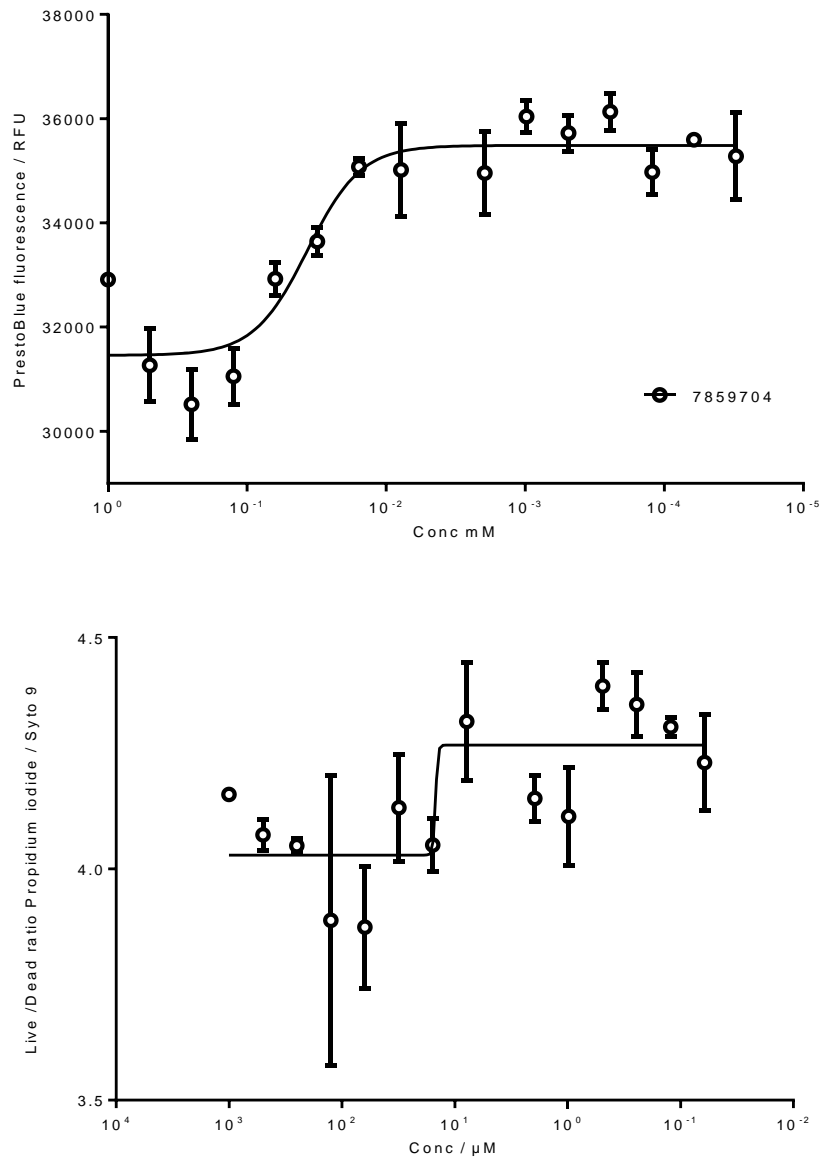


Figure 4.28: Concentration dependent killing from **21**.

Persister culture, generated by treatment with 100X MIC ceftazidime hydrate, was added to a 96 well plate containing two-fold dilutions of compounds in DMSO. Plates were incubated for 24 hours at 37 °C before addition of; Upper: PrestoBlue cell viability reagent; Lower: LIVE/DEAD and reading fluorescence. Results show three biological replicates with error bars indicating standard deviation. pIC_{50} for Upper = 4.4; Lower was inconclusive.

pIC_{50} from dose response assay carried out at DDU was 5.1 with 65 % maximal inhibition and hill slope 1.0. The compound was obtained from ChemBridge (Hit2lead.com) and the name determined from the structure (Figure 4.29)

When repeated at Exeter the pIC_{50} for a dose response assay with PrestoBlue was 4.4, the Hill slope was 1.0 and maximum inhibition = 88% % (Figure 4.30). This result was not repeatable with the LIVE/DEAD assay which gave results indicating a compound effect.

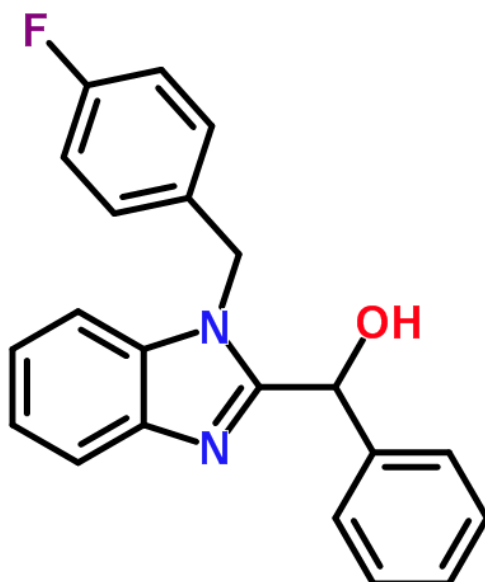


Figure 4.29: Structure of **22**

Also known as [1-(4-fluorobenzyl)-1H-benzimidazol-2-yl](phenyl)methanol.

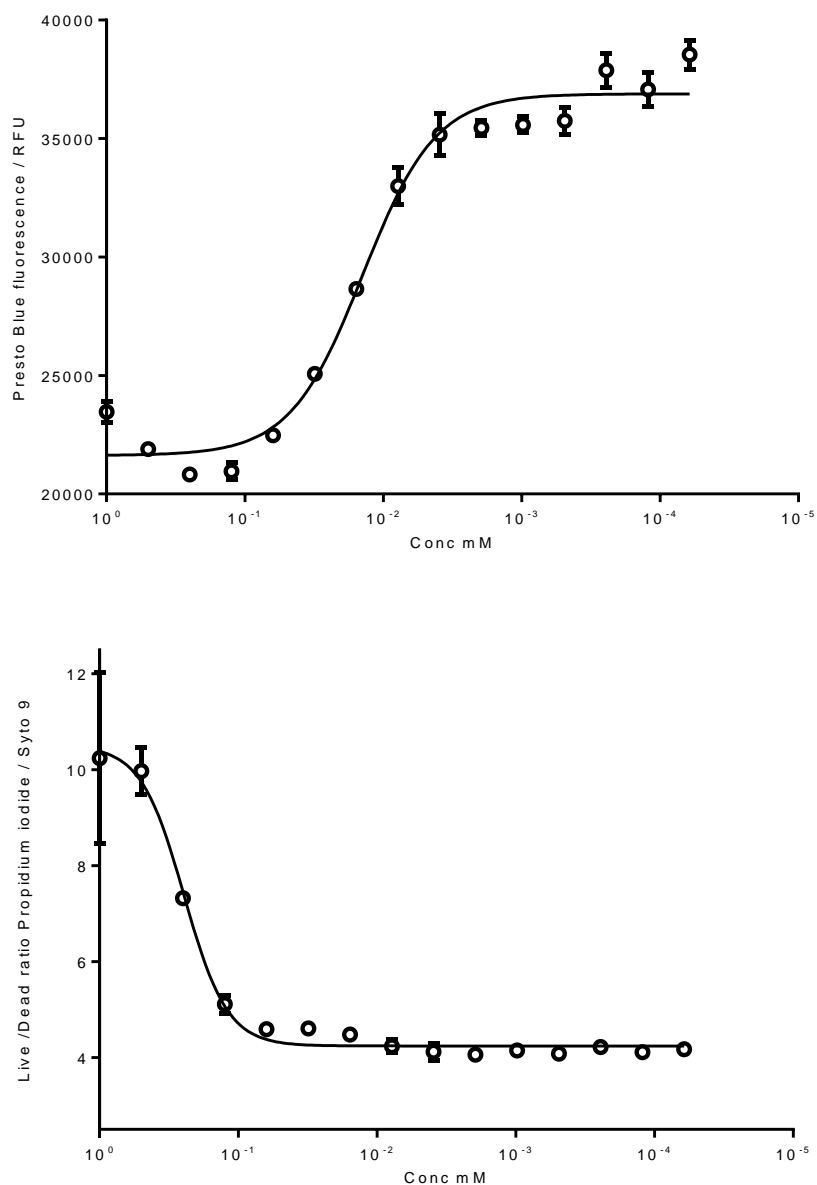


Figure 4.30: Concentration dependent killing from **22**.

Persister culture, generated by treatment with 100X MIC ceftazidime hydrate, was added to a 96 well plate containing two-fold dilutions of compounds in DMSO. Plates were incubated for 24 hours at 37 °C before addition of; Upper: PrestoBlue cell viability reagent; Lower: LIVE/DEAD and reading fluorescence. Results show three biological replicates with error bars indicating standard deviation. p/C_{50} for Upper = 4.4 (95% CI: 4.7 to 4.6); Lower was inconclusive.

23

pIC_{50} from dose response assay carried out at DDU was 5.2 with 55 % maximal inhibition and Hill slope 1.5. The compound was obtained from ChemDiv and the name determined from the structure (Figure 4.31).

When repeated at Exeter the pIC_{50} for a dose response assay with PrestoBlue was 5.1. The LIVE/DEAD assay gave a slightly stronger effect, with a pIC_{50} of 5.5. For PrestoBlue the Hill slope was 2.2 and maximum inhibition = 57 % (Figure 4.32).

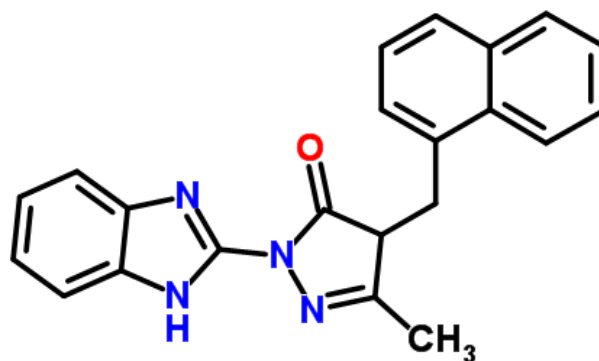


Figure 4.31: Structure of **23**

Also known as 2-(1H-Benzimidazol-2-yl)-5-methyl-4-(1-naphthylmethyl)-2,4-dihydro-3H-pyrazol-3-one.

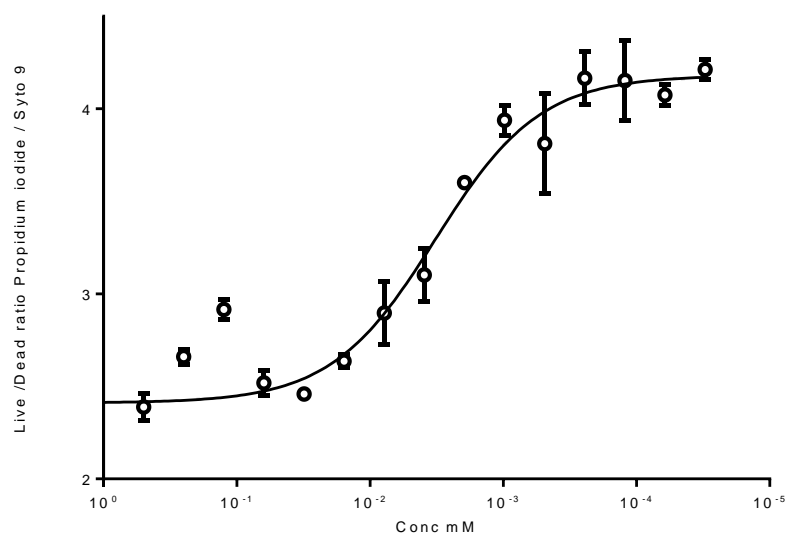
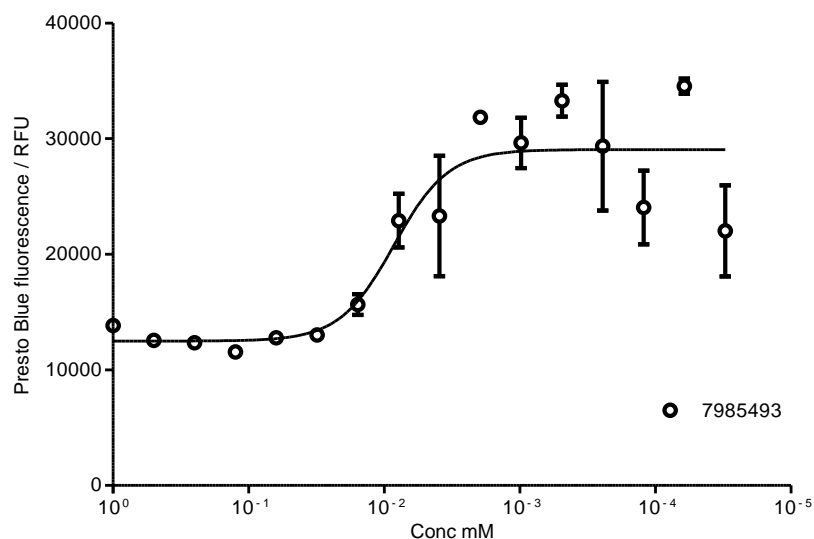


Figure 4.32: Concentration dependent killing from **23**.

Persister culture, generated by treatment with 100X MIC ceftazidime hydrate, was added to a 96 well plate containing two-fold dilutions of compounds in DMSO. Plates were incubated for 24 hours at 37 °C before addition of; Upper: PrestoBlue cell viability reagent; Lower: LIVE/DEAD and reading fluorescence. Results show three biological replicates with error bars indicating standard deviation. pIC_{50} for Upper = 5.1 (95% CI: 5.3 to 4.8); Lower = 5.5 (95% CI: 5.7 to 5.2).

24

pIC_{50} from dose response assay carried out at DDU was 5.7 with 58 % maximal inhibition and Hill slope 2.6. The compound was obtained from ChemDiv and the name determined from the structure (Figure 4.33).

When repeated at Exeter the pIC_{50} for a dose response assay with PrestoBlue was 8.2. This indicates a very strong effect with the top plateau correlating well with other results. This is corroborated with the LIVE/DEAD assay which gave a pIC_{50} of 8.0. For PrestoBlue the Hill slope was 1.3 and maximum inhibition = 50 % (Figure 4.34).

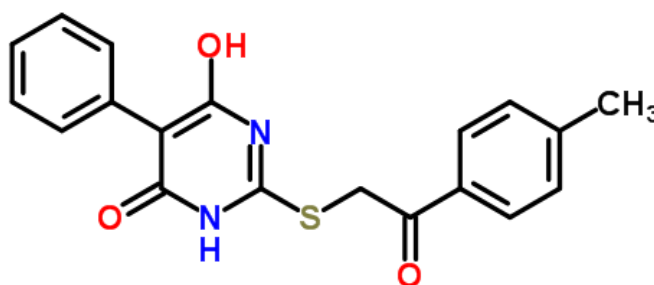


Figure 4.33: Structure of **24**

Also known as 6-hydroxy-2-[[2-(4-methylphenyl)-2-oxoethyl]thio]-5-phenyl-4(3H)-pyrimidinone.

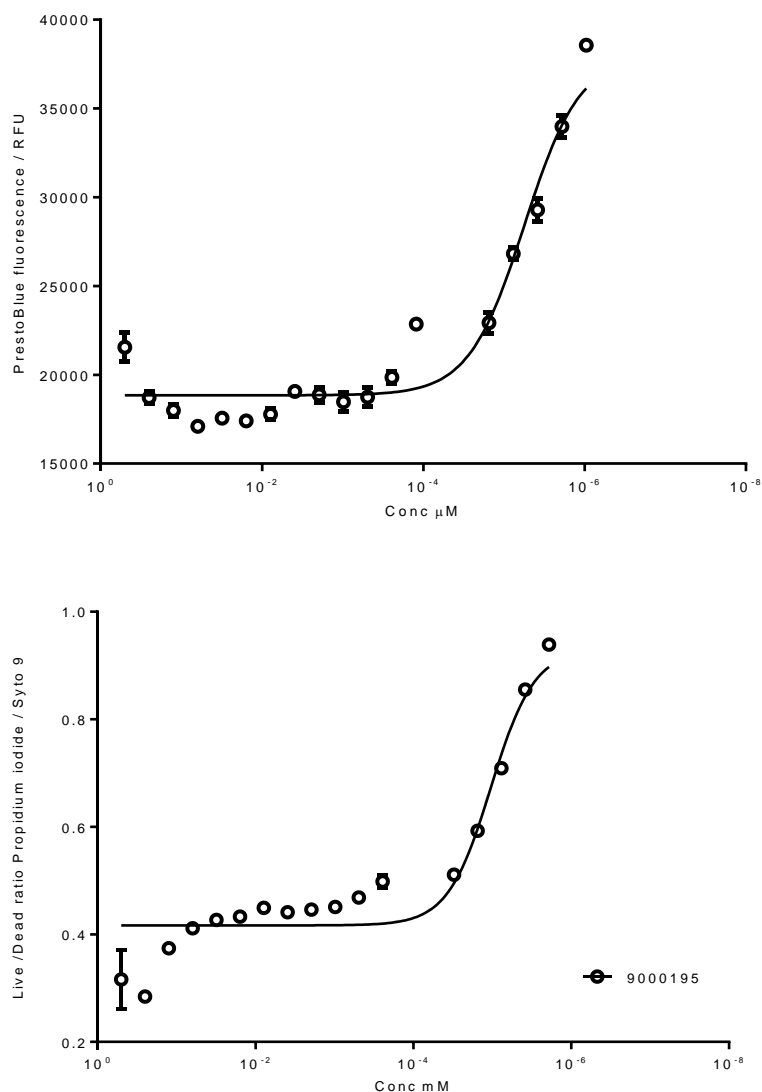


Figure 4.34: Concentration dependent killing from **24**.

Persister culture, generated by treatment with 100X MIC ceftazidime hydrate, was added to a 96 well plate containing two-fold dilutions of compounds in DMSO. Plates were incubated for 24 hours at 37 °C before addition of; Upper: PrestoBlue cell viability reagent; Lower: LIVE/DEAD and reading fluorescence. Results show three biological replicates with error bars indicating standard deviation. Both graphs indicate activity at a $pIC_{50} > 7$ however as the graph does not reach baseline inhibition an accurate pIC_{50} cannot be calculated without constraining the maximum effect. pIC_{50} for Upper = 8.3 (95% CI: 8.3 to 8.1); Lower = 7.9 (95% CI: 8.1 to 7.9).

4.5. Down selection to six compounds

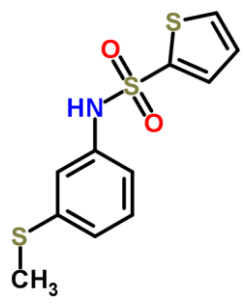
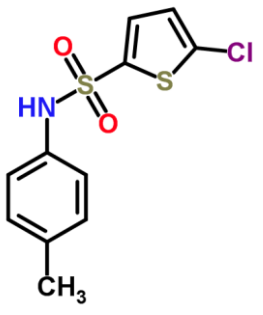
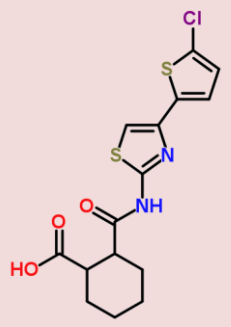
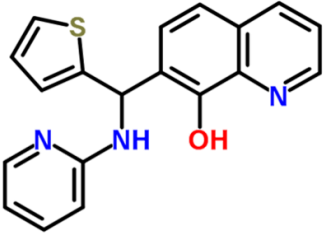
Deciding which hits to take forward to lead identification (the HTL phase) is a crucial step as the downstream optimization phase will require significant time and financial investment.

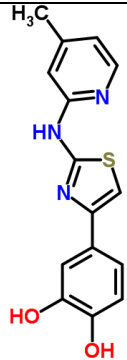
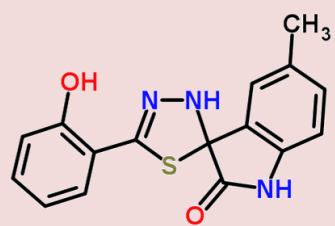
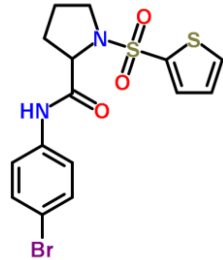
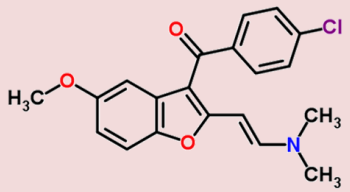
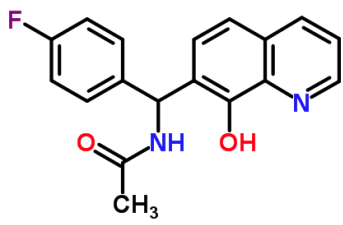
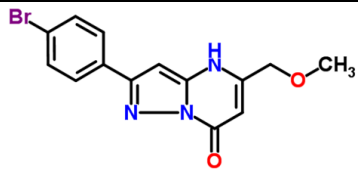
In comparing results of dose response curves to identify the most ideal compounds I considered the pIC_{50} , Hill coefficient and maximal effect. The hill coefficient is a function calculated from the four parameter logistic fit used to calculate potency and, whilst a simplification that needs to be empirically confirmed through models of receptor activation and enzyme activation in an In Vitro assay, the Hill coefficient can give insight into the ratio of ligand to receptor binding. An ideal antimicrobial drug would display a Hill coefficient between 0.5 and 1.8 and a sigmoidal concentration growth inhibition curve reaching maximal 100 % efficacy. This is based on the theory that a high Hill coefficient and a low maximum kill rate indicate “time-dependent antimicrobial effects”, whereas a low Hill coefficient and a high maximum kill rate indicate concentration-dependent effects (Katsuno et al., 2015). However, as none of the compounds met the perfect criteria, six of the most optimal compounds were chosen.

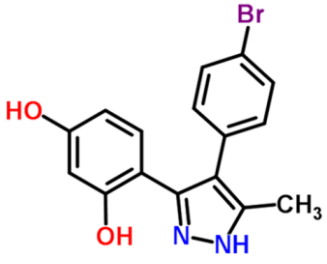
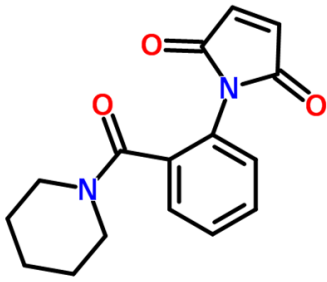
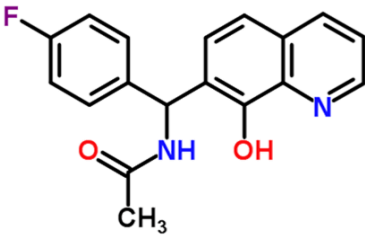
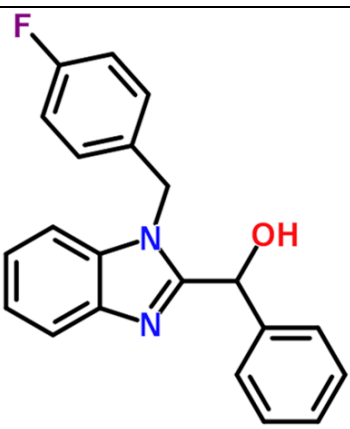
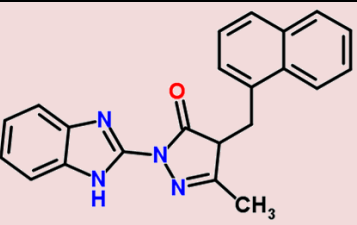
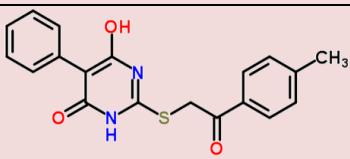
Six compounds: **24**, **16**, **23**, **13**, **7** and chloroxine were chosen from the results of dose response assays (Table 4.2). I decided that six lead series would increase the probability of at least one series being successful, allowing for attrition in future steps, whilst reducing the number of compounds to be studied to a manageable number given time and resources.

Chloroxine (Figure 4.9, Figure 4.10) is already known to be an antibacterial agent and is licenced for use for indications including infectious diarrhoea and inflammatory

bowel disease under the trade name Endiaron and as Capitrol for use with seborrheic dermatitis. Further information about this compound and its properties is given in section 5.3.

Compound	pIC_{50} PrestoBlue	pIC_{50} LIVE/DEAD	Max. Inhibition (%)	Structure
3	4.4	4.5	39	
5	4.4	4.2	43	
7	6.3	5.3	49	
8	4.3	4.3	79	

11	3.9	4.4	67	
13	4.6	4.9	100	
15	4.3	N/A	38	
16	4.6	3.9	42	
17	4.3	4.3	40	
18	4.3	N/A	18	

19	4.8	4.8	37	
20	4.7	4.7	88	
21	4.4	N/A	11	
22	4.4	N/A	88	
23	5.1	5.5	57	
24	8.3	8	50	

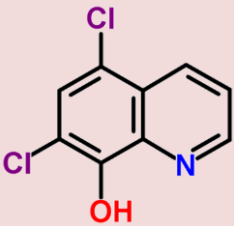
Chloroxine	5.5	N/A	82	
------------	-----	-----	----	---

Table 4.2: Results from activity confirmation.

Down selection of compounds was based upon favourable properties for drug development. Rows shaded in pink were selected for further research based on pIC_{50} , Hill slope and maximal effect.

MIC

MIC was determined for six compounds outlined in chapter 4.5. Results showed that when used as a sole agent without ceftazidime compounds **24**, **16**, **23**, **13**, **7** had no bactericidal or bacteriostatic effects when tested up to a maximum concentration of 1 mM (data not shown). Chloroxine showed weak antimicrobial activity against a culture of *B. thailandensis* with a calculated MIC of 30 μ M (Figure 4.35). Whilst chloroxine displays weak antimicrobial activity, the effect seen for a combination of chloroxine with ceftazidime is markedly greater than for each used as a sole agent (Figure 4.37).

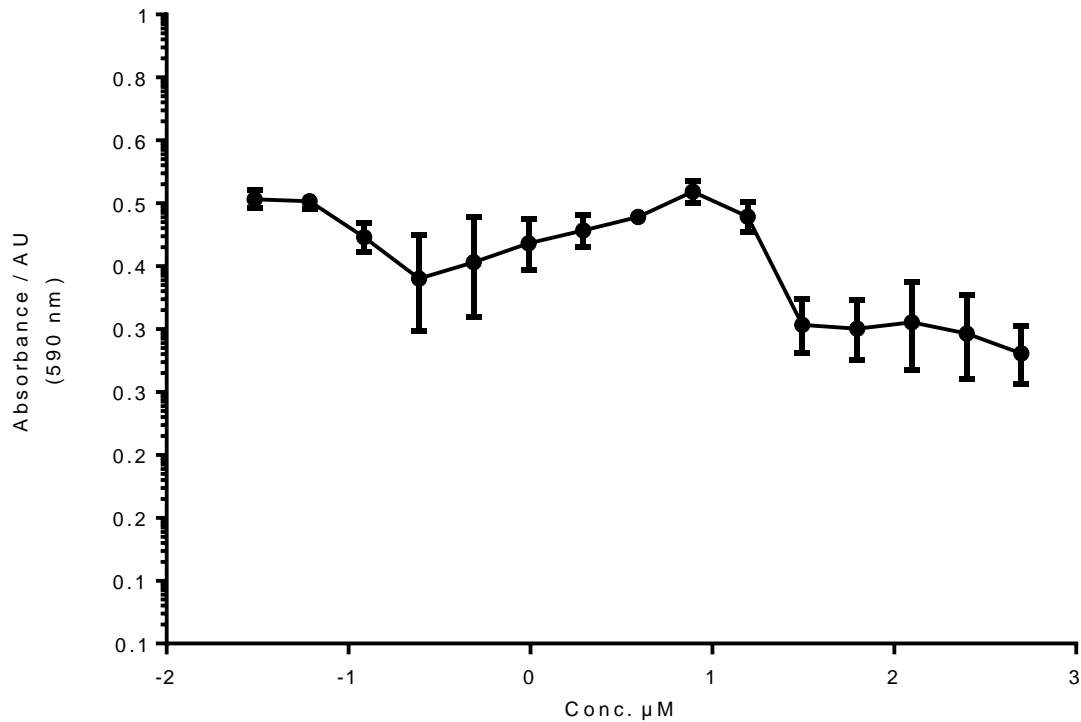


Figure 4.35: A broth microdilution determination of minimum inhibitory concentration (MIC) determination for chloroxine.

MIC was determined as 30 μM. This is the lowest concentration that inhibited growth as detected by absorbance at 590 nm. Results appear to indicate an edge effect at approximately 0.4 μM. Wells with greater error were closer to the plate edge. Results are shown in triplicate, error indicates standard deviation.

Confirmation in *B. pseudomallei*

An experiment was carried out at DSTL to confirm if chloroxine was also active against persister cells in the pathogenic bacteria *B. pseudomallei*. The experiment was performed using an independently sourced, fresh stock of chloroxine and the DSTL reference strain of *B. thailandensis* E264 and *B. pseudomallei*. Raw data was returned to me for analysis.

This experiment (Figure 4.36) was carried out to show that chloroxine is also effective at inhibiting persister cells in a culture of *B. pseudomallei*. Using the PrestoBlue persister assay the experiment was carried out as per methods described in section 4.3. For *B. thailandensis* the $pIC_{50} = 6.5$ which is an order of magnitude more potent than when tested in activity confirmation (Figure 4.10), the 95% confidence intervals were 6.6 to 6.5. Chloroxine was shown to also be effective against *B. pseudomallei* for which $pIC_{50} = 6.0$ (95% confidence interval: 6.1 to 6.0). This confirmed that continuation of research into the use of chloroxine as a potential therapy for melioidosis is justified.

I consider the reproducibility observed in this experiment when carried out by a scientist previously naïve to the project to be a validation of the method development and quality of the PrestoBlue persister assay. The results also validate the use of *B. thailandensis* as a model organism for *B. pseudomallei* for studies of persister cells.

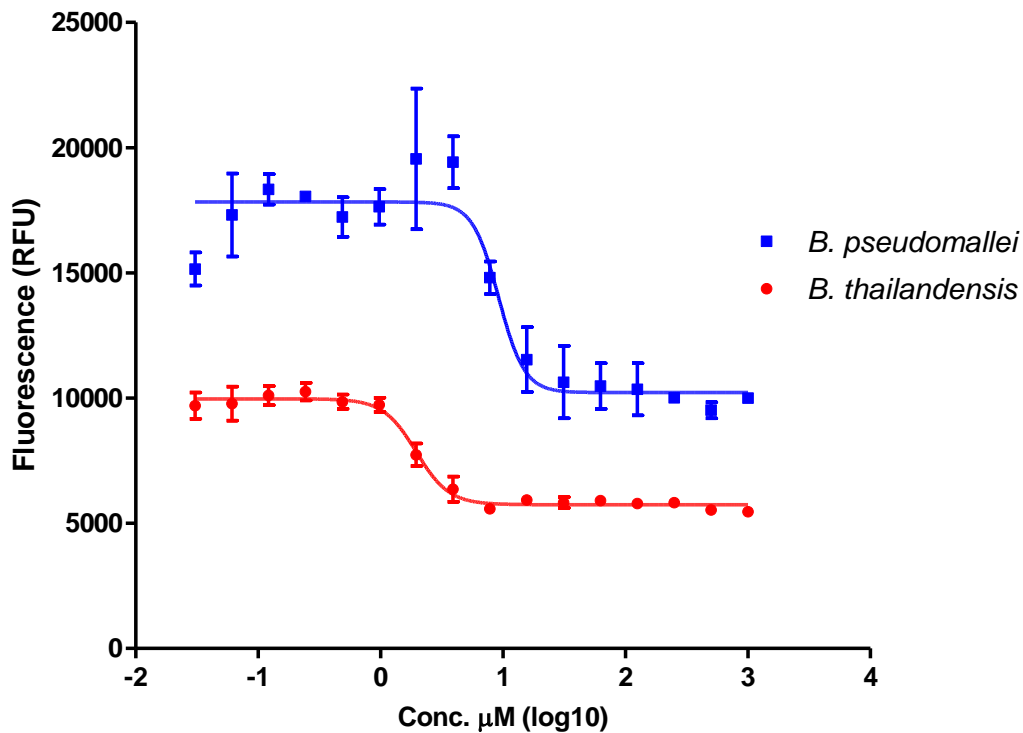


Figure 4.36: Confirmation of chloroxine activity in *B. pseudomallei*. Data provided by DSTL

pIC_{50} was determined using the PrestoBlue™ cell viability assay to compare concentration dependent killing of chloroxine of *B. thailandensis* and *B. pseudomallei*. A persister culture, generated by treatment with 100X MIC ceftazidime hydrate, was added to a 96 well plate containing two-fold dilutions of A in DMSO. Plates were incubated for 24 hours at 37 °C before addition of PrestoBlue™ cell viability reagent and reading fluorescence. Results show three biological replicates with error bars indicating standard deviation. pIC_{50} for *B. thailandensis* = 6.5 (95% CI: 6.6 to 6.5); pIC_{50} for *B. pseudomallei* = 6.0 (95% CI: 6.1 to 6.0).

Time Dependent killing

The six compounds selected in section 4.5 were tested in a time dependent killing experiment where reduction in cell numbers over time was quantified through culture and colony counting. A persister population was treated with ceftazidime and compound at 30 μM (above IC_{50} for all compounds) and reductions quantified. A ceftazidime only control was included. Only one compound, chloroxine was shown to significantly reduce persister cell numbers over a 72 hour period according to this method. The remaining five compounds (**24**, **16**, **23**, and **13**) did not show a significant reduction in colony numbers at this stage of development (Figure 4.37)

As shown previously, chloroxine is weakly antimicrobial when used as a sole agent (Figure 4.35) which may, in part, account for this observation. To improve this experiment, I would retest compounds over a range of concentrations. However, this procedure uses relatively large quantities of compound and so the previous problem of sourcing stocks of compounds prohibited further investigation at this stage. The experiment does indicate that chloroxine is suitable for further investigation.

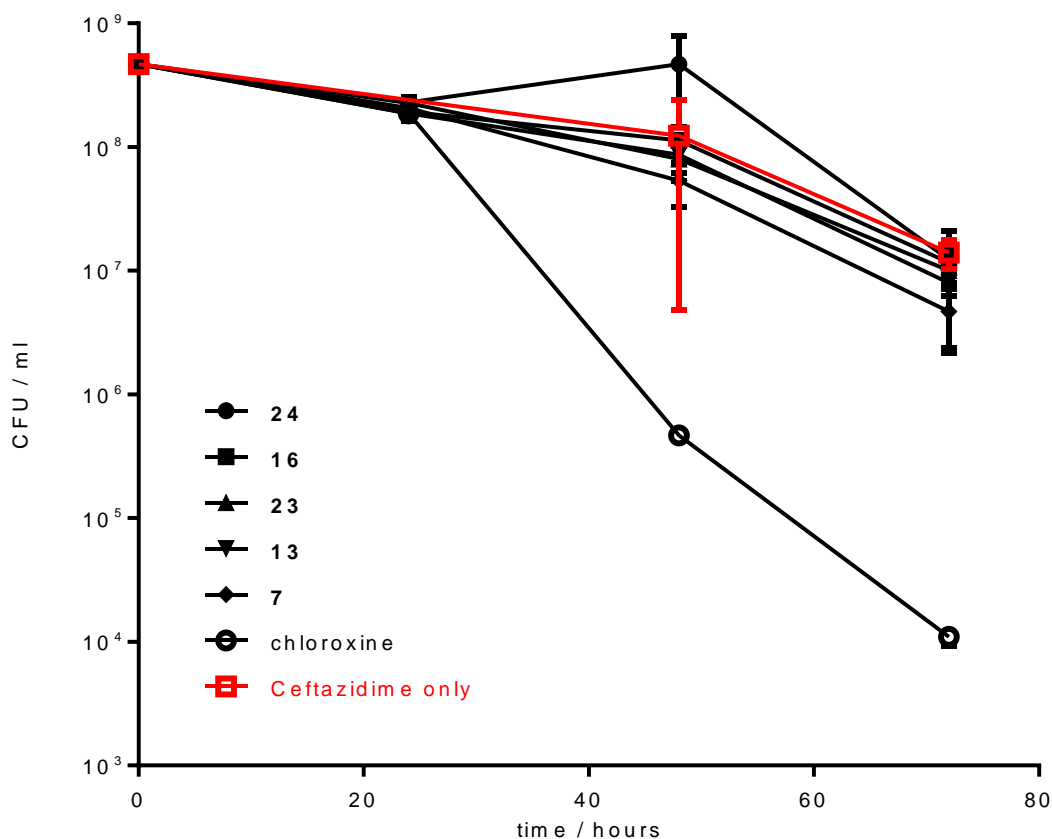


Figure 4.37: Time dependent killing for 6 compounds with promising activity indicated from dose response assays.

Wells of a 24 well plate were seeded with a culture of initial bacterial optical density = 0.4_{600nm}. 1.5 ml was incubated statically with 400 µg/ml ceftazidime hydrate and 30 µM compound in DMSO. Maximum DMSO concentration = 0.1%. Samples were centrifuged, washed and resuspended in LB media. Cells were enumerated by serial dilution in LB media and incubated on LB agar for 24 hours at 37 °C before colonies counted. Persister cell only control is shown in red. Results are in triplicate with error bars indicating standard error. Whilst compounds were active at 30 µM in the cell viability assay this was not observed in the colony-forming unit (CFU) counting experiment shown. As covered in Chapter 2 this may be because enumeration of CFU's is much less sensitive than fluorescence based viability assay. Further

considerations may also include the half-life of compounds in culture and testing against higher concentrations of compound.

4.5. Discussion

It was necessary to confirm hits identified at the DDU using freshly sourced compounds. Test compounds from a screening library are subject to many handling steps by a number of personnel which introduces potential for contamination to occur. Additionally, although masterplates are stored under inert conditions, compounds are stored in a DMSO solution. There is a potential that compounds may have become degraded over time or precipitated out of solution. Hit compounds were confirmed by the DDU through LC-MS after screening. However, it was prudent to repeat assays. By repeating the dose response assays in this section of work I was also able to carry out the experiments with biological triplicates over a larger range of concentrations to obtain more robust fittings of IC_{50} .

A significant frustration was that a good proportion of the compounds, despite being listed in catalogues, were not available for purchase. Ten compounds from the 29 confirmed hits from preliminary screening were not available to buy through commercial suppliers which significantly restricted the flow of work. An alternative to this problem would be to commission synthesis of compounds. However, this would be prohibitively expensive and time consuming for an academically funded project, and so this was not undertaken at this point. Many of these compounds were structurally similar to other hit compounds that were available, and so the loss of these compounds is likely not to have materially affected the following work.

Despite not being able to obtain all hit compounds for hit confirmation, I was able to group hits into series based upon similarities in structure. This family representation

of chemical space that I was able to achieve indicated that the loss of compounds should not significantly affect the work.

Some compounds showed increased fluorescence for the highest concentrations of compound when tested with the PrestoBlue dose response assay. An example of this can be seen in Figure 4.6. As this is observed in the PrestoBlue assay but not the LIVE/Dead assay, I believe that this is due to higher concentrations of the compound reacting with the resazurin in the PrestoBlue giving a false positive result. For the purpose of fitting a line to the data the bottom value for assays where this occurred, the data were truncated at the concentration at which maximum inhibition was observed. The dose response assay for **15** using the Live/Dead assay gave unexpected results. Raw data shows that the SYTO9 component of the assay fluoresced more intensely at greater compound concentrations (Figure 4.16). My conclusion from this is that **15** most likely emits fluorescence at 498 nm or within the same range as SYTO9. This could be tested by reading a solution of **15** in a plate reader at emission wavelength of 498 nm and over a range of excitation wavelengths. Identifying any increase in fluorescence against a negative of DMSO solvent would confirm that **15** is fluorescent at the same wavelength as SYTO9.

This observed difference between LIVE/DEAD and PrestoBlue confirm that it was necessary to have a second, orthogonal assay using a different fluorophore to confirm hits. In addition to giving further confidence in results, this step was deemed important for ensuring the study was of publishable quality.

Notable compounds selected include **13**, which contains a thiadiazole group. Thiadiazoles feature in a number of antiparasitic and antimicrobial agents, but are

more associated with broad spectrum biological activity (Li et al., 2013). **24** appears to show activity at very low concentrations (figure 4.34), which seemed very promising for the development of this compound. A consideration would be that the overall effect is moderate. Further assays were attempted to explore lower concentrations, but these were not successful within the timeframe of the project.

PAINS (Pan Assay Interference Compounds) are compounds that appear frequently in compound screening and have been shown to display promiscuous target binding. Often these compounds can be identified through screening only to fail further down the drug discovery pipeline (Baell and Holloway, 2010). Well established PAINS have been removed from the DDU library or are identified in the analysis of hits through the report creation software. However, it is still possible for promiscuous binding compounds to be selected, which may or may not prove to be good drug candidate. An example of promiscuous binders are PrAT compounds: promiscuous 2-aminothiazoles (Devine et al., 2015). This study was published in January 2015 after activity confirmation and Series expansion (Chapter 5) had been carried out and could potentially include **11** in their number. 2-aminothiazoles have been shown to be photo-reactive and also promiscuous binders (Huth et al., 2007). Despite these concerns there are still a number of compounds containing 2-aminothiazoles in phase I, II and clinical trials (Baell and Holloway, 2010).

ADMET

For a drug candidate to be successful it is important for it to meet criteria in terms of absorption, distribution, metabolism and toxicity (ADMET). These properties may be developed further in the drug development pipeline. However, it is important to consider physiochemical and structural properties from the earliest stage. This is

particularly important for small molecule drugs where the “drug-likeness” (mostly dependent on molecular mass and lipophilicity) are closely linked to the future success of a drug candidate.

A “rule of five” was proposed in 1997 describing predictions of physicochemical properties for suitable drug candidates (Lipinski et al., 2001). The Rule of five is a set of parameters used to estimate “drug-likeness” or bioavailability. It states that for a drug like compound there should be no more than five hydrogen bond donors, ten hydrogen bond acceptors, the compound should have a Mw less than 500 daltons and the octanol-water partition coefficient *logP* should not be greater than 5. Whilst a lot has moved on in drug discovery since then, basic principles such as; improving permeability and oral availability by using smaller molecules with a more favourable ligand efficiency, and reducing the risk of in vivo toxicity and in vitro receptor promiscuity by using molecules with a *cLogP* < 3, can still be applied. The *cLogP* of a compound is a measure of the molecules hydrophilicity. It is calculated as a logarithm of the partition coefficient between n-octanol and water (Collander, 1951). In order to reduce toxicity, *cLogP* should be less than 3 and the total polar surface area (TPSA) should be greater than 75 (Price et al., 2009). High lipophilicity has been hypothesised to increase the probability for promiscuous binding to off target proteins, increasing the likelihood of toxicity (Leeson and Springthorpe, 2007).

5. Series Expansion

5.1. Overview

This section of work was carried out at the University of Exeter from April 2014 to November 2014. In this phase of drug discovery the six compounds identified in section 4.5 were further developed to determine their potential as lead series. To achieve this I focussed on obtaining structure activity relationship (Moule et al.) information for compounds and looked into possible modifications to improve upon confirmed hits.

SAR is the relationship between the chemical or three-dimensional structure of a molecule and its biological activity, in this case measured by ability to reduce persistence. To form the basis of a lead series, clusters of compounds are identified which have related structures but differ in sections or chemical motifs. By testing this series and the core compound and comparing potencies relationships between the structure and activity can be identified (Hughes et al., 2011b).

This phase of work also coincided with the installation of a liquid handling system at the University of Exeter which further improved the reliability of the assays.

5.2. Experimental Procedure

All subsequent liquid handling was automated using an Eppendorf EpMotion liquid handling robot.

Compounds with systematic structural modifications to original hit compounds listed in 4.5 were determined by medicinal chemistry professionals at the DDU. These compounds were sourced through commercial suppliers and dissolved into DMSO

solutions at 36 mM. Compound masterplates were created using an Eppendorf EpMotion 5070 liquid handler to create 16 ten-fold dilutions in DMSO in a final volume of 100 μ l.

From this point a PrestoBlue based dose response assay was performed exactly as described in 4.3.

5.3. Results

Compounds for series expansion were chosen by the DDU around the structures of compounds outlined in section 4.5. By making systematic alteration to R groups around these compound clusters it was hoped primarily to identify closely related compounds with enhanced potency or characteristics better suited to drug use. Another output of this exercise is elucidate structure-activity relationships by observing how manipulation of the compound structure, such as addition or removal of hydrogen bond donors or acceptors for example, can affect the potency of the compound.

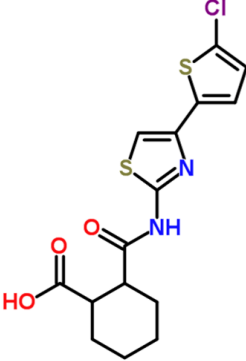
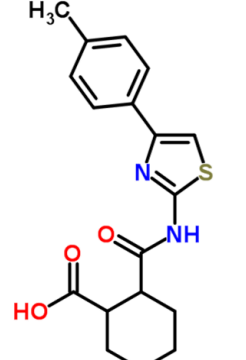
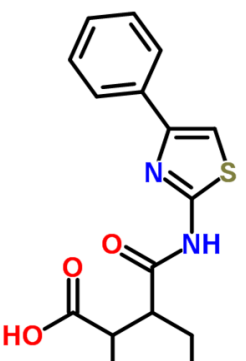
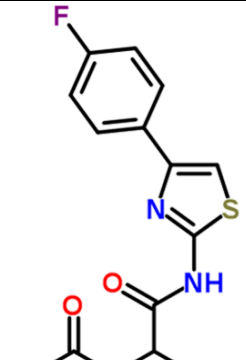
As in section 4, a significant limitation to series expansion was in difficulty obtaining compounds from commercial suppliers. For series expansion, it would be an ideal situation to have modifications for all groups around a structure. Unfortunately, this was not possible. Many compounds advertised online were out of stock indefinitely, and some were not available in the quantities needed for suitable assays. An additional cause for concern with some of the smaller suppliers was that compounds were supplied with very little information as to their process or synthesis and purity from contamination. Many compounds are synthesised using heavy metal catalysts and it is imperative that these are not present in biological assays. These potential impurities could be identified through differential migration using thin layer chromatography (TLC). Contaminants can also be identified by their mass through use

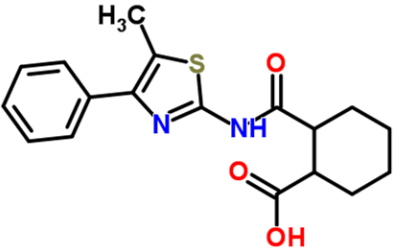
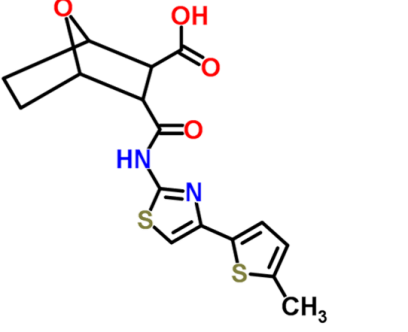
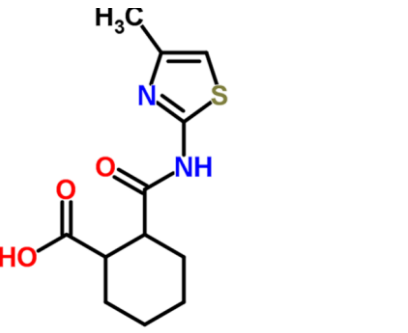
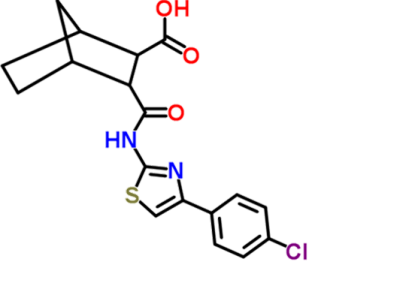
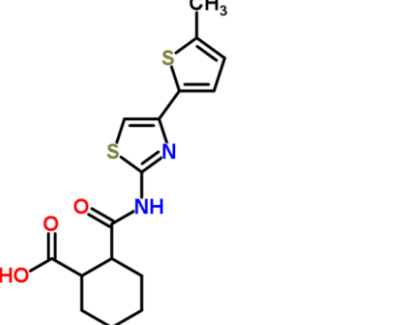
of liquid chromatography mass spectroscopy (LCMS) or by nuclear magnetic resonance spectroscopy (NMR) which identifies chemical and physical properties of molecules through analysis of their NMR spectra. Despite the sub-optimal chemistry resources for this section of work, the resultant data has highlighted two potential lead series. Given the circumstances, the results are surprisingly encouraging.

Series expansion of 7

The parent compound was reordered and retested as shown in Figure 5.1. The compound, obtained from Vitus M Laboratories, is the same as previously supplied by ChemDiv (www.chemdiv.com) with a pIC_{50} determined as 6.3 by the Presto Blue based assay and 5.3 using the LIVE/DEAD assay (Figure 4.6).

Compounds **26, 34, 35, 36, 37, 38** all showed structural modifications that resulted in no dose-dependent relationship being observed. Compounds beginning with the prefix F were brought from Life Chemicals. It is not known if the significantly higher number compounds from this supplier which are not active against persister cells is due to the structural modifications made or some other quality of the chemicals. It is noted that whereas other suppliers provided analytical data on compound identity and purity this was not provided with chemicals from Life Chemicals.

Key	Compound	pIC ₅₀	Hill	Structure	
7	STK959997	6.3 (95% CI: 6.9 to 5.8)	2.0		Figure 5.1
26	STK430229	not converged	N/A		
27	STK414822	5.3 95% CI: 5.4 to 5.1	3.6		Figure 5.3
28	STK430245	6.2 (95% CI: 7.3 to 5.1)	0.7		Figure 5.5

29	STK331592	5.9 (95% CI: 6.1 to 5.6)	4.3		Figure 5.7
30	STK445925	3.5 (95% CI: 1.4 to 5.7)	1.6		Figure 5.9
31	STK414820	4.1 (95% CI: 4.3 to 4.8)	1.7		Figure 5.11
32	STK424172	4.9 (95% CI: 5.7 to 6.2)	0.7		Figure 5.13
33	STK457058	5.7 (95% CI: 5.3 to 6.00)	1.4		Figure 5.15

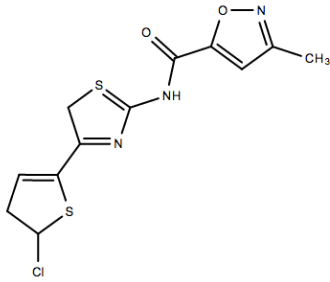
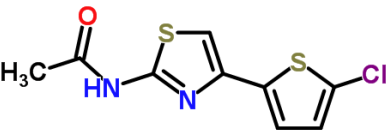
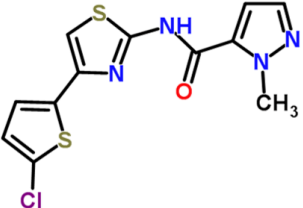
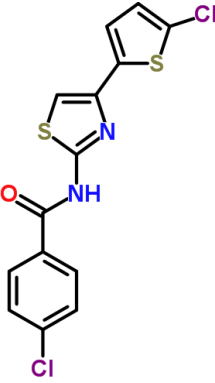
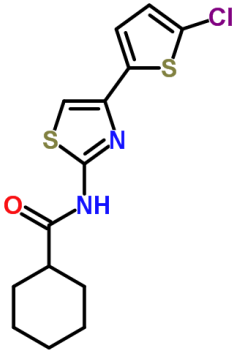
34	F5002-0184	not converged	N/A		
35	F0174-0120	not converged	N/A		
36	F5086-0047	not converged	N/A		
37	F0174-0134	not converged	N/A		
38	F0327-0091	not converged	N/A		

Table 5.1: Series expansion around hit compound 7.

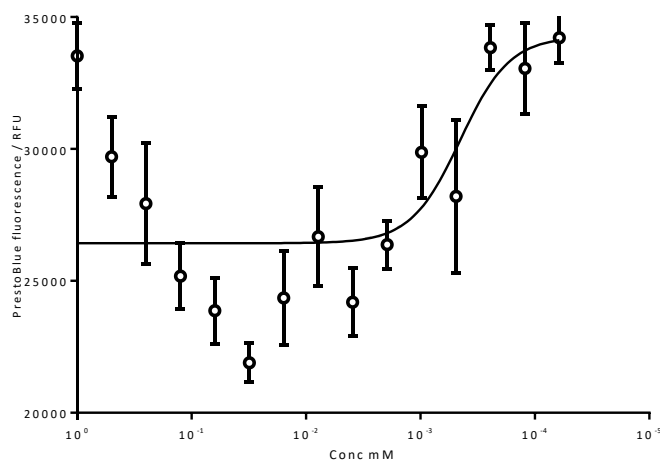


Figure 5.1: Dose response assay for a fresh stock of hit compound **7**. $pIC_{50} = 6.3$ (95% CI: 6.9 to 5.8)

Sourced from VitasM Laboratories, STK959997 is the same as the original hit compound **7** which was sourced from ChemDiv for hit confirmation (Figure 4.5). A dose-response assay using persister culture, generated by treatment with 100X MIC ceftazidime hydrate, was added to a 96 well plate containing two-fold dilutions of compounds in DMSO. Plates were incubated for 24 hours at 37 °C before addition of 10 μ l PrestoBlue cell viability reagent and reading fluorescence. Results are in triplicate, error bars indicate standard error.

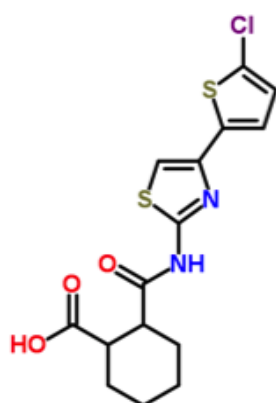


Figure 5.2: Structure of **7**

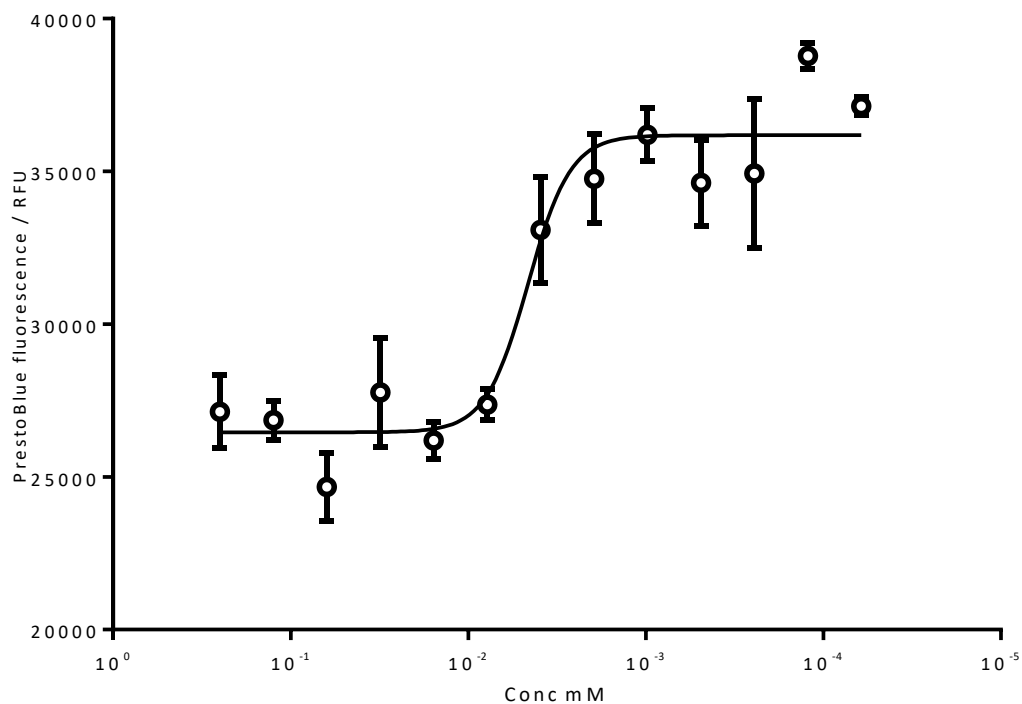


Figure 5.3: **27** from series expansion of **7**.

Replacement of the 2-chlorothiophene group with a benzene group decreases the pIC_{50} from 6.3 to 5.3 (95% CI: 5.4 to 5.1). Results are in triplicate, error bars indicate standard error.

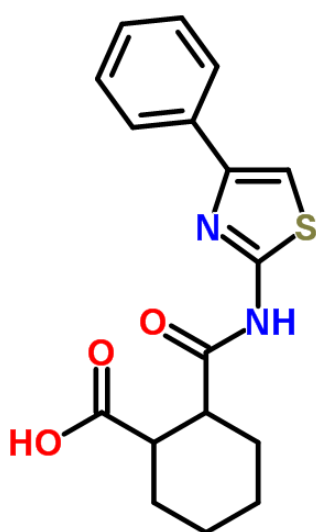


Figure 5.4: Structure of **27**

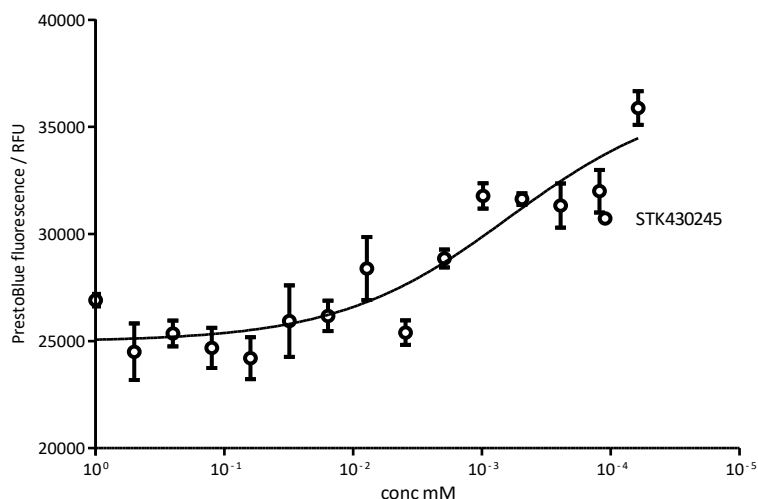


Figure 5.5: **28** from series expansion of **7**.

The 2-chlorothiophene group is replaced with a fluorobenzene group resulting in no change in pIC_{50} from 6.3 to 6.2 (95% CI: 7.3 to 5.1) within error. However this compound is considered less attractive than others in the series with a similar pIC_{50} due to the shallow Hill slope (0.65). Results are in triplicate, error bars indicate standard error.

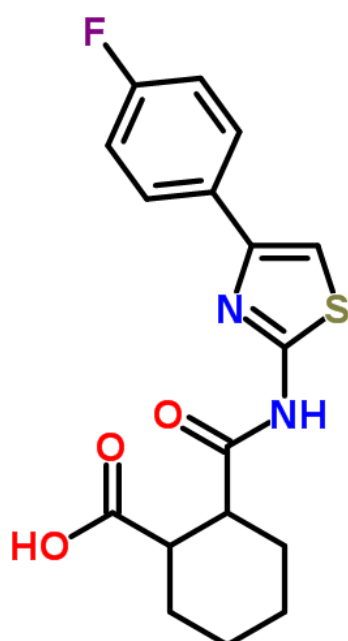


Figure 5.6: Structure of **28**

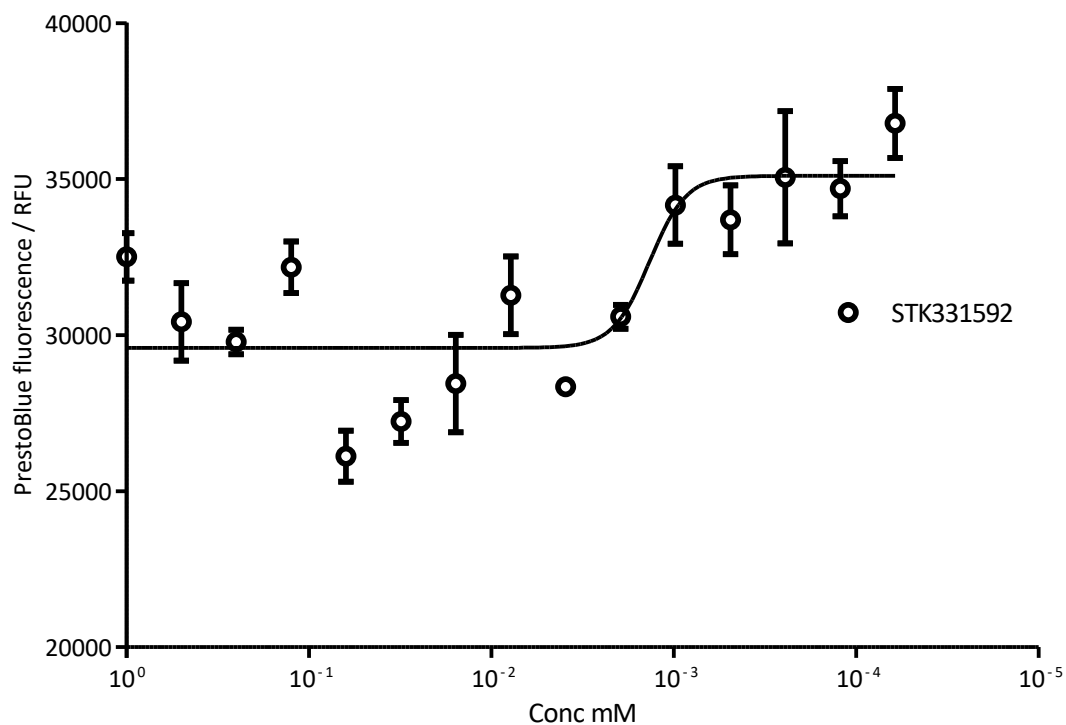


Figure 5.7: **29** from series expansion of **7**.

A benzene group is added to the thiophene group and a methyl group is added to the middle ring resulting in the pIC_{50} increasing from 6.3 to 5.9 (95% CI: 6.1 to 5.6). $R^2 = 0.54$ indicating this may not be a definite result. Results are in triplicate, error bars indicate standard error.

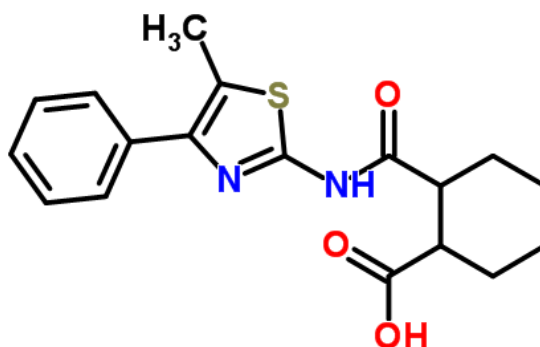


Figure 5.8: Structure of **29**

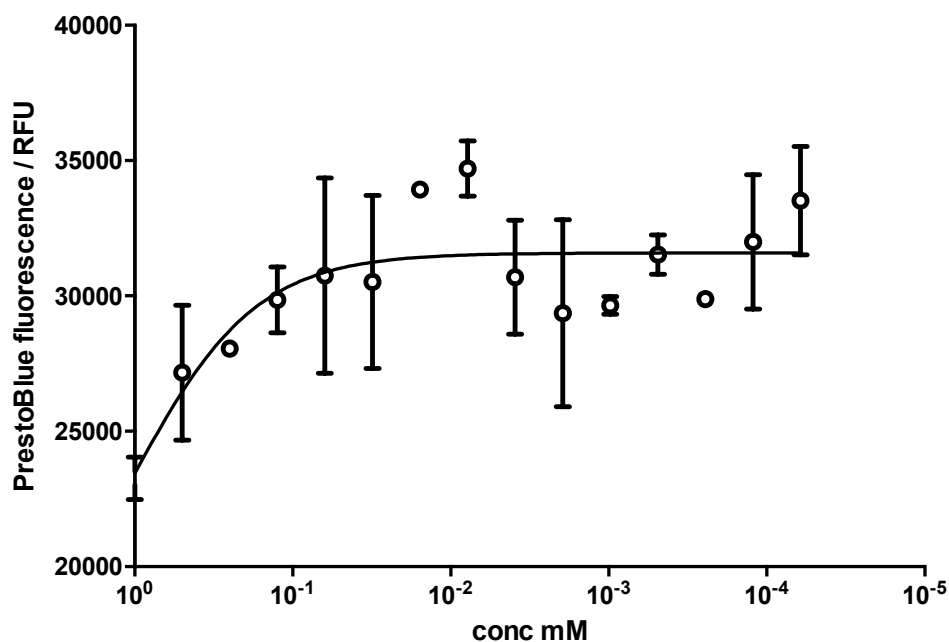


Figure 5.9: **30** from series expansion of **7**.

An oxygen molecule is added across the cyclohexane group creating oxabicyclohexane. The fluoride group is also replaced with a methyl group. The graph shows an increase in pIC_{50} to 3.5. Although the $R^2 = 0.45$ indicates a poor fit, there is clearly a significant loss of activity. Results are in triplicate, error bars indicate standard error.

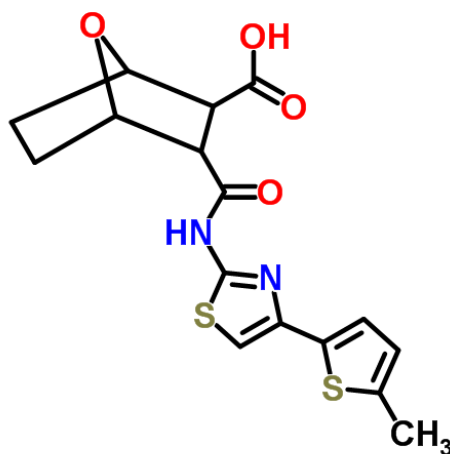


Figure 5.10: Structure of **30**

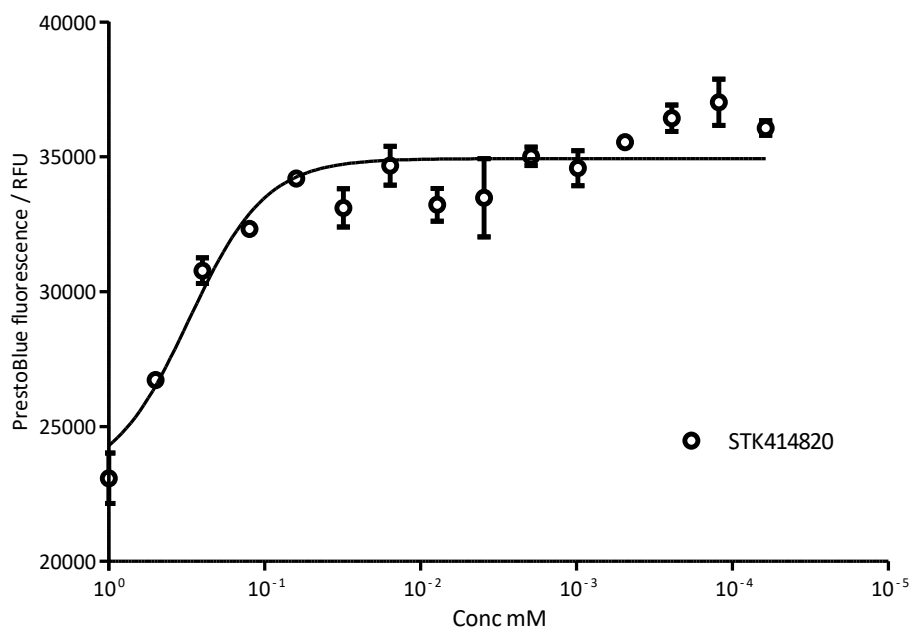


Figure 5.11: **31** from series expansion of 7.

This compound differs from the original structure by removal of the 2-chlorothiophene group and a substitution of as methyl group to create 5-methyl-1,3-thiazole resulting in a reduced pIC_{50} of 3.5. This substitution shows a significant loss of activity. Results are in triplicate, error bars indicate standard error.

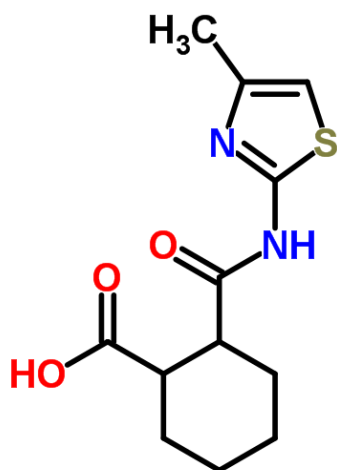


Figure 5.12: Structure of **31**

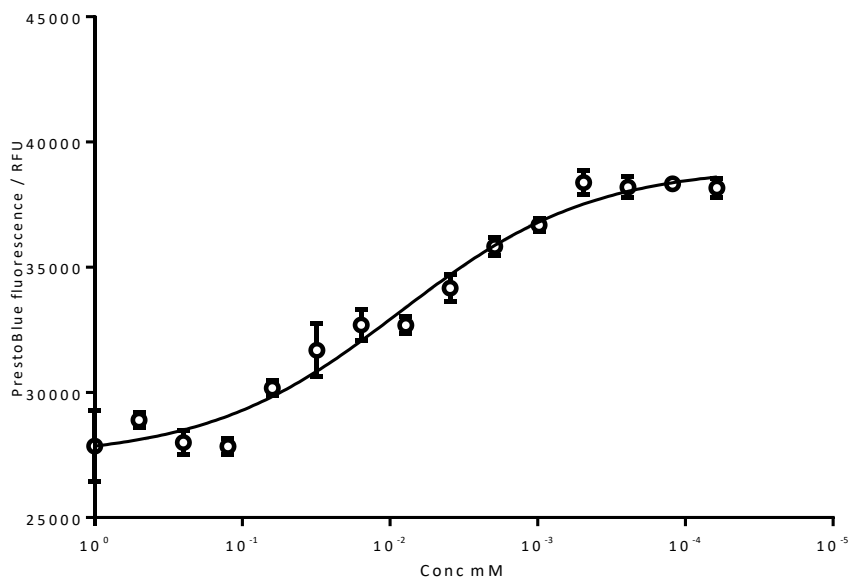


Figure 5.13: **32** from series expansion of **7**.

The structure differs from **7** by the addition of a carbon across the cyclohexane creating a norbornane group and the substitution of the 2-chloro-thiophene for a *para*-chlorobenzene. These combined changes result in an increased pIC_{50} from 6.3 to 4.9 (95% CI: 5.7 to 6.2). Furthermore, there is a significant drop in Hill slope. Results are in triplicate; error bars indicate standard error.

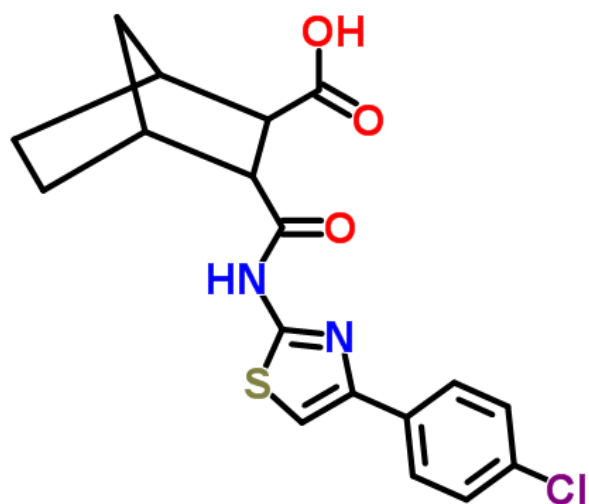


Figure 5.14: Structure of **32**

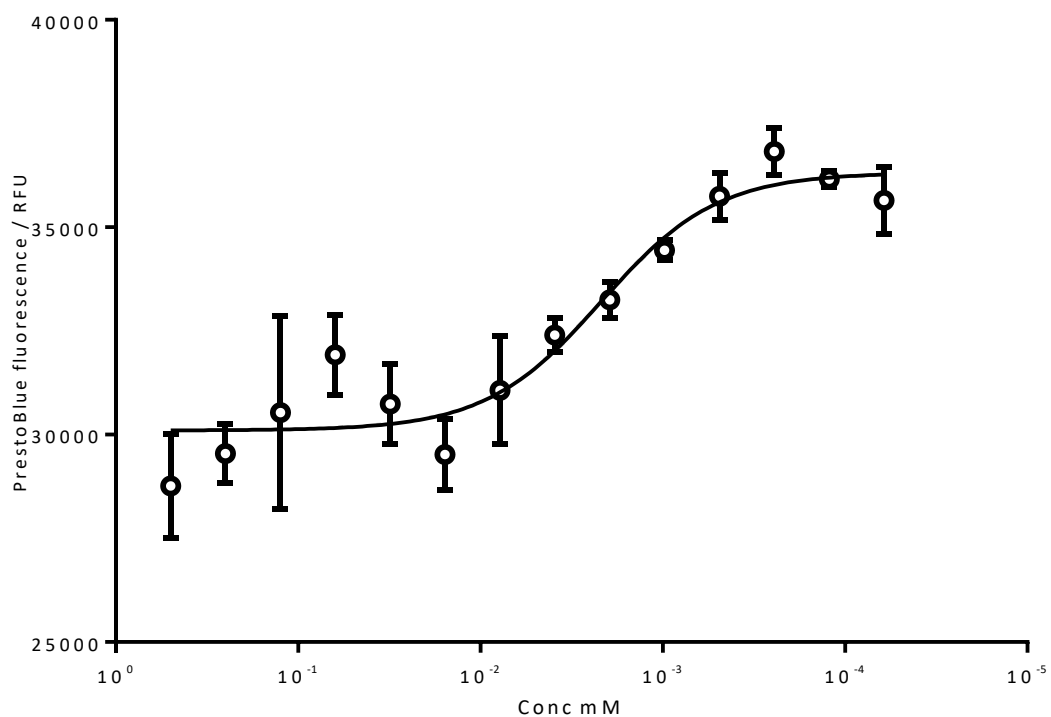


Figure 5.15: **33** from series expansion of **7**.

Substitution of a methyl group for the chloride results in the pIC_{50} reducing from 6.3 to 5.7. Results are in triplicate; error bars indicate standard error.

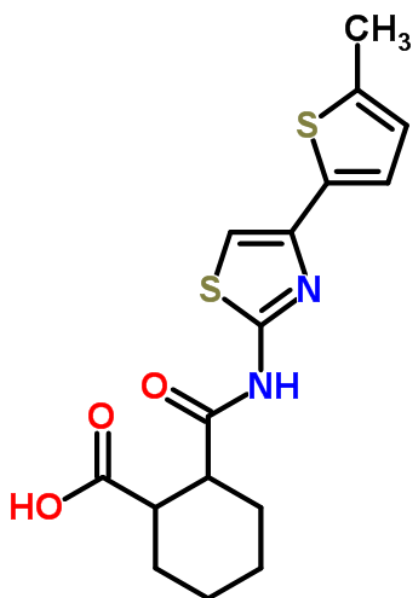


Figure 5.16: Structure of **33**

SAR for 7

For some compounds a poor goodness of fit was observed with high standard deviations observed between replicates. These experiments were carried out in batches using automated liquid handling and avoiding areas of the assay plate where edge effect is most commonly observed (See Chapter 3.2).

A series of modifications to structural groups from compound 7 were made. The critical modifications are shown in Figure 5.17. The first modification made to the parent compound looked at the importance of the chlorine group (shown at the top of the parent molecule). When removed (**27**) a reduction in activity was seen from pIC_{50} 6.3 from 5.3 (Figure 5.5). When substituted for a more electronegative halide, fluoride (**28**) no significant change is observed (Figure 5.7). In **33** the halide group is exchanged for a methyl group resulting in a measurable drop in activity (Figure 5.15).

29 (Figure 5.7) includes a methyl addition to the thiazole group. This results in a significant drop in activity. Compounds with modifications to the cyclohexane group, such as in **32** (Figure 5.13) showed a slight reduction in pIC_{50} although most activity was retained. Another example of this (**32**) features an oxabicyclo heptane instead of the cyclohexane which also severely reduces activity (Figure 5.13).

Compounds **34**, **35**, **36**, **26**, **37**, **38** have lost all inhibiting activity. I have previously mentioned concerns about the chemical supplier. However, this subset of compounds also feature severe modifications or removal of the acid group adjacent to the cyclohexane group. This suggests an SAR indicating this acid group is essential to the compound's activity.

At the other end of the molecule, replacement of the 2-chlorothiophene group with a benzene group decreased the pIC_{50} from 6.3 to 5.3, indicating that both external groups of the molecule have an effect on the activity.

These are clear SAR's, in which modifications to both the acid group and ring structure on both ends of the molecule, result in modulation of potency. This indicates that compound **7** qualifies for development as a lead series.

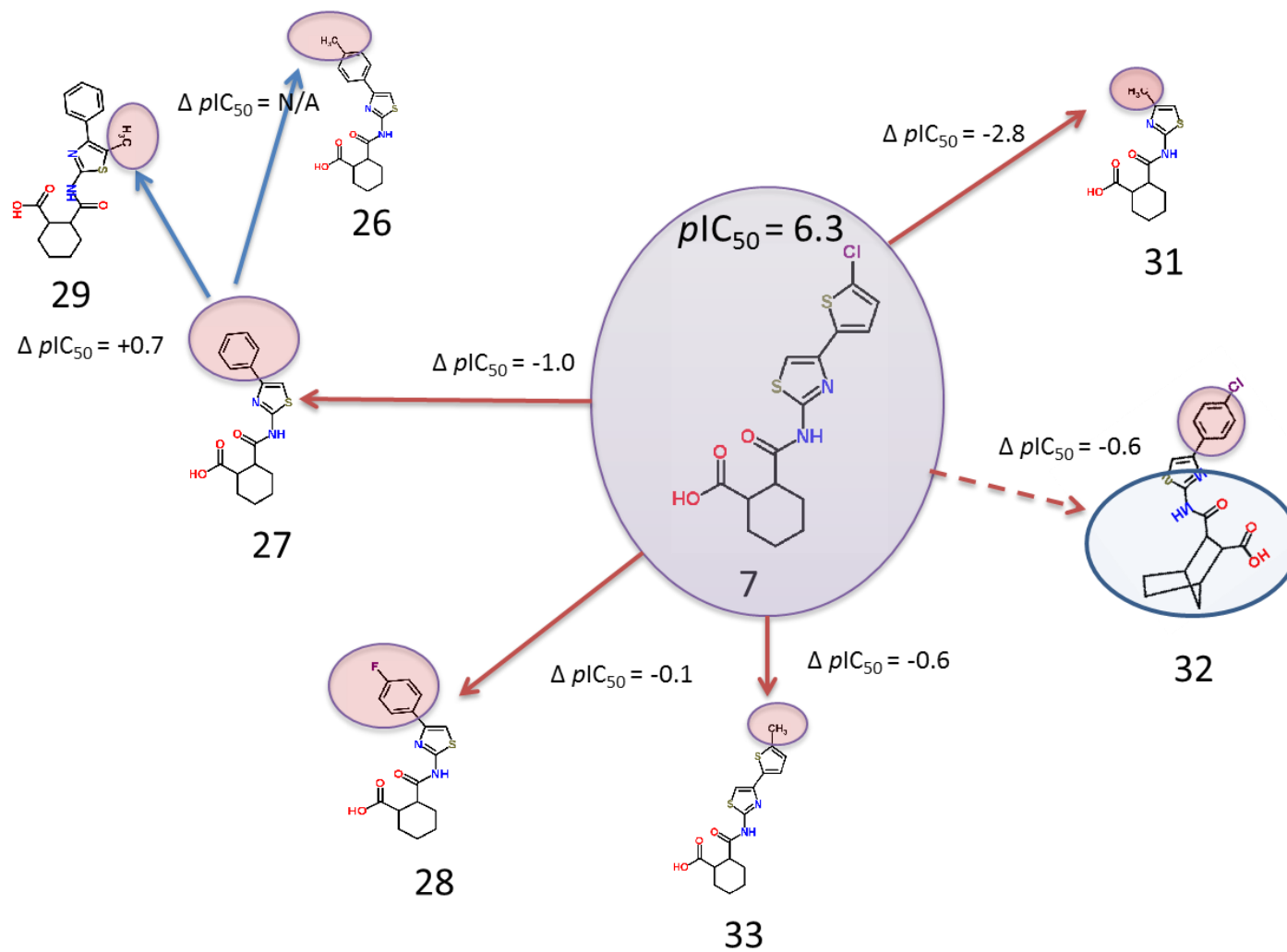


Figure 5.17: SAR for Compound 7 showing evolution of series and effect of manipulation on pIC_{50}

Series expansion of **23**

23, known as 2-(1H-benzimidazol-2-yl)-5-methyl-4-(1-naphthylmethyl)-2,4-dihydro-3H-pyrazol-3-one was sourced from VitasM Laboratories (Chemspider ID 2254810).

The compound complies with the “rule of five” (Lipinski et al., 2001) and has five hydrogen bond acceptors and one hydrogen bond donor. The cLogP is 3.84, which may be considered a bit high, and the molecule contains two rotatable bonds. The Mw of the parent **23** is 354 Da, allowing for some capacity to modify the structure.

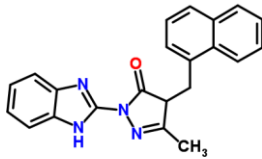
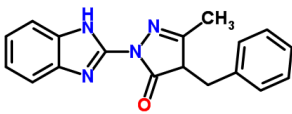
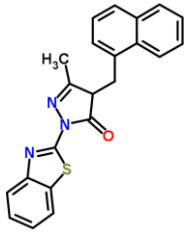
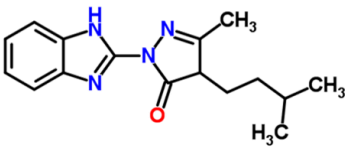
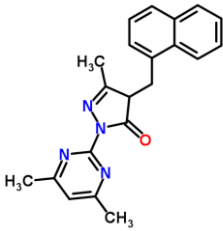
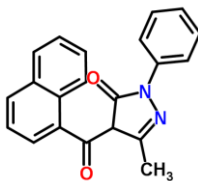
Key	Compound	pIC ₅₀	Hill	Structure	Figure
23	23	5.1	2.1		Figure 5.18
39	STK210203	5.0	2.4		Figure 5.20
40	STK210201	4.3	1.5		Figure 5.22
41	STK210204	4.8	3.4		Figure 5.24
42	STK250052	not converged	N/A		
43	F5229-0026	not converged	N/A		

Table 5.2: Series expansion around parent **23**.

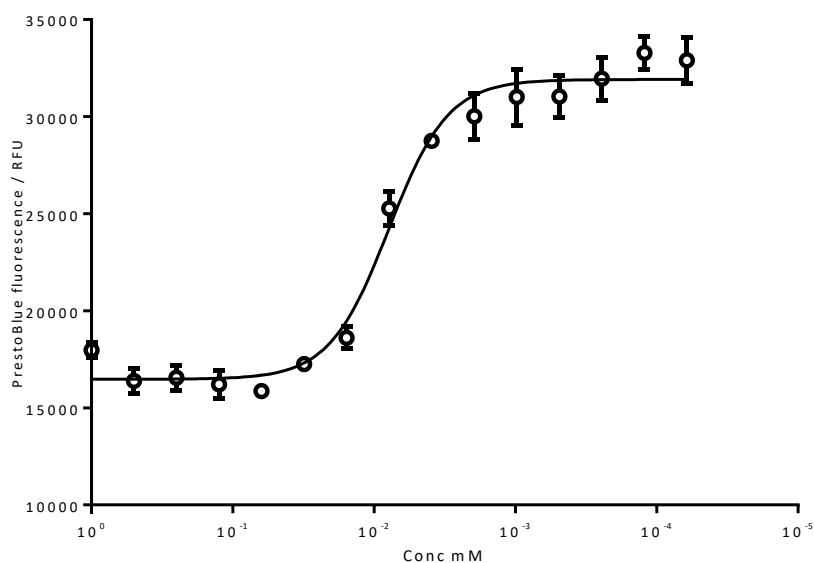


Figure 5.18: Dose response assay for original hit compound **23**.

The parent compound was re-ordered from ChemBridge and the experiment carried out as in Figure 4.32 with the difference being that all liquid handling in this experiment was automated. pIC_{50} was consistent at 5.1 (95% CI: 5.2 to 5.0). Results are in triplicate, error bars indicate standard error.

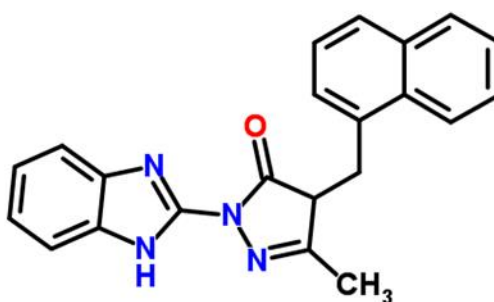


Figure 5.19: Structure of **23**

Also known as (2-(1H-benzimidazol-2-yl)-5-methyl-4-(1-naphthylmethyl)-2,4-dihydro-3H-pyrazol-3-one)

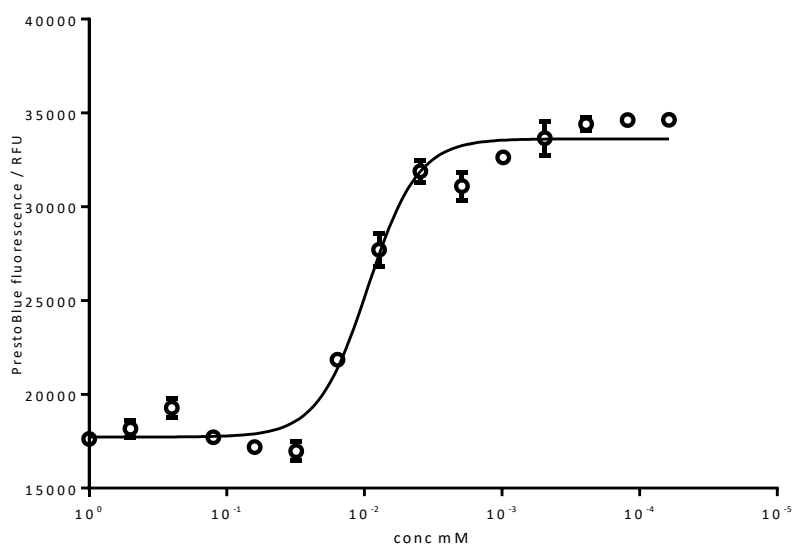


Figure 5.20: **39** from series expansion of **23**.

The structure differs by removal of a benzene ring from the naphthalene group in **23**. $pIC_{50} = 5.02$ indicating little effect on compound activity. This modification, however, significantly reduces the molecular weight. Results are in triplicate; error bars indicate standard error.

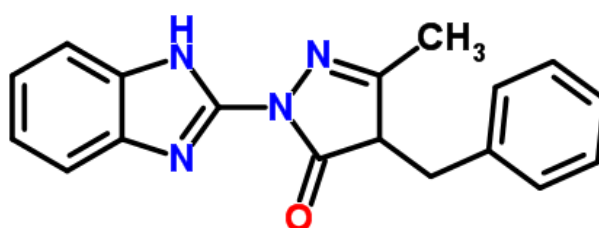


Figure 5.21: Structure of **39**

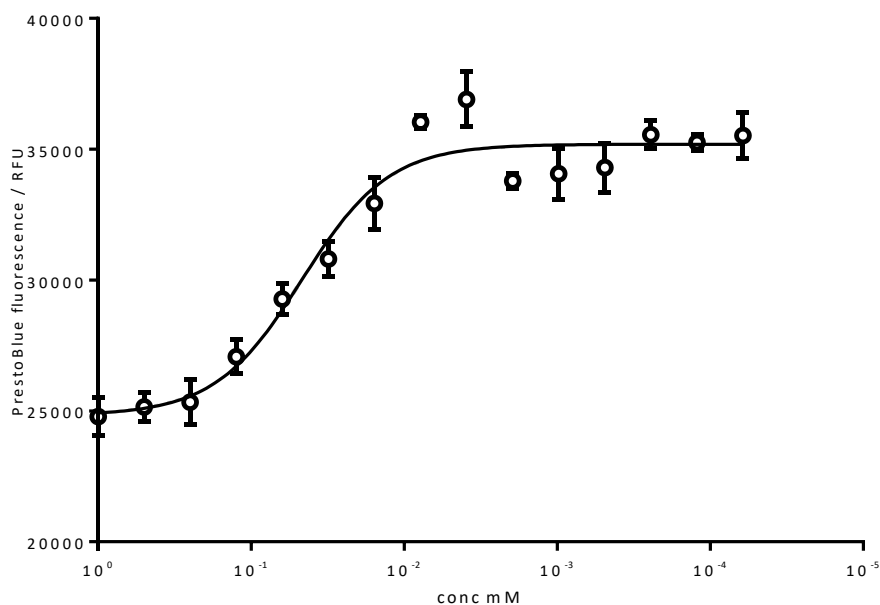


Figure 5.22: Dose response assay for **40** from series expansion of **23**.

Substitution of nitrogen for sulfur produced a benzothiazole group in place of the benzimidazole group in **23** (Figure 5.23). pIC_{50} was decreased from 5.1 to 4.3 indicating this change reduced the compound activity, potentially due to a hydrogen bond donor being required at this position. Results are in triplicate, error bars indicate standard error.

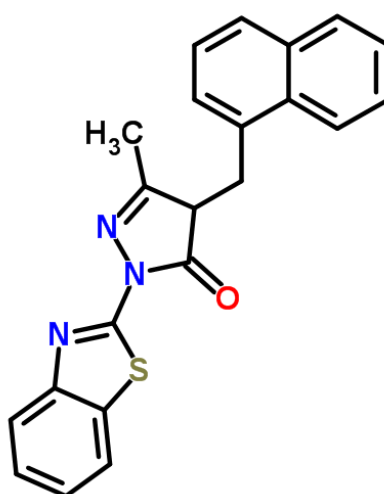


Figure 5.23: Structure of **40**

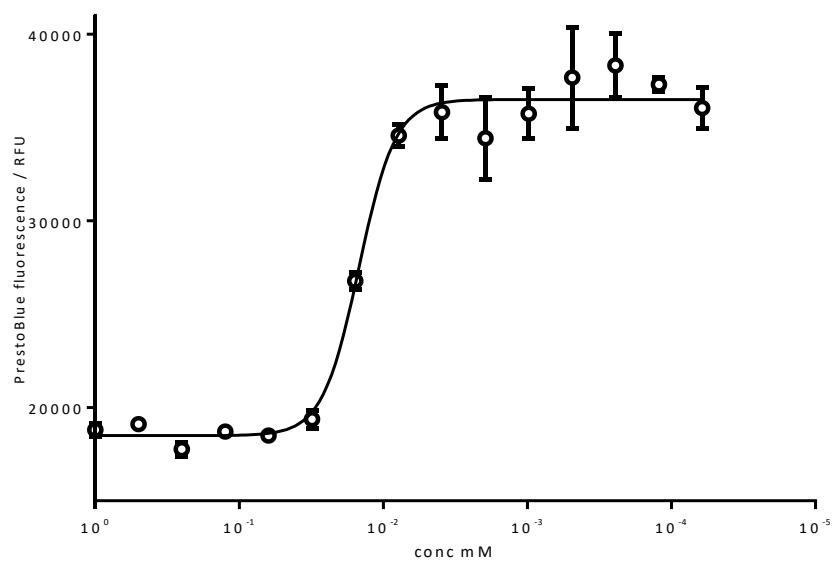


Figure 5.24: **41** from series expansion around the structure of compound **23**.

The naphthalene group from **23** has been removed and replaced with an isobutene group (Figure 5.25). This reduces the pIC_{50} from 5.1 to 4.8 (95% CI: 4.9 to 4.8). However, this reduction is of marginal significance given the errors in these values. Results are in triplicate, error bars indicate standard error.

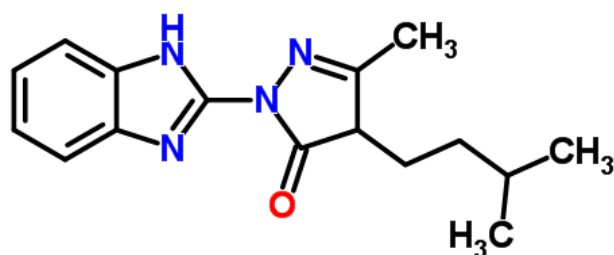


Figure 5.25: Structure of **41**

SAR for 23

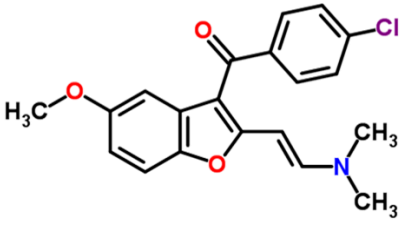
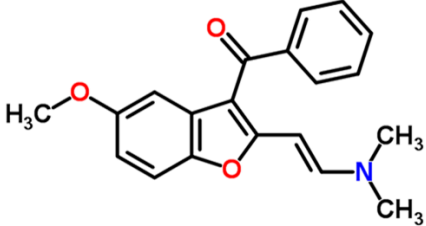
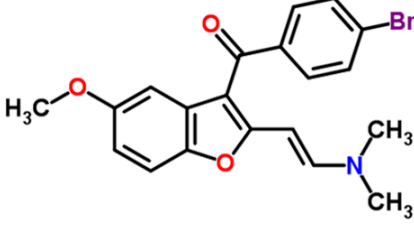
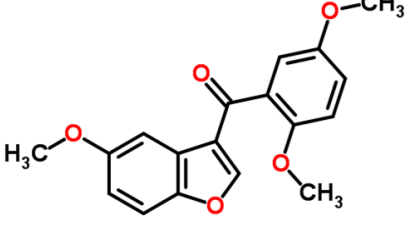
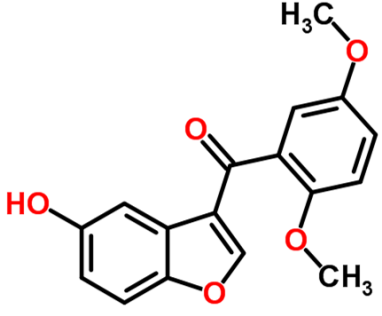
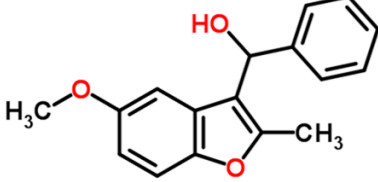
For most modifications made to **23** few significant changes in pIC_{50} were observed. From substitution of a central nitrogen atom for sulphur in **40** (Figure 5.22, Figure 5.23) it can be seen that changes to the central group of hydrogen bond acceptors results in slightly lowered pIC_{50} from 5.1 to 4.3.

As there is some SAR information available for **23** it could be classed as a weak lead series. However there has not been enough dissection of the molecule through systematic series expansion to show any significant improvements upon the parent compound.

23 has a cLogP of 3.135, three rotatable bonds and three hydrogen bond acceptors.

Series expansion of 16

Series expansion around **16** was carried out. The compound, (4-chlorophenyl){2-[(E)-2-(dimethylamino)ethenyl]-5-methoxy-1-benzofuran-3-yl}methanone, has a Mw of 355 and is one of the larger compounds identified. The cLogP = 3.135 and compound contains four hydrogen bond acceptors and no hydrogen bond donors. There are five rotating bonds. The newly sourced compound (Figure 5.27) shows increased activity from pIC_{50} 4.6 (Figure 4.18) to 5.5. This may be a result of using a freshly synthesised compound which has undergone less degradation.

Key	Compound	pIC_{50}	Hill	Structure	Figure
16	STK52587 6	5.5	0.6		Figure 5.27
44	STK52643 5	6.8	1.4		Figure 5.29
45	STK52508 2	4.1	0.8		Figure 5.31
46	STK14913 2	not converged	N/A		
47	STK01317 5	not converged	N/A		
48	STK83253 6	3.7	2.3		Figure 5.33

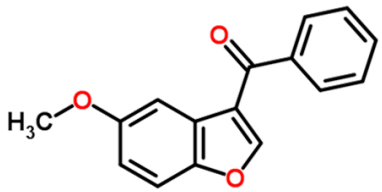
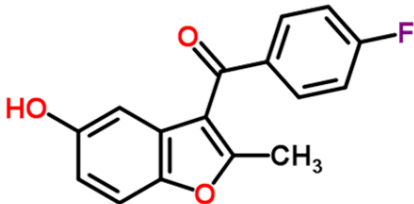
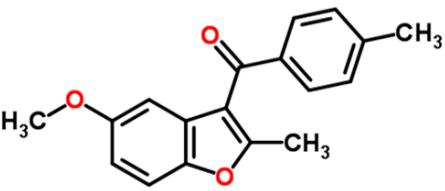
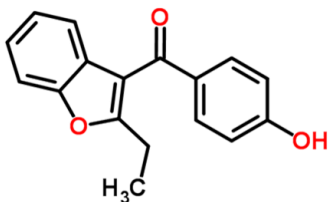
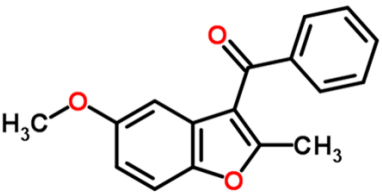
49	STK75182 7	Not converged	N/A		
50	STK83346 3	Not converged	N/A		
51	STK83296 2	Not converged	N/A		
52	L129305	4.2	39.4		Figure 5.35
53	STK52597 7	Not converged	N/A		

Figure 5.26: Series expansion around hit compound 16

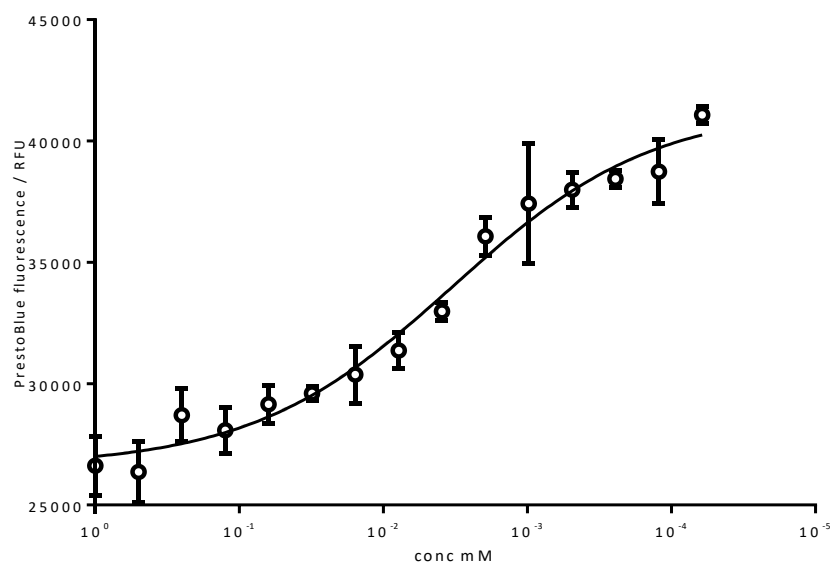


Figure 5.27: Dose response assay for a fresh stock of hit compound **16**.

Compound STK525876, supplied by VitasM Laboratories is structurally the same as **16**, originally supplied by ChemDiv for activity confirmation (Figure 4.18). pIC_{50} was determined as 5.5 (95% CI: 5.9 to 5.1), The Hill slope was 0.6 which is lower than previously observed. Results are in triplicate; error bars indicate standard error.

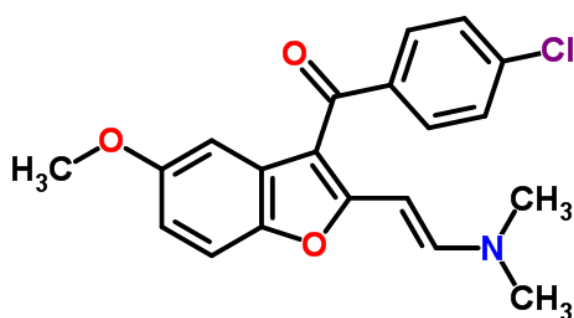


Figure 5.28: Structure of **16**

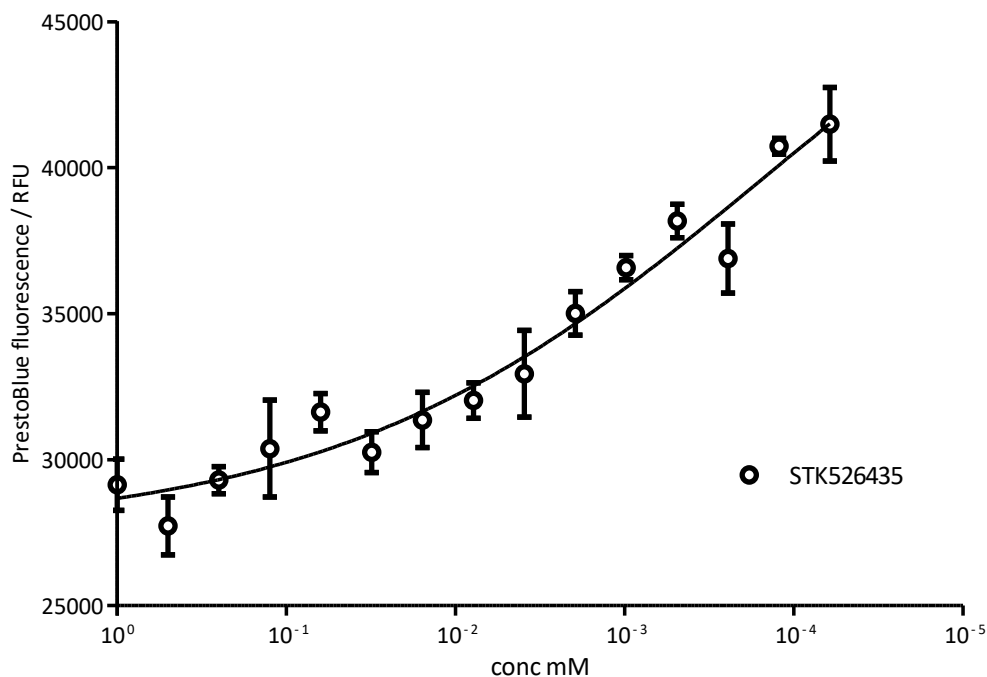


Figure 5.29: Dose response assay for **44** from series expansion of **16**.

Removal of the chloride group shows no significant increase in activity as although $pIC_{50} = 6.8$, the Hill slope is very shallow and lack of a sigmoidal curve results in very wide confidence intervals (95% CI: 10.5 to 3.2). Results are in triplicate, error bars indicate standard error.

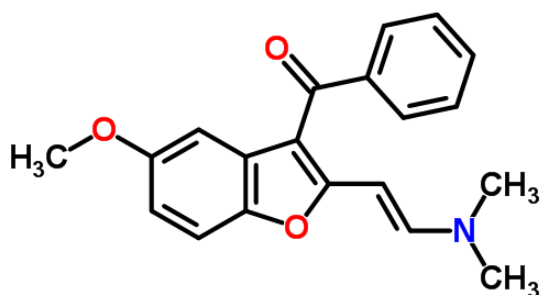


Figure 5.30: Structure of **44**

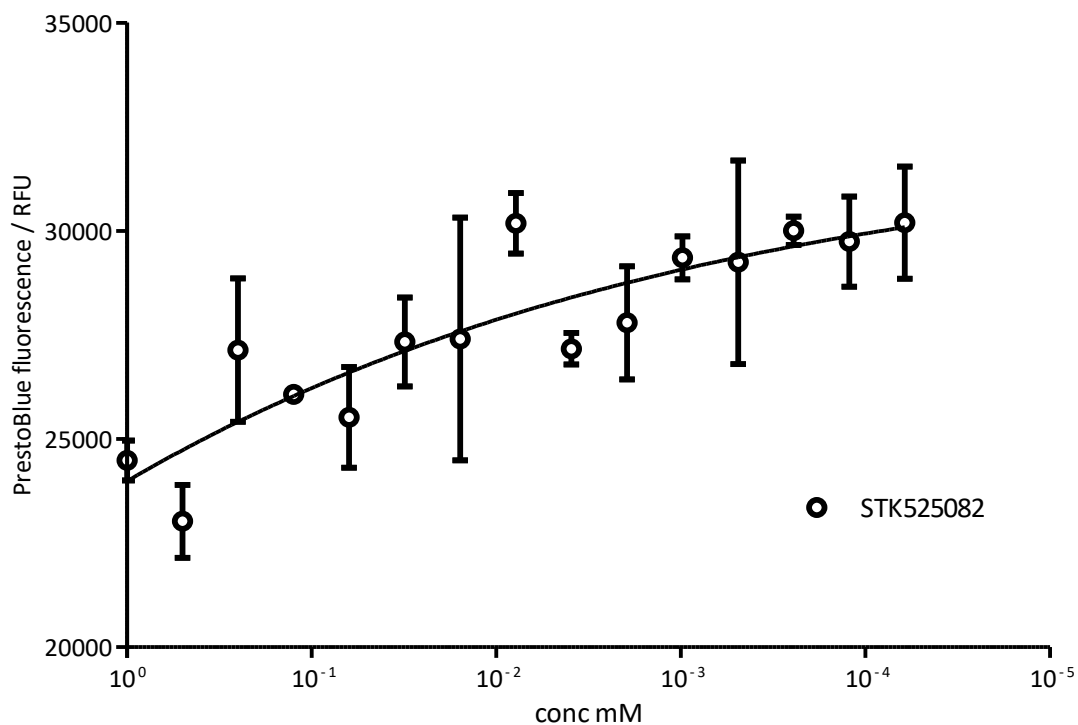


Figure 5.31: Dose response assay for **45** from series expansion of **16**.

Substitution of bromine for the chloride results in a very ambiguous pIC_{50} which due to the shallow hill slope and lack of upper and lower plateaus is not significant. Results are in triplicate; error bars indicate standard error.

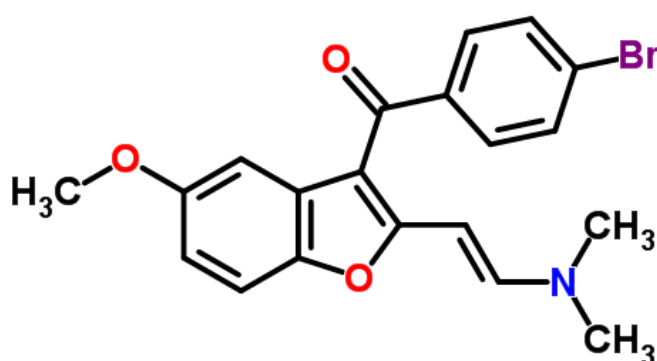


Figure 5.32: Structure of **45**

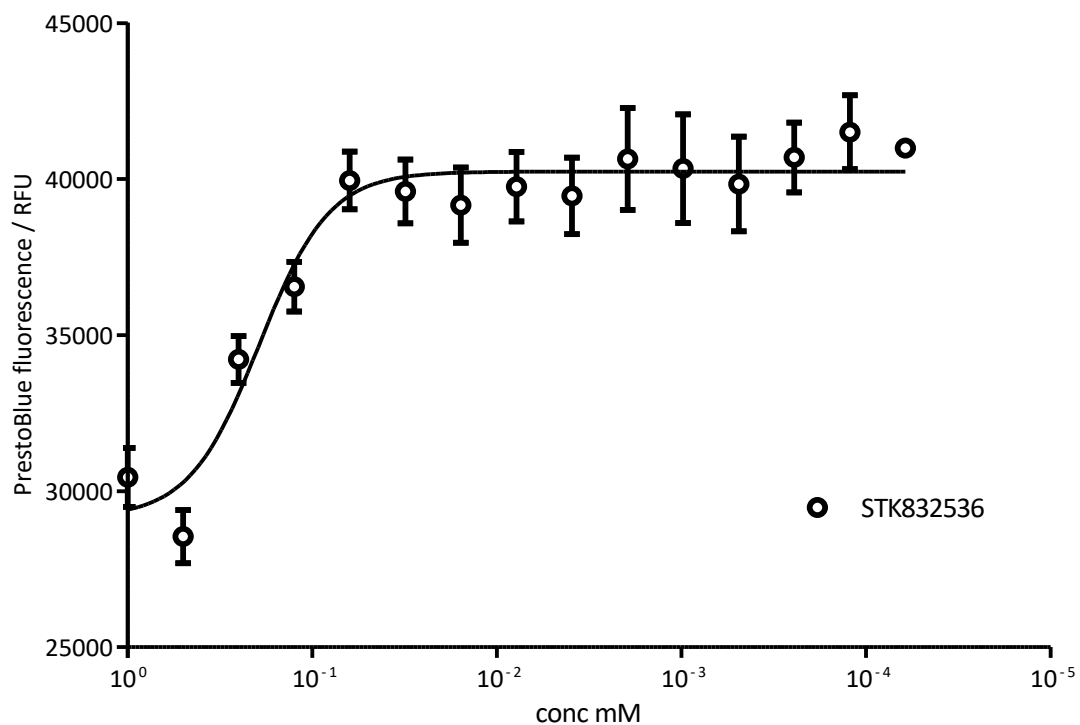


Figure 5.33: Dose response assay for **48** from series expansion of **16**.

Removal of the dimethylamine group results in a significant reduction in pIC_{50} to 3.71 (95% CI: 3.9 to 3.5). Results are in triplicate; error bars indicate standard error.

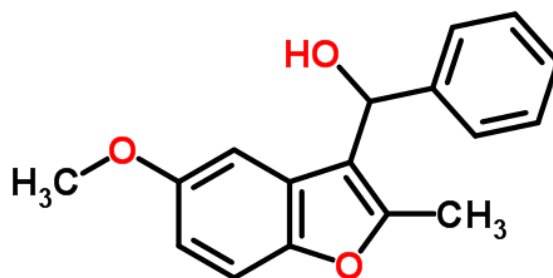


Figure 5.34: Structure of **48**

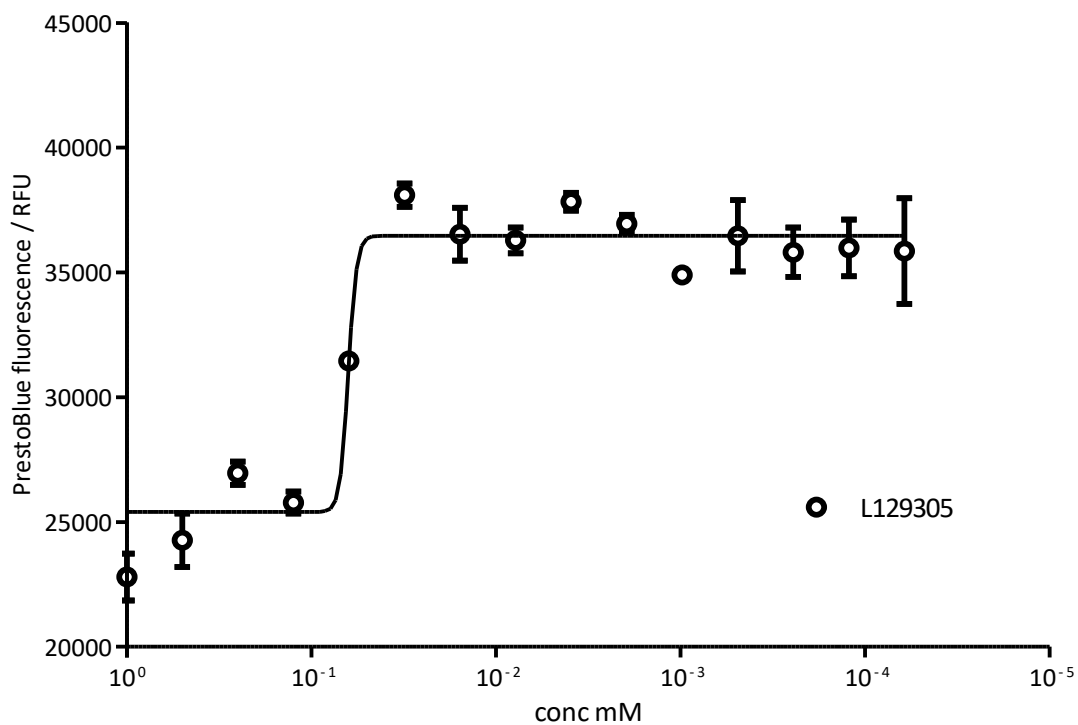


Figure 5.35: Dose response assay for **52** from series expansion of **16**.

The compound differs from the parent compound by removal of the methoxy group from the benzofuran group. The compound is also missing the chlorobenzene group resulting in a reduction of activity: $pIC_{50} = 4.2$ (95% CI: 4.20 to 4.20). Results are in triplicate, error bars indicate standard error.

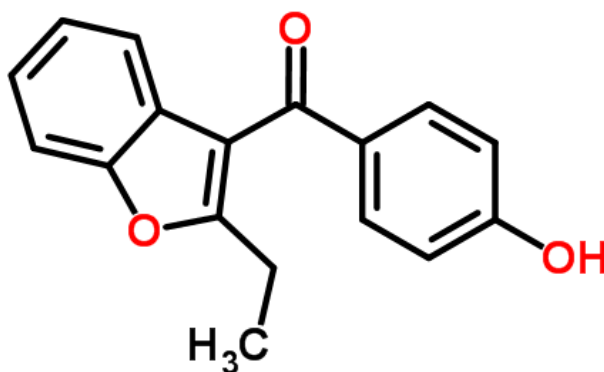


Figure 5.36: Structure of **52**

SAR for 16

It was shown that the presence of the chlorine substituent was crucial to activity, when substituted to another halide; bromide, loss of activity was observed (Figure 5.31).

Dimethylamine group is necessary for activity (Figure 5.33). The presence of this aliphatic group, $(\text{CH}_3)_2\text{NH}$ may be of importance to the compounds solubility and its ability to diffuse across cell membranes.

46 and **47** both showed complete loss of inhibiting activity. This is not unexpected as both molecules are lacking the halide group and the amine group which have both been shown to be necessary for activity.

Compounds **49**, **50**, **51**, and **53** all contained modifications that removed all inhibiting activity. This is not unexpected as the core structure has been heavily modified, significantly changing the 3D shape of the molecules.

Chloroxine

Chloroxine showed the most promising results following hit confirmation; the compound has a low Mw of 214 Da and a pIC_{50} of 5.5.

Chloroxine is a licensed compound used in some shampoos for the treatment of dandruff and seborrheic dermatitis of the scalp. It is already known that chloroxine has an antibacterial action, inhibiting the growth of Gram-positive as well as some Gram-negative organisms. Chloroxine has also shown some antifungal activity against certain dermatophytes and yeasts.

Chloroxine meets most drug requirements as cLogP is 3. It contains two hydrogen bond acceptors and one hydrogen bond donor. The polarised surface area is 33.12 \AA^2 ("Chloroxine | C₉H₅Cl₂NO - Pubchem"). The acute oral LD₅₀ in mice was found to be 200 mg/kg and in rats 450 mg/kg.

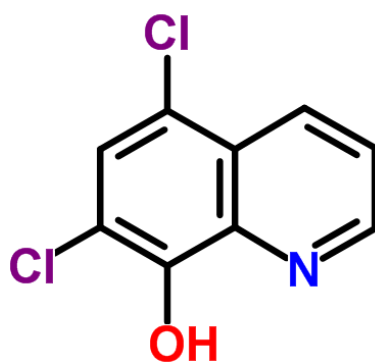
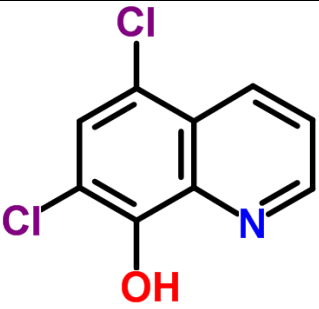
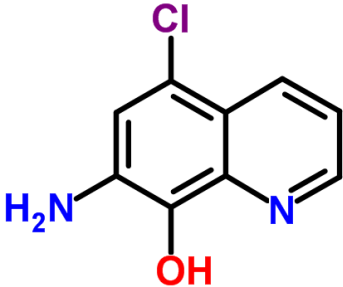
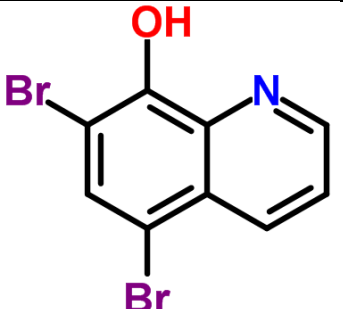
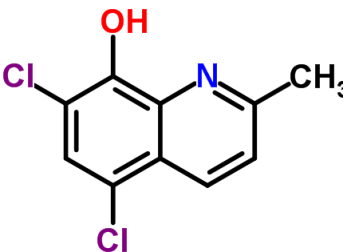
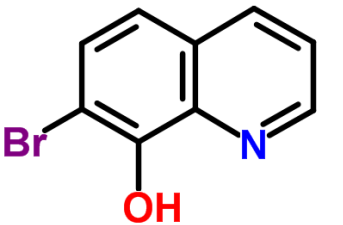
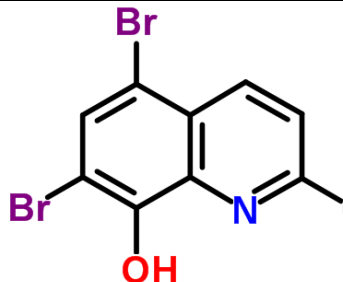
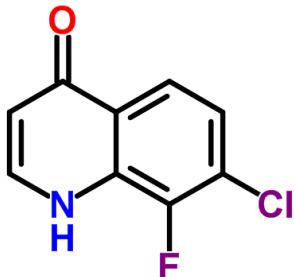
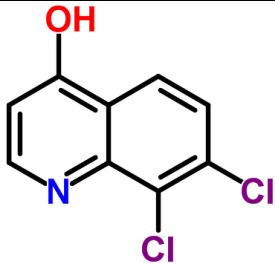
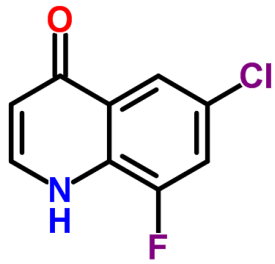
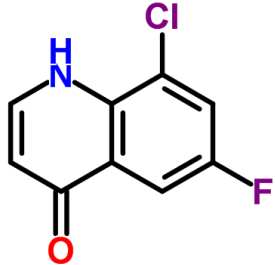
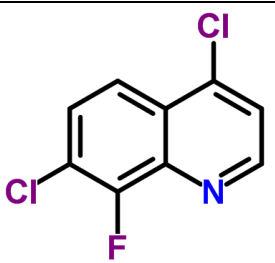
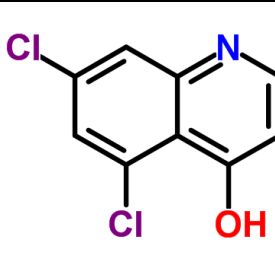
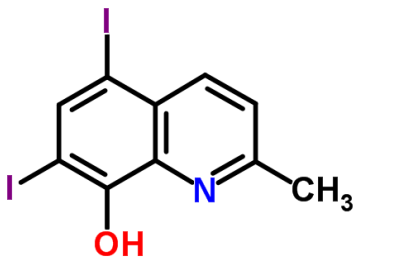


Figure 5.37: Structure of Chloroxine

Key	Compound	pIC_{50}	Hill	Structure	Figure
	Chloroxine	5.5	1.8		Figure 4.10
54	STK735211	3.4	1.9		Figure 5.42
55	STK563617	Not converged	N/A		Figure 5.38
56	LT03330918	Not converged	N/A		
57	LT00423139	5.1	3.5		Figure 5.44
58	LT00453266	Not converged	N/A		

59	17701-66	Not converged	N/A		
60	17709-68	Not converged	N/A		
61	177/01-65	3.4	1.2		Figure 5.46
62	177/01-67	3.1	0.9		Figure 5.48
63	177-01-86	4.1	1.3		Figure 5.50
64	81/09-33	4.1	3.3		Figure 5.52

65	S438189	5.0	3.2	 The image shows the chemical structure of 3-methyl-5,7-diiodoquinolin-8-ol. It consists of a quinoline ring system. The nitrogen atom is at the bottom right of the fused ring system and is colored blue. A methyl group (CH ₃) is attached to the nitrogen atom. The benzene ring of the quinoline system has two iodine atoms (I) at the 5 and 7 positions and a hydroxyl group (OH) at the 8 position. The iodine atoms are colored purple, and the hydroxyl group is colored red.	
----	---------	-----	-----	--	--

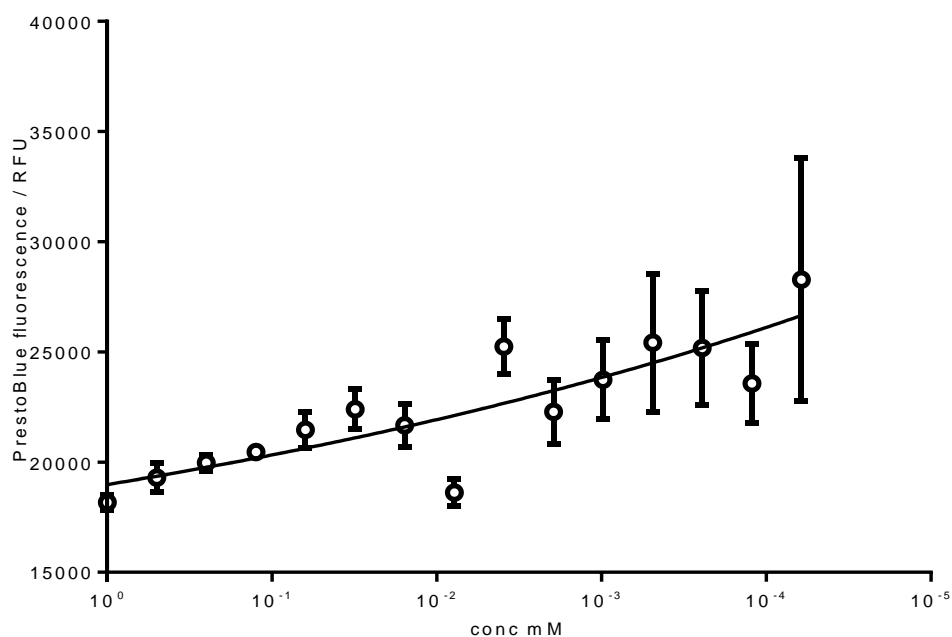


Figure 5.38: Dose response assay for **55** from series expansion of chloroxine.

The replacement of two chloride ions with bromide ions appears to reduce activity and severely reduce the hill slope such that a pIC_{50} cannot accurately be determined. Results are in triplicate; error bars indicate standard error.

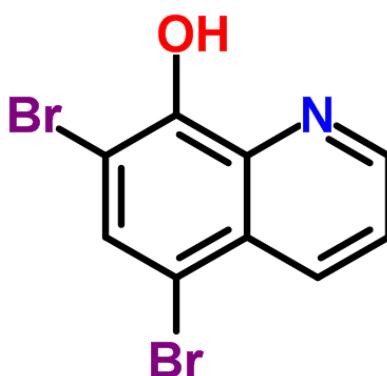


Figure 5.39: Structure of **55**, also known as broxyquinoline.

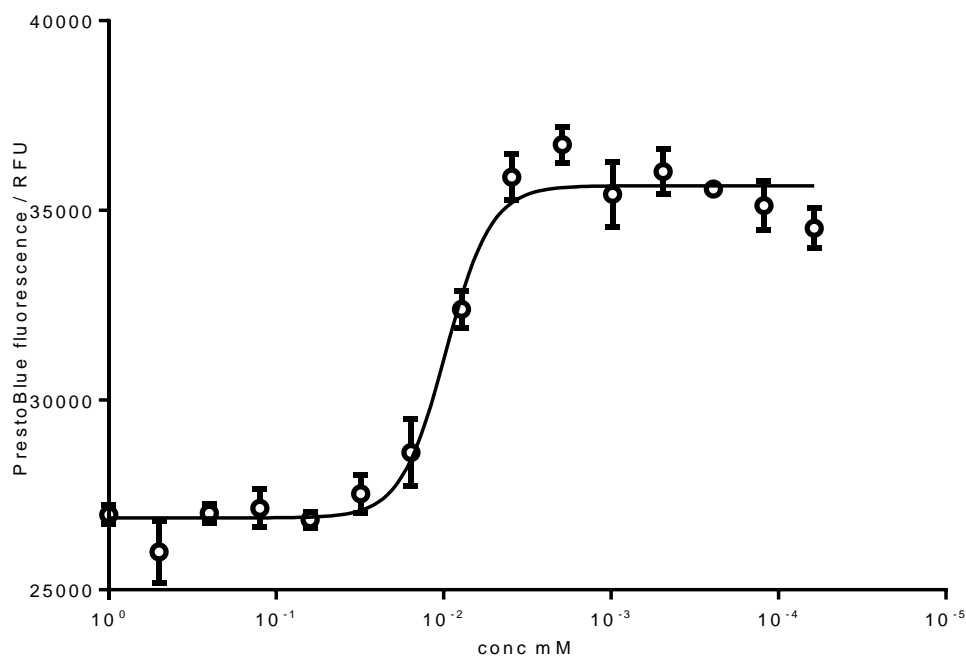


Figure 5.40: Dose response assay for **65** from series expansion of chloroxine

This compound differs from the parent by substitution of the two chlorides for iodide. A methyl group is also added to the nitrogen containing ring. Some activity is lost: $pIC_{50} = 5.0$ (95% CI: 5.1 to 4.9). Results are in triplicate, error bars indicate standard error.

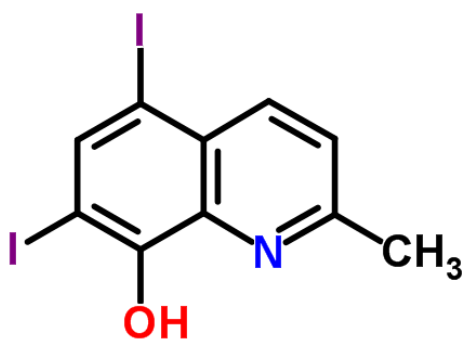


Figure 5.41: Structure of **65**

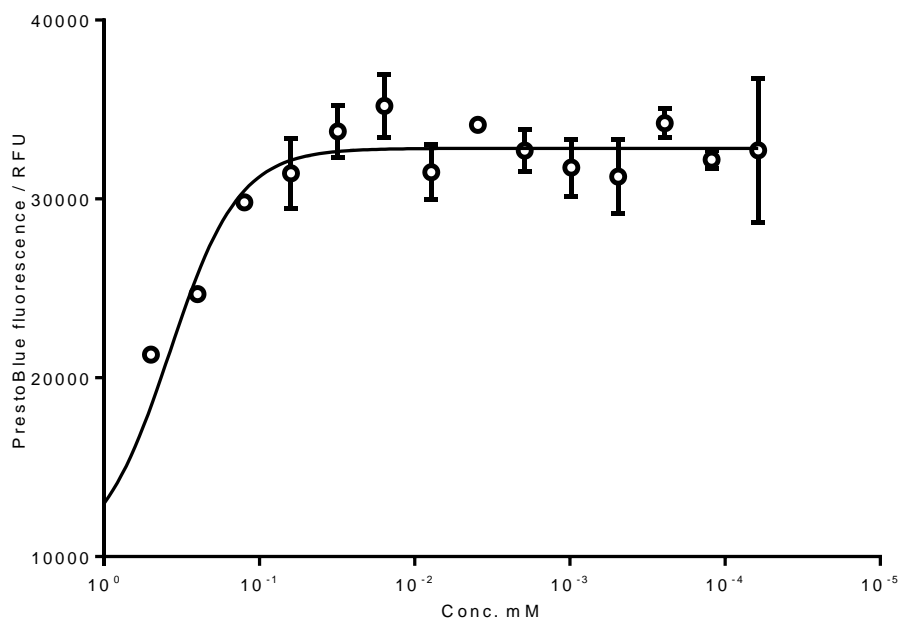


Figure 5.42: Dose response assay for **54** from series expansion of chloroxine.

The substitution of an amine group in replacement of a chloride leads to a decrease in activity to pIC_{50} of 3.4 (95% CI: 3.5 to 3.3). Results are in triplicate; error bars indicate standard error.

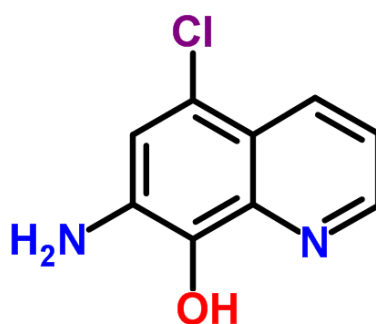


Figure 5.43: Structure of **54**

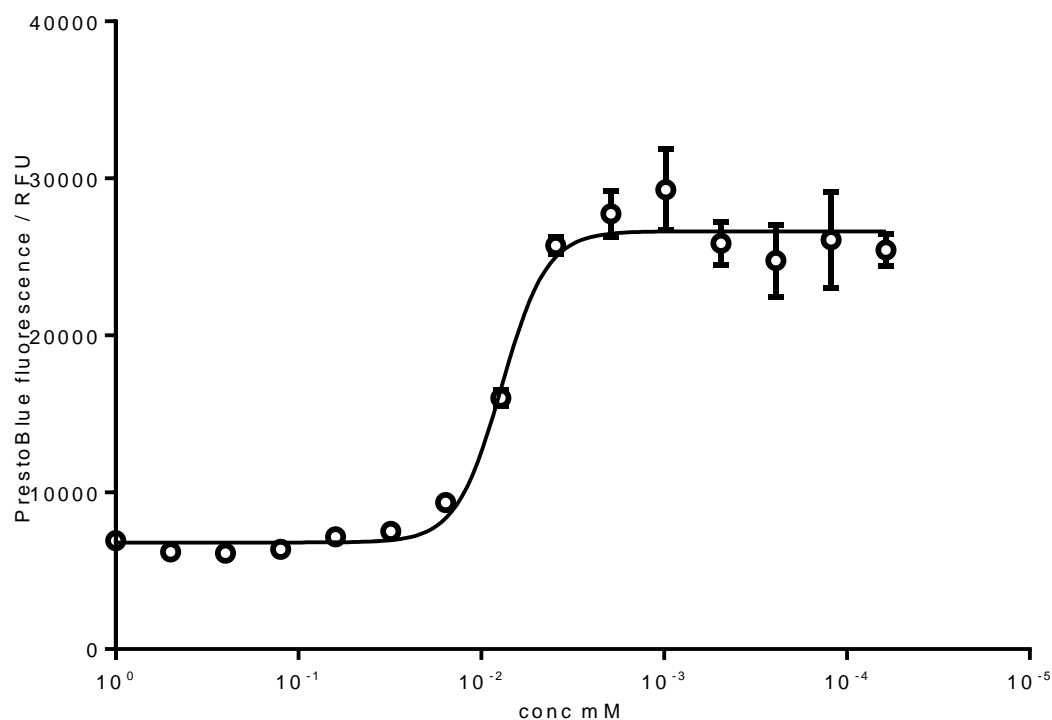


Figure 5.44: Dose response assay for **57** from series expansion of chloroxine.

$pIC_{50} = 5.1$ (95% CI: 5.2 to 5.0) for the compound 7-Bromo-8-quinolinol which is a small decrease from the parent compound. **57** is modified by replacement of the two chloride groups by a single bromide on the quinolinol moiety. Results are in triplicate, error bars indicate standard error.

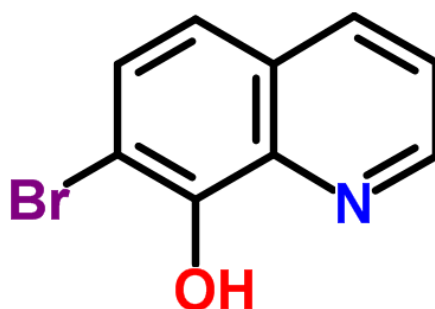


Figure 5.45: Structure of **57**

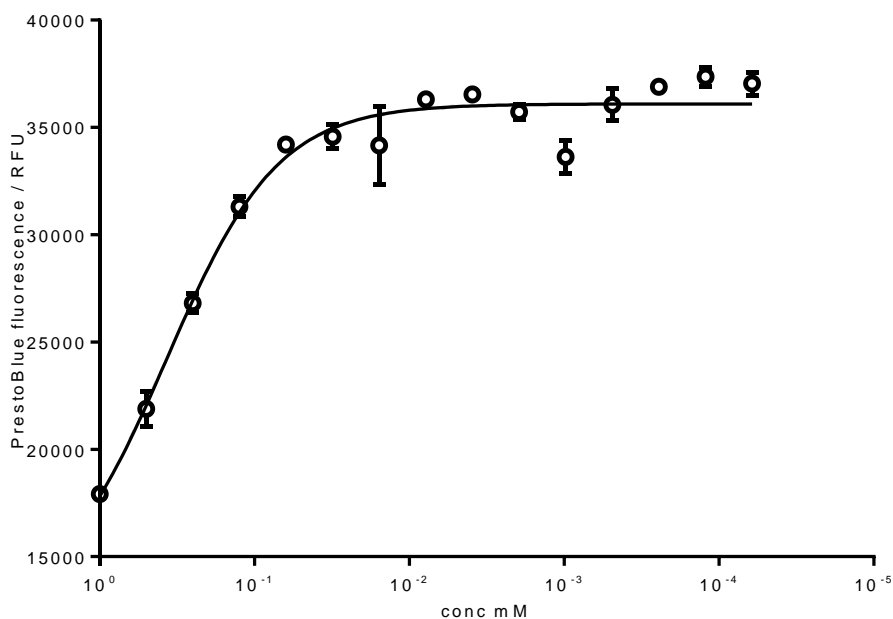


Figure 5.46: Dose response assay for **61** from series expansion for chloroxine.

$pIC_{50} = 3.1$ (95% CI: 3.7 to 3.1), showing a loss of activity. The compound differs from the parent compound through the inclusion of a ketone in place of the hydroxyl group and substitution of fluoride for one of the two chlorides. The nitrogen has also moved position to the other side of the ring. As such loss of activity is expected. Results are in triplicate, error bars indicate standard error.

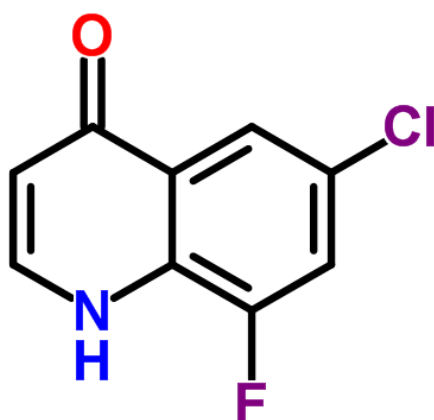


Figure 5.47: Structure of **61**

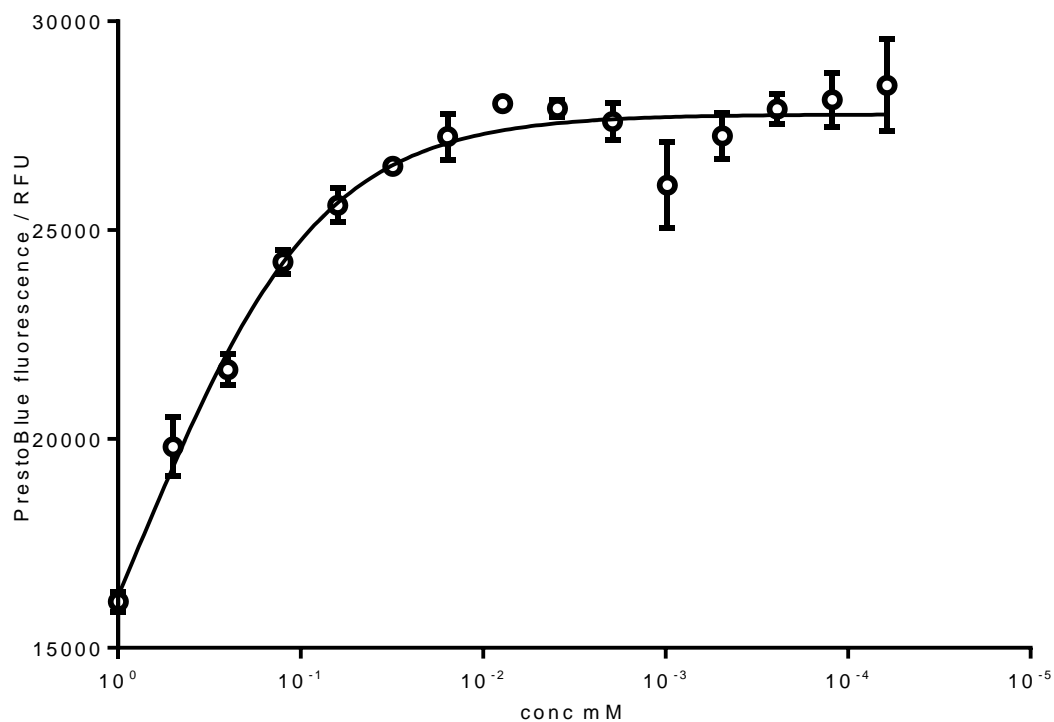


Figure 5.48: Dose response assay for compound **62** from series expansion of chloroxine.

62 is near identical to **61** (Figure 5.47), except for the chloride and fluoride have exchanged positions. This has no significant effect on potency however, as $pIC_{50} = 3.1$ (95% CI: 4.0 to 2.2). Results are in triplicate; error bars indicate standard error.

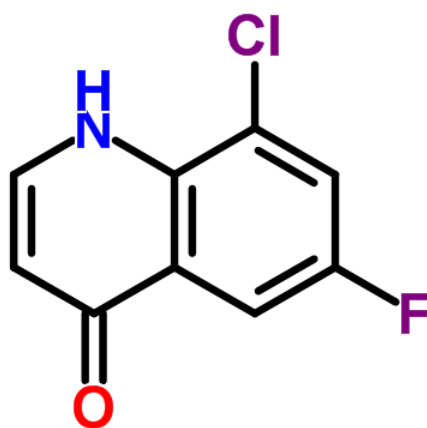


Figure 5.49: Structure of **62**

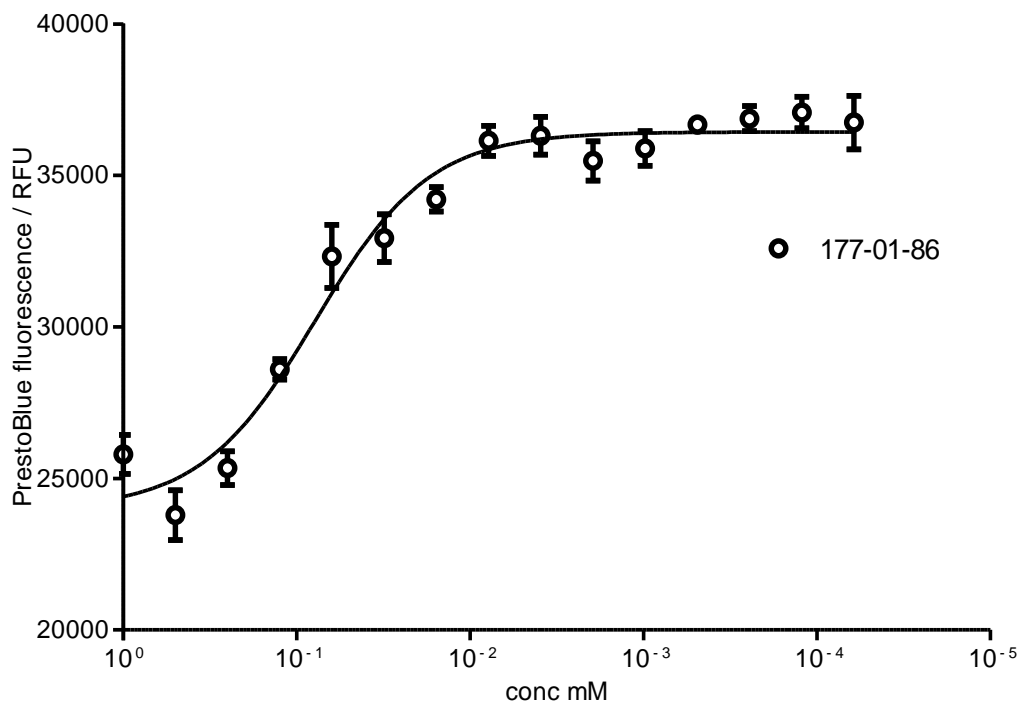


Figure 5.50: Dose response assay for **63** from series expansion of chloroxine.

63 differs from the parent compound through substitution of the hydroxyl group for fluoride, and moving one chloride to the nitrogen containing ring. This causes a reduction in pIC_{50} to 3.1 (95% CI: 4.3 to 4.0). Results are in triplicate, error bars indicate standard error.

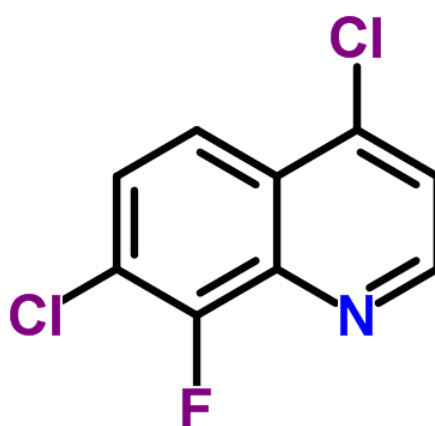


Figure 5.51: Structure of **63**

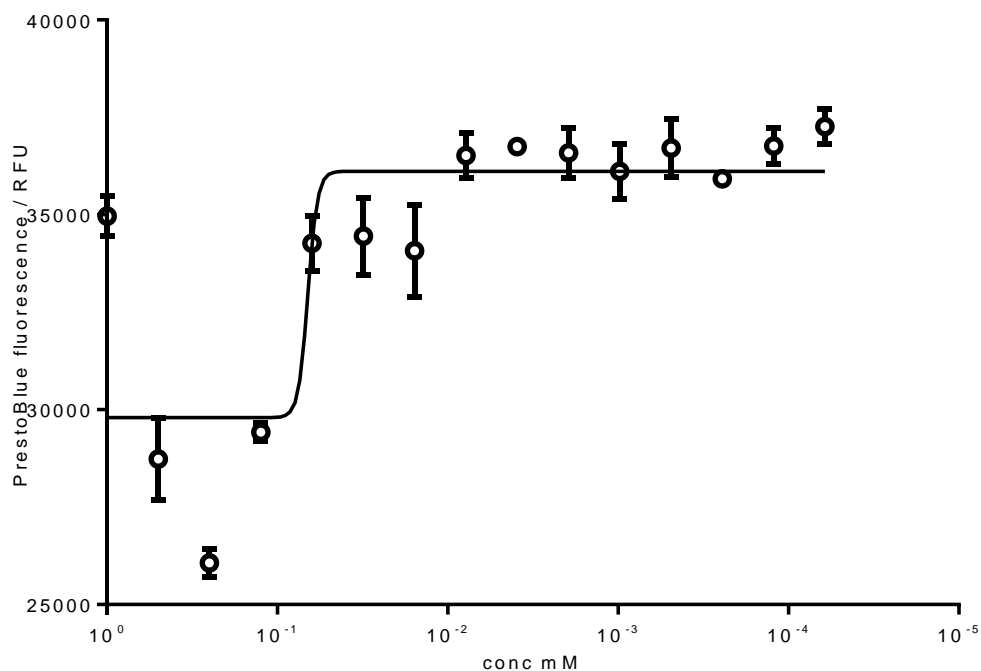


Figure 5.52: Dose response assay for **64** from series expansion of chloroxine.

64 differs from the parent compound only in that the hydroxyl group is moved to the nitrogen containing ring of the quinolinol group. This leads to a reduction in activity; $pIC_{50} = 4.1$ (95% CI: 4.3 to 3.9). Some compound effect is observed at the two highest compound concentrations. Results are in triplicate; error bars indicate standard error.

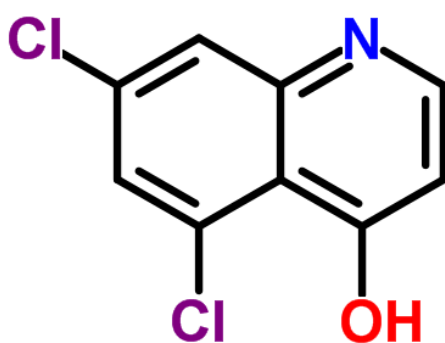


Figure 5.53: Structure of **64**

SAR for Chloroxine

Chloroxine (commercially also known as Capitrol or Endiarol), compound ID CHEMBL1200596 5,7-Dichloroquinolin-8-ol belongs to the class of organic compounds known as hydroxyquinolines. These are compounds containing a quinoline moiety bearing a hydroxyl group.

55 has appeared in screens against antibiotic tolerant cells in *Escherichia coli* biofilms previously (Fleck et al., 2014). The substitution of two bromide ions in place of the chloride appears to reduce activity. However the dose response curve is not a typical sigmoidal curve which may indicate an error with the experiment or an artefact of the PrestoBlue assay (Figure 5.38).

Compound **60**: 7,8-Dichloro-4-quinolinol is a structural isomer of chloroxine with the only change from the parent compound being that the hydroxyl group has moved to the ring containing the nitrogen. The dose response assay (data not shown) failed as high concentrations of the compound appeared to give a compound effect with PrestoBlue. It is predicted that **60** is a reducing agent; as such it would be useful to retest this compound with the secondary LIVE/DEAD assay. **64** also contains a hydroxyl group on the nitrogen containing ring and, whilst reduced activity is observed, the two highest concentrations of compound also show an increase in fluorescence signal. It is also worth noting here that both compounds were obtained from Butt Park Ltd. This chemical supplier was the only available vendor of these compounds and it was difficult to ascertain the reliability of this source as chemicals came with no accompanying purity data and the company has very little internet presence by which to verify. It is a possibility that the compound effect observed is a result of contamination by a manufacturing by-product.

Halide series: as the Mw of the halide ions increases it is expected that the activity of the molecule will decrease. One other route of investigation would be to test 5,7-Difluoro-8-quinolinol as this would be predicted to be even more potent. **65** (Figure 5.40) shows only a small reduction in potency for substitution of the two chloride ions for iodide.

5.4. Discussion

In order to better understand the SAR of hit compounds, a round of series expansion was carried out. This process was a fairly rudimentary experiment to collect SAR data and to try and define the essential aspects of the compounds which are pivotal to their activity.

Overall features of **7**: The presence of a halide ion is preferential to activity. It can be removed, however it cannot be substituted with a methyl group, indicating that a group which draws electron density from the ring structure is preferential. It is also possible that a hydrogen bond acceptor in this position is favoured. Modifications to the thiazole group resulted in a severe drop in activity. As thiazoles are often seen to have biological activity this may be an example of steric hindrance.

The thiophene group is also a modulator of activity, when removed entirely activity drops, however when replaced with benzene most activity is retained.

Overall there appear to be three areas of modification that can be made to modulate activity in **7**. These are the chlorine substituent, the thiophene and cyclohexanecarboxylic acid. The carboxylic acid appears to be critical to activity. As there are several areas where the structure can be modified **7** would be classed as a moderate quality lead. However, as no significant improvements to activity were observed more work is needed to develop a high quality lead series.

Structural modifications to **23** were limited in availability with only three features able to be tested. It was found that modification of the naphthalene group was well tolerated with compounds **39** (Figure 5.20) and **41** (Figure 5.24) showing part and total removal of this group have little effect on the pIC_{50} . These significantly improve the Mw of the compound for drug likeness. The second area tested was the benzothiazole (**40**,

Figure 5.22). In this ring, the sulphur was replaced with nitrogen resulting in a 10-fold reduction in pIC_{50} . The final feature tested was the naphthylmethyl group. Compounds **42** and **43** included reductions in this structure, both resulting in complete loss of activity, indicating that this is the reactive centre of **23**'s activity.

In the series expansion around chloroxine there were two fundamental structural features which could be altered to elicit a change in potency. The first of these is the two chlorine atoms, which were substituted for other halides and moved to different positions around the central quinolinol structure. In addition, the secondary alcohol, which was tested on both cyclohexane rings of the quinolinol as well as oxidised to a ketone and substituted for a chloride ion. It was shown that both of these changes elicited an effect on the compound potency. However, all compounds were less potent than the parent compound, chloroxine.

As there are no examples of motifs around the central structure which can be changed without compromising activity, this would exclude chloroxine from being truly defined as a lead series as no evidence of being able to improve the structure has been shown. However there are a number of potential molecules which have not been tested in this study which would need to be investigated before stating this for sure. Compounds which would have been of use to study are tiliquinol, tilbroquinol (Figure 5.54). These compounds and their analogues have been previously identified as candidate prodrugs in a persister cell study into biofilm survival in *Escherichia coli* (Fleck et al., 2014).

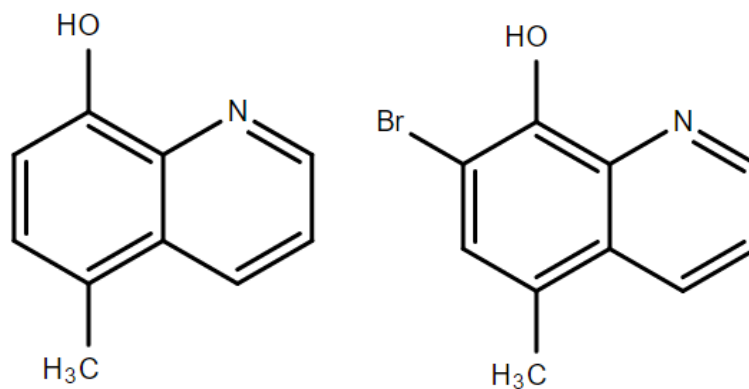


Figure 5.54: Compounds tiliquinol (left) and tilbroquinol (right).

These have both been identified in a previous prodrug screen for activity against persister cells however, were not included in this study. Due to their structural similarity, it would have been useful to have tested these molecules against persister cells in *B. thailandensis*.

Series expansion around **7**, **16**, **23** and chloroxine gave rise to useful SAR information and aided the development of lead series. At this stage **16** is the most promising lead series as there are clear SARs in multiple sites of the structure and importantly, modifications that improve the pIC_{50} have been identified. As described previously, chloroxine is also a very promising compound, although there may not be as much scope for improvement.

Series expansion was encumbered by being unable to obtain compounds from commercial compound suppliers, crucially those compounds around the chloroxine structure which showed the most promise.

Whilst useful, I do not feel that this round of series expansion has delivered results representative of the potential. Because of the limitations described the experiment lacked a systematic and quantitative structure which I think would bring more value out of the data collected. Further progress in developing lead series may be made through use of quantitative SAR (QSAR). QSAR is a method by which molecules are evaluated according to their steric, electronic and lipophilic properties. These properties are converted into mathematical descriptors to allow computer aided quantitative modelling of structures with optimum properties for the desired biological response (Winkler, 2002). QSAR modelling is especially powerful in this kind of study as I am yet to confirm the specific drug target (Wang et al., 2015).

A potential cause of error in series expansion was around inconsistencies within compounds from different suppliers. For one supplier (Butt Park), none of the compounds had any activity. This included a repeat stock of an original hit compound. Whilst the compounds were not supplied with data on purity this could have been

easily determined by LCMS, NMR or thin layer chromatography, however I failed to do this whilst undertaking the project.

One of the challenges I have found in series expansion is a lack of chemistry expertise. Identification of compounds in hit expansion was carried out by a chemist at the DDU who identified a limited series of compounds around the structures of the six confirmed hits. Since completing work on the project I recognise the benefits that could have been gained from reaching out and collaborating with researchers with relevant expertise.

6. Mechanism of action studies

6.1. Overview

Attempts to identify the mechanism of action (MOA) for identified compounds formed the last study in this project, taking place at Exeter from December 2014 to June 2015. Next Generation Sequencing (NGS) was carried out by the Exeter Sequencing Service who also assisted with computational analysis of the resulting data.

Having confirmed compound activities in chapter 5 the following priority was to investigate the MOA for compound inhibition of persister cells.

As discussed in assay development, phenotypic screening can result in hits which are more likely to survive the rigours of tests in animal models and clinical tests as the compound has already shown positive results in a live model. Phenotypic screens can also prevent researcher bias towards preconceived notions of “druggable” targets; leading to evidence led discovery (Eder et al., 2014). However, the benefits of unknown mechanisms of action in primary screening can become a problem further down the drug discovery pipeline (Bourne et al., 2012). At these later stages, it can be integral to lead optimisation to elucidate the targets that are driving phenotypes. This is especially important to SARs where alterations to compound structure may result in different pharmacology, whilst retaining the same broad whole cell response (Futamura et al., 2013). This process of identifying the molecular and genetic targets of active compounds can also be termed “target deconvolution” (Lee and Bogoy, 2013).

6.2. Chemical genetics approach.

I aimed to use a chemical genetics approach to identify proteins associated with persister cell formation and survival. Chemical genetics is the study of genes through small-molecule perturbation (Zanders et al., 2002). This has been made possible through recent advances in the capacity and accessibility of sequencing technologies. Chemical genetics is employed early in the drug discovery process for phenotypically identified drug candidates. This gives useful information early on to be able to select for successful outcomes and avoid wasting resources on non-tractable routes. This should improve the efficiency of drug discovery which is of huge benefit to an academically driven project such as this, which has access to limited resources. Chemical genetics is also attractive in persister cell studies where it is hypothesised that multiple regulatory pathways and gene redundancy are present. As small molecules can inhibit the activity of functional homologues, use of chemical genetics to identify targets can overcome issues of gene redundancy (Knight and Shokat, 2007).

The advances in NGS have made whole genome analysis an attractive and viable tool for target identification. This study performed NGS on an Illumina platform. This technology utilizes sequencing by synthesis (SBS) to track the addition of nucleotide bases through fluorescence as a nucleic acid chain is built (Shen et al., 2005).

Over-expression Library

A plasmid based over-expression library was developed to identify and select for *B. thailandensis* genes. The library was developed by Dr. Marc Fox, Dr. Sarah Harding and Dr. Donna Ford at DSTL, Porton Down. It was designed to give a minimum of four-fold omnidirectional coverage of the entire *B. thailandensis* genome. The library

contained clones of 1.5-3 kbp of genomic DNA. Most genes from *B. thailandensis* are less than 1.5 kbp long, and over 95% are smaller than 3 kbp. This library therefore represents a good compromise between coverage of the entire genome, and avoiding clones with several genes co-expressed. The experiment performed here aimed to identify genetic targets which, when over-expressed, survive the bactericidal effects of ceftazidime and chloroxine combination therapy.

This method has been successfully used in yeast to identify cellular targets of small molecules (Luesch et al., 2005). A benefit of this method is that it is able to identify not only primary targets but “off target” activities of compounds and alternate modes of action (Lum et al., 2004).

6.3. Resistance generation

A pilot experiment to identify genetic targets of chloroxine through development of resistance mutants was designed. The aim was to passage a persister culture through cycles of treatment with a selective dose of chloroxine with the intention of isolating a single resistant clone. Comparative genomic analysis of the resistant clone to the naïve persister genome could then identify the target gene of chloroxine as an anti persister.

6.4. Experimental procedures

Preparation of NGS samples

An aliquot of 250 µl of the over expression library pBBR1-MCS2 in *B. thailandensis* provided by DSTL was added to 3 x 5 ml tubes of LB broth containing 750 µg/ml kanamycin (LB 750kan) and grown overnight with aeration at 37 °C to an approximate optical density of OD₆₀₀ 1.5. The cultures were centrifuged and resuspended in M9

media treated with 400 X MIC ceftazidime, either with or without additional 30 μ M chloroxine. A naïve control of over expression library with only 750 μ g/ml kanamycin to preserve the plasmid was also produced. After static overnight incubation at 37 °C the cultures were centrifuged to pellet cells and the supernatant discarded.

Plasmid DNA was extracted using a GeneJET Plasmid miniprep kit (Fermentas, D00048). A freeze–thaw step was added to improve the survival of DNA preparations. After initial resuspension of the cell pellet in ice-chilled resuspension buffer, reaction tubes were submerged in liquid nitrogen until frozen. Tubes were then thawed on ice with minimal agitation. This step was repeated twice before proceeding as per the standard protocol. DNA was quantified from using the quBit fluorescence assay (ThermoFisher, Q32850).

Library preparation was performed by Exeter Sequencing Service using Nextera and Nextflex protocols. Round one of sequencing was run on a MiSeq and round two was run on a HiSeq (Illumina Sequencing Platform).

Data analysis

Overview: Analysis was carried out by Konrad Paszkiewicz at the Exeter Sequencing Service. This included development of a pipeline to filter the plasmid sequences from pBBR1-MCS to retain only *B. thailandensis* genomic DNA and alignment of these sequences against the annotated *B. thailandensis* E264 reference genome. Coverage of the reference genome by the naïve control library and the ceftazidime only sample was calculated. Peak-calling of paired-end sequences was then performed using a broad peaks with bandwidths > 300 bp. This was carried out using the MACS2 (model based analysis for ChIP-Seq) (Zhang et al., 2008) version 2.0.10.20130712 with a cut off of $p > 0.005$. Differential peaks were then annotated.

Results were visualised in the Integrative Genomics Viewer (IGV, Broad Institute) (Robinson et al., 2011). ChIP-seq (chromatin immunoprecipitation sequencing) results were used to identify and evaluate significance of regions of enrichment (Feng et al., 2012).

Gene sequences were analysed to identify differentially expressed sequences from the samples tested with a combination of ceftazidime and chloroxine (Table 6.1 – rows 7-9) but not in the ceftazidime only control (Table 6.1 – rows 4-6). Peaks identified were cross-referenced with Burkholderia.com database (Winsor et al., 2008) to identify function. Homologues with other *Burkholderia* species were also identified. Potential targets were determined based upon likely significance, and the ease with which a recombinant protein target could be expressed, purified and assayed to show activity and target inhibition with chloroxine.

Resistance Generation

An overnight culture of *B. thailandensis* was grown to stationary phase before being centrifuged at 10 000 X g for 10 minutes to pellet cells and resuspended in LB 750kan to OD₆₀₀ 0.5. A CFU count was carried out on the culture and 3 x 5 ml samples were then treated with 400 µg/ml ceftazidime hydrate and 30 µM chloroxine. A further 3 x 5 ml samples were only treated with 400 µg/ml ceftazidime hydrate as a control group and all samples were incubated statically for 72 hours at 37 °C. Following incubation a second CFU count was performed and survival frequency determined by the equation

$$\frac{CFU/ml\ T72}{CFU/ml\ at\ T0}$$

6.5. Results

The over-expression library used for this work comprised the broad host range plasmid pBBR1-MCS2 (Kovach et al., 1995) containing fragments of genomic DNA of sized between 1.5-3 kb in the *lac* inducible multiple cloning site. This was provided by DSTL. The library was representative of approximately 90,000 clones to give a minimum four-fold, omnidirectional coverage of the *B. thailandensis* genome. This should ensure that 95% of ORFs are expressed at least once in the library.

Two rounds of NGS were carried out using the over-expression library under treatment with ceftazidime and a combined treatment of ceftazidime and chloroxine (Table 6.1).

Plasmid DNA was extracted from surviving cells and run with agarose gel electrophoresis (Figure 6.1). A band size of between 6.2 and 7.7 kb was expected based upon the pBBR1-MCS2 plasmid of 4,707 bp and a gDNA insert of between 1,500 and 3,000 bp. Despite optimisation of the SOP for *B. thailandensis*, plasmids extracted from the bacteria displayed smeared bands when visualised on a gel. There is general consensus (unpublished data) that this is common when extracting plasmid DNA from *Burkholderia sp.* Therefore, instead of using restriction digestion to isolate the gDNA prior to sequencing, I decided to sequence the whole plasmid extraction. An MACS2 pipeline was then designed to isolate the gDNA from the plasmid backbone during data analysis.

Initial analysis confirmed almost total coverage of the *B. thailandensis* genome by the naïve library control. Twelve genes were identified which promoted persister cell survival in the presence of chloroxine and ceftazidime combination treatment, were identified (

Table 6.2). Data shown in appendix 1.

Sample number	Treatment	DsDNA concentration ng/ μ l
1	naïve library	10.02
2	naïve library	19.13
3	naïve library	21.14
4	ceftazidime	15.11
5	ceftazidime	60.31
6	ceftazidime	53.82
7	Chloroxine + ceftazidime	68.05
8	Chloroxine + ceftazidime	20.71
9	Chloroxine + ceftazidime	42.83

Table 6.1: Sample conditions for round one of Next Generation Sequencing

QuBit analysis of plasmid miniprep preparation for NGS. Samples 1 – 3: untreated *B. thailandensis* with over expression library pBBR1-MCS2, 4-6: 24 hours treatment with 400 μ g/ml ceftazidime hydrate, 7-9 24 hours treatment with 400 μ g/ml ceftazidime hydrate and 30 μ M chloroxine.

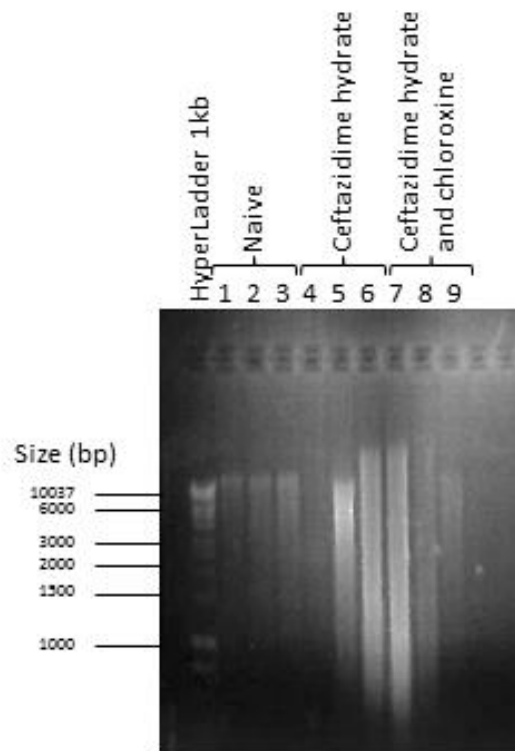


Figure 6.1: Agarose gel (2%) of products of miniprep for Next Generation Sequencing.

Plasmid pBBR1-MCS2 is 4,707 bp, gDNA inserts ranged from 1,500 to 3,000 bp. An expected band of 6.2 – 7.7 was expected. However, the gel shows smearing of DNA over a much wider range of sizes. It is hypothesised that the bands seen are smeared due to the difficult nature of extracting plasmids from *Burkholderia spp.*

	Predicted Name / Function	Round 1	Round 2
BTH_II0108	Outer membrane porin (Caglic et al.) of the NodT family. Function is most likely an efflux protein.	Yes	No
BTH_II0513	Predicted AraC family transcriptional regulator.	Yes	Yes
BTH_II0793	Cellulose Synthase Operon protein C	Yes	Yes
BTH_II2074	Hypothetical protein similar to DoxX family	Yes	Yes
BTH_II2168	Copper-translocating P-type ATPase	Yes	Yes
BTH_II2314	Hypothetical phosphotransferase	Yes	Yes
BTH_I0077	Hypothetical transposase	Yes	Yes
BTH_I0185	5-dehydro-4-deoxyglucarate dehydratase.	Yes	Yes
BTH_I0313	Hydroxymethylglutaryl-CoA-lyase.	Yes	Yes
BTH_I0527	Hypothetical protein	Yes	Yes
BTH_I1209	MotA/TolQ/ExbB proton channel.	Yes	Yes
BTH_I2652	Branched chain amino acid ABC transporter.	Yes	Yes

Table 6.2: Pathways in *B. thailandensis* identified through two rounds of next generation sequencing of persister cells from an over expression library treated with chloroxine.

BTH_II0108 is predicted to be an outer membrane porin (Caglic et al.) involved in the transport and binding of proteins. The gene was present in round one of NGS however, was not identified in round two. It is predicted that BTH_II0108 is part of an outer membrane efflux pump. As such, it is unlikely to be a specific target of chloroxine, but may instead have mitigated the effects of one of the two antibiotics by efflux. No further action was taken at this time.

BTH_II0513 is an AraC family transcriptional regulator. It is most likely located in the cytoplasm. The AraC family of transcriptional regulators is one of the largest groups of regulatory proteins in bacteria. They are involved in transcriptional regulation of carbon metabolism, stress responses and virulence (Santiago et al., 2014) (Yang et al., 2011). AraC activators have been used as targets in small-molecule drug discovery for antibacterial agents previously in *Escherichia coli* (Skredenske et al., 2013). Gene BTH_II0513 was synthesised and marked as a potential avenue of investigation.

BTH_II0793 is predicted to be cellulose synthase operon protein C. Bacterial cellulose is commonly found in biofilms. Cellulose is synthesised and translocated across the inner membrane. This may indicate that over-expression of BTH_II0793 provides protection from antibiotic treatment through reinforcement of biofilm structures (Morgan et al., 2014).

BTH_II2074 is a hypothetical protein with homology to DoxX-like family proteins. Predicted to be localised to the cytoplasmic membrane, DoxX in *M. tuberculosis* is a component of a membrane-associated oxidoreductase complex which protects the bacteria against the oxidative stress of the host environment (Nambi et al., 2015). The gene was synthesised for future investigation, but is likely to be challenging to work with as it is a membrane protein.

BTH_II2168 is a copper-translocating P-type ATPase. This is a large protein comprising a number of transmembrane helices and an ATP binding cassette. It is predicted to be located in the cytoplasmic membrane. Whilst copper is a potent cytotoxin, Cu^{+2+} ions are also required as catalytic cofactors for proteins that carry out essential cellular functions. Copper homeostasis is tightly regulated (Pena et al., 1999) (Argüello et al., 2013). Chloroxine has been shown to be a potent chelator of copper forming very stable complexes with Cu^+ and Cu^{2+} over a wide range of pHs (**Error! Hyperlink reference not valid.**). This gene was synthesised for future investigation. However, due to the complexity involved in developing and enzyme assay to characterise a membrane associated protein, further work on this has been postponed. There is also a significant possibility that, given the predicted action in transport across the cell membrane, this protein may not be a specific target of chloroxine and up-regulation may be a response to antibiotic stress.

BTH_II2314 is a hypothetical protein. One domain of the protein has some homology to aminoglycoside phosphotransferase enzymes. However, the gene is not complete. Aminoglycoside phosphotransferase enzymes have been identified as potential drug targets previously (Lallemand et al., 2012). Although this experiment does not use aminoglycosides it is possible that the O-phosphorylation activity of the enzyme is in some way modifying the compound or a target. A second domain of this protein which is a greater peak in NGS analysis is related to general ATPases. Due to the ambiguities in the likely function of this protein, it has not been a priority for further work.

BTH_II0077 is a hypothetical protein. Very little information is available for this gene. All orthologs are transposases or putative transposases. Because of the lack of information no further action was taken with this gene.

BTH_I0185 is D-5-4-deoxyglucarate dehydratase. This enzyme is part of the ascorbate and aldarate metabolism pathway, which is essential for the biosynthesis of arabinose. The enzyme is in the only pathway to produce arabinose in *B. thailandensis* (Figure 6.2). A coupled assay has been developed in *Acinetobacter baylyi* to characterise this enzyme which was used as a template to characterise it. (Aghaie et al., 2008) This pathway could be further explored. However, the gene is not present in *B. pseudomallei* and so is unlikely to be the target of chloroxine which inhibits persister cells in both species.

BTH_I10185 is also involved in regulation of expression of the divergent *ulaG* and *ulaABCDEF* operons involved in L-ascorbate dissimilation in *Escherichia coli* (Campos et al., 2004) and the ascorbate transporter of *Escherichia coli*. The gene forms part of the phosphotransferase system which is required for anaerobic utilisation of L-ascorbate (Zhang et al., 2003).

BTH_I0313 is hydroxymethylglutaryl-CoA-lyase (HMG-CoA). This lyase plays an essential role in lipid metabolism and degradation of ketone bodies. It is also involved in the degradation of branched chain amino acids (Figure 6.3).

BTH_I0313 is also present in the genome of *B pseudomallei* at locus BPSL0333 and a BLAST search (NCBI) identified hydroxymethylglutaryl-CoA-lyase in the genome of *Pseudomonas aeruginosa* (Altschul et al., 1997) (Altschul et al., 2005). Loss of this enzyme in humans leads to Reye syndrome, as such selectivity is important.

BTH_I0313 was identified as the most promising gene identified from NGS. The gene was synthesised and cloned into a bacterial expression plasmid for investigation. From this recombinant protein may be expressed and purified for use in an in vitro assay to identify if chloroxine inhibits enzyme action. It may also be possible to develop a cell-based assay to see if expression of BTH_I0313 in cells treated with chloroxine restores the persister phenotype.

BTH_I0527 is a hypothetical protein with very little information available. The gene contains two hydrolase domains and orthologs include hydrolases and esterases. There was not enough evidence to prioritise this gene for further study.

BTH_I1209 is a MotA/TolQ/ExbB proton channel family protein. This family includes integral membrane proteins involved in translocation of proteins across membranes. There is a high probability the proteins are proton channels. MotA is an essential component of the flagellar in *E-coli* (Braun et al., 1999). ExbB is part of the TonB-dependent transduction complex. The TonB complex uses the proton gradient across the inner bacterial membrane to transport large molecules across the outer bacterial membrane. I considered that BTH_I1209 was likely to be non-specific to chloroxine, and more likely involved in generic efflux pump activity.

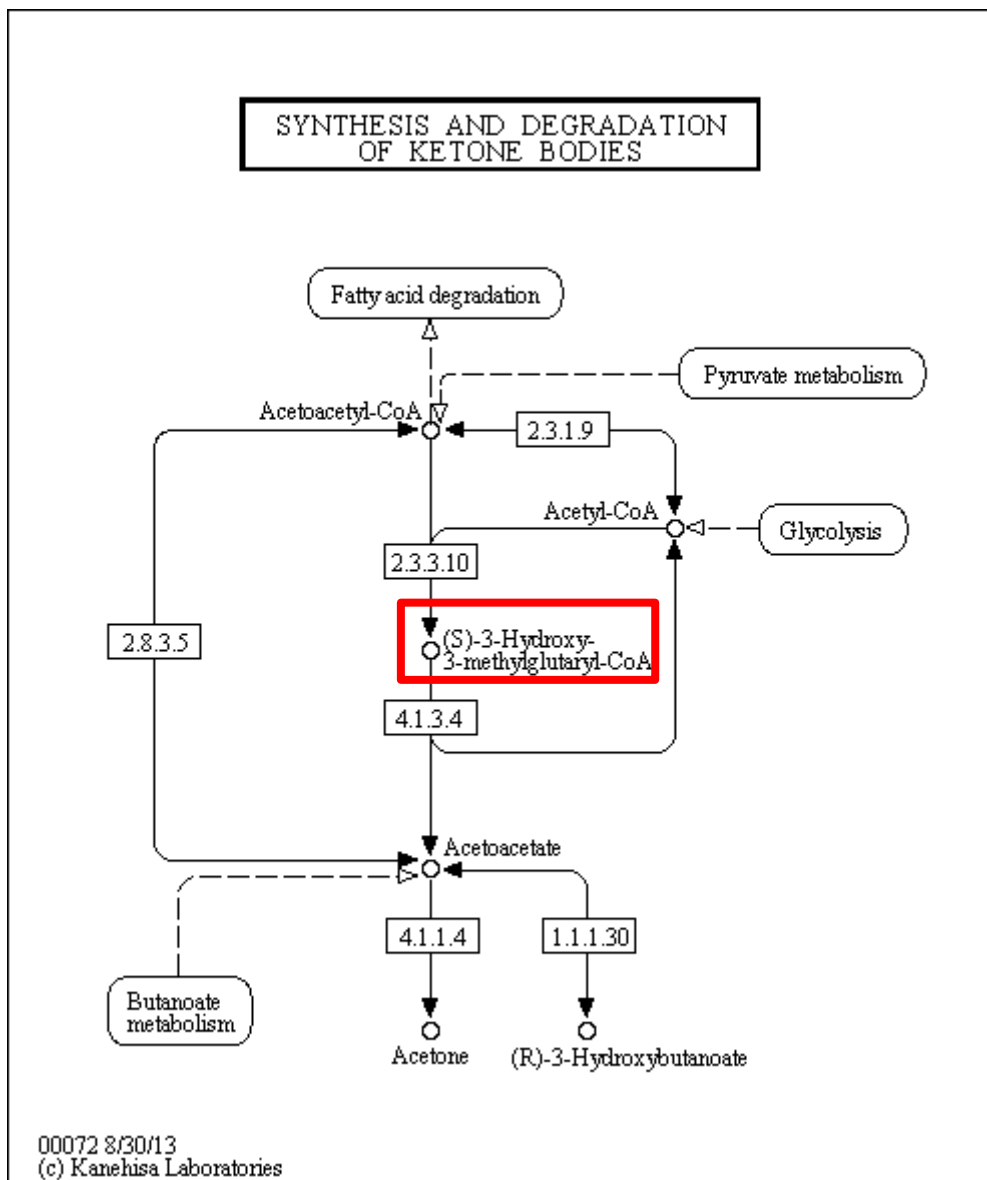


Figure 6.3: Kegg pathway for gene BTH_I0313 a gene included in a pathway for degradation of ketone bodies.

B. thailandensis gene BTH_I0313 encodes hydroxymethylglutaryl-CoA-lyase (red box), an enzyme essential for lipid metabolism and degradation of ketone bodies. It is also involved in the degradation of branched chain amino acids.

BTH_I2652 is a branched-chain amino acid ABC transporter permease/ATP binding protein. The protein is large (741 amino acids) and consists of 11 transmembrane helices. Approximately the last 300 amino acids are all cytoplasmic and form the classic ATP binding fold.

Pfam predicts that the protein consists of 3 domains (Finn et al., 2016). A branched-chain amino acid transport system / permease component (35-305); an ATP-binding domain of ABC transporter (511-667) and a branched-chain amino acid ATP-binding cassette transporter (714-736). BTH_I2652 is predicted to be a metabolite import protein involved in the breakdown of branched chain amino acids. This is promising as this is in the same pathway as the hydroxymethylglutaryl-CoA-lyase from the identified gene BTH_I0313. The gene is a homolog of gene BP1026B in *B. pseudomallei*.

6.6. Discussion

Over Expression Library

Twelve potential genes in the *B. thailandensis* genome were identified through NGS using the overexpression library (

Table 6.2). Through reference to the annotated genome (Winsor et al., 2008), I was able to obtain some insight into the possible functions of these genes. This allowed me to predict the most promising genes that are likely to be involved in persister formation, maintenance and revival.

Six compounds with characteristics suitable for development into drug compounds were identified for further development in chapter 5. I decided to progress into MOA studies using just one compound, chloroxine. Target deconvolution is a time-consuming and expensive process and I decided to develop the methodology using a single compound which would be operationally more feasible. Also, developing methods through successive rounds of experiments would require significant quantities of the compound. As chloroxine is readily available and inexpensive it was a suitable candidate. An additional consideration to this is that within the timescales of this project more meaningful progress can be made towards producing a new therapy to treat persister cells with chloroxine as it is already a licenced drug. As such I decided to use a combination treatment of ceftazidime and chloroxine for initial development of MOA experimental procedures before use with more difficult to obtain or expensive compounds. This decision was further justified as chloroxine was the only compound to show a significant reduction in cell numbers in the biphasic kill assay (Figure 4.37), which is biologically a very similar experiment.

An alternative technique to identify target genes could have been to use transposon directed insertion-site sequencing (TRADIS) or knock-out mutants and assessing the effects of disruption on persister survival. This has been used previously in *Burkholderia* species to identify novel targets for antimicrobial development (Moule et al., 2014). However, deletion mutants can be misleading in identifying pharmacological interactions as transposon insertions may lead to observation of phenotypes independent of persister function increasing the rate of false positive results. This is especially relevant if assay quantification is through a viability readout.

An additional challenge to determining the target of compound inhibition is that protein functions can be regulated by many post-translational modifications such as phosphorylation. They are also dependent on spatial and temporal modifications. In order to elucidate the relevant MOA a more sophisticated experimental design than a traditional deletion mutant approach was required (Cong et al., 2012).

Resistance Generation

An experiment was carried out to identify target genes for chloroxine through development of resistance. The rationale was to passage a persister culture through cycles of treatment so isolate a single resistant clone. Comparative genomic analysis of the resistant clone to a naïve persister culture could then identify the target gene in which mutation gives rise to resistance against chloroxine and ceftazidime. This experiment was run for 3 months. However, conditions such as passage time and treatment concentration required further optimisation. Data is not shown as no scientific advance was made and the experimental procedure requires further work to deliver meaningful results at this stage. The MOA for chloroxine used as an antibiotic has not been previously described in the literature. As the MOA for chloroxine was not

known, a more poignant approach may have been to start by testing chloroxine as a sole agent at 10X MIC. However, after significant attempts to develop a resistant mutant had failed, implementation of this experiment required significantly more time than was available coming towards the end of this project.

Target Validation and Future Developments

The ultimate validation of the target engagement of chloroxine would require the crystal structure of protein-inhibitor complex through purification and crystallisation of the enzyme in complex with chloroxine. It will also be important to determine target specificity and identify any off-target effects. In the first instance toxicity may be predicted by quantifying GI₅₀ through a dose response assay in a selection of immortalised human cell lines.

Further stages of drug discovery that should continue this line of work include in vitro assays to provide further ADME information for chloroxine as well as PK/PD profiling. To move from hit to the lead phase it would be advantageous to refine compound properties to improve drug-like characteristics and potency (Hughes et al., 2011a). However, as previously discussed, chloroxine is already a licenced and well tolerated drug. It may be that expending further efforts to modify chloroxine are unjustified. ADME and PK/PD investigations are still very important in determining correct dosing regimens.

Having identified hydroxymethylglutaryl-CoA-lyase from gene BTH_I0313, the gene was sequenced and cloned into a construct for recombinant expression in *Escherichia coli*. A six histidine residue tag was included in the synthesised sequence to enable purification by nickel affinity chromatography. This was carried out by Eve Chan, an undergraduate student at the University of Exeter. During her final year research

project, Eve was able to express and purify CoA-lyase and design a coupled assay (Figure 6.3). However the time constraints of her project did not allow for inhibition assays with chloroxine. It is hoped that these investigations will be carried out imminently.

Hypothesised MoA's for Chloroxine

Although chloroxine has been used a licenced antimicrobial for over a century, the MOA for this antibiotic is not known. It is therefore impossible to know whether the same pathway is targeted in persister cells as in general antibiotic activity; or whether a secondary target causes the effect on persisters.

A study in 2014 identified that toxin GhoT, from a toxin/antitoxin system, Gho/GhoS slows metabolism in the presence of antimicrobials in *Escherichia coli*. The antimicrobials tested included 5,7-dichloro—hydroxyquinoline (chloroxine). The study found that in the presence of chloroxine, the GhoT toxin damages the cell membrane at the cell poles, thereby depleting cellular energy and disrupting proton motive force (Cheng et al., 2014). GhoT was first described in (Wang et al., 2012) as a component of a novel type V toxin-antitoxin with it's anti-toxin GhoS. GroT is a membrane lytic peptide that causes lysed “ghost cells” with damaged membranes and an increase in persister cell numbers. In non persisters the anti-toxin GhoS was identified as an RNase which cleaves *ghoT* mRNA (Wang et al., 2012). The implication of this research could be that treatment of *Burkholderia* with chloroxine causes cell wall damage leading to cell decay. It was also noted that in cells over expressing GhoT, hyper-permeability of the membrane occurred. This compromise to the membrane may in the case of melioidosis treatment be the basis of the synergy observed when chloroxine and ceftazidime are used together. Alternatively chloroxine may enhance

the persistent state, driving the cells deeper into a lower metabolism state (Figure 4.37). However, a BLAST search of GhoT against the *Burkholderia* genome database (Winsor et al., 2008) did not identify any homologs in any *Burkholderia* species.

The structure of chloroxine suggests stability in low pH environments. This indicates that the compound should retain activity in the stomach. A believed reservoir of *B. pseudomallei* persister cells is the gastrointestinal tract (Goodyear et al., 2012). This has been hypothesised to be instrumental to recurrent disease; as such chloroxine's suitability for treatment of melioidosis is enhanced.

Preliminary results from MOA studies have highlighted two putative genes for further investigation. Results indicate that use of an over-expression library for identifying persister cell genes is justified and could be applied to other lead series. However target inhibitor relationships need to be characterised through enzyme inhibition studies or crystallisation of an enzyme inhibitor complex before this can be absolutely confirmed.

7. Conclusions and Outlook

Work on this investigation started in April 2012 and received funding for three years. Following successful initial findings, an extension of three months was granted to carry out SAR studies.

7.1. Summary of work

The impetus for this project was primarily to develop a drug discovery program to improve treatment options in melioidosis. An equally important focus was to improve the understanding of the role persister cells can play in (treating) chronic and recurrent disease. An aim of the project was to investigate if persister cells are viable targets for antimicrobial treatment. Through these investigations I hoped to learn more about the role of persister cells and the genetic basis of their formation and survival.

To achieve these aims I developed a phenotypic assay to identify compounds that eradicate persister cells. The assay was based on the reduction of the resazurin based dye PrestoBlue and was optimised for HTS of a screening library. The screening library chosen was the diversity library created by the DDU. As previously described, this library has been designed to cover a larger area of chemical space and identify drug-like small molecules. The diversity library has also been strategically designed for antimicrobial drug discovery.

Screening of 61,250 compounds identified 2,127 compounds that gave a statistically significant reduction in persister cell numbers. I then used dose-response assays to triage these results to 29 compounds with a pIC_{50} greater than five. The project benefited from the DDU's expertise in HTS and interpretation of results. This gave me

great confidence that the screening was a success and that the results from the first work package in the project were reliable and biologically significant.

Using extended dose-response assays and structural information, as well as information from the literature, six “best in class” compounds were selected. These included the licensed drug chloroxine. In a time dependent killing assay chloroxine reduced levels of persister cells by three orders of magnitude over 72 hours ($P = 0.01$). This confirmed the compound has activity in both the PrestoBlue assay and using the “gold standard” culture/colony count method.

Series expansion was carried out for the six compounds with differing levels of success. As described in chapter 5, good SAR characteristics were identified for three of the six compounds. Series expansion around chloroxine using commercially available compounds did not identify any more potent compounds, but did highlight key features of the molecule for activity. Compounds **7** and **23** showed areas around the structure that can be modified to modulate activity and have potential for future development into lead series. **16** showed three key structural features integral to activity with at least one structural modification leading to an increase in potency. **16** was the most promising as a lead series for future work. However, in order to make the most progress within the confines of the overall project I chose chloroxine to take forward into MOA studies.

Collaborators at DSTL were able to accurately replicate dose response assays for chloroxine. They were also able to show that chloroxine is active against persister cells formed by *Burkholderia pseudomallei*. This validates the approach that I took in performing the original assays with *B. thailandensis*, and confirms that chloroxine has potential for use in the pathogen.

Following on from activity confirmation and series expansion the project progressed to look at MOA studies for lead series. A chemical genetics approach was taken to identify genes involved in persister cell survival using Next Generation Sequencing of an over expression library. This identified twelve genes which were significantly over represented when compared to a persister culture treated only with ceftazidime ($P < 0.05$). Based on the predicted function of these genes, and the tractability of downstream assays, I selected two putative genes involved in inhibition of persister cells by chloroxine. These genes had viable hypotheses for their action and it was possible to design enzyme assays with which to test activity. I was also able to make predictions from their structure and cellular location about the ease of which the proteins could be expressed and purified for use.

7.2. Future Work

Mass population studies in persister cells are only able to measure averages which can make some analyses impossible (Dhar and McKinney, 2007). One potential method could be single cell micro fluidic analysis of individual persister cells to identify heterogeneity within the population (Helaine and Holden, 2013). To facilitate drug development and testing, it would extremely helpful to have a suitable murine model for chronic and recurrent infection.

Figure 4.36 shows the dose response assay for chloroxine carried out in *B. thailandensis* and *B. pseudomallei* by DSTL. The same assay was attempted for *Pseudomonas aeruginosa*, a Gram-negative bacteria which also causes persistent infections (Mulcahy et al., 2010b). Persister cells in *P. aeruginosa* have already been identified as a target for therapeutic development (Liebens et al., 2016). From a drug discovery perspective, if chloroxine is also active against persister cell targets in

Pseudomonas infections the impact of this project could be far greater. A small amount of funding was acquired by DSTL to investigate this. However, this species is far more sensitive to low concentrations of the DMSO carrier, and so the assay was invalid. If further streams of funding were to become available I am confident the assay could be re-optimised for new species, for example by investigating a wider range of suitable carriers.

There is an additional hurdle to anti-persister therapies, in that the food and drug administration (FDA) only require testing against rapidly growing bacteria. This makes market conditions excellent for a new conventional broad-spectrum antibiotic but is considerably more challenging to develop an anti-persister therapy (Lewis, 2007). For this reason, as chloroxine is already licenced, it is much more attractive as a potential drug for a disease that is not attractive to significant pharmaceutical financial backing.

7.3. Academic Drug Discovery

Not only are we witnessing worrying trends in antibiotic resistance, but emerging pathogens such as *B. pseudomallei* are being diagnosed in ever increasing populations (Limmathurotsakul et al., 2016). It is therefore even more worrying that large pharmaceutical companies have seen a significant reduction in drug discovery programs since the turn of the century. This has led to a dramatic reduction in the number of new molecular entities (NME) to be approved by the FDA and the number of companies actively discovering new compounds to reduce by over half since 2005 (Kinch and Flath, 2014). A significant reason for this reduction in productivity is the attrition observed in potential new drugs in phase II and III clinical trials due to patient safety issues and insufficient compound efficacy (Paul et al., 2010). It can also be speculated that the economic model for drug discovery, particularly for antibiotics, by

large pharmaceutical companies reporting to shareholders is not viable (Pammolli et al., 2011). There are diminishing incentives for companies to invest in antibiotic R&D and push new products to market. Maximising sales volumes to make a return on investment cannot be applied to antibiotics as overuse will drive resistance generation (Hoffman and Outterson, 2015, Kesselheim and Outterson, 2010, Kesselheim and Outterson, 2011); and increasing prices will stop the drugs reaching patients in need.

More recently models of pharmaceutical collaboration with academic groups, biotechnology companies and government are emerging and contributing to new platforms for discovery, leads and some drugs (Everett, 2015, Schultz Kirkegaard and Valentin, 2014). These smaller, diverse companies are the drivers of creativity and innovation able to apply high-risk ideas and concepts. Academic Drug Discovery Centres (ADDC) are an example of industry–academic partnerships (Tralau-Stewart et al., 2009) with the intent to develop drug candidates up to the point at which the risk is suitably low for the product to gain commercial interest. In the case of neglected diseases such as melioidosis, potential drugs would need to meet criteria for further government or humanitarian funding. This urgent need was further recognised in a major communique from the World Economic Forum, Davos 2016 calling for revitalization of the basic scientific research and development required to create new antibiotics.

From this project it became clear that any academic drug discovery programme is reliant on a broad range of expertise and specialities. It is evident that the struggles I encountered with obtaining adequate SAR data was partly due to a lack of chemistry support within the project team. The bulk of the chemical synthesis work was not inherently difficult. However, due to my background as a microbiologist and my lack of experience in chemistry, this was outside of my skillset. The project would have

benefited either from involvement of a postgraduate student or approximately £15,000 available for contracted synthesis of compounds.

7.4. Concluding remarks

It has been postulated that deeper understanding of the mechanisms of persister formation could contribute to the development of persister-specific drugs and improve treatment of chronic infectious diseases (Helaine and Kugelberg, 2014). As a whole the project has been successful and concludes with sufficient data for continuation of research following a number of leads and is at an ideal stage for instigation of a medicinal chemistry program for development of chloroxine as a clinical option for treatment of persistent melioidosis.

References

- AEKPLAKORN, W., CHARİYALERTSAK, S., KESSOMBOON, P., SANGTHONG, R., INTHAWONG, R., PUTWATANA, P., TANEEPANICHSKUL, S. & THAI NATIONAL HEALTH EXAMINATION SURVEY, I. V. S. G. 2011. Prevalence and management of diabetes and metabolic risk factors in Thai adults: the Thai National Health Examination Survey IV, 2009. *Diabetes Care*, 34, 1980-5.
- AGHAIE, A., LECHAPLAIS, C., SIRVEN, P., TRICOT, S., BESNARD-GONNET, M., MUSELET, D., DE BERARDINIS, V., KREIMEYER, A., GYAPAY, G., SALANOUBAT, M. & PERRET, A. 2008. New insights into the alternative D-glucarate degradation pathway. *J Biol Chem*, 283, 15638-46.
- AHMED, K., ENCISO, H. D., MASAKI, H., TAO, M., OMORI, A., THARAVICHIKUL, P. & NAGATAKE, T. 1999. Attachment of *Burkholderia pseudomallei* to pharyngeal epithelial cells: a highly pathogenic bacteria with low attachment ability. *Am J Trop Med Hyg*, 60, 90-3.
- ALLISON, K. R., BRYNILDSEN, M. P. & COLLINS, J. J. 2011a. Heterogeneous bacterial persisters and engineering approaches to eliminate them. *Curr Opin Microbiol*, 14, 593-8.
- ALLISON, K. R., BRYNILDSEN, M. P. & COLLINS, J. J. 2011b. Metabolite-enabled eradication of bacterial persisters by aminoglycosides. *Nature*, 473, 216-+.
- ALTSCHUL, S. F., MADDEN, T. L., SCHAFFER, A. A., ZHANG, J., ZHANG, Z., MILLER, W. & LIPMAN, D. J. 1997. Gapped BLAST and PSI-BLAST: a new generation of protein database search programs. *Nucleic Acids Res*, 25, 3389-402.

- ALTSCHUL, S. F., WOOTTON, J. C., GERTZ, E. M., AGARWALA, R., MORGULIS, A., SCHAFFER, A. A. & YU, Y. K. 2005. Protein database searches using compositionally adjusted substitution matrices. *Febs Journal*, 272, 5101-5109.
- AMBAYE, A., KOHNER, P. C., WOLLAN, P. C., ROBERTS, K. L., ROBERTS, G. D. & COCKERILL, F. R., 3RD 1997. Comparison of agar dilution, broth microdilution, disk diffusion, E-test, and BACTEC radiometric methods for antimicrobial susceptibility testing of clinical isolates of the *Nocardia asteroides* complex. *J Clin Microbiol*, 35, 847-52.
- ARGÜELLO, J. M., RAIMUNDA, D. & PADILLA-BENAVIDES, T. 2013. Mechanisms of copper homeostasis in bacteria. *Frontiers in Cellular and Infection Microbiology*, 3, 73.
- BAELL, J. B. & HOLLOWAY, G. A. 2010. New substructure filters for removal of pan assay interference compounds (PAINS) from screening libraries and for their exclusion in bioassays. *J Med Chem*, 53, 2719-40.
- BALABAN, N. Q. 2011. Persistence: mechanisms for triggering and enhancing phenotypic variability. *Curr Opin Genet Dev*, 21, 768-75.
- BALABAN, N. Q., GERDES, K., LEWIS, K. & MCKINNEY, J. D. 2013. A problem of persistence: still more questions than answers? *Nature Reviews Microbiology*, 11, 587-591.
- BALABAN, N. Q., MERRIN, J., CHAIT, R., KOWALIK, L. & LEIBLER, S. 2004. Bacterial persistence as a phenotypic switch. *Science*, 305, 1622-1625.
- BATHOORN, E., TSIOUTIS, C., DA SILVA VOORHAM, J. M., SCOULICA, E. V., IOANNIDOU, E., ZHOU, K., ROSSEN, J. W., GIKAS, A., FRIEDRICH, A. W. & GRUNDMANN, H. 2016. Emergence of pan-resistance in KPC-2 carbapenemase-producing *Klebsiella pneumoniae* in Crete, Greece: a close call. *J Antimicrob Chemother*.
- BEGLEY, D. W., FOX, D., 3RD, JENNER, D., JULI, C., PIERCE, P. G., ABENDROTH, J., MURUTHI, M., SAFFORD, K., ANDERSON, V., ATKINS, K., BARNES, S. R., MOEN, S. O., RAYMOND, A. C., STACY, R., MYLER, P. J., STAKER, B. L., HARMER, N. J., NORVILLE,

- I. H., HOLZGRABE, U., SARKAR-TYSON, M., EDWARDS, T. E. & LORIMER, D. D. 2014. A structural biology approach enables the development of antimicrobials targeting bacterial immunophilins. *Antimicrob Agents Chemother*, 58, 1458-67.
- BERNIER, S. P., LEBEAUX, D., DEFRANCESCO, A. S., VALOMON, A., SOUBIGOU, G., COPPEE, J. Y., GHIGO, J. M. & BELOIN, C. 2013. Starvation, Together with the SOS Response, Mediates High Biofilm-Specific Tolerance to the Fluoroquinolone Ofloxacin. *Plos Genetics*, 9.
- BIGGER, J. W. 1944. Treatment of staphylococcal infections with penicillin - By intermittent sterilisation. *Lancet*, 2, 497-500.
- BOURNE, C. R., WAKEHAM, N., BUNCE, R. A., BERLIN, K. D. & BARROW, W. W. 2012. Classifying compound mechanism of action for linking whole cell phenotypes to molecular targets. *Journal of molecular recognition : JMR*, 25, 216-223.
- BOWLING, T., MERCER, L., DON, R., JACOBS, R. & NARE, B. 2012. Application of a resazurin-based high-throughput screening assay for the identification and progression of new treatments for human African trypanosomiasis. *International Journal for Parasitology, Drugs and Drug Resistance*, 2, 262-270.
- BRAUN, T. F., POULSON, S., GULLY, J. B., EMPEY, J. C., VAN WAY, S., PUTNAM, A. & BLAIR, D. F. 1999. Function of proline residues of MotA in torque generation by the flagellar motor of Escherichia coli. *Journal of bacteriology*, 181, 3542-3551.
- BRETT, P. J., DESHAZER, D. & WOODS, D. E. 1997. Characterization of Burkholderia pseudomallei and Burkholderia pseudomallei-like strains. *Epidemiol Infect*, 118, 137-48.
- BRETT, P. J., DESHAZER, D. & WOODS, D. E. 1998. Burkholderia thailandensis sp. nov., a Burkholderia pseudomallei-like species. *Int J Syst Bacteriol*, 48 Pt 1, 317-20.

- BROOUN, A., LIU, S. & LEWIS, K. 2000. A dose-response study of antibiotic resistance in *Pseudomonas aeruginosa* biofilms. *Antimicrob Agents Chemother*, 44, 640-6.
- BUSTIN, S. A., BENES, V., GARSON, J. A., HELLEMANS, J., HUGGETT, J., KUBISTA, M., MUELLER, R., NOLAN, T., PFAFFL, M. W., SHIPLEY, G. L., VANDESOMPELE, J. & WITTEWER, C. T. 2009. The MIQE guidelines: minimum information for publication of quantitative real-time PCR experiments. *Clin Chem*, 55, 611-22.
- BUTLER, D. 2012. Viral research faces clampdown. *Nature*, 490, 456.
- BUTT, A., HIGMAN, VICTORIA A., WILLIAMS, C., CRUMP, MATTHEW P., HEMSLEY, CLAUDIA M., HARMER, N. & TITBALL, RICHARD W. 2014a. The HicA toxin from *Burkholderia pseudomallei* has a role in persister cell formation. *Biochemical Journal*, 459, 333-344.
- BUTT, A., HIGMAN, V. A., WILLIAMS, C., CRUMP, M. P., HEMSLEY, C. M., HARMER, N. & TITBALL, R. W. 2014b. The HicA toxin from *Burkholderia pseudomallei* has a role in persister cell formation. *Biochem J*, 459, 333-44.
- CAGLIC, D., KRUTEIN, M. C., BOMPIANI, K. M., BARLOW, D. J., BENONI, G., PELLETIER, J. C., REITZ, A. B., LAIRSON, L. L., HOUSEKNECHT, K. L., SMITH, G. R. & DICKERSON, T. J. 2014. Identification of clinically viable quinolinol inhibitors of botulinum neurotoxin A light chain. *J Med Chem*, 57, 669-76.
- CALVORI, C., FRONTALI L., LEONI L., TECCE G., 1965. Effect of rifamycin on protein synthesis. *Nature*, 995, 417-8
- CAMPOS, E., BALDOMA, L., AGUILAR, J. & BADIA, J. 2004. Regulation of expression of the divergent *ulaG* and *ulaABCDEF* operons involved in LaAscorbate dissimilation in *Escherichia coli*. *J Bacteriol*, 186, 1720-8.

- CENTERS FOR DISEASE, C., PREVENTION, D. O. H. & HUMAN, S. 2012. Possession, use, and transfer of select agents and toxins; biennial review. Final rule. *Fed Regist*, 77, 61083-115.
- CHANTRATITA, N., RHOLL, D. A., SIM, B., WUTHIEKANUN, V., LIMMATHUROTSAKUL, D., AMORNCHAI, P., THANWISAI, A., CHUA, H. H., OOI, W. F., HOLDEN, M. T., DAY, N. P., TAN, P., SCHWEIZER, H. P. & PEACOCK, S. J. 2011. Antimicrobial resistance to ceftazidime involving loss of penicillin-binding protein 3 in *Burkholderia pseudomallei*. *Proc Natl Acad Sci U S A*, 108, 17165-70.
- CHAOWAGUL, W., SUPUTTAMONGKOL, Y., DANCE, D. A., RAJCHANUVONG, A., PATTARA-ARECHACHAI, J. & WHITE, N. J. 1993. Relapse in melioidosis: incidence and risk factors. *J Infect Dis*, 168, 1181-5.
- CHENG, A. C., CHIERAKUL, W., CHAOWAGUL, W., CHETCHOTISAKD, P., LIMMATHUROTSAKUL, D., DANCE, D. A., PEACOCK, S. J. & CURRIE, B. J. 2008. Consensus guidelines for dosing of amoxicillin-clavulanate in melioidosis. *Am J Trop Med Hyg*, 78, 208-9.
- CHENG, A. C., FISHER, D. A., ANSTEY, N. M., STEPHENS, D. P., JACUPS, S. P. & CURRIE, B. J. 2004. Outcomes of patients with melioidosis treated with meropenem. *Antimicrob Agents Chemother*, 48, 1763-5.
- CHENG, H.-Y., SOO, V. W. C., ISLAM, S., MCANULTY, M. J., BENEDIK, M. J. & WOOD, T. K. 2014. Toxin GhoT of the GhoT/GhoS toxin/antitoxin system damages the cell membrane to reduce adenosine triphosphate and to reduce growth under stress. *Environmental Microbiology*, 16, 1741-1754.
- CHOI, S. H. & KOH, Y. 2012. Ceftazidime for respiratory infections. *Expert Opin Pharmacother*, 13, 2097-109.

- COGAN, N. G., SZOMOLAY, B. & DINDOS, M. 2013. Effect of Periodic Disinfection on Persisters in a One-Dimensional Biofilm Model. *Bulletin of Mathematical Biology*, 75, 94-123.
- COHEN, N. R., LOBRITZ, M. A. & COLLINS, J. J. 2013. Microbial persistence and the road to drug resistance. *Cell Host Microbe*, 13, 632-42.
- COLE, J. 1996. Nitrate reduction to ammonia by enteric bacteria: redundancy, or a strategy for survival during oxygen starvation? *FEMS Microbiol Lett*, 136, 1-11.
- COLLANDER, R. 1951. The Partition of Organic Compounds between Higher Alcohols and Water. *Acta Chemica Scandinavica*, 5, 774-780.
- CONG, F., CHEUNG, A. K. & HUANG, S. M. 2012. Chemical genetics-based target identification in drug discovery. *Annu Rev Pharmacol Toxicol*, 52, 57-78.
- CONLON, B. P., NAKAYASU, E. S., FLECK, L. E., LAFLEUR, M. D., ISABELLA, V. M., COLEMAN, K., LEONARD, S. N., SMITH, R. D., ADKINS, J. N. & LEWIS, K. 2013. Activated ClpP kills persisters and eradicates a chronic biofilm infection. *Nature*, 503, 365-70.
- CONLON, B. P., ROWE, S. E. & LEWIS, K. 2015. Persister Cells in Biofilm Associated Infections. *Biofilm-Based Healthcare-Associated Infections, Vol II*, 831, 1-9.
- CORREIA, F. F., D'ONOFRIO, A., REJTAR, T., LI, L., KARGER, B. L., MAKAROVA, K., KOONIN, E. V. & LEWIS, K. 2006. Kinase activity of overexpressed HipA is required for growth arrest and multidrug tolerance in Escherichia coli. *J Bacteriol*, 188, 8360-7.
- CRAGG, G. M. & NEWMAN, D. J. 2013. Natural products: a continuing source of novel drug leads. *Biochim Biophys Acta*, 1830, 3670-95.
- CROCKER, J. C., BEECHAM, E., KELLY, P., DINSDALE, A. P., HEMSLEY, J., JONES, L. & BLUEBOND-LANGNER, M. 2015. Inviting parents to take part in paediatric

- palliative care research: a mixed-methods examination of selection bias. *Palliat Med*, 29, 231-40.
- CURRIE, B. J., FISHER, D. A., ANSTEY, N. M. & JACUPS, S. P. 2000a. Melioidosis: acute and chronic disease, relapse and re-activation. *Trans R Soc Trop Med Hyg*, 94, 301-4.
- CURRIE, B. J., FISHER, D. A., HOWARD, D. M., BURROW, J. N., LO, D., SELVA-NAYAGAM, S., ANSTEY, N. M., HUFFAM, S. E., SNELLING, P. L., MARKS, P. J., STEPHENS, D. P., LUM, G. D., JACUPS, S. P. & KRAUSE, V. L. 2000b. Endemic melioidosis in tropical northern Australia: a 10-year prospective study and review of the literature. *Clin Infect Dis*, 31, 981-6.
- CURRIE, B. J., JACUPS, S. P., CHENG, A. C., FISHER, D. A., ANSTEY, N. M., HUFFAM, S. E. & KRAUSE, V. L. 2004. Melioidosis epidemiology and risk factors from a prospective whole-population study in northern Australia. *Trop Med Int Health*, 9, 1167-74.
- CURRIE, B. J., WARD, L. & CHENG, A. C. 2010. The epidemiology and clinical spectrum of melioidosis: 540 cases from the 20 year Darwin prospective study. *PLoS Negl Trop Dis*, 4, e900.
- DANCE, D. 2014a. Treatment and prophylaxis of melioidosis. *International Journal of Antimicrobial Agents*, 43, 310-318.
- DANCE, D. 2014b. Treatment and prophylaxis of melioidosis. *Int J Antimicrob Agents*, 43, 310-8.
- DE LEENHEER, P. & COGAN, N. G. 2009. Failure of antibiotic treatment in microbial populations. *Journal of Mathematical Biology*, 59, 563-579.
- DEVINE, S. M., MULCAIR, M. D., DEBONO, C. O., LEUNG, E. W., NISSINK, J. W., LIM, S. S., CHANDRASHEKARAN, I. R., VAZIRANI, M., MOHANTY, B., SIMPSON, J. S., BAELL, J. B., SCAMMELLS, P. J., NORTON, R. S. & SCANLON, M. J. 2015. Promiscuous 2-aminothiazoles (PrATs): a frequent hitting scaffold. *J Med Chem*, 58, 1205-14.

- DHAR, N. & MCKINNEY, J. D. 2007. Microbial phenotypic heterogeneity and antibiotic tolerance. *Curr Opin Microbiol*, 10, 30-8.
- DI, L. & KERNS, E. H. 2006. Biological assay challenges from compound solubility: strategies for bioassay optimization. *Drug Discov Today*, 11, 446-51.
- DIAS, D. A., URBAN, S. & ROESSNER, U. 2012. A historical overview of natural products in drug discovery. *Metabolites*, 2, 303-36.
- DORR, T., LEWIS, K. & VULIC, M. 2009. SOS Response Induces Persistence to Fluoroquinolones in Escherichia coli. *Plos Genetics*, 5.
- DORR, T., VULIC, M. & LEWIS, K. 2010. Ciprofloxacin Causes Persister Formation by Inducing the TisB toxin in Escherichia coli. *Plos Biology*, 8.
- DUFFY, B. C., ZHU, L., DECORNEZ, H. & KITCHEN, D. B. 2012. Early phase drug discovery: cheminformatics and computational techniques in identifying lead series. *Bioorg Med Chem*, 20, 5324-42.
- EDER, J., SEDRANI, R. & WIESMANN, C. 2014. The discovery of first-in-class drugs: origins and evolution. *Nat Rev Drug Discov*, 13, 577-587.
- ERLANSON, D. A., MCDOWELL, R. S. & O'BRIEN, T. 2004. Fragment-Based Drug Discovery. *Journal of Medicinal Chemistry*, 47, 3463-3482.
- EVERETT, J. R. 2015. Academic drug discovery: current status and prospects. *Expert Opin Drug Discov*, 10, 937-44.
- FAUVART, M., DE GROOTE, V. N. & MICHIELS, J. 2011. Role of persister cells in chronic infections: clinical relevance and perspectives on anti-persister therapies. *J Med Microbiol*, 60, 699-709.
- FENG, J., AUWAERTER, P. G. & ZHANG, Y. 2015. Drug Combinations against *Borrelia burgdorferi* Persisters In Vitro: Eradication Achieved by Using Daptomycin, Cefoperazone and Doxycycline. *PLoS ONE*, 10, e0117207.

- FENG, J., LIU, T., QIN, B., ZHANG, Y. & LIU, X. S. 2012. Identifying ChIP-seq enrichment using MACS. *Nat Protoc*, 7, 1728-40.
- FINN, R. D., COGGILL, P., EBERHARDT, R. Y., EDDY, S. R., MISTRY, J., MITCHELL, A. L., POTTER, S. C., PUNTA, M., QURESHI, M., SANGRADOR-VEGAS, A., SALAZAR, G. A., TATE, J. & BATEMAN, A. 2016. The Pfam protein families database: towards a more sustainable future. *Nucleic Acids Research*, 44, D279-D285.
- FLECK, L. E., NORTH, E. J., LEE, R. E., MULCAHY, L. R., CASADEI, G. & LEWIS, K. 2014. A Screen for and Validation of Prodrug Antimicrobials. *Antimicrobial Agents and Chemotherapy*, 58, 1410-1419.
- FLEMING, A. 1946. The development and use of penicillin. *Chic Med Sch Q*, 7, 20-8.
- FUTAMURA, Y., MUROI, M. & OSADA, H. 2013. Target identification of small molecules based on chemical biology approaches. *Mol Biosyst*, 9, 897-914.
- GERMAIN, E., CASTRO-ROA, D., ZENKIN, N. & GERDES, K. 2013a. Molecular Mechanism of Bacterial Persistence by HipA. *Molecular Cell*, 52, 248-254.
- GERMAIN, E., CASTRO-ROA, D., ZENKIN, N. & GERDES, K. 2013b. Molecular mechanism of bacterial persistence by HipA. *Mol Cell*, 52, 248-54.
- GILAD, J., HARARY, I., DUSHNITSKY, T., SCHWARTZ, D. & AMSALEM, Y. 2007. Burkholderia mallei and Burkholderia pseudomallei as bioterrorism agents: National aspects of emergency preparedness. *Israel Medical Association Journal*, 9, 499-503.
- GLASS, M. B., GEE, J. E., STEIGERWALT, A. G., CAVUOTI, D., BARTON, T., HARDY, R. D., GODOY, D., SPRATT, B. G., CLARK, T. A. & WILKINS, P. P. 2006. Pneumonia and septicemia caused by Burkholderia thailandensis in the United States. *J Clin Microbiol*, 44, 4601-4.

- GODOY, D., RANDLE, G., SIMPSON, A. J., AANENSEN, D. M., PITT, T. L., KINOSHITA, R. & SPRATT, B. G. 2003. Multilocus sequence typing and evolutionary relationships among the causative agents of melioidosis and glanders, *Burkholderia pseudomallei* and *Burkholderia mallei*. *J Clin Microbiol*, 41, 2068-79.
- GOODYEAR, A., BIELEFELDT-OHMANN, H., SCHWEIZER, H. & DOW, S. 2012. Persistent gastric colonization with *Burkholderia pseudomallei* and dissemination from the gastrointestinal tract following mucosal inoculation of mice. *PLoS One*, 7, e37324.
- GRAPHPAD SOFTWARE, I. 2016. *Analysing Dose-Response Data* [Online]. www.graphpad.com. Available: [http://www.graphpad.com/faq/file/P4-Dose-response curves.pdf](http://www.graphpad.com/faq/file/P4-Dose-response%20curves.pdf) [Accessed 26/01/2016 2016].
- GUBLER, H., SCHOPFER, U. & JACOBY, E. 2013. Theoretical and experimental relationships between percent inhibition and IC50 data observed in high-throughput screening. *J Biomol Screen*, 18, 1-13.
- HALL-STOODLEY, L., COSTERTON, J. W. & STOODLEY, P. 2004. Bacterial biofilms: from the natural environment to infectious diseases. *Nat Rev Microbiol*, 2, 95-108.
- HALSEY, L. G., CURRAN-EVERETT, D., VOWLER, S. L. & DRUMMOND, G. B. 2015. The fickle P value generates irreproducible results. *Nat Meth*, 12, 179-185.
- HARAGA, A., OHLSON, M. B. & MILLER, S. I. 2008a. Salmonellae interplay with host cells. *Nat Rev Microbiol*, 6, 53-66.
- HARAGA, A., WEST, T. E., BRITTNACHER, M. J., SKERRETT, S. J. & MILLER, S. I. 2008b. *Burkholderia thailandensis* as a model system for the study of the virulence-associated type III secretion system of *Burkholderia pseudomallei*. *Infect Immun*, 76, 5402-11.
- HARVEY, A. L. 2008. Natural products in drug discovery. *Drug Discovery Today*, 13, 894-901.

- HARWOOD C. R., C. S. M. 1990. *Chemically defined growth media and supplements*, Chichester, United Kingdom, Wiley.
- HAYES, M. V. & ORR, D. C. 1983. Mode of action of ceftazidime: affinity for the penicillin-binding proteins of *Escherichia coli* K12, *Pseudomonas aeruginosa* and *Staphylococcus aureus*. *J Antimicrob Chemother*, 12, 119-26.
- HELAINÉ, S. & HOLDEN, D. W. 2013. Heterogeneity of intracellular replication of bacterial pathogens. *Curr Opin Microbiol*, 16, 184-91.
- HELAINÉ, S. & KUGELBERG, E. 2014. Bacterial persisters: formation, eradication, and experimental systems. *Trends in Microbiology*, 22, 417-424.
- HEMSLEY, C. M., LUO, J. X., ANDREAE, C. A., BUTLER, C. S., SOYER, O. S. & TITBALL, R. W. 2014. Bacterial drug tolerance under clinical conditions is governed by anaerobic adaptation but not anaerobic respiration. *Antimicrob Agents Chemother*, 58, 5775-83.
- HOFFMAN, S. J. & OUTTERSON, K. 2015. What Will It Take to Address the Global Threat of Antibiotic Resistance? *J Law Med Ethics*, 43, 363-8.
- HOFFMASTER, A. R., AUCCOIN, D., BACCAM, P., BAGGETT, H. C., BAIRD, R., BHENGSRİ, S., BLANEY, D. D., BRETT, P. J., BROOKS, T. J., BROWN, K. A., CHANTRATITA, N., CHENG, A. C., DANCE, D. A., DECUYPERE, S., DEFENBAUGH, D., GEE, J. E., HOUGHTON, R., JORAKATE, P., LERTMEMONGKOLCHAI, G., LIMMATHUROTSAKUL, D., MERLIN, T. L., MUKHOPADHYAY, C., NORTON, R., PEACOCK, S. J., ROLIM, D. B., SIMPSON, A. J., STEINMETZ, I., STODDARD, R. A., STOKES, M. M., SUE, D., TUANYOK, A., WHISTLER, T., WUTHIEKANUN, V. & WALKE, H. T. 2015. Melioidosis diagnostic workshop, 2013. *Emerg Infect Dis*, 21.
- HOLDEN, M. T., TITBALL, R. W., PEACOCK, S. J., CERDENO-TARRAGA, A. M., ATKINS, T., CROSSMAN, L. C., PITT, T., CHURCHER, C., MUNGALL, K., BENTLEY, S. D., SEBAIHIA,

- M., THOMSON, N. R., BASON, N., BEACHAM, I. R., BROOKS, K., BROWN, K. A., BROWN, N. F., CHALLIS, G. L., CHEREVACH, I., CHILLINGWORTH, T., CRONIN, A., CROSSETT, B., DAVIS, P., DESHAZER, D., FELTWELL, T., FRASER, A., HANCE, Z., HAUSER, H., HOLROYD, S., JAGELS, K., KEITH, K. E., MADDISON, M., MOULE, S., PRICE, C., QUAIL, M. A., RABBINOWITSCH, E., RUTHERFORD, K., SANDERS, M., SIMMONDS, M., SONGSIVILAI, S., STEVENS, K., TUMAPA, S., VESARATCHAVEST, M., WHITEHEAD, S., YEATS, C., BARRELL, B. G., OYSTON, P. C. & PARKHILL, J. 2004. Genomic plasticity of the causative agent of melioidosis, *Burkholderia pseudomallei*. *Proc Natl Acad Sci U S A*, 101, 14240-5.
- HOUGHTON, R. L., REED, D. E., HUBBARD, M. A., DILLON, M. J., CHEN, H., CURRIE, B. J., MAYO, M., SAROVICH, D. S., THEOBALD, V., LIMMATHUROTSAKUL, D., WONGSUWAN, G., CHANTRATITA, N., PEACOCK, S. J., HOFFMASTER, A. R., DUVAL, B., BRETT, P. J., BURTNICK, M. N. & AUCOIN, D. P. 2014. Development of a prototype lateral flow immunoassay (LFI) for the rapid diagnosis of melioidosis. *PLoS Negl Trop Dis*, 8, e2727.
- HUDDLESTON, J. R. 2014. Horizontal gene transfer in the human gastrointestinal tract: potential spread of antibiotic resistance genes. *Infection and Drug Resistance*, 7, 167-176.
- HUGHES, J. P., REES, S., KALINDJIAN, S. B. & PHILPOTT, K. L. 2011a. Principles of early drug discovery. *Br J Pharmacol*, 162, 1239-49.
- HUGHES, J. P., REES, S., KALINDJIAN, S. B. & PHILPOTT, K. L. 2011b. Principles of early drug discovery. *British Journal of Pharmacology*, 162, 1239-1249.
- HUTH, J. R., SONG, D., MENDOZA, R. R., BLACK-SCHAEFER, C. L., MACK, J. C., DORWIN, S. A., LADROR, U. S., SEVERIN, J. M., WALTER, K. A., BARTLEY, D. M. & HAJDUK, P. J. 2007. Toxicological evaluation of thiol-reactive compounds identified using a la

- assay to detect reactive molecules by nuclear magnetic resonance. *Chem Res Toxicol*, 20, 1752-9.
- HYATT, J. M., MCKINNON, P. S., ZIMMER, G. S. & SCHENTAG, J. J. 1995. The Importance of Pharmacokinetic-Pharmacodynamic Surrogate Markers to Outcome - Focus on Antibacterial Agents. *Clinical Pharmacokinetics*, 28, 143-160.
- INGLIS, T. J., GOLLEDGE, C. L., CLAIR, A. & HARVEY, J. 2001. Case report: recovery from persistent septicemic melioidosis. *Am J Trop Med Hyg*, 65, 76-82.
- INGLIS, T. J., ROLIM, D. B. & RODRIGUEZ, J. L. 2006. Clinical guideline for diagnosis and management of melioidosis. *Rev Inst Med Trop Sao Paulo*, 48, 1-4.
- JOHN, T. J. 2004. Melioidosis, the mimicker of maladies. *Indian J Med Res*, 119, vi-viii.
- JOHNSON, P. J. T. & LEVIN, B. R. 2013. Pharmacodynamics, Population Dynamics, and the Evolution of Persistence in *Staphylococcus aureus*. *Plos Genetics*, 9.
- JOHNSTON, C. W., SKINNIDER, M. A., DEJONG, C. A., REES, P. N., CHEN, G. M., WALKER, C. G., FRENCH, S., BROWN, E. D., BERDY, J., LIU, D. Y. & MAGARVEY, N. A. 2016. Assembly and clustering of natural antibiotics guides target identification. *Nat Chem Biol*, advance online publication.
- JONES, A. L., BEVERIDGE, T. J. & WOODS, D. E. 1996. Intracellular survival of *Burkholderia pseudomallei*. *Infect Immun*, 64, 782-90.
- KASPY, I., ROTEM, E., WEISS, N., RONIN, I., BALABAN, N. Q. & GLASER, G. 2013a. HipA-mediated antibiotic persistence via phosphorylation of the glutamyl-tRNA-synthetase. *Nature Communications*, 4.
- KASPY, I., ROTEM, E., WEISS, N., RONIN, I., BALABAN, N. Q. & GLASER, G. 2013b. HipA-mediated antibiotic persistence via phosphorylation of the glutamyl-tRNA-synthetase. *Nat Commun*, 4, 3001.

- Leveau JHJ, Lindow SE. 2001. Predictive and Interpretive Simulation of Green Fluorescent Protein Expression in Reporter Bacteria. *Journal of Bacteriology*, 183, 23
- KATSUNO, K., BURROWS, J. N., DUNCAN, K., VAN HUIJSDUIJNEN, R. H., KANEKO, T., KITA, K., MOWBRAY, C. E., SCHMATZ, D., WARNER, P. & SLINGSBY, B. T. 2015. Hit and lead criteria in drug discovery for infectious diseases of the developing world. *Nat Rev Drug Discov*.
- KEREN, I., KALDALU, N., SPOERING, A., WANG, Y. & LEWIS, K. 2004a. Persister cells and tolerance to antimicrobials. *FEMS Microbiol Lett*, 230, 13-8.
- KEREN, I., MULCAHY, L. R. & LEWIS, K. 2012. Persister Eradication: Lessons from the World of Natural Products. *Natural Product Biosynthesis by Microorganisms and Plants, Pt C*, 517, 387-406.
- KEREN, I., SHAH, D., SPOERING, A., KALDALU, N. & LEWIS, K. 2004b. Specialized persister cells and the mechanism of multidrug tolerance in Escherichia coli. *J Bacteriol*, 186, 8172-80.
- KEREN, I., SHAH, D., SPOERING, A., KALDALU, N. & LEWIS, K. 2004c. Specialized persister cells and the mechanism of multidrug tolerance in Escherichia coli. *Journal of Bacteriology*, 186, 8172-8180.
- KESERŰ, G. M. & MAKARA, G. M. 2006. Hit discovery and hit-to-lead approaches. *Drug Discovery Today*, 11, 741-748.
- KESSELHEIM, A. S. & OUTTERSON, K. 2010. Fighting antibiotic resistance: marrying new financial incentives to meeting public health goals. *Health Aff (Millwood)*, 29, 1689-96.
- KESSELHEIM, A. S. & OUTTERSON, K. 2011. Improving antibiotic markets for long-term sustainability. *Yale J Health Policy Law Ethics*, 11, 101-67.

- KINCH, M. S. & FLATH, R. 2014. New drug discovery: extraordinary opportunities in an uncertain time. *Drug Discov Today*.
- KING, H., AUBERT, R. E. & HERMAN, W. H. 1998. Global burden of diabetes, 1995-2025: prevalence, numerical estimates, and projections. *Diabetes Care*, 21, 1414-31.
- KNIGHT, Z. A. & SHOKAT, K. M. 2007. Chemical genetics: where genetics and pharmacology meet. *Cell*, 128, 425-30.
- KOH, S. F., TAY, S. T., SERMSWAN, R., WONGRATANACHEEWIN, S., CHUA, K. H. & PUTHUCHEARY, S. D. 2012. Development of a multiplex PCR assay for rapid identification of *Burkholderia pseudomallei*, *Burkholderia thailandensis*, *Burkholderia mallei* and *Burkholderia cepacia* complex. *J Microbiol Methods*, 90, 305-8.
- KOVACH, M. E., ELZER, P. H., HILL, D. S., ROBERTSON, G. T., FARRIS, M. A., ROOP, R. M., 2ND & PETERSON, K. M. 1995. Four new derivatives of the broad-host-range cloning vector pBBR1MCS, carrying different antibiotic-resistance cassettes. *Gene*, 166, 175-6.
- LAKSHMANAN, U., YAP, A., FULWOOD, J., YICHUN, L., HOON, S. S., LIM, J., TING, A., SEM, X. H., KREISBERG, J. F., TAN, P., TAN, G. & FLOTOW, H. 2014. Establishment of a novel whole animal HTS technology platform for melioidosis drug discovery. *Comb Chem High Throughput Screen*, 17, 790-803.
- LALL, N., HENLEY-SMITH, C. J., DE CANHA, M. N., OOSTHUIZEN, C. B. & BERRINGTON, D. 2013. Viability Reagent, PrestoBlue, in Comparison with Other Available Reagents, Utilized in Cytotoxicity and Antimicrobial Assays. *Int J Microbiol*, 2013, 420601.
- LALLEMAND, P., LEBAN, N., KUNZELMANN, S., CHALOIN, L., SERPERSU, E. H., WEBB, M. R., BARMAN, T. & LIONNE, C. 2012. Transient kinetics of aminoglycoside

- phosphotransferase(3')-IIIa reveals a potential drug target in the antibiotic resistance mechanism. *FEBS Lett*, 586, 4223-7.
- LAM, K. S. 2007. New aspects of natural products in drug discovery. *Trends in Microbiology*, 15, 279-289.
- LAVAN, D. A., LYNN, D. M. & LANGER, R. 2002. Moving smaller in drug discovery and delivery. *Nat Rev Drug Discov*, 1, 77-84.
- LEE, J. & BOGYO, M. 2013. Target deconvolution techniques in modern phenotypic profiling. *Curr Opin Chem Biol*, 17, 118-26.
- LEESON, P. D. & SPRINGTHORPE, B. 2007. The influence of drug-like concepts on decision-making in medicinal chemistry. *Nat Rev Drug Discov*, 6, 881-90.
- LEUNG, V. & LEVESQUE, C. M. 2012. A Stress-Inducible Quorum-Sensing Peptide Mediates the Formation of Persister Cells with Noninherited Multidrug Tolerance. *Journal of Bacteriology*, 194, 2265-2274.
- LEWIS, K. 2001. Riddle of biofilm resistance. *Antimicrob Agents Chemother*, 45, 999-1007.
- LEWIS, K. 2007. Persister cells, dormancy and infectious disease. *Nat Rev Microbiol*, 5, 48-56.
- LEWIS, K. 2008a. Multidrug tolerance of biofilms and persister cells. *Curr Top Microbiol Immunol*, 322, 107-31.
- LEWIS, K. 2008b. Multidrug tolerance of biofilms and persister cells. *Bacterial Biofilms*, 322, 107-131.
- LEWIS, K. 2010. Persister cells. *Annu Rev Microbiol*, 64, 357-72.
- LI, Y., GENG, J., LIU, Y., YU, S. & ZHAO, G. 2013. Thiadiazole-a promising structure in medicinal chemistry. *ChemMedChem*, 8, 27-41.

- LIEBENS, V., DEFRAINE, V. & FAUVART, M. 2016. A Whole-Cell-Based High-Throughput Screening Method to Identify Molecules Targeting *Pseudomonas aeruginosa* Persister Cells. *Methods Mol Biol*, 1333, 113-20.
- LIMMATHUROTSAKUL, D., CHAOWAGUL, W., CHIERAKUL, W., STEPNIEWSKA, K., MAHARJAN, B., WUTHIEKANUN, V., WHITE, N. J., DAY, N. P. & PEACOCK, S. J. 2006. Risk factors for recurrent melioidosis in northeast Thailand. *Clin Infect Dis*, 43, 979-86.
- LIMMATHUROTSAKUL, D., GOLDING, N., DANCE, D. A. B., MESSINA, J. P., PIGOTT, D. M., MOYES, C. L., ROLIM, D. B., BERTHERAT, E., DAY, N. P. J., PEACOCK, S. J. & HAY, S. I. 2016. Predicted global distribution of *Burkholderia pseudomallei* and burden of melioidosis. *Nature Microbiology*, 1, 15008.
- LIMMATHUROTSAKUL, D., WONGRATANACHEEWIN, S., TEERAWATTANASOOK, N., WONGSUVAN, G., CHAISUKSANT, S., CHETCHOTISAKD, P., CHAOWAGUL, W., DAY, N. P. & PEACOCK, S. J. 2010a. Increasing incidence of human melioidosis in Northeast Thailand. *Am J Trop Med Hyg*, 82, 1113-7.
- LIMMATHUROTSAKUL, D., WONGRATANACHEEWIN, S., TEERAWATTANASOOK, N., WONGSUVAN, G., CHAISUKSANT, S., CHETCHOTISAKD, P., CHAOWAGUL, W., DAY, N. P. J. & PEACOCK, S. J. 2010b. Increasing Incidence of Human Melioidosis in Northeast Thailand. *The American Journal of Tropical Medicine and Hygiene*, 82, 1113-1117.
- LING, L. L., SCHNEIDER, T., PEOPLES, A. J., SPOERING, A. L., ENGELS, I., CONLON, B. P., MUELLER, A., SCHABERLE, T. F., HUGHES, D. E., EPSTEIN, S., JONES, M., LAZARIDES, L., STEADMAN, V. A., COHEN, D. R., FELIX, C. R., FETTERMAN, K. A., MILLETT, W. P., NITTI, A. G., ZULLO, A. M., CHEN, C. & LEWIS, K. 2015. A new antibiotic kills pathogens without detectable resistance. *Nature*, 517, 455-+.

- LIPINSKI, C. A., LOMBARDO, F., DOMINY, B. W. & FEENEY, P. J. 2001. Experimental and computational approaches to estimate solubility and permeability in drug discovery and development settings. *Adv Drug Deliv Rev*, 46, 3-26.
- LIPSITZ, R., GARGES, S., AURIGEMMA, R., BACCAM, P., BLANEY, D. D., CHENG, A. C., CURRIE, B. J., DANCE, D., GEE, J. E., LARSEN, J., LIMMATHUROTSAKUL, D., MORROW, M. G., NORTON, R., O'MARA, E., PEACOCK, S. J., PESIK, N., ROGERS, L. P., SCHWEIZER, H. P., STEINMETZ, I., TAN, G., TAN, P., WIERSINGA, W. J., WUTHIEKANUN, V. & SMITH, T. L. 2012. Workshop on treatment of and postexposure prophylaxis for *Burkholderia pseudomallei* and *B. mallei* Infection, 2010. *Emerg Infect Dis*, 18, e2.
- LIU, B., LI, S. & HU, J. 2004. Technological advances in high-throughput screening. *Am J Pharmacogenomics*, 4, 263-76.
- LUESCH, H., WU, T. Y., REN, P., GRAY, N. S., SCHULTZ, P. G. & SUPEK, F. 2005. A genome-wide overexpression screen in yeast for small-molecule target identification. *Chem Biol*, 12, 55-63.
- LUM, P. Y., ARMOUR, C. D., STEPANIANTS, S. B., CAVET, G., WOLF, M. K., BUTLER, J. S., HINSHAW, J. C., GARNIER, P., PRESTWICH, G. D., LEONARDSON, A., GARRETT-ENGELE, P., RUSH, C. M., BARD, M., SCHIMMACK, G., PHILLIPS, J. W., ROBERTS, C. J. & SHOEMAKER, D. D. 2004. Discovering modes of action for therapeutic compounds using a genome-wide screen of yeast heterozygotes. *Cell*, 116, 121-37.
- MADDOX, C. B., RASMUSSEN, L. & WHITE, E. L. 2008. Adapting Cell-Based Assays to the High Throughput Screening Platform: Problems Encountered and Lessons Learned. *JALA Charlottesville Va*, 13, 168-173.
- MAHARJAN, B., CHANTRATITA, N., VESARATCHAVEST, M., CHENG, A., WUTHIEKANUN, V., CHIERAKUL, W., CHAOWAGUL, W., DAY, N. P. & PEACOCK, S. J. 2005. Recurrent

- melioidosis in patients in northeast Thailand is frequently due to reinfection rather than relapse. *J Clin Microbiol*, 43, 6032-4.
- MAISONNEUVE, E., CASTRO-CAMARGO, M. & GERDES, K. 2013. (p)ppGpp controls bacterial persistence by stochastic induction of toxin-antitoxin activity. *Cell*, 154, 1140-50.
- MAJERCZYK, C. D., BRITTNACHER, M. J., JACOBS, M. A., ARMOUR, C. D., RADEY, M. C., BUNT, R., HAYDEN, H. S., BYDALEK, R. & GREENBERG, E. P. 2014. Cross-species comparison of the *Burkholderia pseudomallei*, *Burkholderia thailandensis*, and *Burkholderia mallei* quorum-sensing regulons. *J Bacteriol*, 196, 3862-71.
- MCCUNE, R. M., JR. & TOMPSETT, R. 1956. Fate of *Mycobacterium tuberculosis* in mouse tissues as determined by the microbial enumeration technique. I. The persistence of drug-susceptible tubercle bacilli in the tissues despite prolonged antimicrobial therapy. *J Exp Med*, 104, 737-62.
- MCDONALD, J. C., DUFFY, D. C., ANDERSON, J. R., CHIU, D. T., WU, H. K., SCHUELLER, O. J. A. & WHITESIDES, G. M. 2000. Fabrication of microfluidic systems in poly(dimethylsiloxane). *Electrophoresis*, 21, 27-40.
- MERRITT, A., INGLIS, T. J., CHIDLOW, G. & HARNETT, G. 2006. PCR-based identification of *Burkholderia pseudomallei*. *Rev Inst Med Trop Sao Paulo*, 48, 239-44.
- MESTRES, J., GREGORI-PUIGJANE, E., VALVERDE, S. & SOLE, R. V. 2009. The topology of drug-target interaction networks: implicit dependence on drug properties and target families. *Mol Biosyst*, 5, 1051-7.
- MOKER, N., DEAN, C. R. & TAO, J. S. 2010. *Pseudomonas aeruginosa* Increases Formation of Multidrug-Tolerant Persister Cells in Response to Quorum-Sensing Signaling Molecules. *Journal of Bacteriology*, 192, 1946-1955.

- MONACK, D. M., MUELLER, A. & FALKOW, S. 2004. Persistent bacterial infections: the interface of the pathogen and the host immune system. *Nat Rev Microbiol*, 2, 747-65.
- MORGAN, J. L., MCNAMARA, J. T. & ZIMMER, J. 2014. Mechanism of activation of bacterial cellulose synthase by cyclic di-GMP. *Nat Struct Mol Biol*, 21, 489-96.
- MOULE, M. G., HEMSLEY, C. M., SEET, Q., GUERRA-ASSUNCAO, J. A., LIM, J., SARKAR-TYSON, M., CLARK, T. G., TAN, P. B., TITBALL, R. W., CUCCUI, J. & WREN, B. W. 2014. Genome-wide saturation mutagenesis of *Burkholderia pseudomallei* K96243 predicts essential genes and novel targets for antimicrobial development. *MBio*, 5, e00926-13.
- MOYED, H. S. & BERTRAND, K. P. 1983. Hipa, a Newly Recognized Gene of *Escherichia-Coli* K-12 That Affects Frequency of Persistence after Inhibition of Murein Synthesis. *Journal of Bacteriology*, 155, 768-775.
- MULCAHY, L. R., BURNS, J. L., LORY, S. & LEWIS, K. 2010a. Emergence of *Pseudomonas aeruginosa* Strains Producing High Levels of Persister Cells in Patients with Cystic Fibrosis. *Journal of Bacteriology*, 192, 6191-6199.
- MULCAHY, L. R., BURNS, J. L., LORY, S. & LEWIS, K. 2010b. Emergence of *Pseudomonas aeruginosa* strains producing high levels of persister cells in patients with cystic fibrosis. *J Bacteriol*, 192, 6191-9.
- MULLARD, A. 2015. Industry R&D returns slip. *Nat Rev Drug Discov*, 15, 7.
- NAMBI, S., LONG, JARUKIT E., MISHRA, BIBHUTI B., BAKER, R., MURPHY, KENAN C., OLIVE, ANDREW J., NGUYEN, HIEN P., SHAFFER, SCOTT A. & SASSETTI, CHRISTOPHER M. 2015. The Oxidative Stress Network of *Mycobacterium tuberculosis* Reveals Coordination between Radical Detoxification Systems. *Cell Host & Microbe*, 17, 829-837.

- NGAUY, V., LEMESHEV, Y., SADKOWSKI, L. & CRAWFORD, G. 2005. Cutaneous melioidosis in a man who was taken as a prisoner of war by the Japanese during World War II. *Journal of Clinical Microbiology*, 43, 970-972.
- NGUGI, S. A., VENTURA, V. V., QAZI, O., HARDING, S. V., KITTO, G. B., ESTES, D. M., DELL, A., TITBALL, R. W., ATKINS, T. P., BROWN, K. A., HITCHEN, P. G. & PRIOR, J. L. 2010. Lipopolysaccharide from *Burkholderia thailandensis* E264 provides protection in a murine model of melioidosis. *Vaccine*, 28, 7551-5.
- NGUYEN, D., JOSHI-DATAR, A., LEPINE, F., BAUERLE, E., OLAKANMI, O., BEER, K., MCKAY, G., SIEHNEL, R., SCHAFHAUSER, J., WANG, Y., BRITIGAN, B. E. & SINGH, P. K. 2011. Active starvation responses mediate antibiotic tolerance in biofilms and nutrient-limited bacteria. *Science*, 334, 982-6.
- NHEM, S., LETCHFORD, J., MEAS, C., THANN, S., MCLAUGHLIN, J. C., BARON, E. J. & WEST, T. E. 2014. Detection of *Burkholderia pseudomallei* in Sputum using Selective Enrichment Broth and Ashdown's Medium at Kampong Cham Provincial Hospital, Cambodia. *F1000Res*, 3, 302.
- NIEVES, W., PETERSEN, H., JUDY, B. M., BLUMENTRITT, C. A., RUSSELL-LODRIGUE, K., ROY, C. J., TORRES, A. G. & MORICI, L. A. 2014. A *Burkholderia pseudomallei* outer membrane vesicle vaccine provides protection against lethal sepsis. *Clin Vaccine Immunol*, 21, 747-54.
- NYSTROM, T. 2003. Conditional senescence in bacteria: death of the immortals. *Mol Microbiol*, 48, 17-23.
- OGEIL, R. P., ROOM, R., MATTHEWS, S. & LLOYD, B. 2015. Alcohol and burden of disease in Australia: the challenge in assessing consumption. *Aust N Z J Public Health*, 39, 121-3.

- OKIROR, L., COLTART, C., BILLE, A., GUILLE, L., PILLING, J., HARRISON-PHIPPS, K., ROUTLEDGE, T., LANG-LAZDUNSKI, L., HEMSLEY, C. & KING, J. 2014. Thoracotomy and decortication: impact of culture-positive empyema on the outcome of surgery. *Eur J Cardiothorac Surg*, 46, 901-6.
- OMURA, S. & CRUMP, A. 2004. The life and times of ivermectin - a success story. *Nat Rev Microbiol*, 2, 984-9.
- ORMAN, M. A. & BRYNILDSEN, M. P. 2013. Dormancy Is Not Necessary or Sufficient for Bacterial Persistence. *Antimicrobial Agents and Chemotherapy*, 57, 3230-3239.
- PAGNARITH, Y., KUMAR, V., THAIPADUNGPANIT, J., WUTHIEKANUN, V., AMORNCHAI, P., SIN, L., DAY, N. P. & PEACOCK, S. J. 2010. Emergence of pediatric melioidosis in Siem Reap, Cambodia. *Am J Trop Med Hyg*, 82, 1106-12.
- PALMER, G. H., BANKHEAD, T. & LUKEHART, S. A. 2009. 'Nothing is permanent but change' - antigenic variation in persistent bacterial pathogens. *Cellular Microbiology*, 11, 1697-1705.
- PAMMOLLI, F., MAGAZZINI, L. & RICCABONI, M. 2011. The productivity crisis in pharmaceutical R&D. *Nat Rev Drug Discov*, 10, 428-38.
- PAUL, S. M., MYTELKA, D. S., DUNWIDDIE, C. T., PERSINGER, C. C., MUNOS, B. H., LINDBORG, S. R. & SCHACHT, A. L. 2010. How to improve R&D productivity: the pharmaceutical industry's grand challenge. *Nat Rev Drug Discov*, 9, 203-14.
- PEACOCK, S. J., SCHWEIZER, H. P., DANCE, D. A., SMITH, T. L., GEE, J. E., WUTHIEKANUN, V., DESHAZER, D., STEINMETZ, I., TAN, P. & CURRIE, B. J. 2008. Management of accidental laboratory exposure to *Burkholderia pseudomallei* and *B. mallei*. *Emerg Infect Dis*, 14, e2.
- PENA, M. M., LEE, J. & THIELE, D. J. 1999. A delicate balance: homeostatic control of copper uptake and distribution. *J Nutr*, 129, 1251-60.

- PENDLETON, J. N., GORMAN, S. P. & GILMORE, B. F. 2013. Clinical relevance of the ESKAPE pathogens. *Expert Rev Anti Infect Ther*, 11, 297-308.
- PINK, R., HUDSON, A., MOURIES, M. A. & BENDIG, M. 2005. Opportunities and challenges in antiparasitic drug discovery. *Nat Rev Drug Discov*, 4, 727-40.
- PITMAN, M. C., LUCK, T., MARSHALL, C. S., ANSTEY, N. M., WARD, L. & CURRIE, B. J. 2015. Intravenous therapy duration and outcomes in melioidosis: a new treatment paradigm. *PLoS Negl Trop Dis*, 9, e0003586.
- PREVENTION, C. F. D. C. A. 2015. Conclusion of Select Agent Inquiry into Burkholderia pseudomallei Release at Tulane National Primate Research Center.
- PRICE, D. A., BLAGG, J., JONES, L., GREENE, N. & WAGER, T. 2009. Physicochemical drug properties associated with in vivo toxicological outcomes: a review. *Expert Opin Drug Metab Toxicol*, 5, 921-31.
- PRUKSACHARTVUTHI, S., ASWAPOKEE, N. & THANKERNGPOL, K. 1990. Survival of Pseudomonas pseudomallei in human phagocytes. *J Med Microbiol*, 31, 109-14.
- "Chloroxine | C9h5cl2no - Pubchem". Pubchem.ncbi.nlm.nih.gov. N.p., 2017. Web. 6 Feb. 2017.
- RAINS, C. P., BRYSON, H. M. & PETERS, D. H. 1995. Ceftazidime. An update of its antibacterial activity, pharmacokinetic properties and therapeutic efficacy. *Drugs*, 49, 577-617.
- RAMMAERT, B., BEAUTE, J., BORAND, L., HEM, S., BUCHY, P., GOYET, S., OVERTOOM, R., ANGEBAULT, C., TE, V., TRY, P. L., MAYAUD, C., VONG, S. & GUILLARD, B. 2011. Pulmonary melioidosis in Cambodia: a prospective study. *BMC Infect Dis*, 11, 126.
- RECKSEIDLER, S. L., DESHAZER, D., SOKOL, P. A. & WOODS, D. E. 2001. Detection of bacterial virulence genes by subtractive hybridization: identification of capsular

- polysaccharide of *Burkholderia pseudomallei* as a major virulence determinant. *Infect Immun*, 69, 34-44.
- RECKSEIDLER-ZENTENO, S. L., DEVINNEY, R. & WOODS, D. E. 2005. The capsular polysaccharide of *Burkholderia pseudomallei* contributes to survival in serum by reducing complement factor C3b deposition. *Infect Immun*, 73, 1106-15.
- RESISTANCE, R. O. A. 2016. Declaration by the Pharmaceutical, Biotechnology and Diagnostics Industries on Combating Antimicrobial Resistance. <http://amr-review.org/>.
- REYMOND, J.-L., VAN DEURSEN, R., BLUM, L. C. & RUDDIGKEIT, L. 2010. Chemical space as a source for new drugs. *MedChemComm*, 1, 30-38.
- RICHARDS, D. M. & BROGDEN, R. N. 1985. Ceftazidime - a Review of Its Antibacterial Activity, Pharmacokinetic Properties and Therapeutic Use. *Drugs*, 29, 105-161.
- ŘÍHA, M., KARLÍČKOVÁ, J., FILIPSKÝ, T., MACÁKOVÁ, K., HRDINA, R. & MLADĚNKA, P. 2013. Novel method for rapid copper chelation assessment confirmed low affinity of D-penicillamine for copper in comparison with trientine and 8-hydroxyquinolines. *Journal of Inorganic Biochemistry*, 123, 80-87.
- ROBERTS, M. E. & STEWART, P. S. 2005. Modelling protection from antimicrobial agents in biofilms through the formation of persister cells. *Microbiology*, 151, 75-80.
- ROBINSON, J. T., THORVALDSDÓTTIR, H., WINCKLER, W., GUTTMAN, M., LANDER, E. S., GETZ, G. & MESIROV, J. P. 2011. Integrative Genomics Viewer. *Nature Biotechnology*, 29, 24-26.
- RODE, J. W. & WEBLING, D. D. 1981. Melioidosis in the Northern Territory of Australia. *Med J Aust*, 1, 181-4.
- ROSENTHAL, P. J. 2003. Antimalarial drug discovery: old and new approaches. *J Exp Biol*, 206, 3735-44.

- ROTEM, E., LOINGER, A., RONIN, I., LEVIN-REISMAN, I., GABAY, C., SHORESH, N., BIHAM, O. & BALABAN, N. Q. 2010. Regulation of phenotypic variability by a threshold-based mechanism underlies bacterial persistence. *Proceedings of the National Academy of Sciences of the United States of America*, 107, 12541-12546.
- SANFORD, J. P. & MOORE, W. L., JR. 1971. Recrudescence melioidosis: a southeast asian legacy. *Am Rev Respir Dis*, 104, 452-3.
- SANTIAGO, A. E., RUIZ-PEREZ, F., JO, N. Y., VIJAYAKUMAR, V., GONG, M. Q. & NATARO, J. P. 2014. A large family of antivirulence regulators modulates the effects of transcriptional activators in Gram-negative pathogenic bacteria. *PLoS Pathog*, 10, e1004153.
- SARKAR-TYSON, M., SMITHER, S. J., HARDING, S. V., ATKINS, T. P. & TITBALL, R. W. 2009. Protective efficacy of heat-inactivated *B. thailandensis*, *B. mallei* or *B. pseudomallei* against experimental melioidosis and glanders. *Vaccine*, 27, 4447-51.
- SARKAR-TYSON, M., THWAITE, J. E., HARDING, S. V., SMITHER, S. J., OYSTON, P. C., ATKINS, T. P. & TITBALL, R. W. 2007. Polysaccharides and virulence of *Burkholderia pseudomallei*. *J Med Microbiol*, 56, 1005-10.
- SAROVICH, D. S., PRICE, E. P., LIMMATHUROTSAKUL, D., COOK, J. M., VON SCHULZE, A. T., WOLKEN, S. R., KEIM, P., PEACOCK, S. J. & PEARSON, T. 2012. Development of ceftazidime resistance in an acute *Burkholderia pseudomallei* infection. *Infect Drug Resist*, 5, 129-32.
- SAROVICH, D. S., WARD, L., PRICE, E. P., MAYO, M., PITMAN, M. C., BAIRD, R. W. & CURRIE, B. J. 2014. Recurrent melioidosis in the Darwin Prospective Melioidosis Study: improving therapies mean that relapse cases are now rare. *J Clin Microbiol*, 52, 650-3.

- SCHULTZ KIRKEGAARD, H. & VALENTIN, F. 2014. Academic drug discovery centres: the economic and organisational sustainability of an emerging model. *Drug Discov Today*, 19, 1699-710.
- SCHUMACHER, M. A., BALANI, P., MIN, J., CHINNAM, N. B., HANSEN, S., VULIC, M., LEWIS, K. & BRENNAN, R. G. 2015. HipBA-promoter structures reveal the basis of heritable multidrug tolerance. *Nature*, 524, 59-64.
- SCHUMACHER, M. A., MIN, J., LINK, T. M., GUAN, Z., XU, W., AHN, Y. H., SODERBLOM, E. J., KURIE, J. M., EVDOKIMOV, A., MOSELEY, M. A., LEWIS, K. & BRENNAN, R. G. 2012. Role of unusual P loop ejection and autophosphorylation in HipA-mediated persistence and multidrug tolerance. *Cell Rep*, 2, 518-25.
- SCHUMACHER, M. A., PIRO, K. M., XU, W., HANSEN, S., LEWIS, K. & BRENNAN, R. G. 2009. Molecular mechanisms of HipA-mediated multidrug tolerance and its neutralization by HipB. *Science*, 323, 396-401.
- SEBAUGH, J. L. 2011. Guidelines for accurate EC50/IC50 estimation. *Pharm Stat*, 10, 128-34.
- SELVARAJ, C., TRIPATHI, S. K., REDDY, K. K. & SINGH, S. K. 2011. Tool development for Prediction of pIC50 values from the IC50 values - A pIC50 value calculator. *Current Trends in Biotechnology and Pharmacy*, 5, 1104-1109.
- SHAH, D., ZHANG, Z. G., KHODURSKY, A., KALDALU, N., KURG, K. & LEWIS, K. 2006. Persisters: a distinct physiological state of E-coli. *Bmc Microbiology*, 6.
- SHARMA, B., BROWN, A. V., MATLUCK, N. E., HU, L. T. & LEWIS, K. 2015. *Borrelia burgdorferi*, the Causative Agent of Lyme Disease, Forms Drug-Tolerant Persister Cells. *Antimicrob Agents Chemother*, 59, 4616-24.
- SHEN, R., FAN, J. B., CAMPBELL, D., CHANG, W., CHEN, J., DOUCET, D., YEAKLEY, J., BIBIKOVA, M., WICKHAM GARCIA, E., MCBRIDE, C., STEEMERS, F., GARCIA, F.,

- KERMANI, B. G., GUNDERSON, K. & OLIPHANT, A. 2005. High-throughput SNP genotyping on universal bead arrays. *Mutat Res*, 573, 70-82.
- SIM, B. M., CHANTRATITA, N., OOI, W. F., NANDI, T., TEWHEY, R., WUTHIEKANUN, V., THAI PADUNGPANIT, J., TUMAPA, S., ARIYARATNE, P., SUNG, W. K., SEM, X. H., CHUA, H. H., RAMNARAYANAN, K., LIN, C. H., LIU, Y., FEIL, E. J., GLASS, M. B., TAN, G., PEACOCK, S. J. & TAN, P. 2010. Genomic acquisition of a capsular polysaccharide virulence cluster by non-pathogenic Burkholderia isolates. *Genome Biol*, 11, R89.
- SINGH, S. B. & BARRETT, J. F. 2006. Empirical antibacterial drug discovery - Foundation in natural products. *Biochemical Pharmacology*, 71, 1006-1015.
- SKREDENSKE, J. M., KOPPOLU, V., KOLIN, A., DENG, J., KETTLE, B., TAYLOR, B. & EGAN, S. M. 2013. Identification of a small-molecule inhibitor of bacterial AraC family activators. *J Biomol Screen*, 18, 588-98.
- SMITH, M. D., WUTHIEKANUN, V., WALSH, A. L. & WHITE, N. J. 1996. In-vitro activity of carbapenem antibiotics against beta-lactam susceptible and resistant strains of Burkholderia pseudomallei. *J Antimicrob Chemother*, 37, 611-5.
- SPOERING, A. L. & LEWIS, K. 2001. Biofilms and planktonic cells of Pseudomonas aeruginosa have similar resistance to killing by antimicrobials. *J Bacteriol*, 183, 6746-51.
- STIEFEL, P., SCHMIDT-EMRICH, S., MANIURA-WEBER, K. & REN, Q. 2015. Critical aspects of using bacterial cell viability assays with the fluorophores SYTO9 and propidium iodide. *Bmc Microbiology*, 15.
- SUPUTTAMONGKOL, Y., CHAOWAGUL, W., CHETCHOTISAKD, P., LERTPATANASUWUN, N., INTARANONGPAI, S., RUCHUTRAKOOL, T., BUDHSARAWONG, D., MOOTSIKAPUN, P., WUTHIEKANUN, V., TEERAWATASOOK, N. & LULITANOND, A.

1999. Risk factors for melioidosis and bacteremic melioidosis. *Clin Infect Dis*, 29, 408-13.
- SWINNEY, D. C. & ANTHONY, J. 2011. How were new medicines discovered? *Nat Rev Drug Discov*, 10, 507-19.
- TRALAU-STEWART, C. J., WYATT, C. A., KLEYN, D. E. & AYAD, A. 2009. Drug discovery: new models for industry-academic partnerships. *Drug Discov Today*, 14, 95-101.
- UNGER, M. A., CHOU, H. P., THORSEN, T., SCHERER, A. & QUAKE, S. R. 2000. Monolithic microfabricated valves and pumps by multilayer soft lithography. *Science*, 288, 113-116.
- VADIVELU, J., PUTHUCHEARY, S. D., DRASAR, B. S., DANCE, D. A. & PITT, T. L. 1998. Stability of strain genotypes of *Burkholderia pseudomallei* from patients with single and recurrent episodes of melioidosis. *Trop Med Int Health*, 3, 518-21.
- VALLER, M. J. & GREEN, D. 2000. Diversity screening versus focussed screening in drug discovery. *Drug Discov Today*, 5, 286-293.
- VEBER, D. F., JOHNSON, S. R., CHENG, H.-Y., SMITH, B. R., WARD, K. W. & KOPPLE, K. D. 2002. Molecular Properties That Influence the Oral Bioavailability of Drug Candidates. *Journal of Medicinal Chemistry*, 45, 2615-2623.
- VEGA, N. M., ALLISON, K. R., KHALIL, A. S. & COLLINS, J. J. 2012. Signaling-mediated bacterial persister formation. *Nature Chemical Biology*, 8, 431-433.
- VIVOLI, M., ISUPOV, M. N., NICHOLAS, R., HILL, A., SCOTT, A. E., KOSMA, P., PRIOR, J. L. & HARMER, N. J. 2015. Unraveling the *B. pseudomallei* Heptokinase WcbL: From Structure to Drug Discovery. *Chem Biol*, 22, 1622-32.
- VLIEGHE, E., KRUY, L., DE SMET, B., KHAM, C., VENG, C. H., PHE, T., KOOLE, O., THAI, S., LYNEN, L. & JACOBS, J. 2011. Melioidosis, phnom penh, Cambodia. *Emerg Infect Dis*, 17, 1289-92.

- VORACHIT, M., LAM, K., JAYANETRA, P. & COSTERTON, J. W. 1995. Electron microscopy study of the mode of growth of *Pseudomonas pseudomallei* in vitro and in vivo. *J Trop Med Hyg*, 98, 379-91.
- WALKER, K. K. & LEVINE, A. J. 1996. Identification of a novel p53 functional domain that is necessary for efficient growth suppression. *Proc Natl Acad Sci U S A*, 93, 15335-40.
- WANG, T., WU, M.-B., LIN, J.-P. & YANG, L.-R. 2015. Quantitative structure-activity relationship: promising advances in drug discovery platforms. *Expert Opinion on Drug Discovery*, 10, 1283-1300.
- WANG, X., LORD, D. M., CHENG, H.-Y., OSBOURNE, D. O., HONG, S. H., SANCHEZ-TORRES, V., QUIROGA, C., ZHENG, K., HERRMANN, T., PETI, W., BENEDIK, M. J., PAGE, R. & WOOD, T. K. 2012. A Novel Type V TA System Where mRNA for Toxin GhoT is Cleaved by Antitoxin GhoS. *Nature chemical biology*, 8, 855-861.
- WEINTRAUB, A. 2003. Immunology of bacterial polysaccharide antigens. *Carbohydr Res*, 338, 2539-47.
- WENLOCK, M. C., AUSTIN, R. P., BARTON, P., DAVIS, A. M. & LEESON, P. D. 2003. A comparison of physiochemical property profiles of development and marketed oral drugs. *J Med Chem*, 46, 1250-6.
- WHITE, N. J. 2003. Melioidosis. *Lancet*, 361, 1715-22.
- WHITMORE, A. 1913. An Account of a Glanders-like Disease occurring in Rangoon. *J Hyg (Lond)*, 13, 1-34 1.
- WIERSINGA, W. J., CURRIE, B. J. & PEACOCK, S. J. 2012. Melioidosis. *N Engl J Med*, 367, 1035-44.
- WINKLER, D. A. 2002. The role of quantitative structure - activity relationships (QSAR) in biomolecular discovery. *Briefings in Bioinformatics*, 3, 73-86.

- WINSOR, G. L., KHAIRA, B., VAN ROSSUM, T., LO, R., WHITESIDE, M. D. & BRINKMAN, F. S. 2008. The Burkholderia Genome Database: facilitating flexible queries and comparative analyses. *Bioinformatics*, 24, 2803-4.
- WOLFSON, J. S., HOOPER, D. C., MCHUGH, G. L., BOZZA, M. A. & SWARTZ, M. N. 1990. Mutants of Escherichia-Coli K-12 Exhibiting Reduced Killing by Both Quinolone and Beta-Lactam Antimicrobial Agents. *Antimicrobial Agents and Chemotherapy*, 34, 1938-1943.
- WOOD, T. K., KNABEL, S. J. & KWAN, B. W. 2013. Bacterial persister cell formation and dormancy. *Appl Environ Microbiol*, 79, 7116-21.
- WU, Y. X., VULIC, M., KEREN, I. & LEWIS, K. 2012. Role of Oxidative Stress in Persister Tolerance. *Antimicrobial Agents and Chemotherapy*, 56, 4922-4926.
- WUTHIEKANUN, V., AMORNCHAI, P., SAIPROM, N., CHANTRATITA, N., CHIERAKUL, W., KOH, G. C., CHAOWAGUL, W., DAY, N. P., LIMMATHUROTSAKUL, D. & PEACOCK, S. J. 2011. Survey of antimicrobial resistance in clinical Burkholderia pseudomallei isolates over two decades in Northeast Thailand. *Antimicrob Agents Chemother*, 55, 5388-91.
- YAMAGUCHI, Y. & INOUE, M. 2011a. Regulation of growth and death in Escherichia coli by toxin-antitoxin systems. *Nature Reviews Microbiology*, 9, 779-790.
- YAMAGUCHI, Y. & INOUE, M. 2011b. Regulation of growth and death in Escherichia coli by toxin-antitoxin systems. *Nat Rev Microbiol*, 9, 779-90.
- YANG, J., TAUSCHEK, M. & ROBINS-BROWNE, R. M. 2011. Control of bacterial virulence by AraC-like regulators that respond to chemical signals. *Trends in Microbiology*, 19, 128-135.

- YOSHIDA, H., MAKI, Y., KATO, H., FUJISAWA, H., IZUTSU, K., WADA, C. & WADA, A. 2002. The ribosome modulation factor (RMF) binding site on the 100S ribosome of *Escherichia coli*. *Journal of Biochemistry*, 132, 983-989.
- YU, Y., KIM, H. S., CHUA, H. H., LIN, C. H., SIM, S. H., LIN, D., DERR, A., ENGELS, R., DESHAZER, D., BIRREN, B., NIERMAN, W. C. & TAN, P. 2006. Genomic patterns of pathogen evolution revealed by comparison of *Burkholderia pseudomallei*, the causative agent of melioidosis, to avirulent *Burkholderia thailandensis*. *BMC Microbiol*, 6, 46.
- ZANDERS, E. D., BAILEY, D. S. & DEAN, P. M. 2002. Probes for chemical genomics by design. *Drug Discovery Today*, 7, 711-718.
- ZHANG, J. H., CHUNG, T. D. & OLDENBURG, K. R. 1999. A Simple Statistical Parameter for Use in Evaluation and Validation of High Throughput Screening Assays. *J Biomol Screen*, 4, 67-73.
- ZHANG, Y., LIU, T., MEYER, C. A., EECKHOUTE, J., JOHNSON, D. S., BERNSTEIN, B. E., NUSBAUM, C., MYERS, R. M., BROWN, M., LI, W. & LIU, X. S. 2008. Model-based analysis of ChIP-Seq (MACS). *Genome Biol*, 9, R137.
- ZHANG, Z., ABOULWAFI, M., SMITH, M. H. & SAIER, M. H., JR. 2003. The ascorbate transporter of *Escherichia coli*. *J Bacteriol*, 185, 2243-50.
- ZIPPER, H., BRUNNER, H., BERNHAGEN, J. & VITZTHUM, F. 2004. Investigations on DNA intercalation and surface binding by SYBR Green I, its structure determination and methodological implications. *Nucleic Acids Res*, 32, e103.

